THE MINOR PLANET BULLETIN

BULLETIN OF THE MINOR PLANETS SECTION OF THE ASSOCIATION OF LUNAR AND PLANETARY OBSERVERS

VOLUME 51, NUMBER 2, A.D. 2024 APRIL-JUNE 89.

ROTATION PERIODS OF THREE ASTEROIDS THROUGH DIFFERENTIAL PHOTOMETRY

Shayaan Zari
Kent Montgomery
Texas A&M University-Commerce
P.O. Box 3011
Commerce, TX 75429-3011
Kent.Montgomery@tamuc.edu

(Received: 2024 January 12 Revised: 2024 February 12)

Lightcurves and rotation periods were determined for three main belt asteroids. The rotation periods found for each asteroid were: 5.778 ± 0.006 h for 3519 Ambiorix, 2.788 ± 0.001 h for 4569 Baerbel, and 5.632 ± 0.004 h for 7468 Anfimov.

In order to create lightcurves and determine rotation periods for each of the chosen asteroids, data were collected over the course of several nights. The asteroids studied were: 3519 Ambiorix, 4569 Baerbel, and 7519 Anfimov.

Asteroid 3519 Ambiorix has a semi-major axis of 2.17 AU and an orbital eccentricity of 0.176. It was discovered in 1984 by H. Debehogne at the La Silla Observatory (JPL, 2023). Asteroid 4569 Baerbel has a semi-major axis of 2.59 AU and an orbital eccentricity of 0.0621. It was discovered in 1985 by C.S. Shoemaker at the Palomar Observatory (JPL, 2023). Asteroid 7468 Anfimov has a semi-major axis of 3.04 AU and an orbital eccentricity of 0.120. It was discovered in 1990 by L.I. Chernykh at the Crimean Astrophysics Observatory (JPL, 2023).

The asteroids used in this study were selected on the basis of several specific criteria: the opposition date, the declination at the time of observing, and the magnitude. Objects that were in opposition 2-3 weeks prior to the current date were chosen so that by sunset, the asteroid would already be around 20° above the horizon. A declination greater than -15° is ideal when observing in the northern hemisphere. Accounting for both opposition date and declination serves to ensure the longest viewing interval per night. Observed objects possessed a magnitude of 16 or less to achieve the maximum signal-to-noise ratio.

The aforementioned parameters were used with the Collaborative Asteroid Lightcurve Link (CALL) database (Warner, 2021). After selecting possible targets, each asteroid's position for that particular night was then found using *TheSkyX* software program (Diffraction Limited). Depending on the time, date, and the observatory's location, the software provided a detailed chart of the asteroid's position against the night sky. Finally, asteroids which traveled too close to many stars were filtered out.

Methods

Images of the field containing the target asteroid as well as several possible reference stars were taken using 180 second exposures. All data were taken through a Luminance 3 filter, which is permeable to visible light while preventing infrared and UV light. The telescope was focused hourly.

At a latitude of 33° N, the 0.7-meter CDK 700 Planewave telescope belonging to the Texas A&M University-Commerce was utilized for all asteroids. Attached to the telescope is an Andor iKon-XL CCD Camera, which was thermoelectrically cooled to -20°C.

After raw data were collected, they were then processed using three kinds of calibration frames which were acquired each night prior to the light images: bias, dark, and flat frames. Flat frames were taken against the twilight sky each night. The image processing program *Maxim DL* (Diffraction Limited) was utilized to produce calibrated images as well as aligning all the images. Differential photometry was performed on these calibrated and aligned images using the software MPO Canopus v10.8.1.1 (Warner, 2019).

For each calibrated image the brightness of five reference stars was determined and these reference stars were chosen based on their magnitude and position on the field. The software then compared the brightness of the asteroid with the average brightness of the

Number	Name	yr mm/dd	Phase	L_{PAB}	B_{PAB}	Period(h)	P.E.	Amp	A.E.	Grp
3519	Ambiorix	2023 06/16-06/17	12.9,13.5	247.2	-0.3	5.778	0.006	0.24	0.04	MB
4569	Baerbel	2023 07/19-07/20	14.3,14.5	272.4	18	2.788	0.001	0.17	0.02	MB
7468	Anfimov	2022 12/14-12/14	6.0, 6.4	69	-1.2	5.632	0.004	0.51	0.02	MB

Table I. Observing circumstances and results. The phase angle is given for the first and last date. If preceded by an asterisk, the phase angle reached an extrema during the period. L_{PAB} and B_{PAB} are the approximate phase angle bisector longitude/latitude at mid-date range (see Harris et al., 1984). Grp is the asteroid family/group (Warner et al., 2009). Additional data is from *MPO Canopus* v10.8.1.1. (Warner, 2019).

comparison stars. The variation of the brightness versus time allowed the creation of a lightcurve. The light frames taken when the target moved in proximity of a star were eliminated to increase accuracy. Lastly, a Fourier transform of the lightcurve was used to determine the target's rotation period and associated error.

Results

3519 Ambiorix. Two nights were spent observing 3519 Ambiorix; 175 images were taken on 2023 June 16 and 171 on 2023 June 17. The resulting lightcurve yielded a rotation period of 5.778 ± 0.006 h with an amplitude of 0.24 mag. Colazo et al. (2021) determined a similar period of 5.78 ± 0.03 h with an amplitude of 0.29 mag.

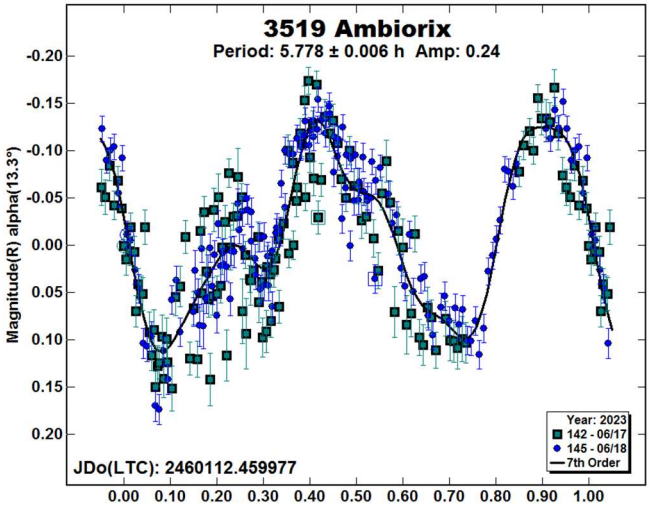

4569 Baerbel. This asteroid was observed over two nights; 67 images were taken on 2023 July 19 and 90 on 2023 July 21. The resulting lightcurve yielded a rotation period of 2.788 ± 0.001 h with an amplitude of 0.17 mag. Brinsfield (2010) obtained a similar period of 2.737 ± 0.001 h with an amplitude of 0.24 mag.

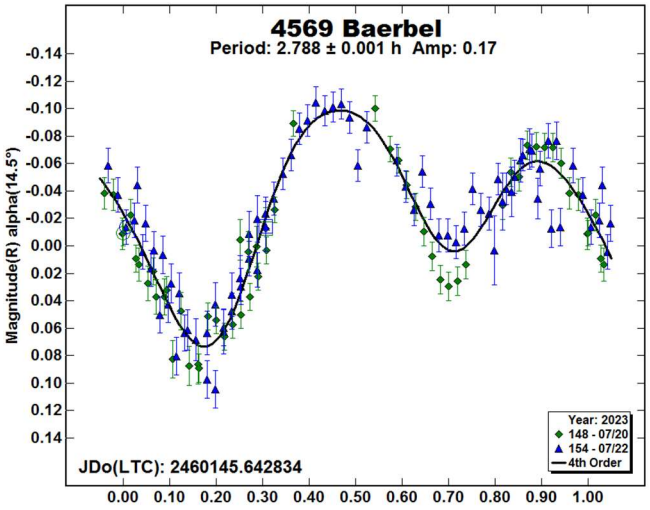

7468 Anfimov. Asteroid 7468 Anfimov was observed over two nights; 100 images were taken on 2022 December 14 and 69 on 2022 December 15. The resulting lightcurve yielded a rotation period of 5.632 ± 0.004 h with an amplitude variance of 0.51 mag. Casalnuovo (2023) reports a period of 6.40 ± 0.01 h with an amplitude of 0.67 mag.

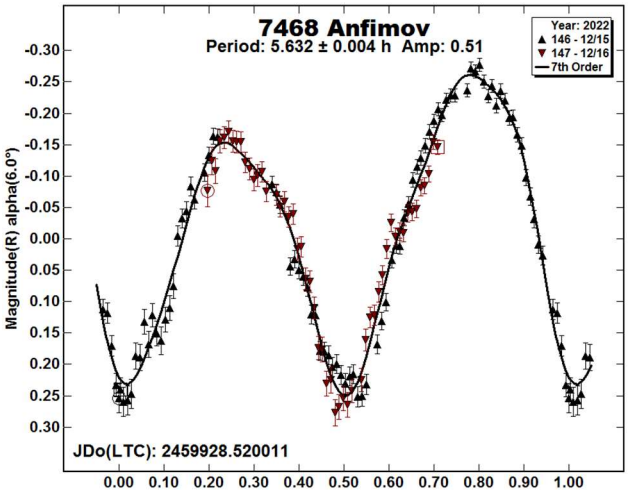

Acknowledgements

This research was supported by the Physics and Astronomy Research Experiences for Undergraduates (REU) Program at the Texas A&M University-Commerce funded by NSF Grant No. 2050277.

References

Brinsfield, J.W. (2010). "Asteroid Lightcurve Analysis at the Via Capote Observatory: 2010 February-May." *Minor Planet Bulletin* **37**, 146-147.

Casalnuovo, G.B. (2023). "Lightcurve Analysis for Four Main Belt Asteroids." *Minor Planet Bulletin* **50**, 215-216.

Colazo, M.; Stechina, A.; Fornari, C.; Santucho, M.; Mottino, A.; Pulver, E.; Melia, R.; Suárez, N.; Scotta, D.; Chapman, A.; Oey, J.; Meza, E.; Bellocchio, E.; Morales, M.; Speranza, T. and 9 colleagues (2021). "Asteroid Photometry and Lightcurve Analysis at Gora Observatories." *Minor Planet Bulletin* **48**, 50-55.

Diffraction Limited MaxIm DL - Astronomy and Scientific Imaging Software.
https://diffractionlimited.com/product/maxim-dl/

Harris, A.W.; Young, J.W.; Scaltriti, F.; Zappala, V. (1984). "Lightcurves and phase relations of the asteroids 82 Alkmene and 444 Gyptis." *Icarus* **57**, 251-258.

JPL (2023). Small-Body Database Lookup.
https://ssd.jpl.nasa.gov/tools/sbdb_lookup.html#/

Warner, B.D.; Harris, A.W.; Pravec, P. (2009). "The Asteroid Lightcurve Database." *Icarus* **202**, 134-146. Updated 2023 June. *http://www.MinorPlanet.info/php/lcdb.php*

Warner, B.D. (2019). MPO Canopus Software Version 10.8.1.1. Bdw Publishing.
https://minplanobs.org/BdwPub/php/displayhome.php

Warner, B.D. (2021). Collaborative Asteroid Lightcurve Link (CALL). *https://www.minorplanet.info/php/call.php*

DETERMINING THE LIGHTCURVES AND ROTATION PERIODS OF FOUR MAIN-BELT ASTEROIDS

Kaitlyn Kalisek
Kent Montgomery
Texas A&M University-Commerce
P.O. Box 3011
Commerce, TX 75429-3011
Kent.Montgomery@tamuc.edu

(Received: 2024 January 12 Revised: 2024 February 12)

Lightcurves and rotation periods were determined for the following four main-belt asteroids: 2854 Rawson: 4.775 ± 0.001 h, 5142 Okutama: 3.803 ± 0.001 h, (14362) 1988 MH: 3.645 ± 0.001 h, and 28248 Barthelemy: 3.128 ± 0.002 h.

This research was conducted in order to determine the rotation period of four main belt asteroids: 2854 Rawson, 5142 Okutama, (14362) 1988 MH, and 28248 Barthelemy. Photometric data were taken over the course of several nights; the resulting magnitudes were then plotted versus time to create lightcurves and analyzed to determine the asteroid's rotation period. Asteroids were chosen based on apparent magnitude, declination, and opposition date. To maximize the amount of data obtained each night, asteroids at or near opposition were chosen; additionally, these asteroids needed a magnitude of 16 or brighter for an optimal signal to noise ratio and have positive declinations because the telescope used was located in the northern hemisphere.

Asteroid 2854 Rawson was discovered by D. McLeish at the Argentine National Observatory in Córdoba in 1964. It has an orbital eccentricity of 0.123 and a semi-major axis of 2.21 AU (JPL, 2023). Asteroid 5142 Okutama was discovered by T. Hioki and S. Hayakawa at Okutama in 1990. It has an orbital eccentricity of 0.277 and a semi-major axis of 2.54 AU (JPL, 2023). Asteroid (14362) 1988 MH was discovered by E.F. Helin at the Palomar Observatory in 1988. It has an orbital eccentricity of 0.192 and a semi-major axis of 2.60 AU (JPL, 2023). Asteroid 28248 Barthelemy was discovered by the OCA-DLR Asteroid Survey (ODAS) at the CERGA Observatory in Caussols in 1999. It has an orbital eccentricity of 0.212 and a semi-major axis of 2.60 AU (JPL, 2023).

Method

The telescope used to obtain the data is located at the Texas A&M University-Commerce Observatory in Commerce, Texas at latitude 33ºN. It is a 0.7-m CDK 700 Planewave telescope equipped with an Andor iKon-XL CCD Camera. To reduce background noise, the camera was thermoelectrically cooled between -40ºC and -60ºC.

Flats, bias, and dark calibration images were taken each night in order to calibrate the images. Flat field images were taken against the twilight sky and exposed for gradually increasing amounts of time, and darks were exposed for three minutes, which is the same exposure time as the light images. All images were taken through a luminance filter which blocks the infrared and UV, therefore allowing only the visible light to be captured by the camera.

Light images were calibrated and aligned using *Maxim DL* software (Diffraction Limited). Then, photometry on each image was performed using *MPO Canopus* v.10.8.1.1 (Warner, 2019). Five comparison stars along with the asteroid were selected and aperture photometry was used to measure the brightness of the comparison stars and the asteroid. These data were then used to find the average difference in magnitude between the comparison stars and the asteroid for every image and plotted versus time to produce a lightcurve. If the asteroid passed close to a star, these data were deleted from the lightcurve, and a Fourier transform was also applied to the lightcurve to determine the rotation period and associated error in the period.

Results

2854 Rawson. Asteroid 2854 Rawson was imaged on 2021 December 1 for 86 times and on 2021 December 2 for 110 times. A rotation period of 4.775 ± 0.001 h with an amplitude variance of 0.78 mag was found. Black et al. (2016) found a similar period of 4.7755 ± 0.0003 h with an amplitude of 0.63 mag. Durech et al. (2019) found a similar period of 4.775587 ± 0.000002 h.

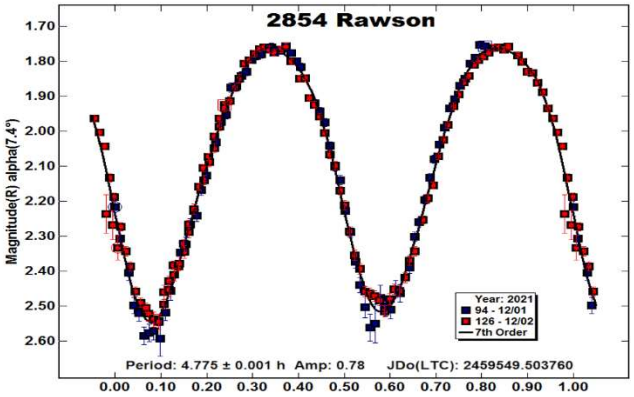

5142 Okutama. Asteroid 5142 Okutama was imaged on 2022 September 15 for 60 times and on 2022 September 17 for100 times. A rotation period of 3.803 ± 0.001 h with an amplitude variance of 0.61 mag was found. Ditteon and Hawkins (2007) found the same period of 3.803 ± 0.001 h with an amplitude of 0.27 mag.

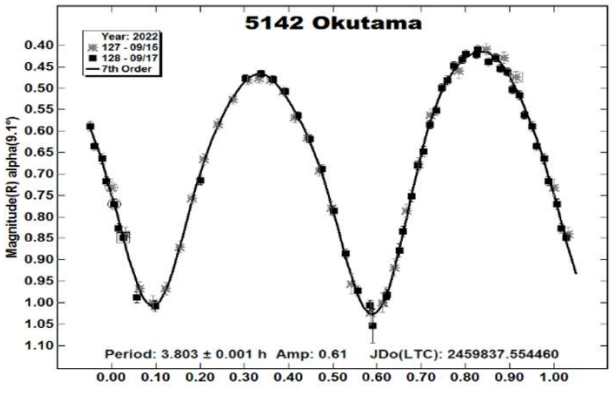

Number	Name	yyyy mm/dd	Phase	L_{PAB}	B_{PAB}	Period(h)	P.E.	Amp	A.E.
2854	Rawson	2021 12/01-12/02	7.86	259.4	-1.9	4.775	0.001	0.78	0.02
5142	Okutama	2022 09/15-09/17	10.13	132.9	-5.4	3.803	0.001	0.61	0.01
14362	1988 MH	2022 09/22-09/29	15.83	97.4	5.3	3.645	0.001	0.43	0.02
28248	Barthelemy	2022 10/14-10/15	8.44	120.6	1.1	3.128	0.002	0.44	0.04

Table I. Observing circumstances and results. The phase angle is given for the first and last date. If preceded by an asterisk, the phase angle reached an extrema during the period. L_{PAB} and B_{PAB} are the approximate phase angle bisector longitude/latitude at mid-date range (see Harris et al., 1984). Grp is the asteroid family/group (Warner et al., 2009).

(14362) 1988 MH. Asteroid (14362) 1988 MH was imaged on 2022 September 22 for 100 times, on 2022 September 23 for 100 times, and on 2022 September 29 for 100 times. A rotation period of 3.645 ± 0.001 h with an amplitude variance of 0.43 mag was found. Behrend (2001web) found a similar period of 3.639 ± 0.002 h with an amplitude of 0.44 mag. Durech and Hanus (2018) found a similar period of 3.64387 ± 0.00002 h.

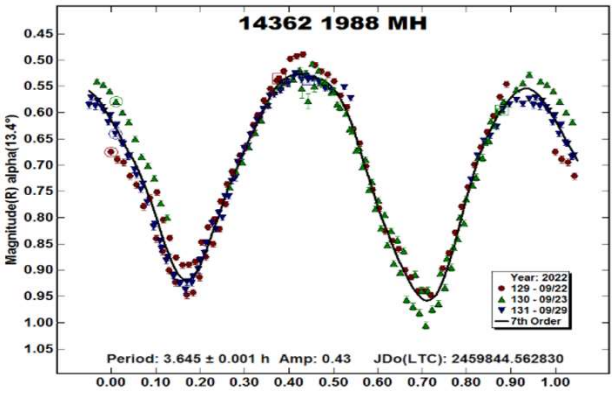

28248 Barthelemy. Asteroid 28248 Barthelemy was imaged on 2022 October 14 for 100 times and on 2022 October 15 for 100 times. A rotation period of 3.128 ± 0.002 h with an amplitude variance of 0.44 mag was found. No previous studies regarding the rotation period were found in either the JPL Small-Body Database (NASA, n.d.) or the Minor Planet Light Curve Database (Warner et al., 2009).

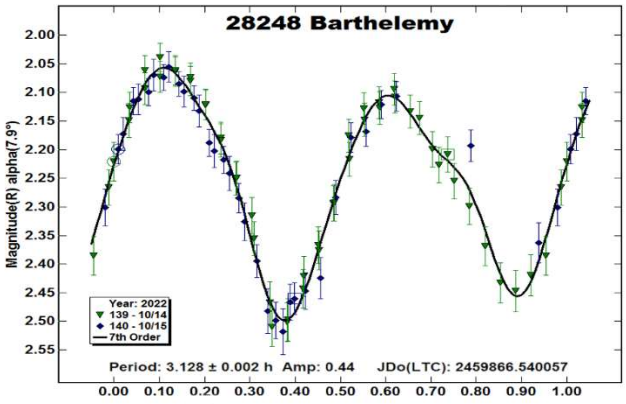

References

Behrend, R. (2001web) Observatoire de Geneve web site. *http://obswww.unige.ch/~behrend/page_cou.html*

Black, S.; Linville, D.; Michalik, D.; Wolf, M.; Ditteon, R. (2016). "Lightcurve Analysis of Asteroids Observed at the Oakley Southern Sky Observatory: 2015 December - 2016 April." *Minor Planet Bull.* **43**, 287-289.

Diffraction Limited Maxim DL - Astronomy and Scientific Imaging Software. *https://diffractionlimited.com/product/maxim-dl/*

Ditteon, R.; Hawkins, S. (2007). "Asteroid Lightcurve Analysis at the Oakley Observatory - October-November 2006." *Minor Planet Bull.* **34**, 59-64.

Durech, J.; Hanus, J. (2018). "Reconstruction of asteroid spin states from Gaia DR2 photometry." *Astron. Astrophys.* **620**, A91.

Durech, J.; Hanus, J.; Vanco, R. (2019). "Inversion of asteroid photometry from Gaia DR2 and the Lowell Observatory photometric database." *Astron. Astrophys* 631, A2.

Harris, A.W.; Young, J.W.; Scaltriti, F.; Zappala, V. (1984). "Lightcurves and phase relations of the asteroids 82 Alkmene and 444 Gyptis." *Icarus* **57**, 251-258.

JPL (2023). Small Body Database Search Engine. *http://ssd.jpl.nasa.gov/sbdb_query.cgi*

NASA. (n.d.). JPL Small-Body Database Lookup. *https://ssd.jpl.nasa.gov/tools/sbdb_lookup.html#/*

Warner, B.D.; Harris, A.W.; Pravec, P. (2009). "The Asteroid Lightcurve Database." *Icarus* **202**, 134-146. Updated 2023 Sep 16. *https://www.minorplanet.info/php/lcdb.php*

Warner, B.D. (2019). *MPO Canopus* software. Version 10.8.1.1. Bdw Publishing. *http://www.minorplanetobserver.com/*

LIGHTCURVE AND ROTATION PERIODS OF FOUR ASTEROIDS

Mamosa Mohoto
Kent Montgomery
Texas A&M University-Commerce
P.O. Box 3011
Commerce, TX 75429-3011
Kent.Montgomery@tamuc.edu

(Received: 2024 January 12 Revised: 2024 February 12)

The following rotation periods were obtained for four main-belt asteroids: 3332 Raksha: 4.816 ± 0.002 h, 3894 Williamcooke: 2.629 ± 0.001 h, 3896 Pordenone: 4.002 ± 0.001 h and 7365 Sejong: 2.580 ± 0.001 h.

Research was conducted in order to determine the rotation period of each of the following asteroids: 3332 Rasksha, 3894 Williamcooke, 7365 Sejong and 3896 Pordenone. These asteriods were selected using the Collaborative Asteroid Lightcurve Link (CALL) website. These chosen asteroids were required to have an apparent magnitude less than 16 and greater than 13. The asteroids were also required to have an opposition date roughly two weeks prior to the observation date. For observations done in Commerce, Texas, asteroids typically had a positive declination and for observations in Chile they had a negative declination.

The asteroid 3332 Raksha was discovered by L. Chernykh in 1978 July 4 at the Crimean Astrophysical Observatory, located in Nauchnyi. It was first observed 1936 March 27. This asteroid has a semi-major axis of 2.21 AU, an eccentricity of 0.086 and an absolute magnitude of 11.68 (JPL, 2023). Asteroid 3894 Wiiliamcooke was discovered by P. Jekabsons and M.P. Candy in 1980 at the Perth Observatory, located in Bickley, Western Australia. It was first observed 1978 March 6. The asteroid has a semi-major axis of 2.54 AU, an eccentricity of 0.172 and an absolute magnitude of 12.26 (JPL, 2023). 3896 Pordenone was discovered by J.M. Baur in 1987 November 18 at Chions, located in Italy. It was first observed 1950 October 13. The asteroid has a semi-major axis of 3.00 AU, an eccentricity of 0.043 and an absolute magnitude of 11.58 (JPL, 2023). The asteroid 7365 Sejong was discovered by K. Watanabe on 1996 August 18 in Sapporo, Japan. It was first observed 1950 August 6. This asteroid has a semi-major axis of 2.21 AU, an eccentricity of 0.213 and an absolute magnitude of 13.78 (JPL, 2023).

Method

Images were taken at the Texas A&M University-Commerce (TAMUC) Observatory using a Planewave CDK 700 27-inch telescope and the 0.6-m Southern Association for Research in Astronomy telescope (SARA-S) located at the Cerro-Tololo Observatory in Chile. Both telescopes were equipped with Apogee Andor CCD cameras. To reduce thermal noise, the cameras were thermoelectrically cooled. The camera used at the TAMUC Observatory was cooled to a temperature range between -20℃ to -35℃. The camera used in Chile was cooled to a temperature of -75℃. For both telescopes the light passed through a luminance filter before hitting the CCD chip. This filter is a passband for all visible light but blocks all IR and UV light. Observations for each asteroid were performed over two to three nights.

Calibration images were taken each night. These calibration images included bias frames, dark frames, and twilight flat field images. Bias frames were taken at the beginning of each night. Two to three dark frames were taken with an exposure time of 180 s, equivalent to the light frame exposure times. Flat field images were taken against the twilight sky. The number of flat field images taken varied for each night of observations. Master images of all the calibrations images were created using *Maxim DL* (Diffraction Limited). These master images were then used to reduce all the asteroid images.

To measure the relative brightness of the asteroids, aperture photometry was performed on each of the asteroid and five comparison stars in each image using the *MPO Canopus* v.10.3.0.0. software (Warner, 2011). The average brightness difference between each asteroid and comparison star was determined for each 3-minute image. These magnitudes were then plotted versus time to produce a lightcurve. Observations revealing the asteroid near or passing in front of a star were removed. A Fourier Transform of the lightcurve was then taken to find the best rotation period for the observed asteroid.

Results

3332 Raksha. Asteroid 3332 Raksha was observed on two nights, both nights using the TAMUC telescope. A total of 184 images were captured for this asteroid. The first night of data collection was on 2022 June 20, and the second night of data collected was on 2022 June 22. Each night had 92 images. Analysis of the lightcurve showed a period of 4.816 ± 0.002 h and an amplitude of 0.23 mag. A study done by Klinglesmith III et al. (2013) resulted in a similar rotation period of 4.806 ± 0.002 h.

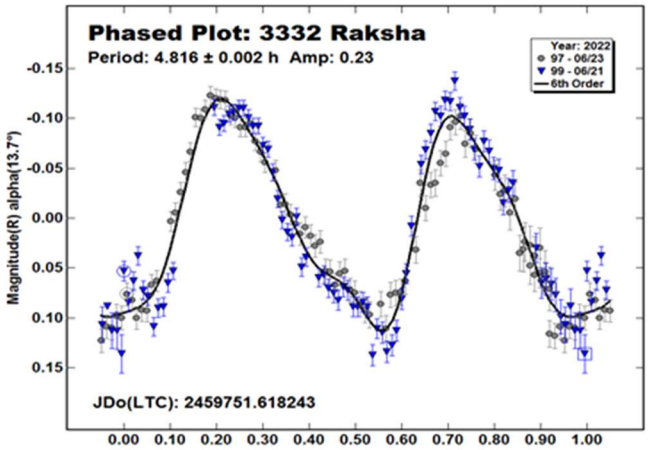

3894 Williamcooke. Three nights of observation were used for 3894 Williamcooke, with a total of 251 images obtained. The first night of data collection was on 2022 June 30, with a total of 109 images using the SARA-S telescope. On the second and third nights, research was done using the TAMUC telescope. 2022 July 1 yielded a total of 82 images and 2022 July 6 a total of 91 images. Analysis of the lightcurve shows 3894 Williamcooke having an amplitude of 0.07 mag and a period of 2.629 ± 0.001 h. Previous research done by Stephens and Warner (2019) indicates a rotation period of 4.16 ± 0.01 h. Another study by Macias (2015) reveals a rotation period of 3.10 ± 0.05 h. The vastly different rotation periods show that this asteroid may require additional research.

Number	Name	2021 mm/dd		Phase	L_{PAB}	B_{PAB}	Period(h)	P.E.	Amp	A.E.
3332	Raksha	2022	06/20-06/22	12.5,13.1	242.7	17.45	4.816	0.002	0.23	0.04
3894	Williamcooke	2022	06/29-07/09	12.7,14.5	255.25	16.95	2.629	0.001	0.07	0.02
3896	Pordenone	2022	08/02-08/06	5.8, 6.8	299.4	11.2	4.002	0.001	0.41	0.02
7365	Sejong	2022	06/30-07/06	11.3,16.1	262.1	9.55	2.580	0.001	0.11	0.02

Table I. Observing circumstances and results. The phase angle is given for the first and last date. If preceded by an asterisk, the phase angle reached an extrema during the period. L_{PAB} and B_{PAB} are the approximate phase angle bisector longitude/latitude at mid-date range (see Harris et al., 1984). Grp is the asteroid family/group (Warner et al., 2009). Additional data are from *MPO Canopus* v10.3.0.0. (Warner, 2011).

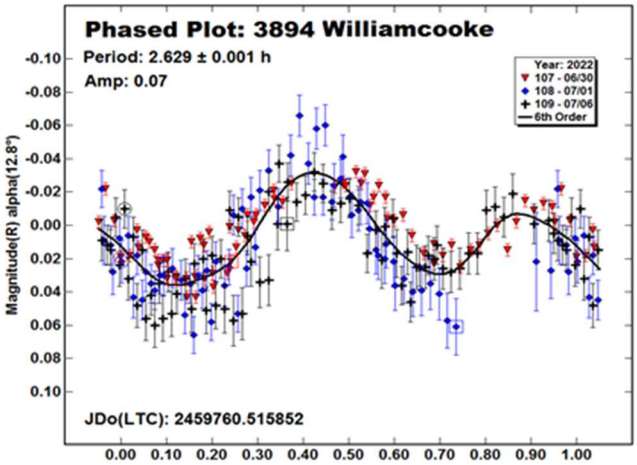

3896 Pordenone. Three nights of observation were used for 3896 Pordenone, with a total of 313 captured images. The first night of data collection was on 2022 August 2 and the second night on 2022 August 3. Both nights resulted in 104 total images. The third night was on 2022 August 6 resulting in 105 total images captured. All three nights of observations were taken using the TAMUC telescope. Analysis of the lightcurve shows a period of 4.002 ± 0.001 h and an amplitude of 0.41 mag. A previous study conducted by Hanus et al. (2013) suggests a rotation period of 4.400366 ± 0.0000005 h. Other research done by Kurtenkov et al. (2014), Waszczak et al. (2015) and Durech et al. (2020) reveal similar rotation periods of 4.00 ± 0.01 h, 4.003 ± 0.0031 h and 4.00368 ± 0.00001 h.

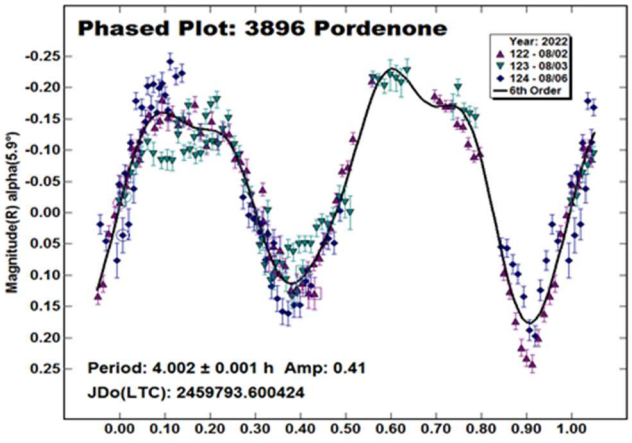

7365 Sejong. Three nights of observation were used for 7365 Sejong, with a total of 269 images obtained. The first night on 2022 June 29 produced 88 images taken with the SARA-S telescope. The second night was 2022 June 29 where 85 images were captured using TAMUC telescope. 2022 July 9, the last night of data collection, resulted in 123 images using the SARA-S telescope. Analysis of the lightcurve shows a period of 2.580 ± 0.001 h and an amplitude of 0.11 mag. Previous research conducted by Polakis (2020) and Yeh et al. (2020) suggests that 7365 Sejong has a rotation period of 2.579 ± 0.001 h. Results were based on research that they estimated may have a 30 percent chance of error (JPL, 2023).

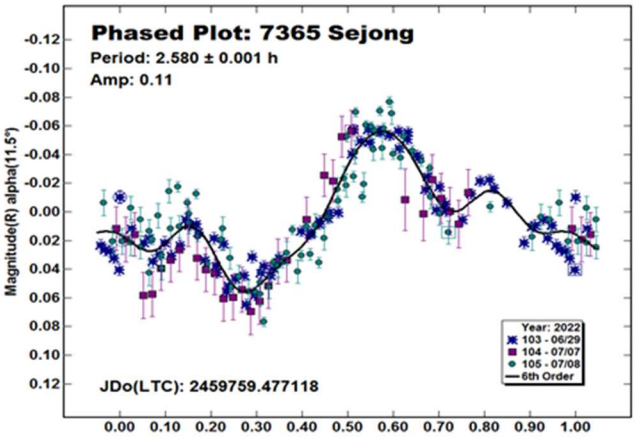

Acknowledgements

This research was fully funded by the National Science Foundation (NSF) grant no. 2050277. The opportunity to conduct this research was made possible through the Physics and Astronomy Research Experiences for Undergraduates (REU) at Texas A&M University-Commerce. Observatories that made research possible include the SARA-S Observatory and TAMUC Observatory.

References

Collaborative Asteroid Lightcurve Link (CALL): Potential Lightcurve Targets. *http://www.minorplanet.info/PHP/call_OppLCDBQuery.php*

Diffraction Limited Maxim DL - Astronomy and Scientific Imaging Software. *https://diffractionlimited.com/product/maxim-dl/*

Durech, J.; Tonry, J.; Erasmus, N.; Denneau, L.; Heinze, A.N.; Flewelling, H.; Vanco, R. (2020). "Asteroid models reconstructed from ATLAS photometry." *Astron. Astrophys.* **643**, A59.

Hanus, J.; Broz, M.; Durech, J.; Warner, B.D.; Brinsfield, J.; Durkee, R.; Higgins, D.; Koff, R.A.; Oey, J.; Pilcher, F.; Stephens, R.; Strabla, L.P. Ulisse, Q.; Girelli, R. (2013). "An anisotropic distribution of spin vectors in asteroid families." *Astron. Astrophys.* **559**, A134.

Harris, A.W.; Young, J.W.; Scaltriti, F.; Zappala, V. (1984). "Lightcurves and phase relations of the asteroids 82 Alkmene and 444 Gyptis." *Icarus* **57**, 251-258.

JPL (2023). Small Body Database Search Engine. *http://ssd.jpl.nasa.gov/sbdb_query.cgi*

Klinglesmith III, D.A.; Hanowell, J.; Risley, E.; Turk, J.; Vargas, A.; Warren, C.A. (2013). "Inversion Model Candidates." *Minor Planet Bull.* **40**, 190-193.

Kurtenkov, A.; Teneva, D.; Todorov, L.; Stoyanov, S. (2014). "Rotation Period Determination for 682 Hagar." *Minor Planet Bull.* **41**, 36.

Macias, A.A. (2015). "Asteroid Lightcurve Analysis at Isaac Aznar Observatory, Aras de Los Olmos, Valencia Spain." *Minor Planet Bull.* **42**, 4-6.

Polakis, T. (2020). "Photometric Observations of Ten Minor Planets." *Minor Planet Bull.* **47**, 13-17.

Stephens, R.D.; Warner, B.D. (2019). "Asteroids Observed from CS3: 2018 July - September." *Minor Planet Bull.* **46**, 66-71.

Warner, B.D. (2011). MPO Canopus software. Version 10.3.0.0. Bdw Publishing. *http://www.minorplanetobserver.com/*

Waszczak, A.; Chang, C.-K.; Ofeck, E.O.; Laher, R.; Masci, F.; Levitan, D.; Surace, J.; Cheng, Y.-Ch.; Ip, W.-H.; Kinoshita, D.; Helou, G.; Prince, T.A.; Kulkarini, S. (2015). "Asteroid Light Curves from the Palomar Transient Factory Survey: Rotation Periods and Phase Functions from Sparse Photometry." *Astron. J.* **150**, 75-109.

Yeh, T.-S.; Li, B.; Chang, C.-K.; Zhao, H.-B.; Ji, J.-H.; Lin, Z.-Y.; Ip, W.-H. (2020). "The Asteroid Rotation Period Survey Using the China Near-Earth Object Survey Telescope (CNEOST)." *Astron. J.* **160**, id. 73.

THE ROTATION PERIOD OF 717 WISIBADA COULD NOT BE FOUND

Frederick Pilcher
Organ Mesa Observatory (G50)
4438 Organ Mesa Loop
Las Cruces, NM 88011 USA
fpilcher35@gmail.com

Jesús Delgado Casal
Observatorio Nuevos Horizontales (Z73)
Calle Hermanos Quintero 17
Camas (Sevilla - Spain) CP 41900

(Received: 2023 October 26 Revised: 2023 November 9)

For 29 sessions including more than 200 hours of photometry of 717 Wisibada by the two authors, no magnitude variations not attributable to instrumental error or catalog errors of calibration star magnitudes could be found. We find $V - R = 0.42$ and in the V band $H = 11.19$, $G = 0.26$.

The observations by Pilcher to produce the results reported in this paper were made at the Organ Mesa Observatory with a Meade 35-cm LX200 GPS Schmidt-Cassegrain, SBIG STL-1001E CCD, 60 to 120 second exposures, unguided, clear filter. Observations by Delgado are with an 11-inch Celestron Schmidt-Cassegrain, Atik 4.14 EX CCD, 60 to 120 second exposures.

Image measurement and lightcurve construction were with *MPO Canopus* software with calibration star magnitudes for solar colored stars from the CMC15 catalog reduced to the Cousins R band. To reduce the number of data points on the lightcurves and make them easier to read, data points have been binned in sets of 3 with maximum time difference 5 minutes.

717 Wisibada. Minor planet 717 Wisibada achieved a brightest magnitude of 13.7 at its 2023 October opposition. Despite its brightness, no previous photometric data were found in the Lightcurve Data Base (Warner et al., 2009). This absence suggested that 717 Wisibada would be a very difficult object, with other observers failing to obtain meaningful data and not publishing. What an enormous understatement this turned out to be!

The two authors obtained more than 200 hours of photometric data in 29 sessions between 2023 Aug. 29 at phase angle 21° to 2023 Oct. 19 at phase angle 1°. Variations on some but not all individual sessions, as well as from one session to another, exceeded the scatter in data points. No repeatable pattern attributed to any rotational variation of the target asteroid could be found. Most of the magnitude variations can be attributed to instrumental errors and catalog errors of calibration star magnitudes. We present several sample raw lightcurves showing data obtained over a short time interval of a few days. The complete data set has been uploaded to *www.ALCDEF.org* with sharing allowed. The reader is invited to download these data and make his own investigation.

Number	Name	yyyy/mm/dd	Phase	L_{PAB}	B_{PAB}	Period(h)	P.E	Amp	A.E.
717	Wisibada	2023/08/30-2023/10/19	20.9 - 0.9	24.2	1.2	NA	NA	NA	NA

Table I. Observing circumstances and results. The phase angle is given for the first and last date, unless a minimum (second value) was reached. L_{PAB} and B_{PAB} are the approximate phase angle bisector longitude and latitude at mid-date range (see Harris et al., 1984).

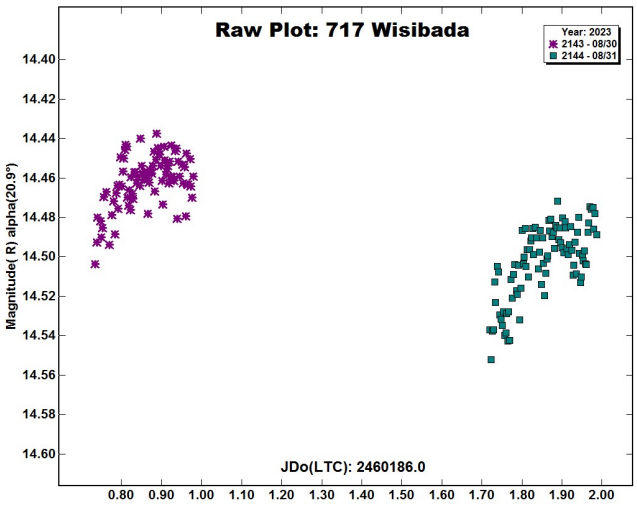
Raw Plot: 717 Wisibada
Year: 2023
2143 - 08/30
2144 - 08/31
Magnitude(R) alpha(20.9°)
JDo(LTC): 2460186.0

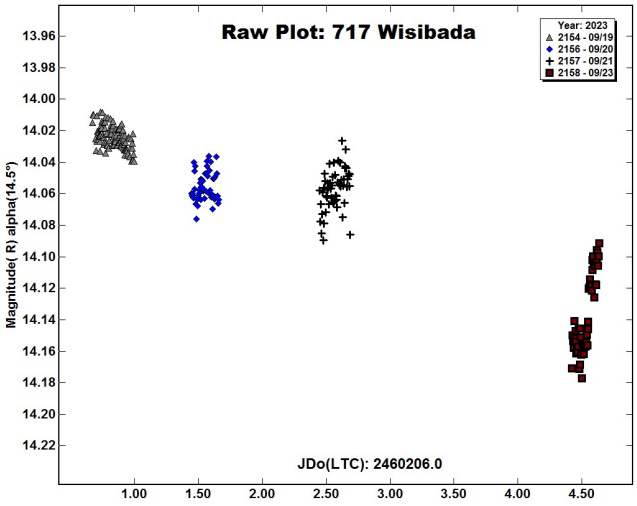
Raw Plot: 717 Wisibada
Year: 2023
2154 - 09/19
2156 - 09/20
2157 - 09/21
2158 - 09/23
Magnitude(R) alpha(14.5°)
JDo(LTC): 2460206.0

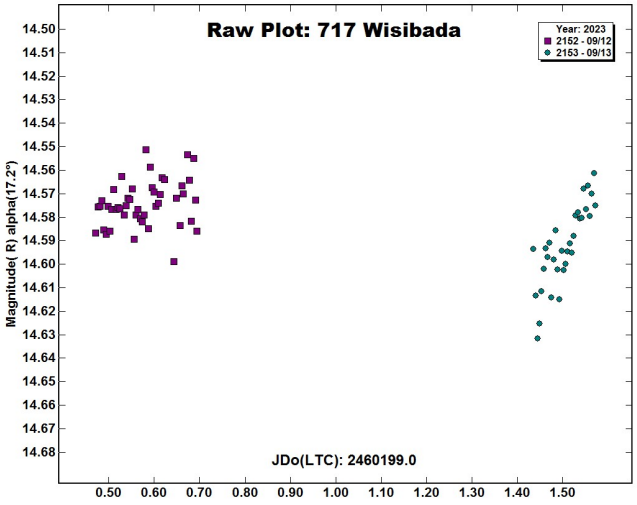
Raw Plot: 717 Wisibada
Year: 2023
2152 - 09/12
2153 - 09/13
Magnitude(R) alpha(17.2°)
JDo(LTC): 2460199.0

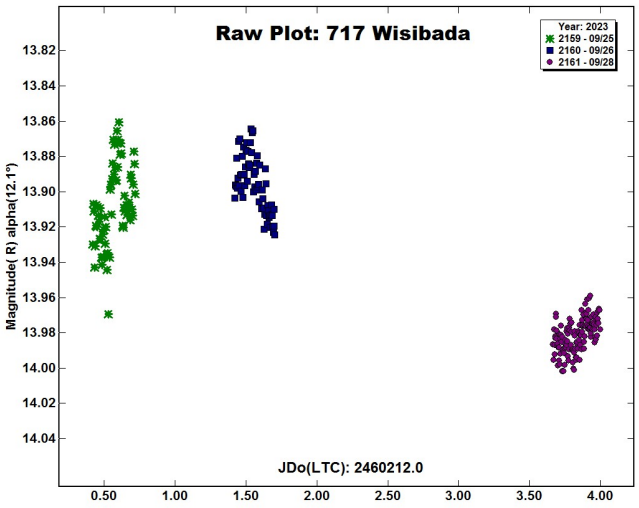
Raw Plot: 717 Wisibada
Year: 2023
2159 - 09/25
2160 - 09/26
2161 - 09/28
Magnitude(R) alpha(12.1°)
JDo(LTC): 2460212.0

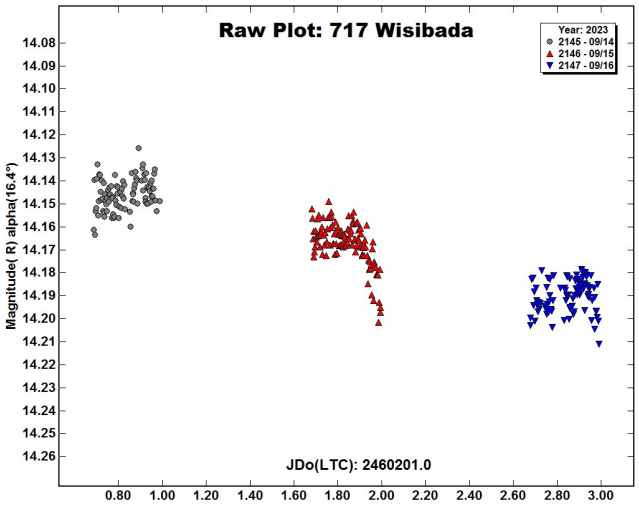
Raw Plot: 717 Wisibada
Year: 2023
2145 - 09/14
2146 - 09/15
2147 - 09/16
Magnitude(R) alpha(16.4°)
JDo(LTC): 2460201.0

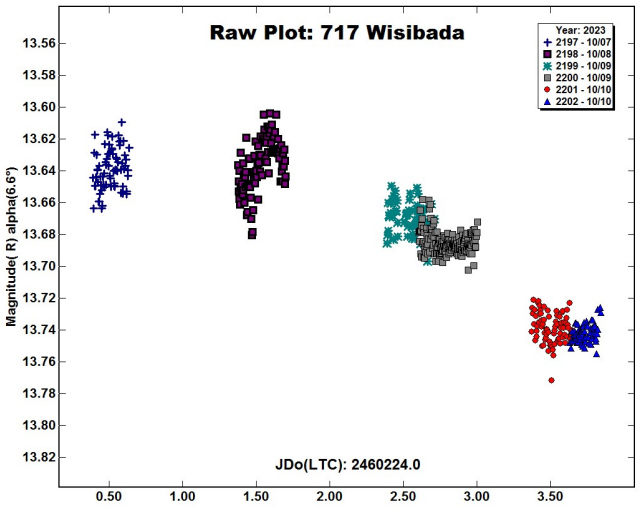
Raw Plot: 717 Wisibada
Year: 2023
2197 - 10/07
2198 - 10/08
2199 - 10/09
2200 - 10/09
2201 - 10/10
2202 - 10/10
Magnitude(R) alpha(6.6°)
JDo(LTC): 2460224.0

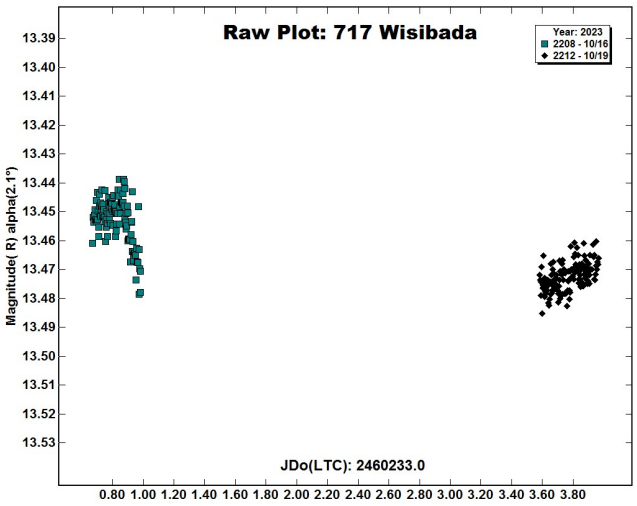

Petr Pravec kindly examined all of our data and concludes:

Indeed, it is a tough case for its low amplitude (most of the time) and probably a long-ish period. It would be needed to get homogeneous data taken with a single camera+filter combination and absolutely calibrated with a high accuracy, resulting in a consistency of the data over all nights on a level of a 0.02 mag or so. Unless you can get such highly homogeneous data, I'm afraid that the case cannot be solved.

On 2023 Oct. 12, twenty images were obtained alternately with the *R* and *V* filters. Both image sets were measured with the same calibration stars. The method of extracting their *R* and *V* colors is explained in Pilcher et al. (2016). The composite lightcurve shows that *V* - *R* = 0.42. The calibrated R magnitudes found for each session were converted to *V* magnitudes by adding 0.42. An *H* - *G* plot in the *V* band shows that *H* = 11.187 ± 0.031, *G* = 0.260 ± 0.040.

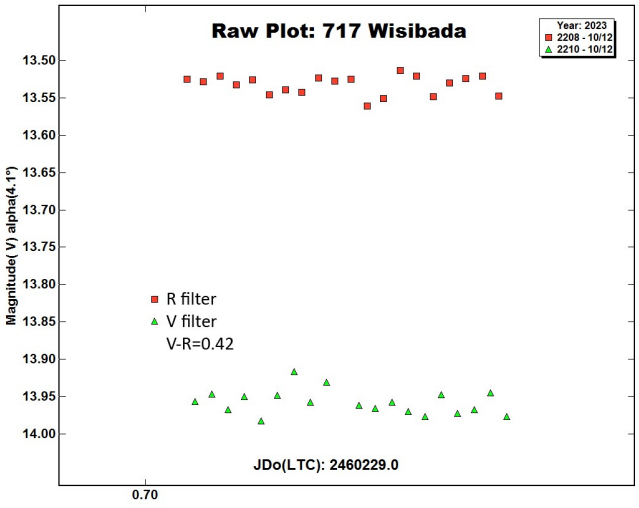

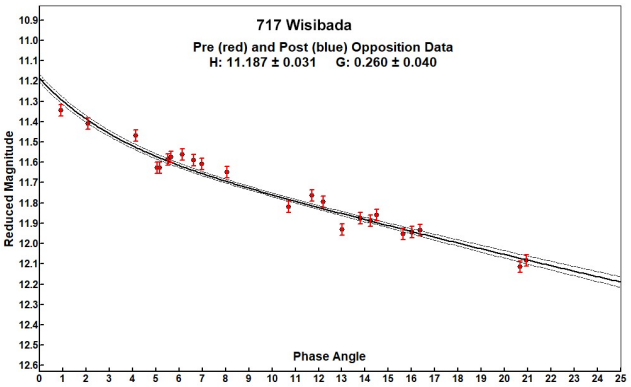

Acknowledgments

The authors thank Lorenzo Franco for preparing the *H* - *G* diagram and Petr Pravec for his independent analysis of our data.

References

Harris, A.W.; Young, J.W.; Scaltriti, F.; Zappala, V. (1984). "Lightcurves and phase relations of the asteroids 82 Alkmene and 444 Gyptis." *Icarus* **57**, 251-258.

Pilcher, F.; Benishek, V.; Klinglesmith, D.A. (2016). "Rotation period, color indices, and H-G parameters for 49 Pales." *Minor Planet Bull.* **43**, 182-183.

Warner, B.D.; Harris, A.W.; Pravec, P. (2009). "The Asteroid Lightcurve Database." *Icarus* **202**, 134-146. Updated 2023 April. *http://www.minorplanet.info/lightcurvedatabase.html*

CALL FOR OBSERVATIONS

Frederick Pilcher
4438 Organ Mesa Loop
Las Cruces, NM 88011 USA
fpilcher35@gmail.com

(Received: 2024 January 9)

Observers who have made visual, photographic, or CCD measurements of positions of minor planets in calendar 2023 are encouraged to report them to this author on or before 2024 April 15. This will be the deadline for receipt of reports which can be included in the "General Report of Position Observations for 2023," to be published in *MPB* Vol. 51, No. 3.

LIGHTCURVE AND ROTATION PERIOD OF 358 APOLLONIA

Frederick Pilcher
Organ Mesa Observatory (G50)
4438 Organ Mesa Loop
Las Cruces, NM 88011 USA
fpilcher35@gmail.com

Jesús Delgado Casal
Observatorio Nuevos Horizontes (Z73)
Calle Hermanos Quintero 17
Camas (Sevilla - Spain) CP 41900

(Received: 2023 December 6)

For 358 Apollonia we find a synodic rotation period of 25.304 ± 0.002 hours, amplitude 0.16 ± 0.02 magnitudes, and an irregular lightcurve for our observations near celestial longitude 65 degrees.

The observations by Pilcher to produce the results reported in this paper were made at the Organ Mesa Observatory with a Meade 35 cm LX200 GPS Schmidt-Cassegrain, SBIG STL-1001E CCD, 60 to 120 second exposures, unguided, clear filter. Observations by Delgado are with an 11-inch Celestron Schmidt-Cassegrain, Atik 4.14 EX CCD, 60 to 120 second exposures.

Image measurement and lightcurve construction were with *MPO Canopus* software with calibration star magnitudes for solar colored stars from the CMC15 catalog reduced to the Cousins *R* band. To reduce the number of data points on the lightcurves and make them easier to read, data points have been binned in sets of 3 with maximum time difference 5 minutes.

358 Apollonia. The Asteroid Lightcurve Database (Warner et al., 2009) lists two previous rotation period determinations. Buchheim (2009) published a synodic period of 50.6 hours, amplitude 0.12 magnitudes, with a symmetrical but nonuniform lightcurve that looks as if it could be phased to half of that period with a comparably good fit. Durech et al. (2020) published a sidereal period of 25.3108 hours.

New observations obtained on 12 nights 2023 Oct. 20 - Dec. 5 provide an excellent fit to an irregular lightcurve with synodic period 25.304 ± 0.002 hours and amplitude 0.16 ± 0.02 magnitudes. A split halves plot shows that the entire 50.611-hour double period was sampled and that the two halves are identical within observational error and reasonable lightcurve shape change between phase angles 17.1° and 3.0°. The double period is ruled out and a period of 25.304 hours may be considered secure. This period is consistent with Durech et al. (2020) and with Buchheim (2009) if his lightcurve data are rephased to 25.3 hours.

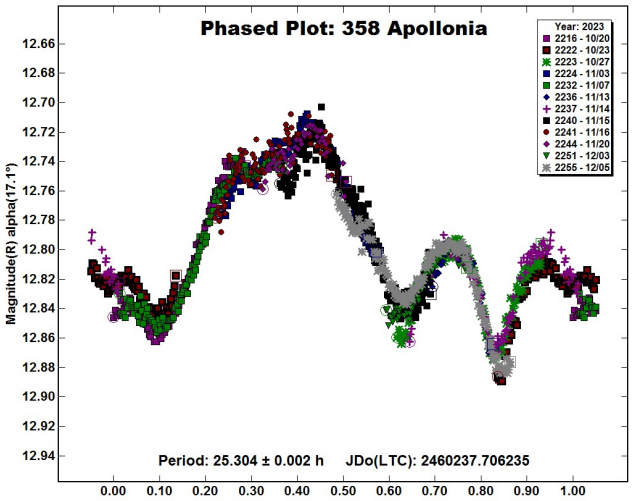

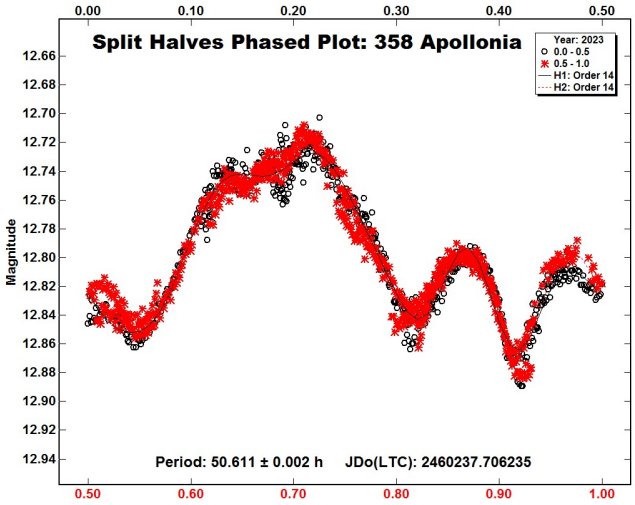

References

Buchheim, R.K. (2009). "Lightcurves of asteroids 358 Apollonia, 734 Benda, and 8356 Wadhwa." *Minor Planet Bull.* **36**, 84-85.

Durech, J.; Tonry, J.; Erasmus, N.; Denneau, L.; Heinze, A.N.; Flewelling, H.; Vančo, R. (2020). "Asteroid models reconstructed from ATLAS photometry." *Astron. Astrophys.* **643**, A59.

Harris, A.W.; Young, J.W.; Scaltriti, F.; Zappala, V. (1984). "Lightcurves and phase relations of the asteroids 82 Alkmene and 444 Gyptis." *Icarus* **57**, 251-258.

Warner, B. D.; Harris, A.W.; Pravec, P. (2009). "The Asteroid Lightcurve Database." *Icarus* **202**, 134-146. Updated 2023 June. *http://www.minorplanet.info/lightcurvedatabase.html*

Number	Name	yyyy/mm/dd	Phase	L_{PAB}	B_{PAB}	Period(h)	P.E	Amp	A.E.
358	Apollonia	2023/10/20-2023/12/05	*17.1 - 3.0	65.5	-4.3	25.304	0.002	0.16	0.02

Table I. Observing circumstances and results. The phase angle is given for the first and last date. Preceded by an asterisk indicates the phase angle reached a minimum during the period. L_{PAB} and B_{PAB} are the approximate phase angle bisector longitude and latitude at mid-date range (see Harris et al., 1984).

LIGHTCURVE ANALYSIS OF 1485 ISA

Rafael González Farfán (Z55)
Observatorio Uraniborg
Écija (Sevilla, SPAIN)
uraniborg16@gmail.com

Francisco J. Benarque Fonseca
Observatorio Ras Algethi (Y91)
Ronda (Málaga, SPAIN)

Esteban Fernández Mañanes (Y90)
Noelia Graciá Ribes
Observatorio Estelia
Ladines (Asturias, SPAIN)

Received: (2023 November 7)

We report on our observations and data analysis of the asteroid 1485 Isa, finding a period of 35.601 ± 0.020 hours, and an amplitude of 0.50 ± 0.03 magnitudes.

All observations reported here were unfiltered, except those that we took from Calar Alto Observatory, Almería, Spain (R-Cousins filter). The images were calibrated in the standard way (bias, darks and flats). Images were measured, and periods analysis were done using *FotoDif* (2021), *Tycho Traker* (2022), and *Periodos* (2020) packages. All data were light-time corrected. The results are summarized below.

Our studies on 1485 Isa began at the end of 2023 September and were extended into October and November. We used amateur telescopes of between 0.25-m to 0.30-m, and the 1.23-m telescope of the Calar Alto observatory, in Almería, thanks to the participation in a project of the Europlanet network, whose objective was to determine the period and lightcurve of this asteroid.

1485 Isa is an asteroid orbiting between Mars and Jupiter in the main portion of the asteroid belt. It orbits the sun every 1920 days (5.26 years), coming as close as 2.67 au and reaching as far as 3.39 AU from the sun. Isa is about 17.34 kilometers in diameter. Its absolute magnitude is 11.92, and 0.117 is its albedo. The asteroid was discovered on 1938 July 28, by Karl Wilhelm Reinmuth at Heidelberg. We found no previously reported rotation period, lightcurve, or 3-D model.

Due to its relatively small size, telescopes with a certain aperture (0.25-m and larger) along with good night skies with little light pollution and good seeing were necessary to monitor and study the asteroid. In addition to our own observations, we decided to submit an observing project to the Europlanet network to use the 1.23-m telescope of the Calar Alto observatory (Almería, Spain) on the nights of 2023 October 23 to 26.

In total, eleven reports were obtained from three different observatories between 2023 September 28 (phase angle 16.9º, elongation 125.5º) and November 6 (phase angle 5.5º, elongation 164.2º). We obtained 1409 points for our lightcurves. Most of our data were uploaded to ALCDEF and MPC sites. The analysis of the data obtained allowed us to deduce a rotation period of 35.601 ± 0.020 hours, and an amplitude of 0.50 ± 0.03 magnitudes.

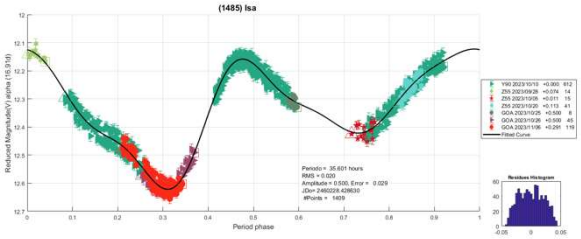

Acknowledgments

Europlanet 2024 RI received funding from the European Union's Horizon 2020 research and innovation program under grant agreement No 871149. This paper is based on observations collected at the Centro Astronómico Hispano en Andalucía (CAHA) at Calar Alto, operated jointly by Junta de Andalucía and Consejo Superior de Investigaciones Científicas (IAA-CSIC). Thanks to all CAHA staff, and specially the support astronomer Ana Guijarro and Ignacio Vico.

References

ALCDEF (2022). Asteroid Lightcurve Data Exchange Format web site. *https://alcdef.org/*

Calar Alto Observatory (CAHA). *https://www.caha.es/*

Europlanet. *https://www.europlanet-society.org/*

FotoDif (2021). *http://astrosurf.com/orodeno/fotodif/index.htm*

Minor Planet Center. *https://minorplanetcenter.net/*

Periodos (2020).
http://www.astrosurf.com/salvador/Programas.html

Tycho Traker (2022). *https://www.tycho-tracker.com/*

Number	Asteroid	20yy mm/dd	Phase	Period(h)	P.E.	Amp	A.E.
1485	Isa	23/09/28-23/11/06	16.9-05.5	35.601	0.020	0.500	0.029

Table I. Observing circumstances and results. Phase is the solar phase angle given at the start and end of the date range. If preceded by an asterisk, the phase angle reached an extrema during the period.

SPIN-SHAPE MODEL FOR 357 NININA

Lorenzo Franco
Balzaretto Observatory (A81), Rome, ITALY
lor_franco@libero.it

Frederick Pilcher
Organ Mesa Observatory (G50)
4438 Organ Mesa Loop
Las Cruces, NM 88011 USA

Julian Oey
Blue Mountains Observatory (Q68)
94 Rawson Pde. Leura, NSW, AUSTRALIA

Alessandro Marchini, Riccardo Papini
Astronomical Observatory, University of Siena (K54)
Via Roma 56, 53100 - Siena, ITALY

Giulio Scarfi
Iota Scorpii Observatory (K78), La Spezia, ITALY

Marco Iozzi
HOB Astronomical Observatory (L63)
Capraia Fiorentina, ITALY

Nello Ruocco
Osservatorio Astronomico Nastro Verde (C82)
Sorrento, ITALY

Paolo Bacci, Martina Maestripieri
GAMP - San Marcello Pistoiese (104), Pistoia, ITALY

Nico Montigiani, Massimiliano Mannucci
Osservatorio Astronomico Margherita Hack (A57)
Florence, ITALY

(Received: 2023 November 28)

We present a shape and spin axis model for main-belt asteroid 357 Ninina. The model was achieved with the lightcurve inversion process, using combined dense photometric data acquired from five apparitions between 2007-2023 and sparse data from USNO Flagstaff. Analysis of the resulting data found a sidereal period P = 35.9840 ± 0.0005 hours and two mirrored pole solutions at (λ = 49°, β = 0°) and (λ = 230°, β = 36°) with an uncertainty of ± 10 degrees.

The minor planet 357 Ninina was observed by the authors for five oppositions from 2007 to 2023 and, to improve the coverage at various aspect angles, we also used the sparse data from USNO Flagstaff Station, according Durech et al. (2009). Most of the dense data were downloaded from ALCDEF (ALCDEF, 2021) and sparse data from the Asteroids Dynamic Site (AstDyS-2, 2020).

The observational details of the dense data used are reported in Table I with the reference, the mid-date, number of the lightcurves used for the inversion process, longitude and latitude of phase angle bisector (LPAB, BPAB). The dense data points were binned in sets of 5 with maximum time difference 5 minutes, in order to reduce the overall processing time. The PAB longitude/latitude distribution of the dense and sparse data are shown on Figure 1, while Figure 2 shows the phase curve obtained with the sparse data.

#	Reference	Mid-date	# LC	LPAB	BPAB
1	Oey (2014)	2007-07-27	8	310	3
2	Oey (2008) (*)	2008-10-10	3	39	18
3	Oey (2014)	2013-09-15	17	343	-9
4	Pilcher (2021)	2021-01-10	16	112	-8
5	Pilcher (2023)	2023-05-30	18	251	17

Table I. Observational details for the dense data used in the lightcurve inversion process for 357 Ninina.
(*) Item 2 published only on 'alcdef.org' web site.

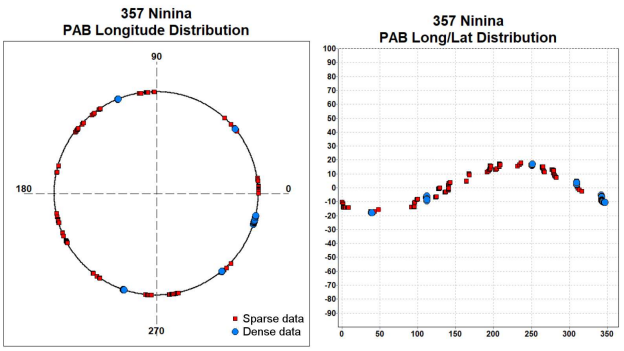

Figure 1: PAB longitude/latitude distribution for the dense and sparse data used in the lightcurve inversion process.

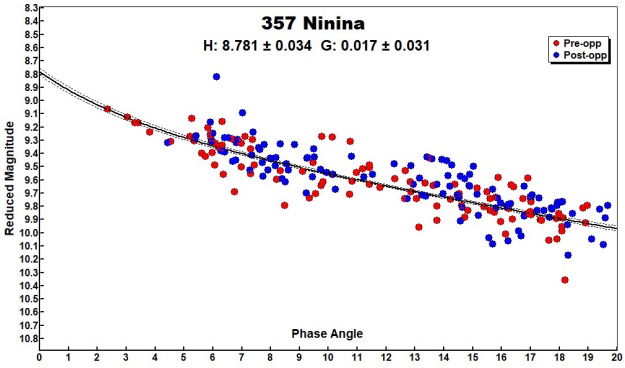

Figure 2: Phase curve obtained from sparse data (reduced magnitude vs phase angle).

Lightcurve inversion was performed using MPO LCInvert v.11.8.4.1 (MPO LCInvert, 2022). For a description of the modeling process see LCInvert Operating Instructions Manual, Durech et al. (2010); and references therein.

In the analysis the processing weighting factor was set, according the data quality of the single dataset, to: 1.0 [#4, #5]; 0.9 [#1, #3]; 0.4 [#2] for dense data and 0.3 for sparse data. The "dark facet" weighting factor was set to 0.5 to keep the dark facet area below 1% of total area and the number of iterations was set to 50.

In lightcurve inversion work, the most critical step is to find an accurate sidereal rotation period. An inaccurate sidereal period can lead to completely incorrect results, regarding the spin axis and the model.

The period search scan was started around 3-sigma interval centered on the average of the synodic periods relative to the dense data used for the inversion process. We found one well isolated sidereal period with a Chi-Sq below to the 9% limit for P=35.9842 h (Figure 3).

In order to verify this result, we plotted the observed synodic periods versus daily change rate of the phase angle bisector longitude (Figure 4). In this plot the intercept of the regression line with the stationary point (ΔPABL/day=0) represents the sidereal period. We found a value of the intercept (35.9814 ± 0.0105 h), consistent with the sidereal period found through the period search scan step (35.9842 h.) and this positive verification reassures us for the subsequent pole searching step. Moreover, the increasing trend of the regression line suggest a prograde rotation.

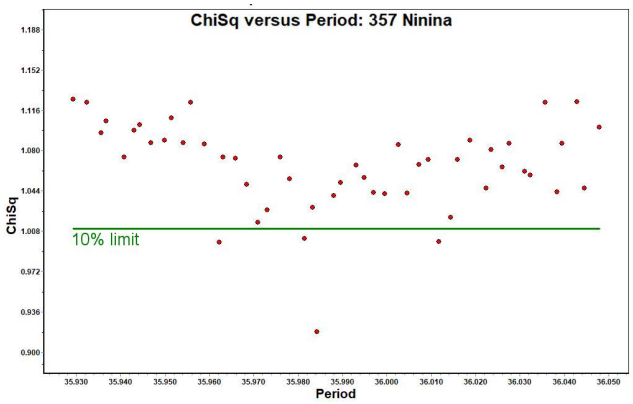

Figure 3: The period scan for 357 Ninina shows one isolated sidereal period with a Chi-Sq below to the 9% limit for P=35.9842 h.

Date (from-to)	PAB_L/day	Syn Period (h)	Period Err (h)
2007-07-13 – 2007-08-11	-0.00395	35.9640	0.0100
2013-07-24 – 2013-11-14	0.07205	36.0105	0.0001
2020-12-07 – 2021-02-13	0.01360	35.9840	0.0010
2023-05-03 – 2023-06-26	-0.00055	36.0000	0.0100

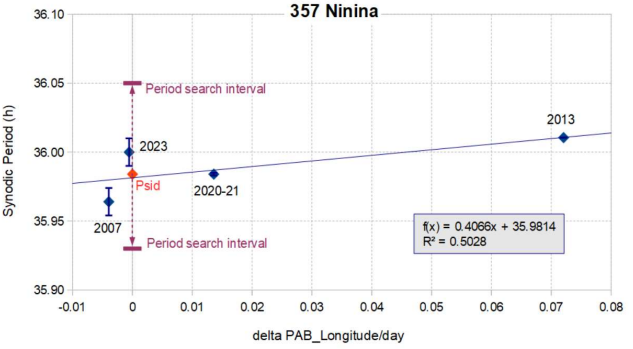

Figure 4: The observed synodic periods versus daily change rate of the phase angle bisector longitude. The synodic period was recalculated for the 2007 data and it is a bit different from published one. The two horizontal bars indicate the interval used for the period search scan. The intercept of the stationary point (ΔPABL/day=0) with the regression line at 35.9814 ± 0.0105 h is consistent with the sidereal period (35.9842 h) found from the period scan step (red point). The increasing trend suggest a prograde rotation.

The pole search was started using the "medium" search option (312 fixed pole position with 15° longitude-latitude steps) and the previously found sidereal period set to "float". From this step we found two roughly mirrored solution with lower Chi-Sq (Figure 5) separated by 180° in longitude, close to ecliptic longitude-latitude pairs (45°, 0°) and (225°, 30°).

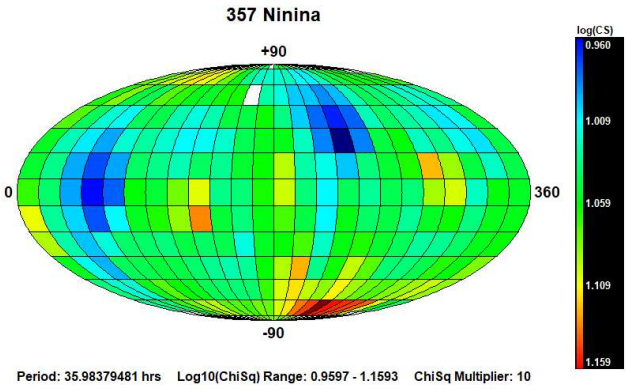

Figure 5: Pole distribution produced by the "medium" search option. The dark blue region indicates the smallest Chi-Sq value while the dark red region indicates the largest. The two roughly mirrored pole solution are approximately centered close to (45°, 0°) and (225°, 30°) with a radius of 30°.

For best focusing the position of the two pole solutions, a "fine" search option (with 49 fixed pole steps with 10° longitude-latitude pairs set to "float") was started with radius of ± 30° on the approximate pole positions found previously. The analysis shows two clustered solutions within 10° of radius that had Chi-Sq values within 10% of the lowest value, approximately centered at ecliptic longitude-latitude (50°, 3°) and (228°, 35°) (Figure 6).

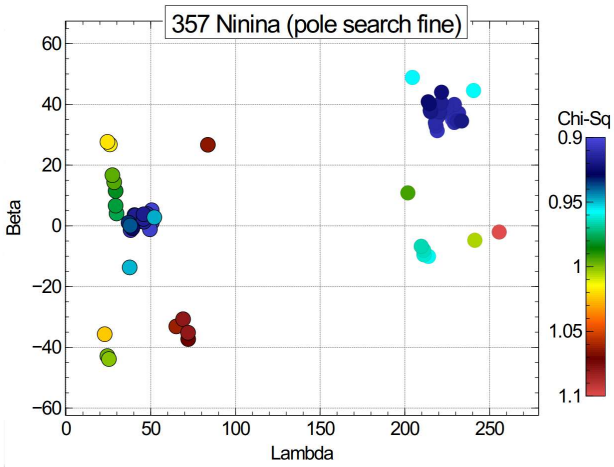

Figure 6: The "fine" pole search shows two clustered solutions (dark blue color) approximately centered near ecliptic longitude-latitude pairs (50°, 3°) and (228°, 35°) with a radius of 10° and Chi-Sq values within 10% of the lowest value.

Moreover, we used the option "none" for refining the two mirrored pole solutions and the relative sidereal periods, found with the previous search option. The two refined solutions are reported in Table II with some statistical data. The reported sidereal period was obtained by averaging the values found into this last step. Typical errors in the pole solution are ± 10° and the uncertainty in sidereal period has been evaluated as a rotational error of 20° over the total time span of the dense data set. We prefer the prograde solution (230°, 36°), consistent with the increasing trend of the regression line on the plot of the synodic periods vs daily change rate PABL.

λ °	β °	Sidereal Period (hours)	RMS	a/b ratio	Ratio of Moments	Angle Phi°
49	0	35.9840 ± 0.0005	0.0187	1.040	1.0010	+5.8
230	36		0.0188	1.031	1.0003	+2.6

Table II. The two refined spin axis solutions for 357 Ninina (ecliptic coordinates) with an uncertainty of ± 10 degrees. The sidereal period was the average of the two solutions found in the pole search process.

Figure 7 shows the shape model while Figure 8 shows the fit between the model (black line) and some observed lightcurves (red points). The fit appears to be good in relation to the very low amplitude of the lightcurves (< 0.12 mag) and the poor quality of some data.

Finally, to check the reliability of the obtained model, we carried out positively some of the tests [1, 4, 5, 6, 8] proposed by Durech et al. (2016) in the section 2.6.

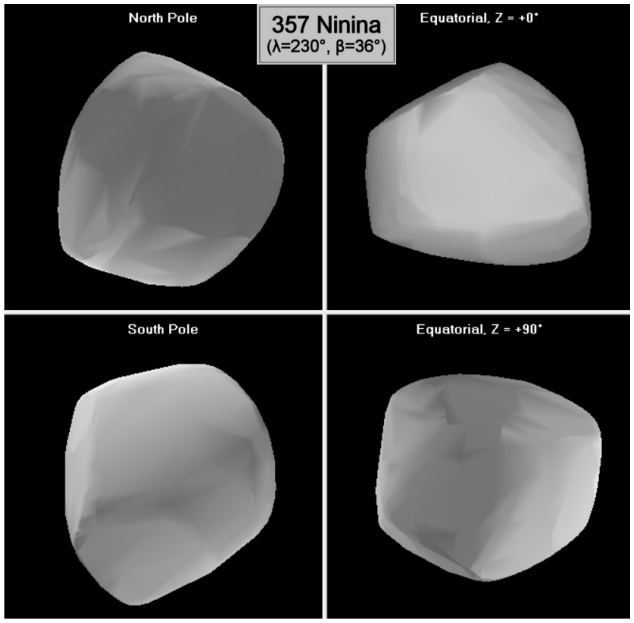

Figure 7: The shape model for 357 Ninina (λ = 230°, β = 36°).

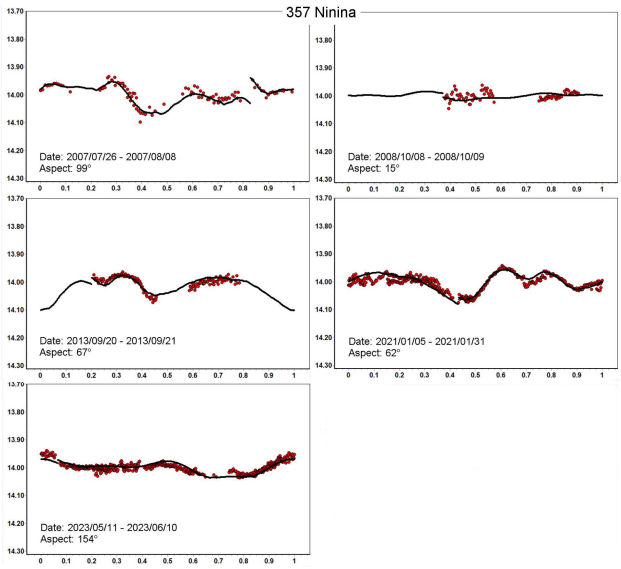

Figure 8: Model fit (black line) versus observed lightcurves (red points) for (λ = 230°, β = 36°) solution.

References

ALCDEF (2021). Asteroid Lightcurve Data Exchange Format web site. *http://www.alcdef.org/*

AstDyS-2 (2020), Asteroids - Dynamic Site. *https://newton.spacedys.com/astdys/*

Durech, J.; Kaasalainen, M.; Warner, B.D.; Fauerbach, M.; Marks, S.A.; Fauvaud, S.; Fauvaud, M.; Vugnon, J.-M.; Pilcher, F.; Bernasconi, L.; Behrend, R. (2009) "Asteroid models from combined sparse and dense photometric data." *A&A* **493**, 291-297.

Durech, J.; Sidorin, V.; Kaasalainen, M. (2010). "DAMIT: a database of asteroid models." *A&A* **513**, A46.

Durech, J.; Hanus, J.; Oszkiewicz, D.; Vanco, R. (2016). "Asteroid models from Lowell photometric database." *A&A* **587**, A48, 1-6.

MPO LCInvert (2022). *https://minplanobs.org/BdwPub/php/mpolcinvert.php*

Oey, J. (2014). "Lightcurve Analysis of Asteroids from Blue Mountains Observatory in 2013." *Minor Planet Bulletin* **41**, 276-281.

Pilcher, F.; Franco, L.; Marchini, A.; Oey, J. (2021). "357 Ninina and 748 Simeisa - Two Asteroids with Earth Commensurate Rotation Periods." *Minor Planet Bulletin* **48**, 233-235.

Pilcher, F.; Franco, L.; Marchini, A.; Papini, R.; Scarfi, G.; Iozzi, M.; Ruocco, N.; Bacci, P.; Maestripieri, M.; Montigiani, N.; Mannucci, M. (2023). "A New Lightcurve of 357 Ninina." *Minor Planet Bulletin* **50**, 255-256.

A PHOTOMETRIC INVESTIGATION OF 526 JENA

Frederick Pilcher
Organ Mesa Observatory (G50)
4438 Organ Mesa Loop
Las Cruces, NM 88011 USA
fpilcher35@gmail.com

Lorenzo Franco
Balzaretto Observatory (A81), Rome, ITALY

Pietro Aceti, Massimo Banfi
Seveso Observatory (C24), Seveso, ITALY

Giorgio Baj
M57 Observatory (K38), Saltrio, ITALY

Alessandro Marchini
Astronomical Observatory, University of Siena (K54)
Via Roma 56, 53100 - Siena, ITALY

(Received: 2023 November 20)

We find for 526 Jena a synodic rotation period 11.877 ± 0.001 h; amplitude 0.25 ± 0.02 mag; color index *V* - *R* = 0.37; and in the *V* band *H* = 10.07, *G*=0.10.

Earlier published rotation periods of 526 Jena suggested a period slightly less than 2/5 of the Earth's rotation period: Barucci et al. (1994), 9.474 h; Behrend (2008web), 9.48 h; Hamanowa and Hamanowa (2011), 9.479 h. More recently Erasmus et al. (2020) published a period 11.877 hours, slightly less than ½ of the Earth's rotation period, and 5/4 of the earlier published period. All showed moderate amplitude bimodal lightcurves. Ambiguity arose as to whether there were 4 or 5 maxima and minima in a time of about 23.75 hours, slightly less than the Earth's rotation period.

The authors of this paper, widely spaced in longitude in North America and Europe, respectively, agreed to collaborate to obtain full phase coverage of the lightcurve of 526 Jena. An equipment list for all observers is provided in Table II. Image measurement and lightcurve construction were with *MPO Canopus* software with calibration star magnitudes for solar colored stars from the CMC15 catalog reduced to the Cousins R band. Zero-point adjustments of a few ×0.01 magnitude were made for best fit. To reduce the number of data points on the lightcurves and make them easier to read, data points have been binned in sets of 3 with maximum time difference 5 minutes.

Ten sessions 2023 Oct. 7 - Nov. 13 provide a very good fit to a slightly asymmetric bimodal lightcurve with synodic period 11.877 ± 0.001 hours and amplitude 0.25 ± 0.02 magnitudes with full phase coverage. The period spectrum between 5 hours and 25 hours shows that a period near 9.48 hours can be definitively ruled out. This new result agrees with Erasmus et al. (2020).

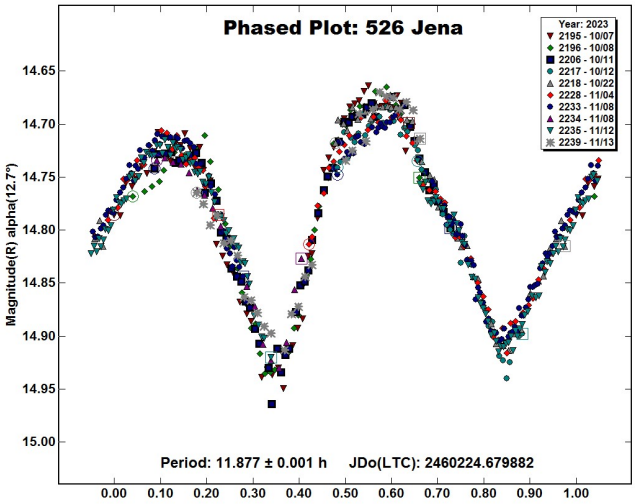

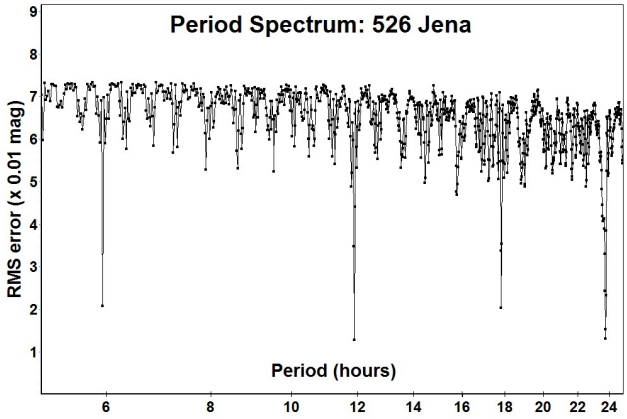

On 2023 Nov. 13, P. Aceti and M. Banfi obtained alternating data points in the *V* and *R* filters that show *V* - *R* = 0.37 ± 0.03. This value is within the usual range 0.38 ± 0.05 for asteroids with C-type taxonomic classifications (Shevchenko and Lupishko, 1998).

Number	Name	2023/mm/dd	Phase	LPAB	BPAB	Period(h)	P.E	Amp	A.E.
526	Jena	10/07-11/13	12.7, 1.1	50	-3	11.877	0.001	0.25	0.02

Table I. Observing circumstances and results. The phase angle is given for the first and last date, except that a * denotes a minimum was reached between these dates. LPAB and BPAB are the approximate phase angle bisector longitude and latitude at mid-date range (see Harris et al., 1984).

Observatory (MPC code)	Telescope	CCD	Filter
Organ Mesa Observatory (G50)	0.35-m SCT f/10	SBIG STL-1001E	C
Seveso Observatory (C24)	0.30-m SCT f/10	QSI KAF 8300 (bin 3×3)	V, R_c
M57 (K38)	0.35-m RCT f/5.5	SBIG STT1603ME	R_c
Astronomical Observatory, University of Siena (K54)	0.30-m MCT f/5.6	SBIG STL-6303e(bin 2×2)	C

Table II. Observing Instrumentations. MCT: Maksutov-Cassegrain, RCT: Ritchey-Chretien, SCT: Schmidt-Cassegrain.

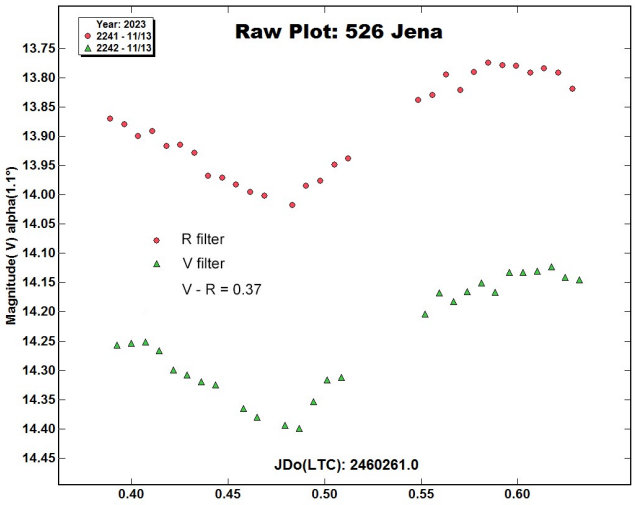

We also present an *H* - *G* plot in the *V* magnitude system for phase angles from 12.7° down to 1.1°. We find $H = 10.07 \pm 0.04$ and $G = 0.10 \pm 0.05$. For this plot the *R* band magnitudes were converted to *V* band, adding the color index *V* - *R* and evaluating, for each lightcurve, the half peak-to-peak magnitudes.

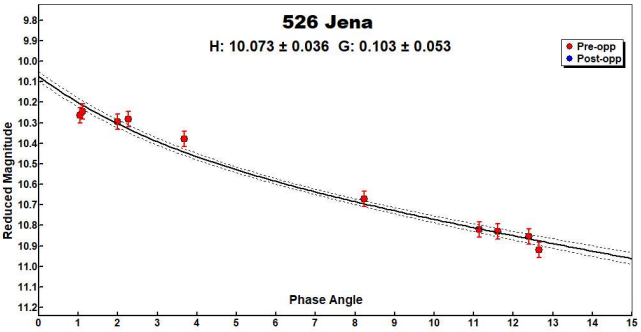

References

Barucci, M.A.; di Martino, M.; Dotto, E.; Fulchignoni, M.; Rotundi, A.; Burchi, R. (1994). "Rotational properties of small asteroids: Photoelectric observations of 16 asteroids." *Icarus* **109**, 267-273.

Behrend, R. (2008web). Observatoire de Geneve web site. *http://obswww.unige.ch/~behrend/page_cou.html*

Erasmus, N.; Navarro-Meza, S.; McNeill, A.; Trilling, D.E.; Sickafoose, A.A.; Denneau, L.; Flewelling, H.; Heinze, A.; Tonry, J.L. (2020). "Investigating taxonomic diversity within asteroid families through ATLAS dual-band photometry." *Ap. J. Suppl. Ser.* **247**, A13.

Hamanowa, H.; Hamanowa, H. (2011). *http://www2.ocn.ne.jp/~hamaten/astlcdata.htm*

Harris, A.W.; Young, J.W.; Scaltriti, F.; Zappala, V. (1984). "Lightcurves and phase relations of the asteroids 82 Alkmene and 444 Gyptis." *Icarus* **57**, 251-258.

Shevchenko, V.G.; Lupishko, D.F. (1998). "Optical properties of Asteroids from Photometric Data." *Solar System Research* **32**, 220-232.

Warner, B.D., Harris, A.W., Pravec, P. (2009). "The Asteroid Lightcurve Database." *Icarus* **202**, 134-146. Updated 2023 June. *https://minplanobs.org/MPInfo/php/lcdb.php*

LIGHTCURVES AND ROTATION PERIODS OF 738 ALAGASTA AND 1011 LAODAMIA, AND A NOTE ON 991 MCDONALDA

Frederick Pilcher
Organ Mesa Observatory (G50)
4438 Organ Mesa Loop
Las Cruces, NM 88011 USA
fpilcher35@gmail.com

(Received: 2024 January 11)

Synodic rotation periods and amplitudes are found for 738 Alagasta 17.882 ± 0.002 hours, 0.06 ± 0.01 magnitudes; 1011 Laodamia 5.1722 ± 0.0001 hours, 0.43 ± 0.02 magnitudes. The period of 991 McDonalda was not found and may be long.

The new observations to produce the results reported in this paper were made at the Organ Mesa Observatory with a Meade 35 cm LX200 GPS Schmidt-Cassegrain, SBIG STL-1001E CCD, 60 to 120 second exposures, unguided, clear filter. Image measurement and lightcurve construction were with *MPO Canopus* software with calibration star magnitudes for solar colored stars from the CMC15 catalog reduced to the Cousins R band. Zero-point adjustments of a few ×0.01 magnitude were made for best fit. To reduce the number of data points on the lightcurves and make them easier to read, data points have been binned in sets of 3 with maximum time difference 5 minutes.

738 Alagasta. Previously published rotation periods for 738 Alagasta are by Sada et al. (2005), 17.83 hours; Behrend (2009web), >12 hours; Garcerán et al. (2016), 18.86 hours; Polakis (2020), 17.89 hours. New observations on 9 nights 2023 Dec. 6 to 2024 Jan. 11 provide a good fit to an irregular lightcurve with period 17.882 ± 0.002 hours, amplitude 0.06 ± 0.01 magnitudes. The split halves plot of the double period 35.763 hours shows close overlap of both halves of the plot and rules out the double period. The period found by this study is consistent with Sada et al. (2005) and Polakis. (2020), but not with Garcerán et al. (2016).

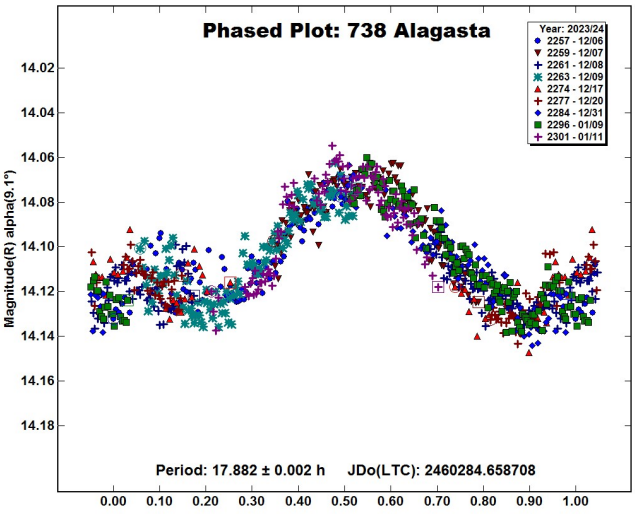

Number	Name	yyyy/mm/dd	Phase	L_{PAB}	B_{PAB}	Period(h)	P.E	Amp	A.E.
738	Alagasta	2023/12/06-2024/01/11	* 9.1 - 4.9	98	- 2	17.882	0.002	0.06	0.01
991	McDonalda	2023/12/04	3.7	82	1	----	----	>0.06	----
1011	Laodamia	2023/12/11-2024/01/10	6.0 - 20.0	82	- 6	5.1722	0.0001	0.43	0.02

Table I. Observing circumstances and results. The phase angle is given for the first and last date, unless a minimum (second value) was reached. L_{PAB} and B_{PAB} are the approximate phase angle bisector longitude and latitude at mid-date range (see Harris et al., 1984).

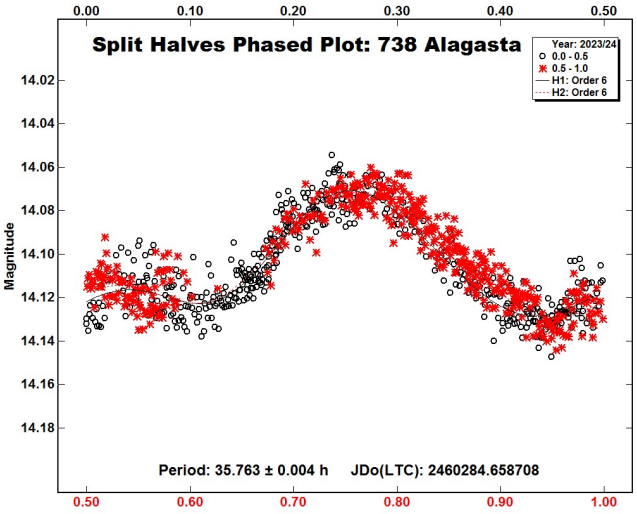

991 McDonalda. The Asteroid Lightcurve Data Base (Warner et al., 2009) lists no published rotation period for 991 McDonalda. probably because this object is very faint. At magnitude 16, the equipment of the Organ Mesa Observatory could have found a reliable rotation period only if the amplitude was fairly large, certainly >0.1 magnitudes, and the period was fairly short. A single ten-hour session on 2023 Dec. 4 showed that this was not the case. From JD 2460282.60 until near JD 2460282.9 the magnitude brightened by 0.06 magnitudes, then faded by 0.03 magnitudes when the session ended at JD 2460283.03. The period is unlikely to be longer than 2 to 4 days. But it was evident after the first session that a very large amount of telescope time would be needed to find a solution that might not be accurate and reliable, and that this telescope time would be more productive if assigned to other targets.

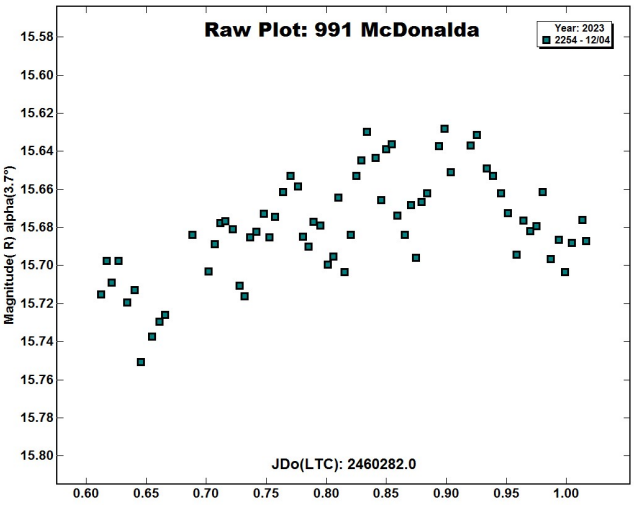

1011 Laodamia. Previously published rotation periods for 1011 Laodamia are by Behrend (2002web), 5.17247 hours; Ivanova et al. (2002), 5.17 hours; Apostolovska (2011), 5.175 hours. New observations on 5 nights 2023 Dec 11 to 2024 Jan 10 provide an excellent fit to a lightcurve with period 5.1722 ± 0.0001 hours, amplitude 0.43 ± 0.02 magnitudes. This result is compatible with other published values.

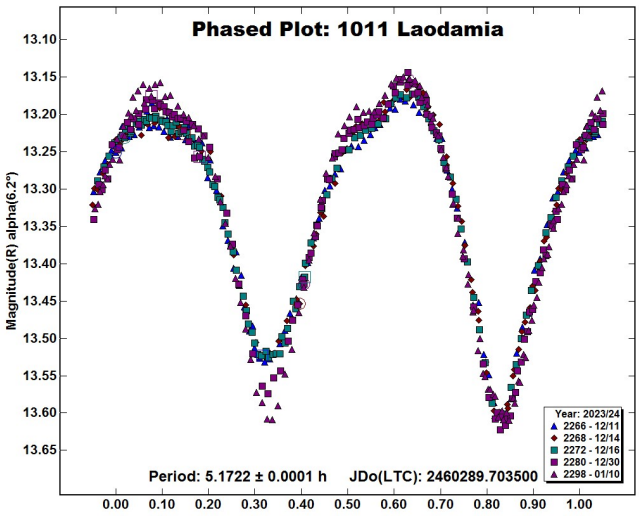

References

Apostolovska, G.; Kostov, A.; Belkina, B.I.; Ivanova, V.G.; Donchev, Z. (2011). "Asteroid Lightcurves for Shape Modeling Obtained at the NAO Rozhen" *Bulgarian J. Phys.* **38**, 325-328.

Behrend, R. (2002web, 2009web). Observatoire de Geneve web site. *http://*obswww.unige.ch/*~behrend/page_cou.html*

Garcerán, A.C.; Aznar, A.; Mansego, E.A.; Rodriguez, P.B.; de Haro, J.L.; Fornas Silva, A.; Fornas Silva, G.; Martinez, V.M.; Chiner, O.R. (2016). "Nineteen asteroids lightcurves at Asteroid Observers (OBAS) - MPPD: 2015 April - Spetember." *Minor Planet Bull.* **43**, 92-97.

Harris, A.W.; Young, J.W.; Scaltriti, F.; Zappala, V. (1984). "Lightcurves and phase relations of the asteroids 82 Alkmene and 444 Gyptis." *Icarus* **57**, 251-258.

Ivanova, V.G.; Apostolovska, G.; Borisov, G.B.; Bilkina, B.I. (2002). "Results from photometric studies of asteroids at Rozhen National Observatory, Bulgaria." *Proceedings of Asteroids, Comets, Meteors - ACM 2002 International Conference*, 29 July - 2 August, Berlin, Germany. Ed. Barbara Warmbein, ESA SP-500. Noordwijk, Netherlands. ESA Publications Division, ISBN 92-9092-810-7, 505-508.

Polakis, T. (2020). "Photometric observations of twenty-seven minor planets." *Minor Planet Bull.* **47**, 314-321.

Sada, P.V.; Canizales, E.D.; Armada, E.M. (2005). "CCD photometry of asteroids 651 Antikleia, 738 Alagasta, and 2151 Hadwiger using a remote commercial telescope." *Minor Planet Bull.* **32**, 73-75.

Warner, B.D.; Harris, A.W.; Pravec, P. (2009). "The Asteroid Lightcurve Database." *Icarus* **202**, 134-146. Updated 2023 Oct. *https://minplanobs.org/MPInfo/php/lcdb.php*

LIGHTCURVE ANALYSIS FOR EIGHT MAIN-BELT ASTEROIDS AND ONE MARS CROSSER

Fernando Huet
Observatorio Polop (Z93)
Apdo. 61 03520 Polop (SPAIN)
fhuet@me.com

Gonzalo Fornas
Centro Astronómico del Alto Turia (J57)
Asociación Valenciana de Astronomía (AVA) SPAIN

Alvaro Fornas
Centro Astronómico del Alto Turia (J57)
Asociación Valenciana de Astronomía (AVA) SPAIN

(Received: 2024 January 9)

Photometric observations of eight main-belt asteroids and one Mars-crosser were obtained from 2023 April 15 to December 30. We derived the following synodic rotational periods: 222 Lucia, 7.8370 ± 0.006 h; 862 Franzia, 7.5235 ± 0.0004 h; 1259 Ogyalla, 17.3000 ± 0.0013 h; 1305 Pongola, 8.0648 ± 0.0015 h; 1308 Halleria, 6.0313 ± 0.0005 h; 1412 Lagrula, 5.9165 ±.0.0008 h; 6025 Naotosato, 27.017 ± 0.004 h; 14835 Holdridge, 16.6717 ± 0.0013 h; and (16591) 1992 SY17, 2.73715 ± 0.00009 h. We also obtained the sidereal rotation period for: 222 Lucia, 7.836690 ± 0.000014 h; 862 Franzia, 7.521938 ± 0.000013 h; 1305 Pongola, 8.063733 ± 0.000015 h; and 6025 Naotosato, 27.02452 ± 0.00019 h.

We report on the photometric analysis result for eight main-belt and one Mars-crossing asteroids. This work was done from Observatorio Polop MPC Z93 (Alicante) operated by members of the Valencian Astronomy Association (AVA) (*http://www.astroava.org*). This database shows graphic results of the data (lightcurves), with the plot phased to a given period.

Observatory	Telescope	CCD
Polop Z93	SC 8"	ASI 2600 MM

Table I. List of instruments used for the observations.

We concentrated on asteroids with no reported period and those where the reported period was poorly established and needed confirmation. We also prioritized those asteroids for which we had dense data collected by our team in previous years in order to attempt finding sidereal periods using *MPO LCInvert* (Bdw Publishing, 2023). All the targets were selected from the Collaborative Asteroid Lightcurve (CALL, 2023) and Minor Planet Center (MPC, 2023) websites. The Asteroid Lightcurve Database (LCDB; Warner et al., 2009) was consulted to locate previously published results.

Images were calibrated in *MaximDL* (Diffraction, 2023) and measured using *MPO Canopus* (Bdw Publishing, 2023) with a differential photometry technique. The comparison stars were restricted to near-solar color to reduce the effects of color dependencies, especially at larger air masses. The lightcurves give the synodic rotation period. The amplitude (peak-to-peak) that is shown is that for the Fourier model curve and not necessarily the true amplitude.

If we found enough data in ALCDEF to add to our ours, we tried finding the sidereal period using *MPO LCInvert* (Bdw Publishing, 2023), which uses the inversion method described by Kaasalainen and Torppa (2001a). This software uses the C code for a routine called "Period Scan" that was written by Ďurech based on the original FORTRAN code written by Kaasalainen (2001). The advantage of this method is that it allows combining *dense* data, such as ours and those in the ALCDEF database (ALCDEF, 2023), with *sparse* data such as those produced by all-sky surveys, e.g., Catalina, USNO, ATLAS, Palomar, etc.

This is an iterative method that starts with an initial estimate based on a known synodic period and scans a range of possible sideral periods to find a *global* minimum of χ^2. The procedure starts with six initial poles for each trial period and selects the period that gives the lowest χ^2. If there is a clear minimum in χ^2 when plotted as a function of the period, the associated period is very likely the correct solution. Getting a clear solution is not always certain. Here, we reference only those asteroids with an apparently valid result.

When using *MPO LCInvert*, we assign weighting coefficients to consider the different densities and quality of the data. A value of 1.0 is assigned to *dense* data and 0.3 to sparse data, which is generally appropriate for higher-quality *sparse* data.

Error estimates for inversion method are not obvious. The smallest separation, ΔP, of the *global* minimum (Kaasalainen et al., 2001b), in the period parameter space is roughly given by

$$\Delta P \approx 0.5 * P^2/\Delta t$$

where Δt is the full epoch range of the data set expressed in the same units as the period. This derives from the fact that the maxima and minima of a double sinusoidal lightcurve for periods P and $P \pm \Delta P$ are at the same epochs after Δt time.

Quoting from Kaasalainen et al. (2001b), "The period error is mostly governed by the epochs of the lightcurves. If the best local χ^2 minimum of the period spectrum is clearly lower than the others, one can obtain an error estimate of, say, a hundredth part of the smallest minimum width ΔP since the edge of a local minimum ravine always lies much higher than its bottom."

Ďurech proposes an estimate of error of

$$\Delta P \approx (1/10 * 0.5) * P^2/\Delta t$$

The factor 1/10 means that the period accuracy is 1/10 of the difference between local minima in the periodogram. When using *MPO LCInvert,* we use Ďurech's formula as error estimate.

It's important to note that the period scan must cover a sufficient range of periods so that a true *global* minimum is found, i.e., the minimum across the entire probable period range. In many cases, there are *local*, less deep minimums. Scanning on too small a range can find one of those *local* minimums and not the true *global* minimum.

222 Lucia. This outer main-belt asteroid belongs to the Themis family. It was discovered by Johann Palisa on 1882 Feb 9 in Vienna and is named after the daughter of Austro-Hungarian explorer Graf Wilczek. Based upon analysis of infrared spectra, it has a diameter of 59.8 ± 0.8 km. From our data we derive a synodic rotation period of 7.8370 ± 0.0002 h and an amplitude of 0.38 mag. This is consistent with Oszkiewicz et al. (2017), who found 7.8371 h.

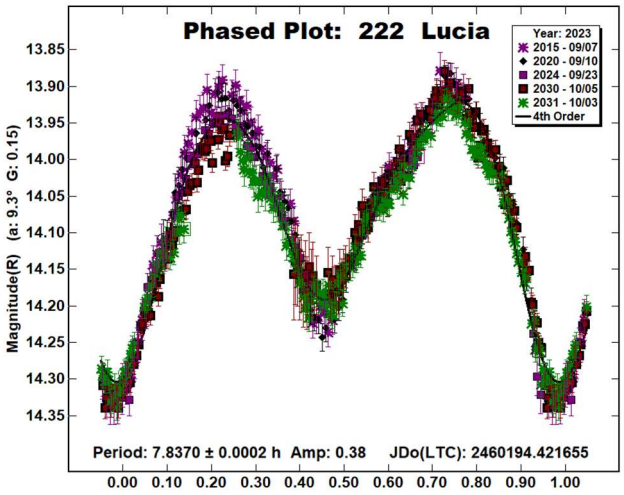

For this asteroid, we had additional *dense* data from our AVA Team obtained in 2016. On ALCDEF we found data from Warner (1999), Stephens (2008), and Oszkiewicz (2016). We also used *sparse* data from Catalina (361 points 2003-2021), Palomar (86 points 2014-2021), USNO (192 points 1998-2010), ATLAS (734 points 2017-2022), and LONEOS (40 points 1999-2008).

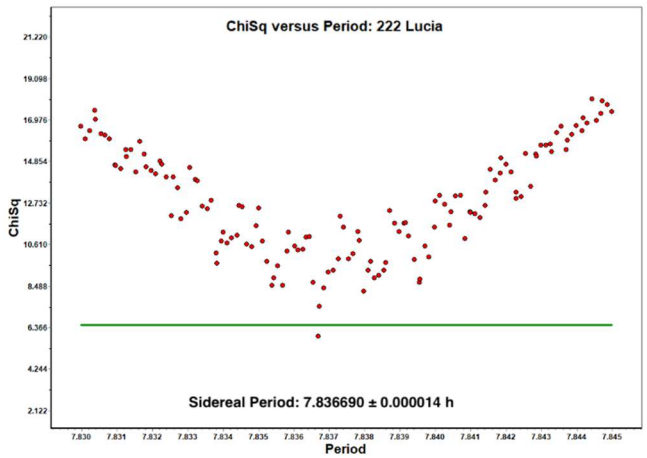

MPO LCInvert found what appears to be a unique sidereal rotation period of 7.836690 ± 0.000014 h. That is consistent with Hanus et al. (2013; 7.83671 h) and Wang et al. (2018; 7.83668 h). The green line represents a level 10% greater than the lowest χ^2.

862 Franzia. This middle main-belt asteroid was discovered on 1917 Jan 28 by M.F. Wolf at Heidelberg. We made observations on 2023 Sep 9 to Oct 11. From our data, the period is ambiguous, it depending on adopting a mono- or bimodal lightcurve. We assume it as bimodal, with a period of 15.0480 ± 0.0009 h and an amplitude of 0.13 mag, but it could be monomodal with a period of 7.5235 ± 0.0004 h.

Both halves of the 15.0480-hour lightcurve of are very similar, which makes the monomodal solution possible, but not certain. In fact, at low amplitudes and phase angles, the true solution may have three or more minimum/maximum pairs (Harris et al., 2014).

Previous results include Behrend (2011web; 2014web, 7.52 h), Behrend (2018web, 7.5236 h). Warner (2005; 15.05 h), Warner (2010, 7.65 h). Aznar Macias et al. (2016, 16.299 h), Ferrero (2020, 7.523 h, and Polakis (2020, 7.52 h).

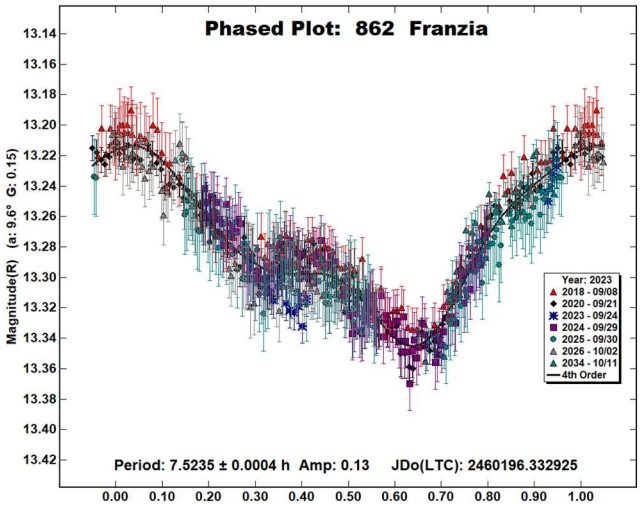

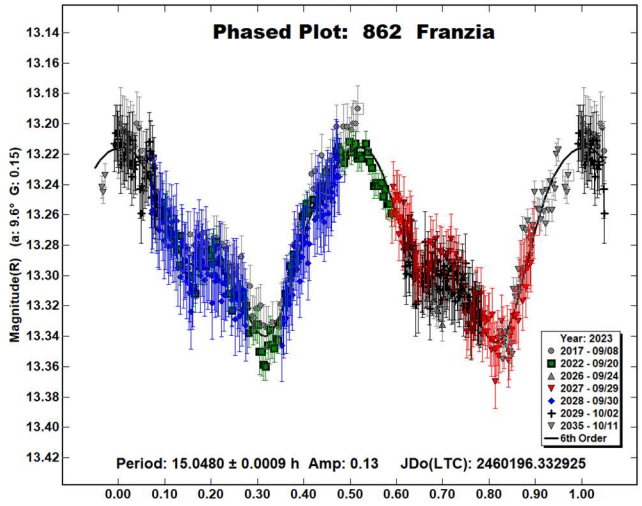

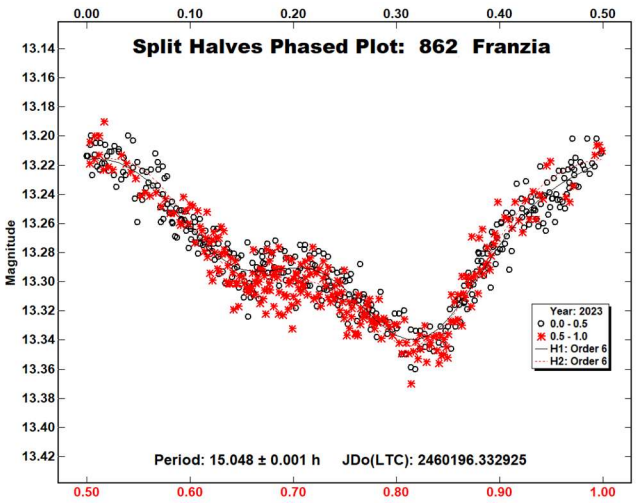

ALCDEF (2023) had *dense* data from Warner (2000; 2004), Brinsfield (2011), Fornas (2016), and Polakis (2020). We added *sparse* data from: USNO (177 points, 1998-2008), Catalina (299 points 2006-2023), ATLAS (841 points, 2017-2023), and Palomar (91 points, 2018-2021). After including our 2023 *dense* data, we tried to get a clear sideral period solution in *MPO LCInvert*.

Unfortunately, the solution was ambiguous with two likely and four not as likely solutions when confining the search to around 7.5 h. The "best" sidereal period there was 7.521938 ± 0.000013 h. When searching around 15.05 h, the best solution was 15.041127 ± 0.000050 h. Both had very similar χ^2 minimums. A search covering 7-16 hours would have taken *much* longer, but it would have shown the possibility of more than one local minimum.

Since they were nearly equal, the *global* minimum was ambiguous. What might favor 7.52 h is that the number of solutions below the 10% χ^2 green line is considerably less than for the longer solution.

In this case, a different, more critical analysis would be warranted, such as that proposed and expanded on by Slivan (2012; 2013; 2014) and Slivan et al. (2023).

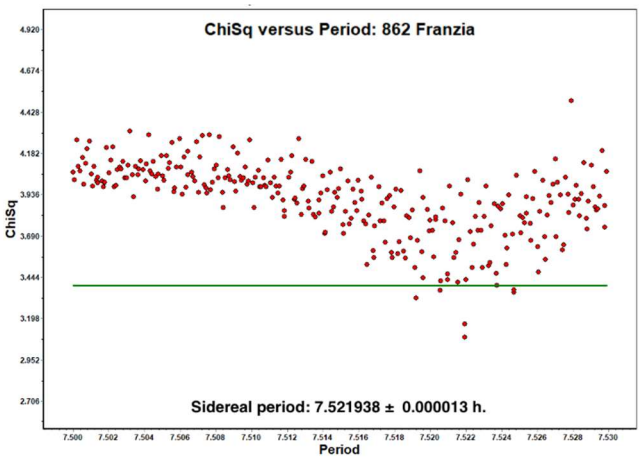

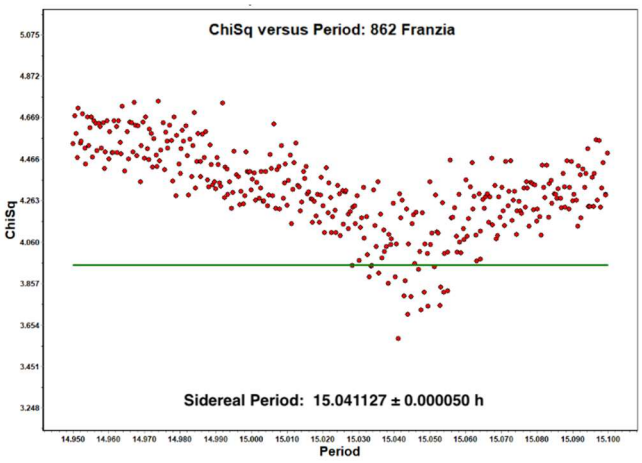

1259 Ogyalla. This outer main-belt asteroid was discovered on 1933 Jan 29 by K. Reinmuth at Heidelberg. We made observations on 2023 Sep 7 to Oct 5. We derived a rotation period of 17.3000 ± 0.0013 h and an amplitude of 0.34 mag. Previous results include Waszczak et al. (2015, 17.304 h), Mansego et al. (2016, 17.334 h) and Erasmus et al. (2020, 17.296 h).

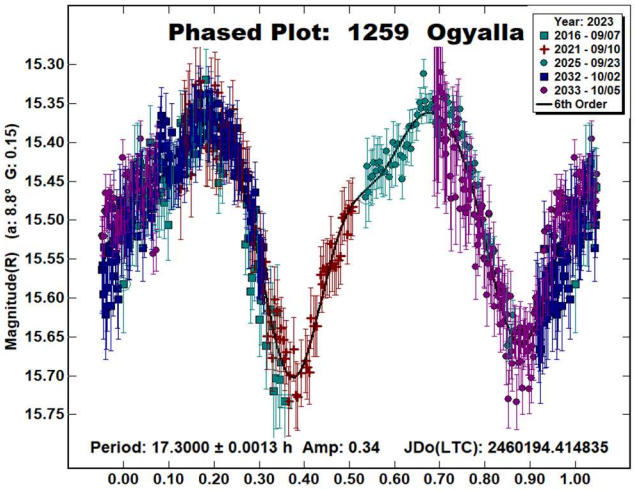

1305 Pongola. This outer main-belt asteroid was discovered on 1928 Jul 16 by H.E. Wood at Johannesburg. We made observations on 2023 Aug 12-30. From our data, we derived a rotation period of 8.0648 ± 0.0015 h and an amplitude of 0.18 mag.

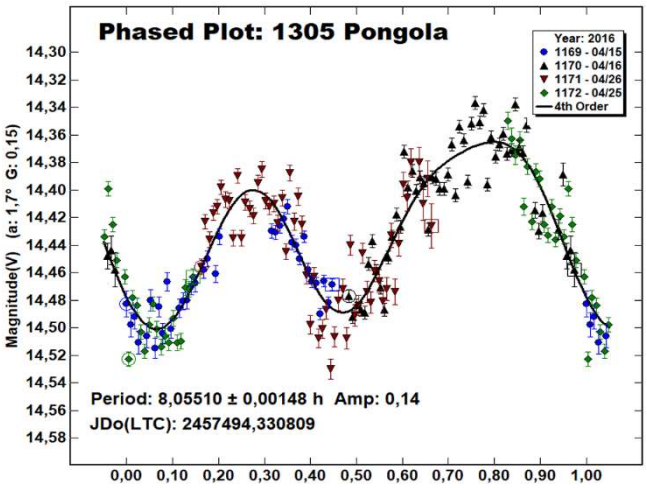

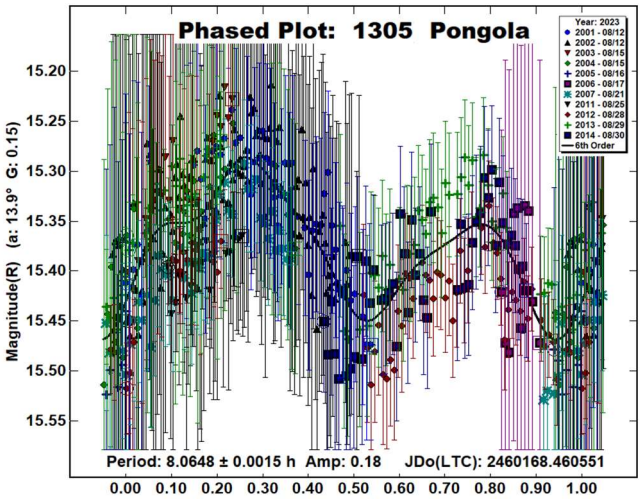

There are several consistent results in the LCDB, among them are Binzel (1987, 8.03 h), Ditteon et al. (2012, 8.06 h), and Sada et al. (2017, 8.0585 h). We re-processed our 2016 data to see they could fit a period similar to ours from the 2023. We were successful, finding 8.055 ± 0.0015 h and amplitude of 0.14 mag.

We downloaded data from the ALCDEF site from Waszczak et al. (2015, *sparse*) and Fornas (2016, *dense*). We also used *sparse* data from Catalina (335 points 2003-2023), Palomar (95 points 2013-2022), USNO (125 points 1998-2008), ATLAS (652 points 2017-2021), and LONEOS (29 points 1999-2007). We used those along with our 2023 *dense* data for a sideral period search using *MPO LCInvert*, which led to P = 8.063733 ± 0.000015 h. The error is based on the data from 1999 to 2023.

Given the number of solutions below the 10% green line, the reported period cannot be considered reliable to any degree.

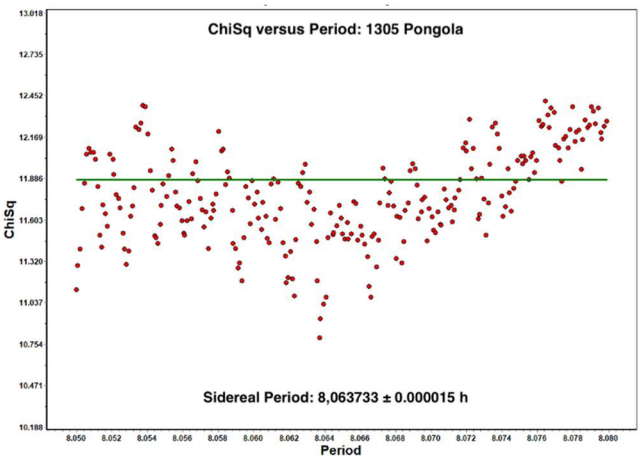

1308 Halleria is a carbonaceous Charis-family asteroid in the outer main-belt and has a diamater of about 43 km. It was discovered on 1931 March 12 by German astronomer Karl Reinmuth at the Heidelberg-Königstuhl State Observatory. We made observations from 2023 December 8-30 and obtained a rotation period of 6.0313 ± 0.0005 h and an amplitude of 0.19 mag.

Previous results include Behrend (2008web, 6.026 h) and Pray (2011web, 6.013 h), which are consistent with our result.

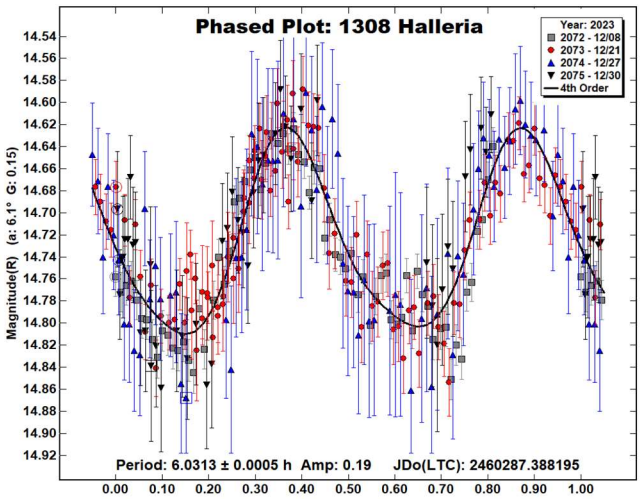

1412 Lagrula. This inner main-belt asteroid was discovered on 1937 January 19 by French astronomer Louis Boyer at the North African Algiers Observatory in Algeria. We made observations from 2023 April 15-21. Our data produced a rotation period of 5.9165 ± 0.0008 h and an amplitude of 0.79 mag. Casalnuovo et al. (2013) found 5.9176 h; team member Aznar et al. (2016) reported 5.882 h; Ďurech et al. (2020) found a sidereal period of 5.917404 h.

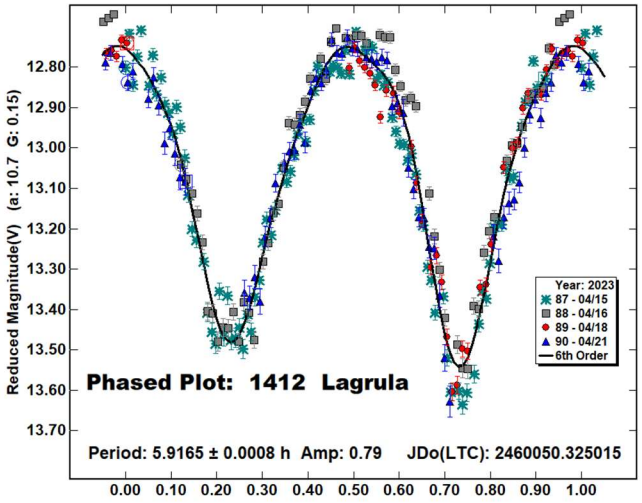

6025 Naotosato. This outer main-belt asteroid was discovered on 1992 Dec 30 by T. Urata at Oohira Observatory, Japan. We made observations from 2022 Aug 15 to Sep 4 (Huet et al., 2023) and found a rotation period of 27.016 h. We had another apparition opportunity in 2023 and repeated the study. Those data led to a rotation period of 27.017 ± 0.004 h and an amplitude of 0.31 mag, The lightcurve has a slightly different shape from our earlier result, as by seen comparing the two.

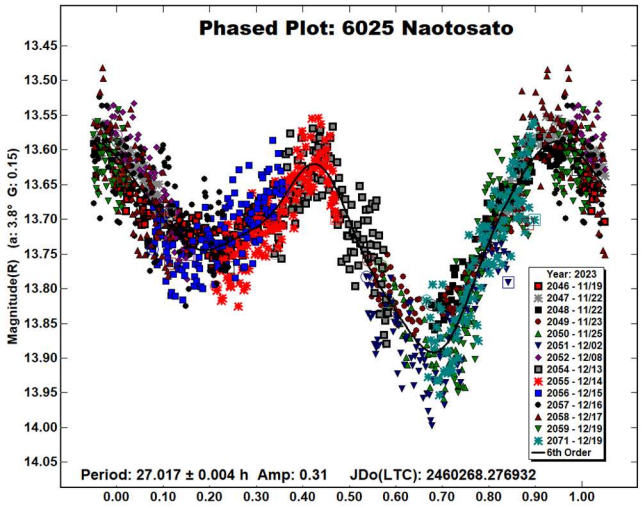

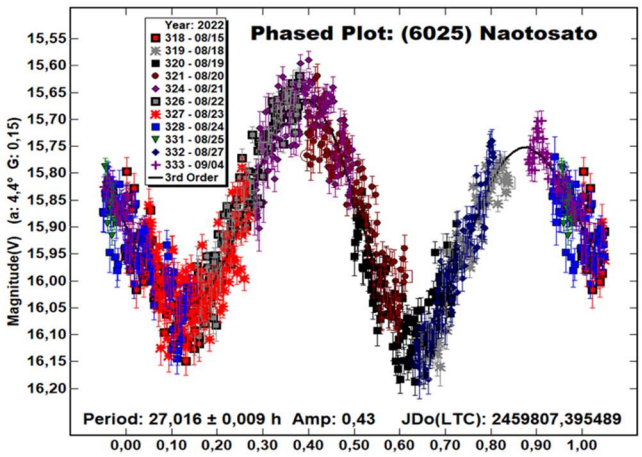

The only dense data in ALCDEF was our own from 2022. We added sparse data from Catalina (282 points, 2003-2023), Palomar (52 points, 2017-2022), USNO (28 points, 2004-2011), ATLAS (839 points, 2021-2023), and LONEOS (28 points 2001-2007). We used those and our two dense data sets from 2022 and 2023 in *MPO LCInvert*. The result was 27.02452 ± 0.00019 h. We used the interval from 2001-2023 to estimate the error.

In the lower graph, we show the χ^2 value as a function of the period; it clearly shows a convergence of the solutions but, with at least five of them below the 10% green line, our result is not certain.

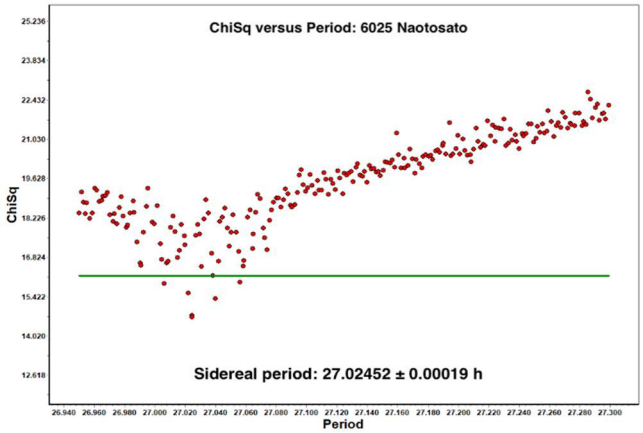

Number	Name	Sidereal Period (h)	P. Error (h)
222	Lucia	7.836690	0.000014
862	Franzia*	7.521938	0.000013
1305	Pongola	8.063733	0.000015
6025	Naotosato	27.02452	0.00019

Table II. Sidereal rotation period obtained from LCINVERT, when available. *Sidereal period corresponding to minimum χ^2.

14835 Holdridge. This main-belt asteroid was discovered on 1987 Nov 26 by C.S. Shoemaker and E.M. Shoemaker at Palomar. We observed this asteroid from 2023 Oct 6 to Nov 17. We found a synodic period of 16.6717 ± 0.0013 h and amplitude of 0.20 mag. This differs considerably from the one by Dose (2023, 164.401 h).

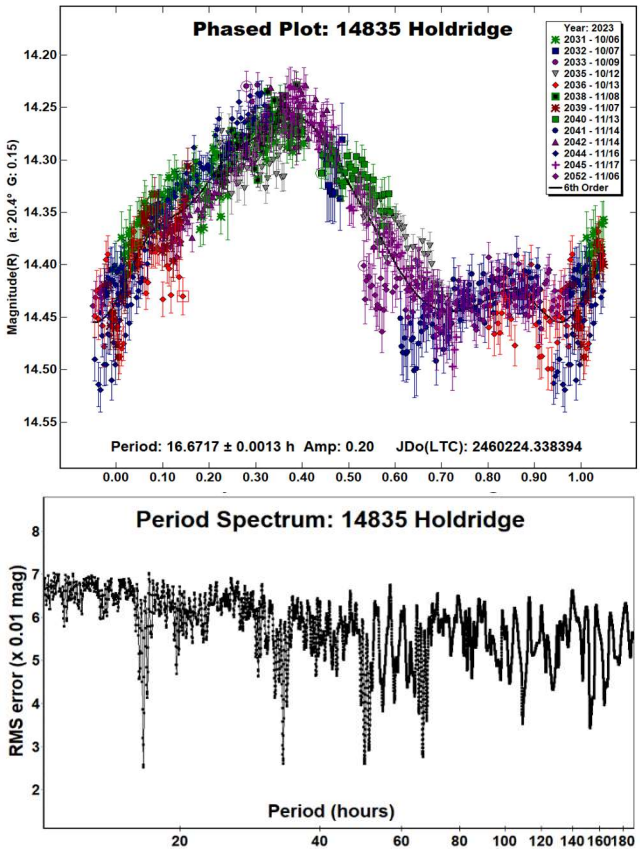

(16591) 1992 SY17. This Marscrosser was discovered on 1992 September 30 by H.E. Holt at Palomar. We made observations from 2023 Jul 29 to Aug 23 to derive a rotation period of 2.73715 ± 0.00009 h and amplitude of 0.15 mag. Pravec et al. (2013web) 2.73728 h.

Number	Name	2023 mm/dd	Phase	L_{PAB}	B_{PAB}	Period(h)	P.E.	Amp	A.E.	Grp
222	Lucia	09/07-10/03	9.0,0.9	9	-2	7.8370	0.0002	0.38	0.02	MB-O
862	Franzia	09/08-10/11	*9.6,10.0	`	16	7.5235	0.0004	0.13	0.01	MB-M
1259	Ogyalla	09/07-10/05	8.5,1.2	9	-2	17.3000	0.0013	0.34	0.02	MB-O
1305	Pongola	04/15-04/26	11.9,13.6	340	-2	8.0648	0.0015	0.18	0.02	MB-O
1308	Halleria	12/08-12/30	6.1,13.2	62	7	6.0313	0.0005	0.19	0.02	MB-O
1412	Lagrula	04/15-04/21	11.1,13.3	185	5	5.9165	0.0008	0.79	0.03	MB-I
6025	Naotosato	11/19-12/19	3.7,10.2	61	7	27.017	0.004	0.31	0.02	MB-I
14835	Holdridge	10/06-11/17	*20.4,15.2	33	15	16.6717	0.0013	0.20	0.01	MB-I
16591	1992 SY17	07/29-08/23	*12.8,16.8	313	14	2.73715	0.00009	0.15	0.01	MC

Table III. Observing circumstances and results. The Phase angle values are for the first and last date. If preceded by an asterisk, the phase angle reached an extrema during the period. L_{PAB} and B_{PAB} are the approximate phase angle bisector longitude and latitude at mid-date range (see Harris et al., 1984). Grp is the asteroid family/group (Warner et al., 2009). ERI: Erigone; EUN: Eunomia; MB-I/O: Main-belt inner/outer; MC: Mars-crosser; NEA: near-Earth; THM: Themis; TRJ: Jupiter Trojan.

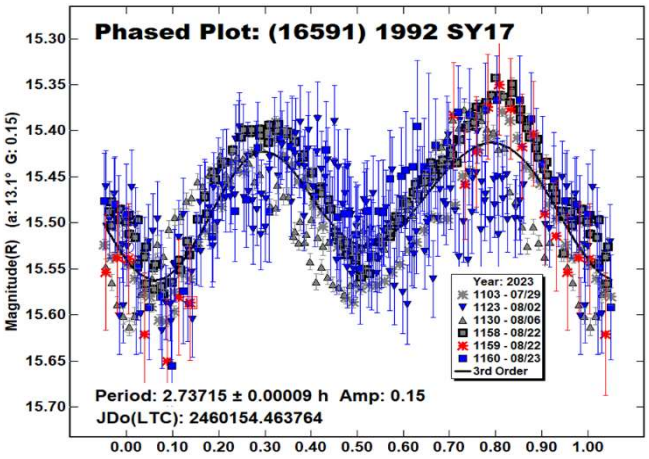

Acknowledgements

We would like to express our gratitude to Brian Warner for supporting the CALL web site and his kind suggestions and interest in asteroid 862 Franzia, and to Gonzalo Fornas, for discovering and helping me use *MPO LCInvert*.

References

ALCDEF (2023). Asteroid Lightcurve Data Exchange Format web site. *https:// alcdef.org*

Aznar Macias, A.; Carreno Garcerain, A.; Arce Masego, E.; Brines Rodriques, P.; Lozano de Haro, J.; Fonas Silva, A.; Fornas Silva, G.; Mas Martinez, V.; Rodrigo Chiner, O.; Herrero Porta, D. (2016). "Twenty-one Asteroid Lightcurves at Group Observadores de Asteroides (OBAS): Late 2015 to Early 2016." *Minor Planet Bull.* **43**, 257-263.

Behrend, R. (2008web; 2011web, 2014web; 2018web). Observatoire de Geneve web site. *http://obswww.unige.ch/~behrend/page_cou.html*

Bdw Publishing (2023). *MPO Canopus* and *MPO LCInvert* software. *https://bdwpublishing.com*

Binzel, R.P. (1987). "A photoelectric survey of 130 asteroids." *Icarus* **72**, 135-208.

CALL (2023). Collaborative Asteroid Lightcurve Link web site. *https://www.minorplanet.info/php/call.php*

Casalnuovo, G.B. (2013). "Lightcurve Photometry, H-G Parameters and Estimated Diameter for 1412 Lagrula." *Minor Planet Bull.* **40**, 188.

Diffraction (2023). *MaximDL* software. *https://www.cyanogen.com/product/maxim-dl/*

Ditteon, R.; Horn, L.; Kamperman, A.; Vorjohan, B.; Kirkpatrick, E. (2012). "Asteroid Lightcurve Analysis at the Oakley Southern Sky Observatory: 2011 April-May." *Minor Planet Bull.* **39**, 26-28.

Ďurech, J.; Tonry, J.; Erasmus, N.; Denneau, L.; Heinze, A.N.; Flewelling, H. Vančo, R. (2020). "Asteroid models reconstructed from ATLAS photometry." *Astron. Astrophys.* **643**, A59.

Dose, E.V. (2023). "Lightcurves of eighteen asteroids." *Minor Planet Bull.* **51**, 42-49.

Erasmus, N.; Navarro-Meza, S.; McNeill, A.; Trilling, D.E.; Sickafoose, A.A.; Denneau, L.; Flewelling, H.; Heinze, A.; Tonry, J.L (2020) "Investigating Taxonomic Diversity within Asteroid Families through ATLAS Dual-band Photometry." *Ap. J. Suppl. Ser.* **247**, A13.

Ferrero, A. (2020). "Photometric Lightcurves of Eight Main-belt Asteroids." *Minor Planet Bull.* **47**, 172-174.

Hanus, J.; Ďurech, J.; Broz, M.; Marciniak, A.; Warner, B.D. and 115 colleagues (2013). "Asteroids' physical models from combined dense and sparse photometry and scaling of the YORP effect by the observed obliquity distribution." *Astron. Astrophys.* **551**, A67.

Harris, A.W.; Young, J.W.; Scaltriti, F.; Zappala, V. (1984). "Lightcurves and phase relations of the asteroids 82 Alkmene and 444 Gyptis." *Icarus* **57(2)**, 251-258.

Harris, A.W.; Pravec, P.; Galad, A.; Skiff, B.A.; Warner, B.D.; Vilagi, J.; Gajdos, S.; Carbognani, A.; Hornoch, K.; Kusnirak, P.; Cooney, W.R.; Gross, J.; Terrell, D.; Higgins, D.; Bowell, E.; Koehn, B.W. (2014). "On the maximum amplitude of harmonics on an asteroid lightcurve." *Icarus* **235**, 55-59.

Huet, F.; Fornas, G.; Fornas, A. (2023). "Lightcurve analysis for Six main-belt asteroids." *Minor Planet Bull.* **50**, 170-172.

Kaasalainen, M. (2001). "Interpretation of lightcurves of precessing Asteroids." *Astron. and Astrophysics* **376**, 302-309.

Kaasalainen, M; Torppa, J. (2001a). "Optimization Methods for Asteroid Lightcurve Inversion. I Shape determination." *Icarus* **143**, 24-36.

Kaasalainen, M; Torppa, J: Muinonen, K. (2001b). "Optimization Methods for Asteroid Lightcurve Inversion. II The complete Inversion Problem." *Icarus* **153**, 37-51.

Mansego, E.A.; Rodriguez, P.B.; de Haro, J.L.; Chiner, O.R.; Silva, A.F.; Porta, D.H.; Martinez, V.M.; Silva, G.F.; Garceran, A.C. (2016). "Eighteen Asteroids Lightcurves at Asteroides Observers (OBAS) - MPPD: 2016 March-May." *Minor Planet Bull.* **43**, 332-336.

MPC (2023). Minor Planet Center web site. *https://www.minorplanetcenter.net/*

Oszkiewicz, D.A.; Skiff, B.A.; Moskovitz, N.; Kankiewicz, P.; Marciniak, A.; Licandro, J.; Galiazzo, M.A.; Zeilinger, W. (2017). "Non-Vestoid candidate asteroids in the inner main belt." *Astron. Astrophys.* **599**, A107.

Polakis, T. (2020). "Photometric Observations of Thirty Minor Planets." *Minor Planet Bull.* **47**, 177-186.

Pravec, P.; Wolf, M.; Sarounova, L. (2013web). *http://www.asu.cas.cz/~ppravec/neo.htm*

Pray, D.P. (2011). *http://www.geocities.com/dppray_2000/*

Sada, P.V.; Olguín, L.; Saucedo, J.C.; Loera-González, P.; Cantú-Sánchez, L.; Garza, J.R.; Ayala-Gómez, S.A.; Avilés, A.; Pérez-Tijerina, E.; Navarro-Meza. S.; Silva, J.S.; Reyes-Ruíz, M.; Segura-Sosas, J.; López-Valdivia, R.; Álvarez-Santana, F.(2017). "Results of the 2016 Mexican Asteroid Photometry Campaign." *Minor Planet Bull.* **44**, 239-242.

Slivan, S.M. (2012). "Epoch Data in Sidereal Period Determination. I. Initial Constraint from Closest Epochs." *Minor Planet Bull.* **39**, 204-206.

Slivan, S.M. (2013). "Epoch Data in Sidereal Period Determination. II. Combining Epochs from Different Apparitions." *Minor Planet Bull.* **40**, 45-48.

Slivan, S.M. (2014). "Sidereal Photometric Astrometry as Efficient Initial Search for Spin Vector." *Minor Planet Bull.* **41**, 282-284.

Slivan, S.M.; McLellan-Cassivi, C.J.; Serra-Ricart, M.; Alarcón, M.R. (2023). "Lightcurve and Constraints on the Spin Vector of Koronis Family Member (1840) Hus: Illustrating Analysis of a Combined Data Set." *Minor Planet Bull.* **50**, 190-193.

Wang, Y.-B.; Xu, Y.; Fan, C.-B.; Liu, C.-Z. (2018). "Study on the spin states of asteroids using a simplistic shape model." *Astron. Nach.* **339**, 457-464.

Warner, B.D. (2005). "Asteroid lightcurve analysis at the Palmer Divide Observatory - Fall 2004" *Minor Planet Bull.* **32**, 29-32.

Warner, B.D. (2010). "Upon Further Review: I. An Examination of Previous Lightcurve Analysis from the Palmer Divide Observatory." *Minor Planet Bull.* **37**, 127-130.

Warner, B.D.; Harris, A.W.; Pravec, P. (2009). "The Asteroid Lightcurve Database." *Icarus* **202**, 134-146. Updated 2021 April. *https://www.minorplanet.info/php/lcdb.php*

Waszczak, A.; Chang, C.-K.; Ofeck, E.O.; Laher, R.; Masci, F.; Levitan, D.; Surace, J.; Cheng, Y.-Ch.; Ip, W.-H.; Kinoshita, D.; Helou, G.; Prince, T.A.; Kulkarini, S. (2015). "Asteroid Light Curves from the Palomar Transient Factory Survey: Rotation Periods and Phase Functions from Sparse Photometry." *Astron. J.* **150**, 75-109.

LIGHTCURVES AND ROTATION PERIODS OF ASTEROIDS 1861 KOMENSKY, 2096 VAINO, 3127 BAGRATION, 3289 MITANI, 3582 CYRANO, 3589 LOYOLA, 3811 KARMA, 4226 DAMIAAN, 4458 OIZUMI, 6086 VRCHLICKY, 6875 GOLGI, (18118) 2000 NB24 AND 29185 REICH

Geoffrey Stone
First Light Observatory Systems
17908 NE 391st St
Amboy, WA 98601 USA
geoff@first-light-systems.com

(Received: 2024 January 14)

We present lightcurves and synodic rotation periods for 1861 Komensky, 2096 Vaino, 3127 Bagration, 3289 Mitani, 3582 Cyrano, 3589 Loyola, 3811 Karma, 4226 Damiaan, 4458 Oizumi, 6086 Vrchlicky, 6875 Golgi, (18118) 2000 NB24 and 29185 Reich observed from 2023 September through 2024 January.

Photometric observation of thirteen asteroids was conducted from 2023 September through 2024 January at Dimension Point Observatory (MPC V42) located near Mayhill, NM.

Images were acquired using a 0.43-m *f*/6.8 Corrected Dall-Kirkham telescope and FLI Kepler KL400 back-illuminated CMOS camera on a PlaneWave Instruments L-500 direct-drive mount. The equipment was operated remotely using *ACP Expert* (Denny, 2023) and *MaximDL* (George et al., 2021). Orbital elements, ephemeris and other information were obtained from the Minor Planet Center (*http://www.minorplanet.net*) the JPL Solar System Dynamics (*http://ssd.jpl.nasa.gov*) and the Lowell Observatory Minor Planet Services (*http://asteroid.lowell.edu*) websites.

Images were made unfiltered in HDR mode, utilizing camera internal stacking every 30 seconds. Exposure duration varied based on the target brightness and apparent motion but were typically 120 seconds.

Image calibration, plate solving, measurement and period analysis were performed using *Tycho-Tracker* V11.0 (Parrott, 2023). Comparison stars of near solar color were chosen from the ATLAS refcat2 star catalog (Tonry et al., 2018) using the comparison star selection feature of *Tycho-Tracker*.

1861 Komensky is an outer main-belt asteroid discovered in 1970 by L. Kohoutek at Bergedorf. We observed in on ten nights in 2023 November through 2024 January resulting in a total of 561 observations. A search of the LCDB found no reported rotation periods. Analysis of the data resulted in a best fit period of 61.8341±0.009925 hours with an amplitude of 0.639±0.06 mag. Coverage is incomplete so this result could be wrong.

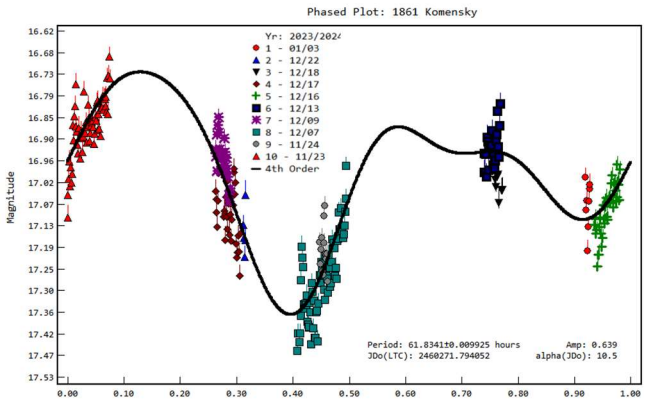

2096 Vaino is an inner main-belt asteroid discovered in 1939 by Y. Vaisala at Turku. It is named for Vainamoinen, an old and wise magician in Finnish folklore. The name also honors Vaino Vaisala, brother of the discoverer. We observed Vaino on nine nights in 2023 September and October resulting in a total of 614 observations. A search of the LCDB resulted in four reports. Mainzer et. al. (2011) and Waszczak et. al. (2015) reported 3.32 hours. Fauerbach and Fauerbach (2019) reported 5.55 and 3.70 hours. Our analysis resulted in a period of 3.3228±0.000425 hours with an amplitude of 0.104±0.02 mag, in close agreement with Mainzer and Waszczak.

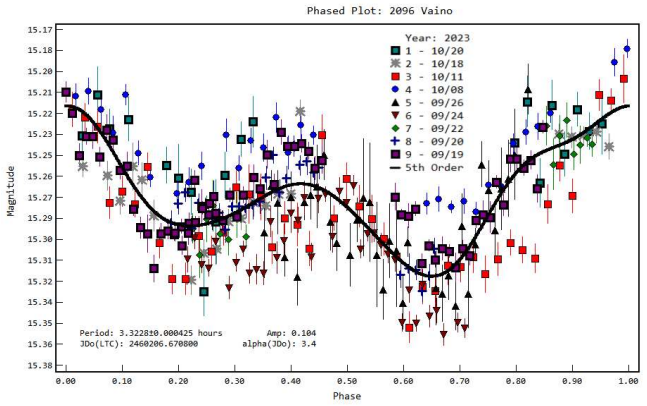

3127 Bagration is a middle main-belt asteroid discovered in 1973 by L. Chernykh at Nauchnyj. We observed it on eight nights resulting in 768 observations. A search of the LCDB resulted in two reports by Behrend in 2015 and 2019 showing >12 hours and >16 hours respectively. There were no references given to the reports themselves. Analysis of the data resulted in a period of 23.4816±0.001925 hours with an amplitude of 0.237±0.02 mag. Coverage of the cycle was incomplete so this result could be wrong. The period spectrum indicates this result is close to the correct value.

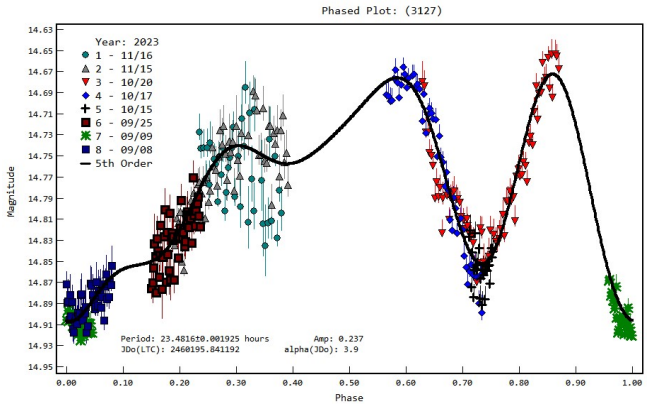

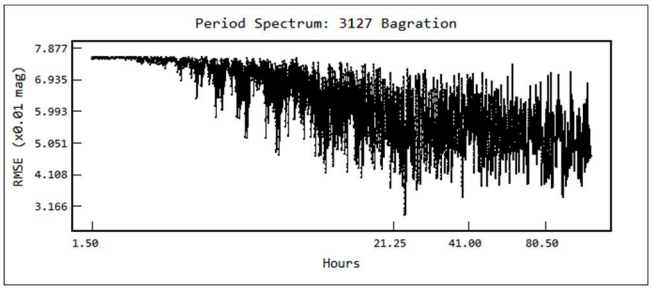

3289 Mitani is an inner main-belt asteroid discovered in 1934 by K. Reinmuth, at Heidelberg. We observed it on nine nights in 2023 November through 2024 January resulting in a total of 577 observations. A search of the LCDB showed no prior rotation period reports. Analysis of the data resulted in a best fit period of 7.822±0.002425 hours with an amplitude of 0.218±0.03 mag.

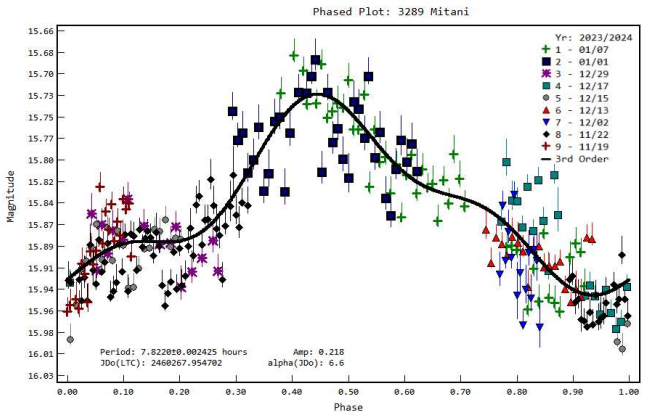

3582 Cyrano is an outer main-belt asteroid discovered in 1986 by P. Wild at Zimmerwald. We observed it on thirteen nights in 2023 December and 2024 January resulting in a total of 643 observations. No prior rotation periods were found in a search of the LCDB. Analysis of the data resulted in a best fit of 33.4180±0.005925 hours with an amplitude of 0.234±0.03 mag.

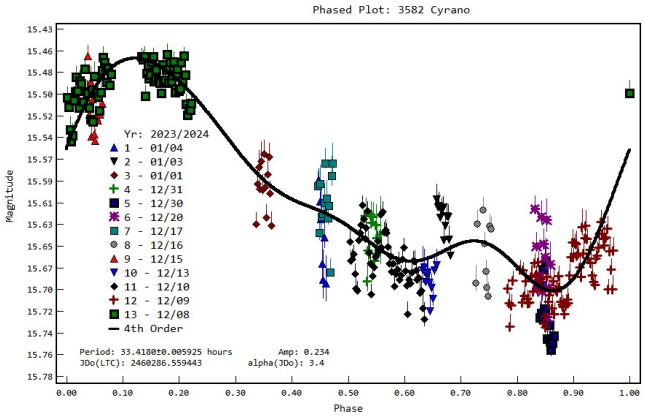

3589 Loyola is an inner main-belt asteroid discovered by J. Wagner at Flagstaff in 1984. We observed it on five nights during 2023 October resulting in 427 total observations. A search of the LCDB resulted in two reports of 4.165750 hours by Ďurech et al. (2020) and 4.166 hours by Erasumus et al. (2020). Analysis of our data resulted in a period of 4.1654±0.000525 hours with an amplitude of 0.813±0.03 mag. Coverage was more than two complete cycles so this result can be considered secure.

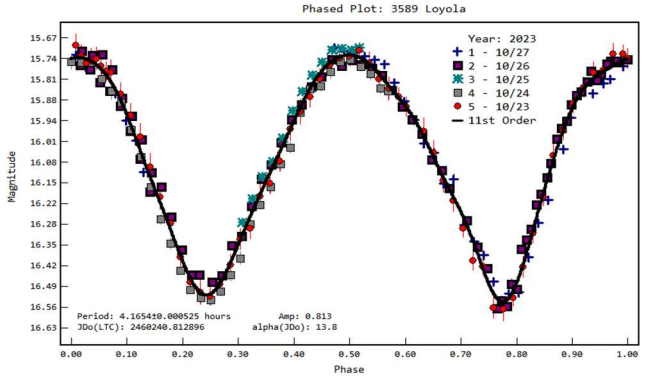

3811 Karma is a main-belt asteroid that is a member of the Karma family (Pavela et al., 2021) situated in the middle part of the main asteroid belt. It was discovered in 1953 by L. Oterma at Turku. We observed it on ten nights in 2023 September and October, resulting in 1032 total observations. A search of the Asteroid Lightcurve Database found four synodic periods reported by Behrend in 2007, Aznar in 2016, Ďurech et al. (2020) and Yeh et al. (2020) with periods between 11.23 and 14.4234 hours and a summary period of 13.32 hours. A recent report from Dose (2023) gives a period of 14.421 hours.

Analysis of our data resulted in a period of 14.4262 ± 0.0005 hours and an amplitude of 0.659 ± 0.03 mag, in close agreement with the more recent reports. The resulting lightcurve shape closely matches that shown in Yeh et al. (2020). The initial period analysis revealed a spread at the minima. Dual period analysis found a signal with period of 28.643±0.004 hours with an amplitude of 0.203±0.002 mag. Subtracting this signal resulted in a period of 14.4298±0.004425 hours and amplitude 0.576±0.002 mag. Plots with and without this secondary signal are shown.

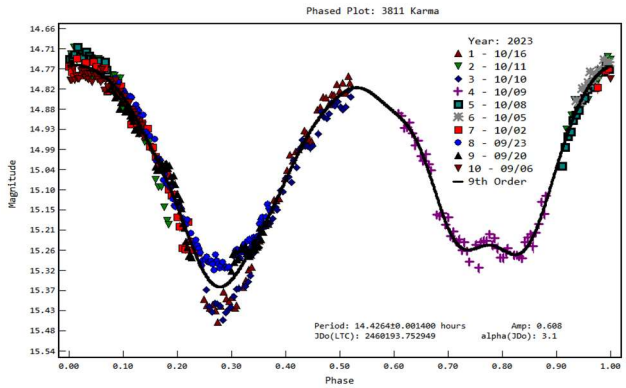

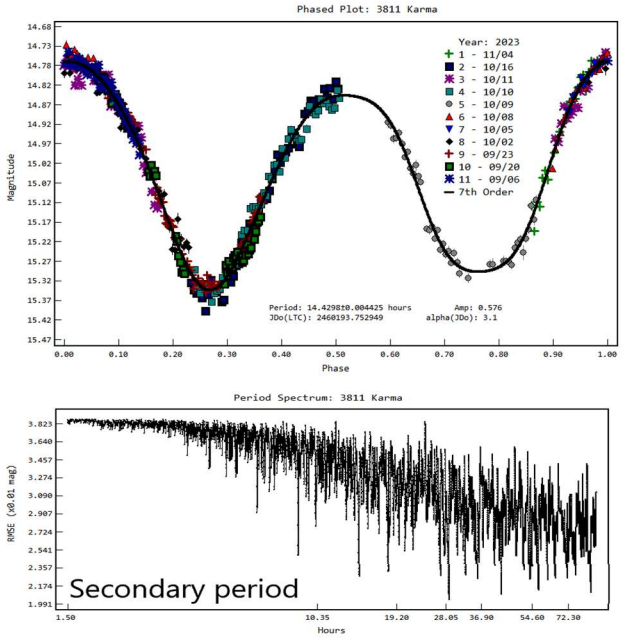

4226 Damiaan is an outer main-belt asteroid discovered in 1989 by E.W. Elst at Haute Provence. We observed it on ten nights resulting in a total of 826 observations. A search of the LCDB resulted in one reported period of 24 hours that is marked “Behrend 2004Web”. We were unable to find a proper reference for this report. Analysis of the data resulted in a best fit period of 30.4458±0.002925 hours with an amplitude of 0.106±0.01 mag. Coverage is incomplete and some of the data is very noisy so this result could be wrong.

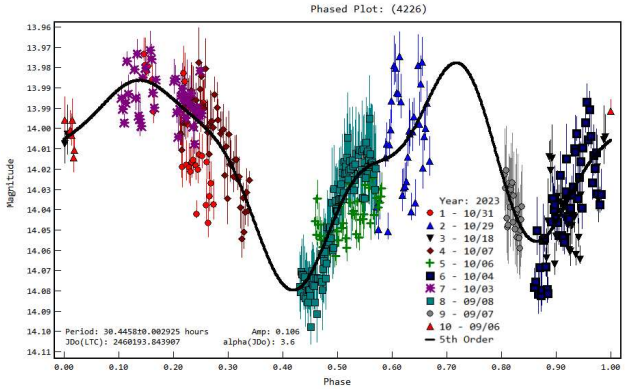

4458 Oizumi is an inner main-belt asteroid discovered in 1990 by Kushida and Muramatsu at Yatsugatake. We observed is on four nights resulting in a total of 682 observations.

A search of the LCDB resulted in two reported periods. Ďurech, et al. (2018) reported 11.04650 hours and Ďurech, et al. (2019) reported 11.40655 hours. Our analysis resulted in 11.3948±0.005925 hours with an amplitude of 0.753±0.03 mag in close agreement with the prior report.

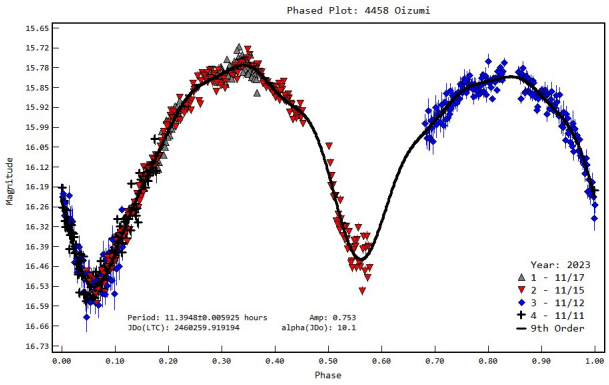

6086 Vrchlicky is a middle main-belt asteroid discovered in 1987 by Z. Vavrove at Klet. It is named for Jaroslav Vrchlicky, a Czech poet. We observed it on three nights in 2023 September for a total of 363 observations. A search of the LCDB revealed one report by Pál, et al. (2020) with a period of 2.76772 hours. Their analysis of the TESS data shows two spikes of approximately equal magnitude, one at the reported period and another between 4 and 5 hours. Analysis of our data resulted in a period of 4.5165±0.001 hours with an amplitude of 0.159±0.03 mag.

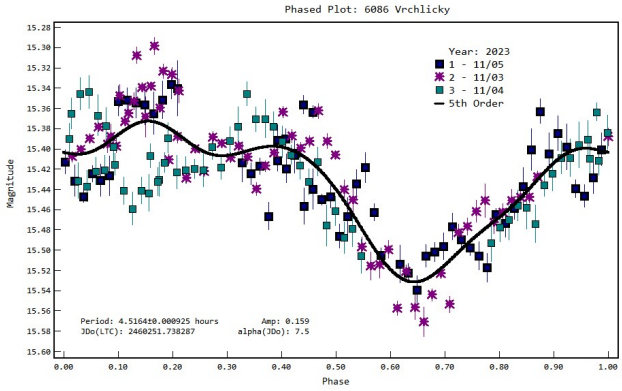

6875 Golgi is an inner main-belt asteroid discovered in 1994 by E.F. Helin at Palomar. It is named for Camillo Golgi, an Italian scientist, physician and biologist. Golgi was awarded the Nobel Prize in Medicine for his studies on the structure of the nervous system. We observed 6875 Golgi on thirteen nights in 2023 November and December resulting in a total of 1260 observations. No prior rotation periods were found in a search of the LCDB. Analysis of the data resulted in a best fit period of 38.6557±0.005925 hours with an amplitude of 0.484±0.05 mag.

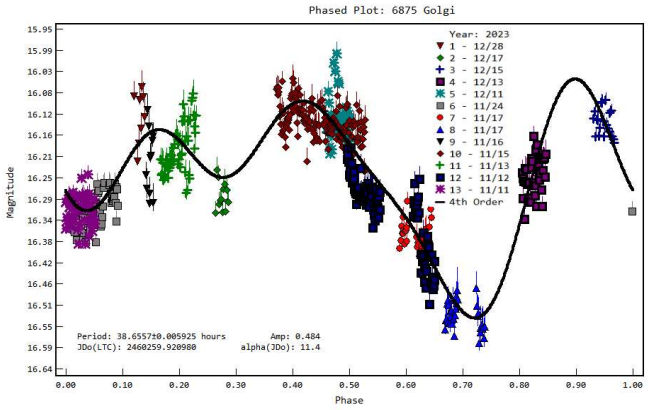

18118 2000 NB24 is an inner main-belt asteroid discovered in 2000 by Spacewatch at Kitt Peak. We observed it on eight nights in 2023 October and November resulting in a total of 342 observations. A search of the LCDB found a report by Waszczak et al. (2015) of 2.524±0.0004 hours. Analysis of our data resulted in a best fit period of 21.3256±0.002925 hours with an amplitude of 0.409±0.06 mag, quite different from the prior result. While the period spectrum shows a spike near 3.8 hours, it is not as large as the best fit. Coverage is a sparse so this result could be wrong.

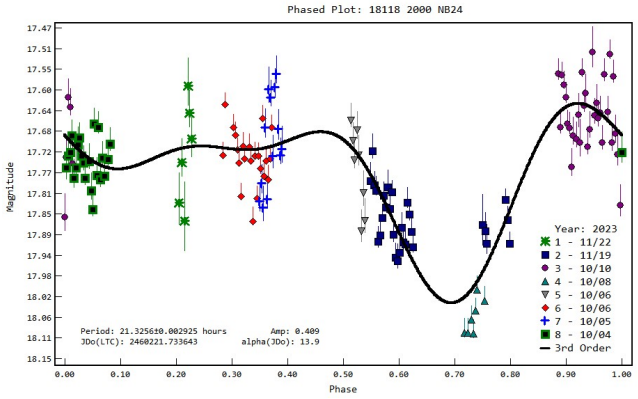

29185 Reich is an outer main-belt asteroid discovered in 1990 by Schmadel and Börngen at Tautenburg. It is named for Ludwig Reich, a professor of Mathematics at the University of Graz. We observed 29185 Reich on five nights in 2023 December and 2024 January resulting in a total of 217 observations. A search of the LCDB revealed no prior rotation period reports. Analysis of the data resulted in a best fit period of 6.0275±0.00245 hours and an amplitude of 0.57±0.09 mag.

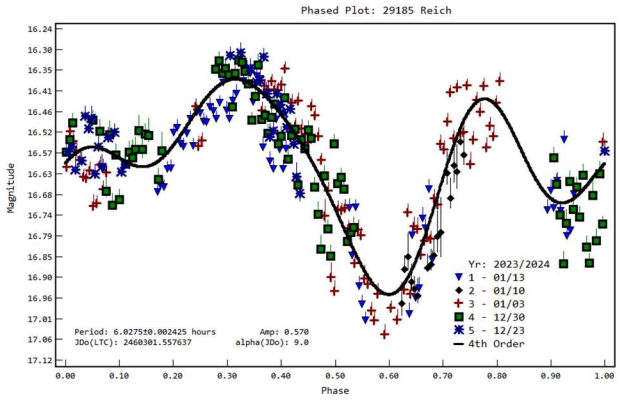

Number	Name	yyyy mm/dd	Phase	L_{PAB}	B_{PAB}	Period(h)	P.E.	Amp	A.E.	Grp
1861	Komensky	2023 11/23-01/03	10.4, 6.2	89	11	61.834	0.010	0.64	0.06	MB-O
2096	Vaino	2023 09/19-10/20	*3.3,15.0	1	1	3.3228	0.001	0.10	0.02	MB-I
3127	Bagration	2023 09/08-11/16	*3.8,24.7	351	6	23.4816	0.002	0.237	0.02	MB-M
3289	Mitani	2023 11/19-01-07	*6.6,20.9	68	1	7.822	0.002	0.218	0.03	MB-I
3582	Cyrano	2023 12/08-01/04	3.4,13.5	68	3	33.418	0.006	0.23	0.03	MB-O
3589	Loyola	2023 10/23-10/27	13.8,11.6	48	-6	4.1654	0.001	0.81	0.03	MB-I
3811	Karma	2023 09/06-11/04	3.9,23.4	339	2	14.4262	0.001	0.659	0.03	MB-M
4226	Damiaan	2023 09/06-10/31	*3.6,22.8	346	5	30.4458	0.003	0.106	0.01	MB-O
4458	Oizumi	2023 11/11-11/17	10.0, 6.9	65	4	11.3948	0.006	0.753	0.03	MB-I
6086	Vrchlicky	2023 11/03-11/05	*7.0, 6.5	53	3	4.5165	0.001	0.159	0.03	MB-M
6875	Golgi	2023 11/11-12/28	*11.4,17.4	65	3	38.6557	0.006	0.484	0.05	MB-I
18118	2000 NB24	2023 10/04-11/22	*13.8,15.2	32	0	21.3256	0.003	0.409	0.06	MB-I
29185	Reich	2023 23/23-01/13	9.0,14.7	85	18	6.0275	0.002	0.570	0.09	MB-O

Table I. Observing circumstances and results. The phase angle is given for the first and last date. If preceded by an asterisk, the phase angle reached an extrema during the period. L_{PAB} and B_{PAB} are the approximate phase angle bisector longitude/latitude at mid-date range (see Harris et al., 1984). Grp is the asteroid family/group (Warner et al., 2009).

Acknowledgements

The author gratefully acknowledges the generosity of Dr. Richard Post for ongoing use of one of his domes in New Mexico to house the author's telescope and Mr. Gary Walker, who has made available the CMOS camera used to collect the observations used in this research. This research used data from the Asteroid Terrestrial-impact Last Alert System (ATLAS) project. ATLAS is primarily funded to search for near earth asteroids through NASA grants NN12AR55G, 80NSSC18K0284, and 80NSSC18K1575. The ATLAS science products have been made possible through the contributions of the University of Hawaii Institute for Astronomy, the Queen's University Belfast, the Space Telescope Science Institute, and the South African Astronomical Observatory. Funding for PDS observations, analysis, and publication was provided by NASA grant NNX13AP56G. Work on the asteroid lightcurve database (LCDB) was funded in part by National Science Foundation grants AST-1210099 and AST-1507535.

References

Denny, R. (2023). ACP Expert software, version 9.1. DC-3 Dreams. *https://acpx.dc3.com*

Dose, E. (2023). "Lightcurves of eighteen asteroids." *The Minor Planet Bull* **51**, 42-49.

Ďurech, J.; Hanuš, J.; Ali-Lagoa, V. (2018). "Asteroid models reconstructed from the Lowell Photometrics Database and WISE data." *Astronomy & Astrophysics,* **617,** id. A57, 8pp.

Ďurech, J.; Hanuš, J.; Vančo, R., (2019). "Inversion of asteroid photometry from the Gaia DR2 and the Lowell Observatory photometric database." *Astronomy & Astrophysics* **631**, id. A2, 4pp.

Ďurech, J.; Tonry, J.; Erasmus, N.; Denneau, L.; Heinze, A.N.; Flewelling, J.; Vanco, R. (2020). "Asteroid models reconstructed from ATLAS photometry." *Astronomy & Astrophysics* **642**, id. A59, 5pp.

Erasmus, N.; Navarro-Meza, S.; McNeill, A.; Trilling, D.E.; Sickapoose, A.A.; Denneau, L.; Flewilling, H.; Heinze, A.; Tonry, J.L. (2020). "Investigating Taxonomic Diversity withing Asteroid Families through ATLAS Dual-Band Photometry." *ApJS* **247**, 7pp.

Fauerbach, M.; Fauerbach, M. (2020). "Photometric Observations of 2096 Vaino and 5104 Skripnichenko." *The Minor Planet Bulletin* **47**, 18-19.

George, D. et. al. (2021). Maxim DL V6.28. *https://diffractionlimited.com/*

Harris, A.W.; Young, J.W.; Scaltriti, F.; Zappala, V. (1984). "Lightcurves and phase relations of the asteroids 82 Alkmene and 444 Gyptis." *Icarus* **57(2)**, 251-258.

Mainzer, A.; Grav, T.; Masiero, J.; Bauer, J.; Hand, E.; Tholen, D.; McMillan, R.S.; Spahr, T.; Cutri, R.M.; Wright, E.; Mo, W.; Maleszewski, C. (2011). "NEOWISE Studies of Spectrophotometrically Classified Asteroids: Preliminary Results." *The Astrophysical Journal* **741**, Issue 2, article id. 90, 22pp. doi:10.1088/0004-637X/741/2/90.

Pál, A.; Szakáts, R.; Kiss, C.; Bódi, A.; Bognár, Z.; Kalup, C.; Kiss, L.L.; Marton, G.; Molnár, L.; Plachy, E.; Sárneczky, K.; Szabó, G.M.; Szabó, R. (2020). "Solar System Objects Observed with TESS - First Data Release: Bright Main-belt and Trojan Asteroids from the Southern Survey." *Ap. J. Suppl Ser*. **247**, id. 26.

Parrott, D. (2023). Tycho-Tracker V10.8.5. *http://www.tycho-tracker.com*

Pavela, D.; Novakovic, B.; Carruba, V.; Radovic, V. (2021). "Analysis of the Karma asteroid family." Monthly Notices of the Royal Astronomical Society **501**, 356-366.

Tonry, J.L.; Denneau, L.; Flewelling, H.; Heinze, A.N.; Onken, C.A.; Smartt, S.J.; Stalder, B.; Weiland, H.J.; Wolf, C. (2018). "The ATLAS All-Sky Stellar Reference Catalog." *Astrophys. J.* **867**, A105.

Warner, B.D.; Harris, A.W.; Pravec, P. (2009). "The asteroid lightcurve database." *Icarus* **202**, 134-146. Updated 2023 April 24. *https://www.alcdef.org*

Waszczak, A.; Chang, C.-K.; Ofeck, E.O.; Laher, R.; Masci, F.; Levitan, D.; Surace, J.; Cheng, Y.-Ch.; Ip, W.-H.; Kinoshita, D.; Helou, G.; Prince, T.A.; Kulkarini, S. (2015). "Asteroid Light Curves from the Palomar Transient Factory Survey: Rotation Periods and Phase Functions from Sparse Photometry." *Astron. J.* **150**, 75-109.

Yeh, T.-S.; Li, B.; Chang, C.-K.; Zhao, H.-B.; Ji, J.-H.; Lin, Z.-Y.; Ip, W.-H. (2020). "The Asteroid Rotation Period Survey Using the Chine Near-Earth Object Survey Telescope (CNEOST)." *The Astronomical Journal* **160**, id.73.

LIGHTCURVES OF EIGHTEEN ASTEROIDS

Eric V. Dose
3167 San Mateo Blvd NE #329
Albuquerque, NM 87110
mp@ericdose.com

(Received: 2024 January 15)

We present lightcurves and synodic rotation periods for eighteen asteroids.

We present asteroid lightcurves obtained via the workflow process described by Dose (2020) and later improved (Dose, 2021a). This workflow applies to each image an ensemble of typically 25-100 nearby comparison ("comp") stars selected from the ATLAS refcat2 catalog (Tonry et al., 2018). This abundance of comp stars and our custom diagnostic plots allow for rapid identification and removal of outlier, variable, and poorly measured comp stars.

The product of this custom workflow is one night's time series of absolute magnitudes, on Pan-STARRS r′ (PR) catalog basis, for one target asteroid. These absolute magnitudes are corrected for instrument transforms, sky extinction, and image-to-image ("cirrus") fluctuations, and thus they represent magnitudes at the top of earth's atmosphere. These magnitudes are imported directly into *MPO Canopus* software (Warner, 2021) where they are adjusted for distances and phase-angle dependence, fit by Fourier analysis including identifying and ruling out of aliases, and plotted.

Phase-angle corrections are made by applying an H-G model to the night's phase angle, using the *G* value minimizing best-fit RMS error across all nights' data. For campaigns in which we cannot estimate an asteroid's *G* value, usually due to a narrow range of phase angles, we apply the Minor Planet Center's default value of 0.15. No nightly zero-point adjustments (Delta Comps in *MPO Canopus*) were made to any session, other than by estimating *G*.

Lightcurve Results

Eighteen asteroids were observed from New Mexico Skies observatory at 2310 meters elevation in southern New Mexico. Images were acquired by using a 0.50-meter PlaneWave OTA on a PlaneWave L-500 mount and equatorial wedge and an SBIG AC4040M CMOS camera cooled to -15°C or to -22°C (after December 13) that was fitted with a GG495 yellow filter (Schott).

This equipment was operated remotely via *ACP* software (DC-3 Dreams), running one-night plan files generated by python scripts (Dose, 2020). Exposure times targeted 2.5-5.0 millimagnitudes uncertainty in asteroid instrumental magnitude, subject to a minimum exposure of 90 seconds to ensure suitable comp-star photometry, and to a maximum of 480 seconds.

FITS images were calibrated using temperature-matched, exposure-matched, median-averaged dark images and recent flat images of a flux-adjustable light panel. Calibrated images were plate-solved by *TheSkyX* (Software Bisque), and target asteroids were identified in *Astrometrica* (Herbert Raab). All photometric images were visually inspected; the author excluded images with poor tracking, excessive interference by cloud or moon, or having stars, satellite tracks, cosmic ray artifacts, residual image artifacts, or other apparent light sources within 12 arcseconds of the target asteroid's signal centroid. Images passing these screens were submitted to the workflow.

The GG495 yellow filter used here requires only modest first-order transforms to yield magnitudes in the standard Pan-STARRS r′ (PR) passband. In our hands, using a light-yellow filter (rather than a clear filter or no filter) improves night-to-night reproducibility to a degree outweighing loss of signal-to-noise ratio caused by ~15% loss of measured flux.

Comparison stars from the ATLAS refcat2 catalog were selected only if they had a distance of at least 15 arcseconds from image boundaries and from other catalogued flux sources, no catalog VARIABLE flag, PR magnitude within [-2, +1] of the target asteroid's PR magnitude on that night (except that very faint asteroids used comp stars with magnitudes in the range 14 to 16), PR-I color value within [0.10, 0.34], and absence of variability as seen in session plots of each comp star's instrumental magnitude vs time.

In this report, "period" refers to an asteroid's synodic rotation period and "mmag" denotes millimagnitudes (0.001 magnitude). In the lightcurves, *MPO Canopus* v10 shows "SR" for both Pan-STARRS and Sloan r′ values. The *G* value given in the lightcurve plot is that which optimized the Fourier fit.

526 Jena. For this asteroid of the Themis family, we estimate a synodic rotation period of 11.877 ± 0.001 h, agreeing with two recent survey results (11.877 h, Erasmus et al., 2020; 11.87651 h, Martikainen et al., 2021) but differing from other known reports (9.474 h, Barucci et al., 1994; 9.48 h, Behrend, 2008web; 9.479 h, Hamanowa and Hamanowa, 2011web; 9.51664 h, Hanuš et al., 2016), all of which appear to have captured an alias by one-half period per day of the actual rotation period.

The lightcurve is clearly bimodal in shape. Our best *G* value of 0.10 gave a modest fit improvement over the MPC default value of 0.15; our Fourier-fit RMS error is 7 mmag.

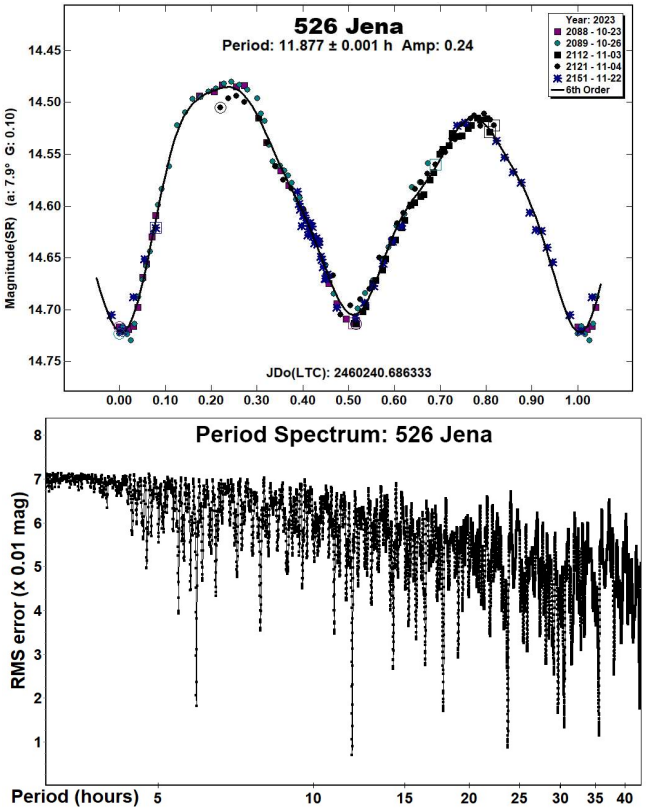

Suppression of aliases was greatly aided by our long observing sessions of which two were more than eight hours in duration, enough to capture two adjacent brightness minima or maxima. The often-reported alias near 9.48 h does not appear in our period spectrum.

549 Jessonda. Most reported estimates of the rotation period for this bright middle main-belt asteroid appear to have assumed a monomodal interpretation (2.97 h, Behrend, 2002web; 2.9709 h, Behrend, 2005web; 2.971 h, Warner, 2011; 2.962 h, Stephens, 2015; 2.9713 h, Pilcher, 2020; 2.972 h, Polakis, 2020b; but note 5.938 h, Warner, 2006 as a precursor to Warner, 2011), and except in one case (4.5 h, Brincat, 2002web) were near 2.97 h or twice that value. The similarity between successive cycles in the lightcurve and the uniformly low amplitude both present weak evidence that a monomodal interpretation is correct, but it always remains possible that the lightcurve is still bimodal and that the asteroid's two physical sides are very similar.

We were intrigued by some fine structure emerging in the recent lightcurves of Pilcher and Polakis, which our new data confirm. We suggest that this fine structure is the best evidence yet for the monomodal character of this lightcurve, because higher-order modality would require that opposite physical sides of the asteroid would have to match in their shapes, which seems unlikely (our three sessions were offset by an odd number of period cycles, so that, under bimodality, we would have sampled both sides of the asteroid). We conclude that the true rotation period of 549 Jessonda is 2.971 h.

Our new estimate of 2.9710 ± 0.0005 h matches recent consensus. We adopted the MPC default *G* value of 0.15, and our Fourier fit RMS error is 5 mmag.

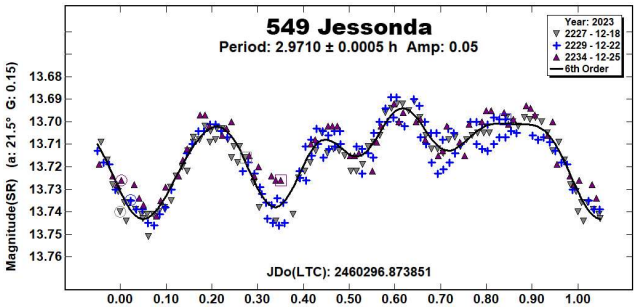

The period spectrum appears unequivocal. No meaningful signals appeared at periods longer than 15 h.

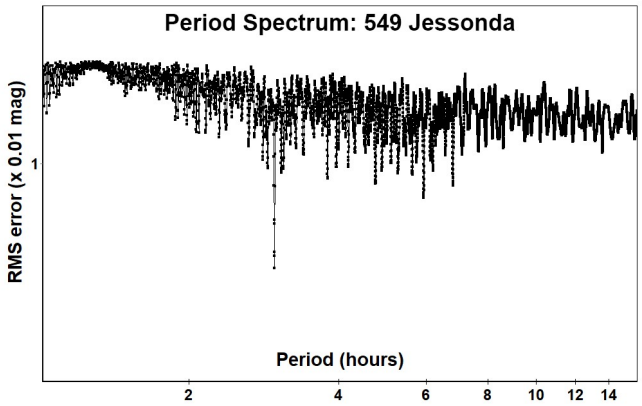

717 Wisibada. Arriving at a Fourier solution for this outer main-belt asteroid was exceptionally difficult due to its long rotational period and its atypical lightcurve shape. Indeed, we know of no previous period reports, which remains true of very few low-numbered asteroids. From 30 nights' observations, we report a bimodal lightcurve with period 609.06 ± 0.49 h. Adopting our best *G* value of 0.27 markedly decreased the fit RMS error to 10 mmag.

No periods shorter than 600 h can satisfactorily fit our data.

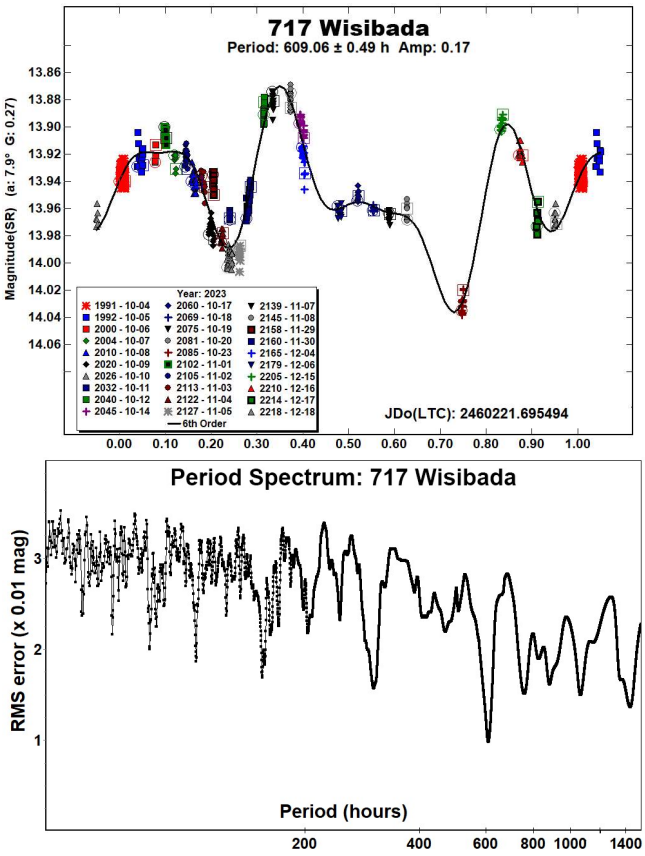

722 Frieda. We confirm the tumbling apparent in previous lightcurves (Polakis, 2019; Dose, 2021b), and we report here a rotation period of 130.284 ± 0.153 h, in reasonable agreement with most previous reports (131.166 h, Ďurech et al., 2019; 131.1 h, Polakis, 2019; 128.99 h, Dose, 2021b). We cannot explain one differing report of 30.06 h (Olguin et al., 2020) via multiples or aliases but note that its phase coverage was incomplete.

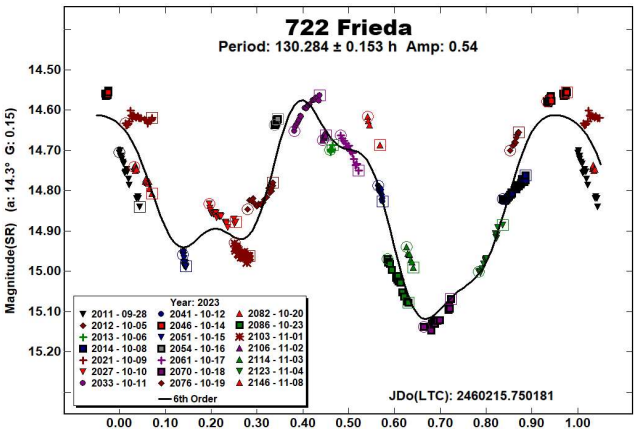

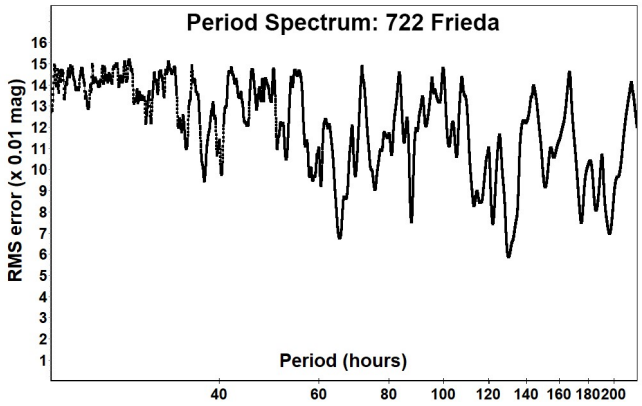

Night-to-night brightness variations caused by tumbling appear to have had several effects: scatter in reported periods around 130 h, our high Fourier fit RMS error of 59 mmag, and very low sensitivity of the fit to *G* value for which we kept MPC's default of 0.15.

The period spectrum is not as clear as wished even with 21 nights' data, but the preponderance of recent reports around 130 h and the lightcurve's high amplitude support 130 hours as 722 Frieda's correct rotational period.

However, if one extends the period spectrum, a dominant new signal appears near 395 h, close to three times the bimodal period, and its RMS error is much lower than that for the bimodal period.

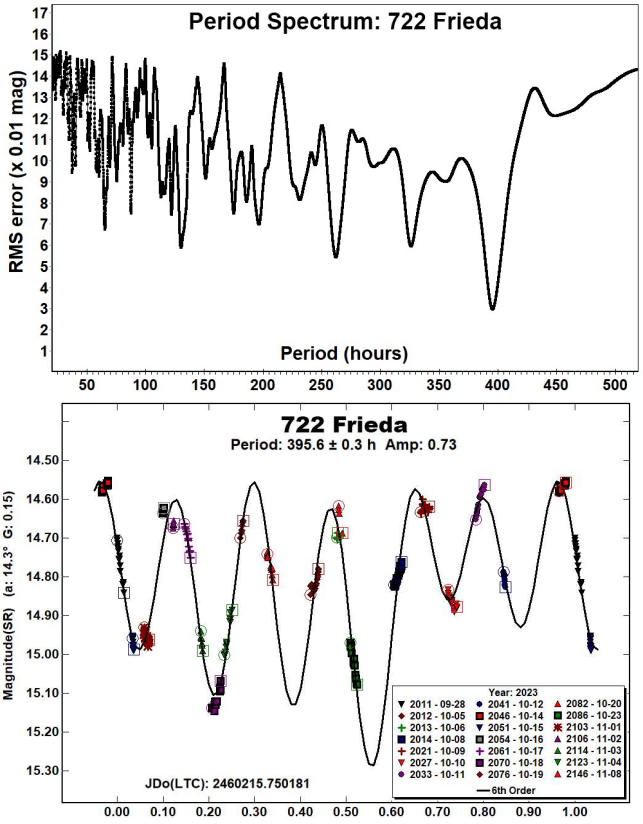

Of course, a hexamodal Fourier fit is unrealistic for rotation alone, but this period so strikingly matches our data - even within nights - as to suggest a precession period near 3 times the rotational period. However, it is important to note that *MPO Canopus* is not designed to analyze tumbling asteroids properly and that the longer period might be at a "beat frequency" of the true periods of rotation and precession.

1112 Polonia. For this asteroid of the Eos family, we find a nominally bimodal lightcurve dominated by one maximum and a rotation period of 18.574 ± 0.011 h, in fair agreement with two reports (18.605 h, Behrend, 2018web; 18.71 h, Polakis, 2020a) but differing from another, earlier report (82.5 h, Warner, 2008). A period of 82.5 h represents an alias of our value by one period per day. Our best *G* value is 0.25 and our Fourier fit RMS error for this bright asteroid is 4 mmag.

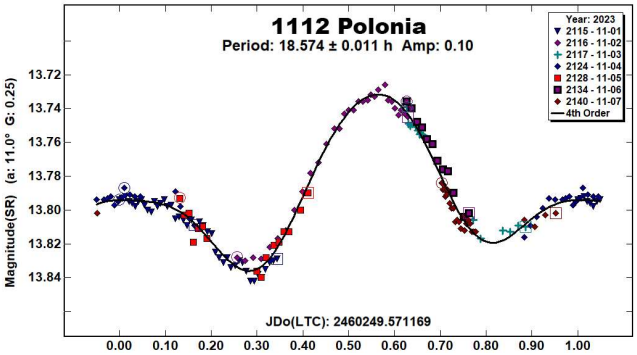

The period spectrum is unambiguous except for a double-period signal near 37 h. Our fortunate series of seven consecutive observation nights strongly suppressed aliases, including that at 82.5 h.

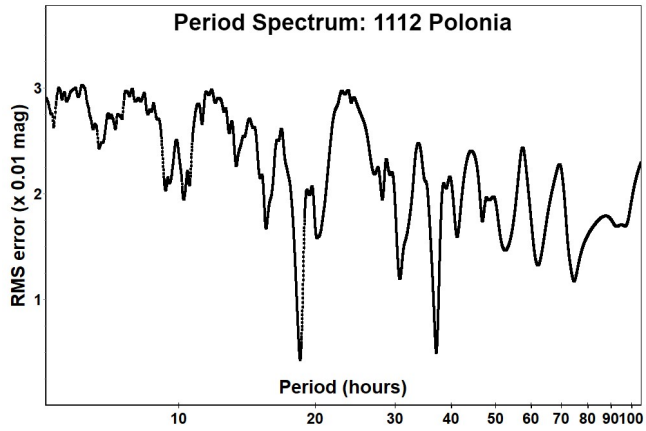

1408 Trusanda. For this asteroid of the Eos family, we report a rotation period of 29.357 ± 0.015 h and an asymmetric bimodal lightcurve. We know of no previous period reports. We adopted a default *G* value of 0.15, and the Fourier fit RMS error is 9 mmag.

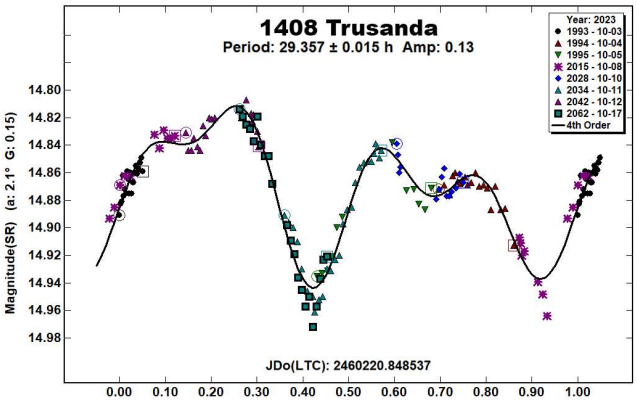

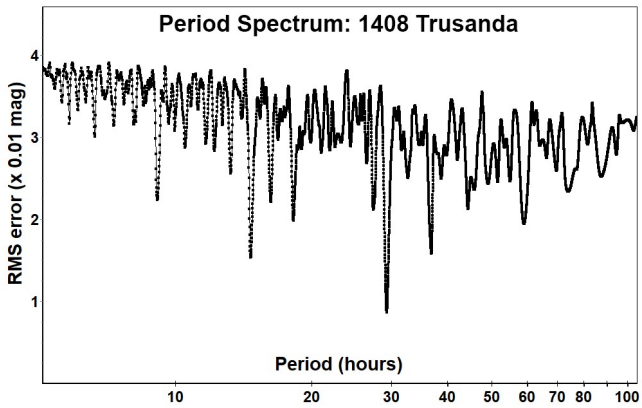

1429 Pemba. Finding a Fourier solution for this inner main-belt asteroid was complicated by its long period and its unusual, nominally bimodal lightcurve shape. After twenty nights' observation extending over more than three periods, we report a period of 421.31 h ± 0.25 h, consistent with one previously reported lower limit (> 20 h, Harris et al., 1999); we know of no reported central estimates of the period. The lightcurve shows little evidence of tumbling effect. A *G* value of 0.23 markedly decreased our Fourier fit RMS error, which is 22 mmag.

No periods shorter than about 400 h can fit our observations.

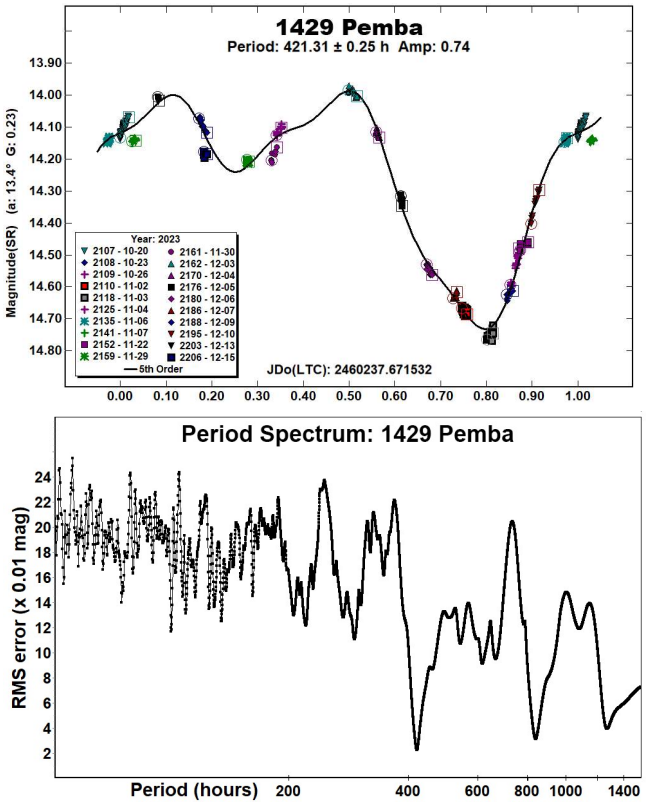

1604 Tombaugh. For this Eos-family asteroid, we add to the growing rotation-period consensus (8.2 h, Lagerkvist, 1978; 7.04 h, Binzel, 1987; 6.15 h, Sárneczky et al., 1999; 7.047 h, Albers et al., 2010; 7.056 h, Strabla et al., 2013; 7.24 h, Behrend, 2017web; 7.0359 h, Ďurech and Hanuš, 2018; 7.03598 h, Ďurech et al., 2019) with our estimate of 7.0360 ± 0.0005 h. Our best *G* value of 0.13 modestly improved the fit over a default value or 0.15; our Fourier fit RMS error is 9 mmag.

Our period spectrum is dominated by signals at multiples of one-half our proposed period, as expected for a nearly symmetric bimodal lightcurve.

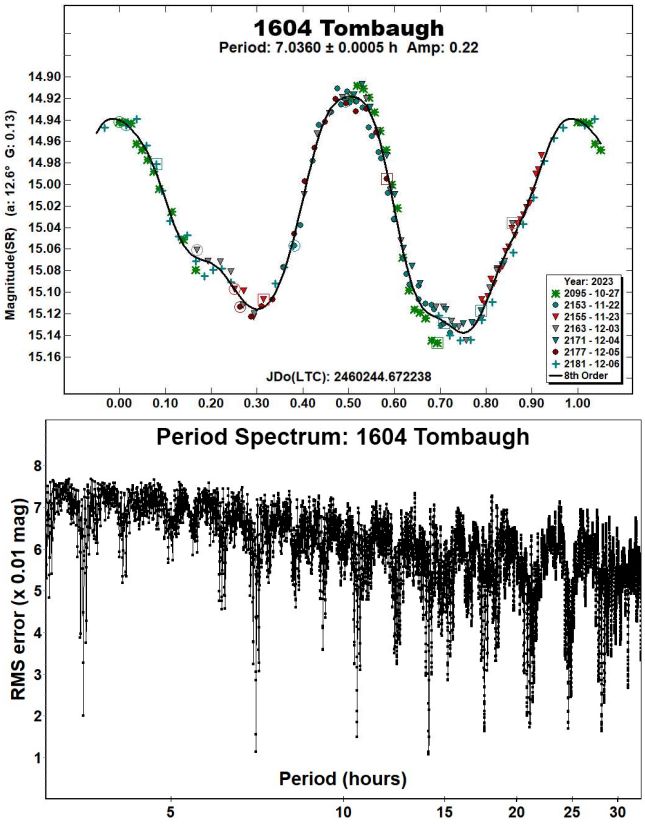

2122 Pyatiletka. Our period estimate of 8.902 ± 0.002 h for this inner main-belt asteroid agrees with two previous reports from surveys (8.899 h, Waszczak et al., 2015; 8.90167 h, Ďurech et al., 2020). The lightcurve is clearly bimodal. Our best *G* value is 0.32, and our Fourier fit RMS error is 14 mmag.

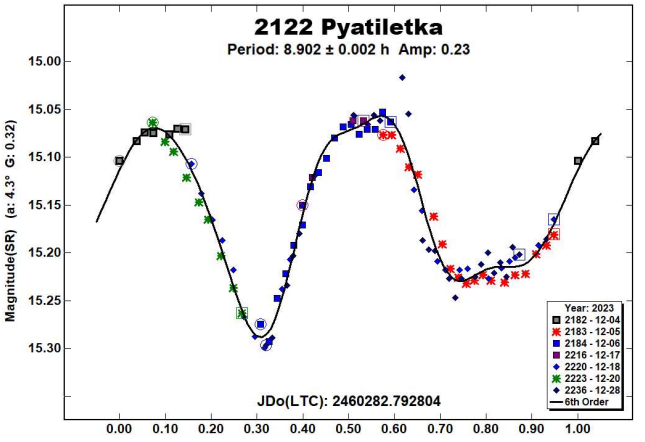

2374 Vladvysotskij. For this asteroid of the Meliboea family, we report a rotational period of 5.412 ± 0.001 h, in agreement with two previous survey reports (5.398 h, Waszczak et al., 2015; 5.41401 h, Ďurech et al., 2018). The lightcurve is bimodal. The Fourier fit was insensitive to *G* value, given the small phase angle range covered, and its RMS error is 8 mmag.

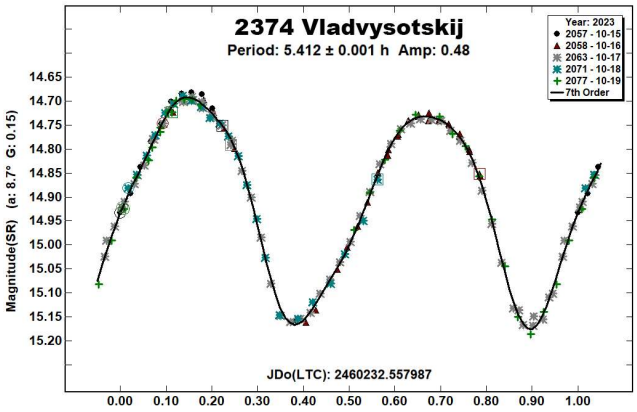

2967 Vladisvyat. For this Ursula-family asteroid, we report a rotation period of 8.375 ± 0.001 h. The LCDB lists no previous period reports. The lightcurve is bimodal with the two halves differing only slightly. Our best *G* value is -0.06 and our Fourier fit RMS error is 9 mmag.

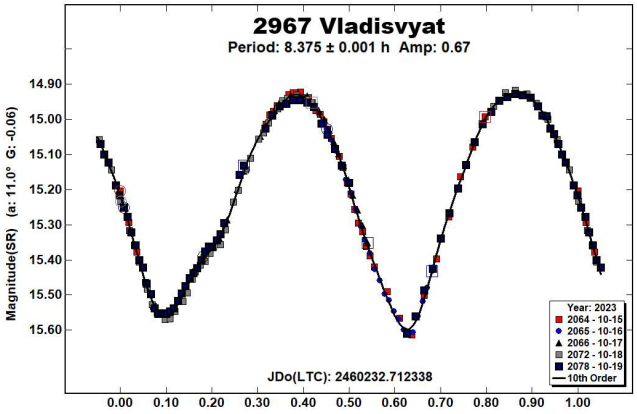

The period spectrum is dominated by signals at multiples of one-half period, consistent with a slightly asymmetric bimodal lightcurve. Complete phase coverage, with overlaps, was made possible by observing for 60% or more of the period during three of the five consecutive nights. The relatively large lightcurve amplitude also supports our bimodal interpretation.

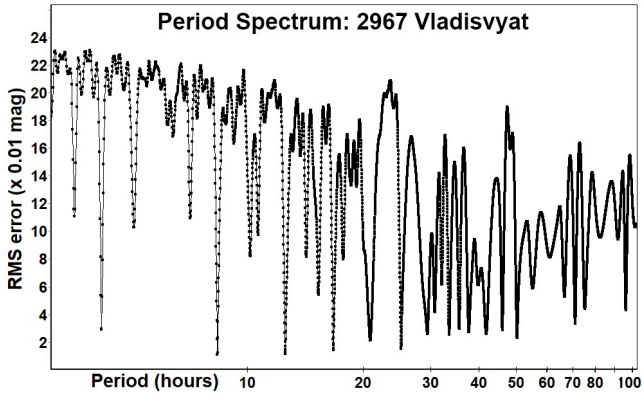

3530 Hammel. For this faint Hertha-family asteroid, we report a rotation period of 4.609 ± 0.001 h, in reasonable agreement with two previous reports (4.53 h, Erasmus et al., 2019; 4.59 h, Behrend, 2023web). The lightcurve is bimodal with very large amplitude and differing minimum brightnesses. Given the narrow phase-angle range covered, we could not distinguish our best *G* value from the MPC default of 0.15 and so we adopted the latter. Our Fourier fit RMS error is 52 mmag.

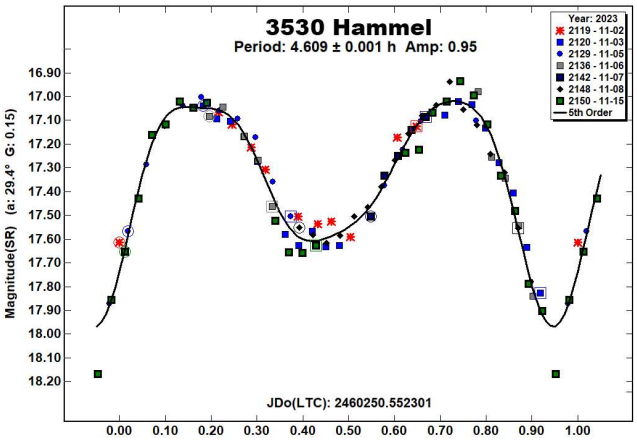

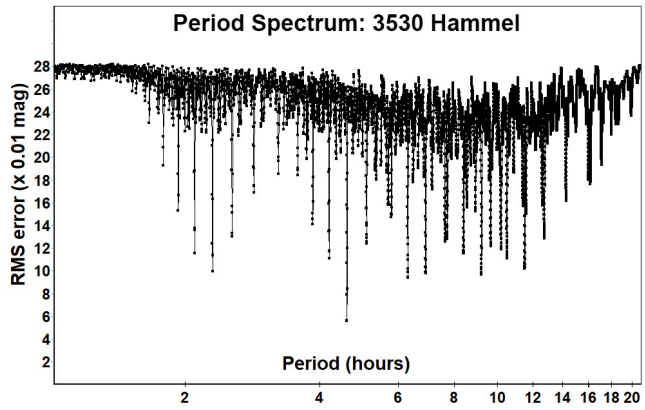

3759 Piironen. Previous attempts to determine the period for this outer main-belt asteroid have resulted in three widely differing reported periods (15.02 h, Behrend, 2011web; 8.213 h, Klinglesmith et al., 2015; 409.848 h, Waszczak et al., 2015). Our result of 406.70 ± 0.25 h, based on 19 nights' observations over 13 weeks (more than 5 periods), agrees fairly well with that of Waszczak, and the lightcurve is bimodal. Our best *G* value is 0.20; our Fourier fit RMS error is 26 mmag. We saw little or no effect of any tumbling.

The period spectrum's primary signal falls at our proposed period, and two secondary signals fall at one- and three-halves of that period.

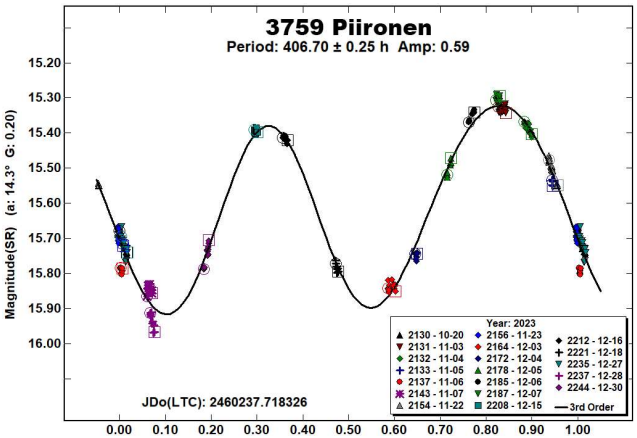

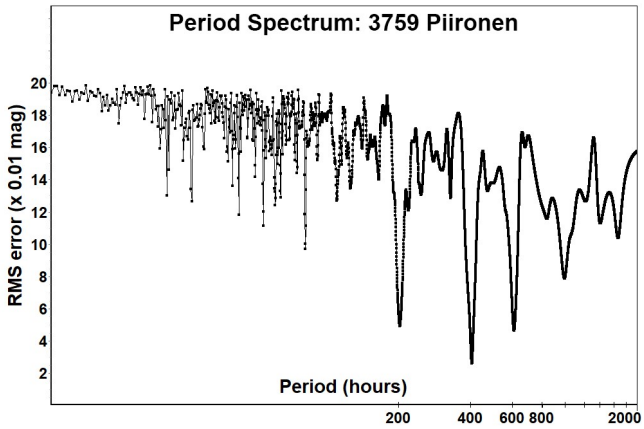

5740 Toutoumi. Previous rotation period estimates for this middle main-belt asteroid have been based on monomodal (5.83981 h, Pál et al., 2020) and bimodal (11.68 h, Vander Haagen, 2007; 11.686 h, McNeill et al., 2019; 11.67974 h, Ďurech et al., 2020) assumed shapes for the lightcurve. Our lightcurve shape strongly confirms the bimodal interpretation and our estimate for the rotation period is 11.681 ± 0.002 h. Our narrow range of phase angles caused us to adopt the MPC default *G* value of 0.15, and our Fourier fit RMS error is 16 mmag.

Our period spectrum confirms the bimodal interpretation.

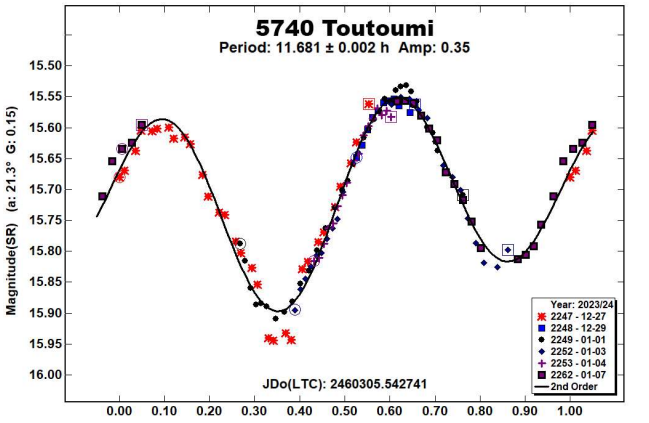

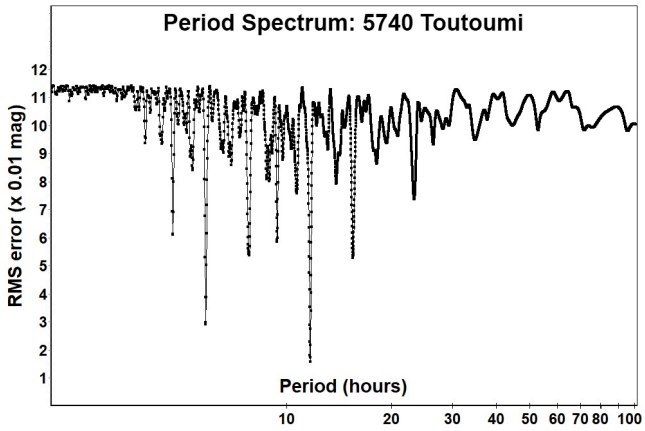

6790 Pingouin. For this inner main-belt asteroid, we find a bimodal lightcurve with period 123.851 ± 0.011 h, in agreement with one previously reported result (124.16 h; Ďurech et al., 2020) but differing from another (6.38 h, Clark, 2007). Even with 26 nights' observations over a campaign of five months (30 rotational periods), the phase coverage is imperfect. The lightcurve amplitude is very large, supporting the bimodal lightcurve shown. Our best *G* value was indistinguishable from the MPC default of 0.15, and our Fourier fit RMS error is 36 mmag. We saw no clear suggestion of tumbling effect.

The period spectrum is dominated by signals at multiples of one-half of our proposed period.

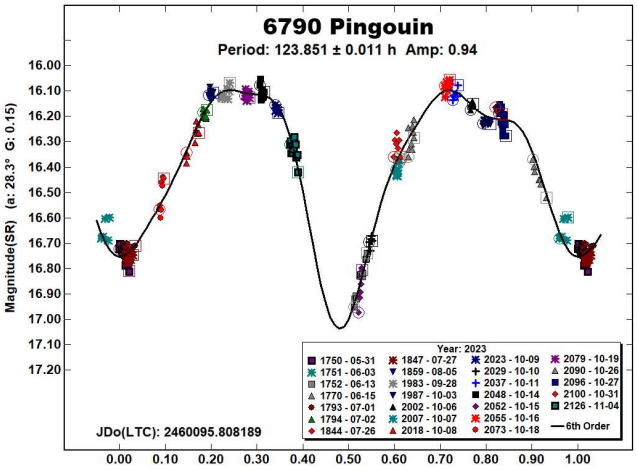

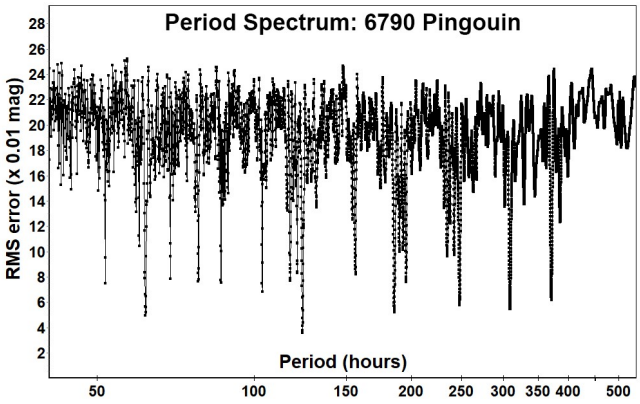

7169 Linda. Several previous attempts to determine the rotation period of this Matterania-family asteroid have led to widely differing reported estimates (> 28 h; Higgins and Gonçalves, 2007; 8.355 h, Clark, 2008; 27.864 h, Hanuš et al., 2013; 341.68 h, Waszczak et al., 2015; 336.276 h, Pál et al., 2020).

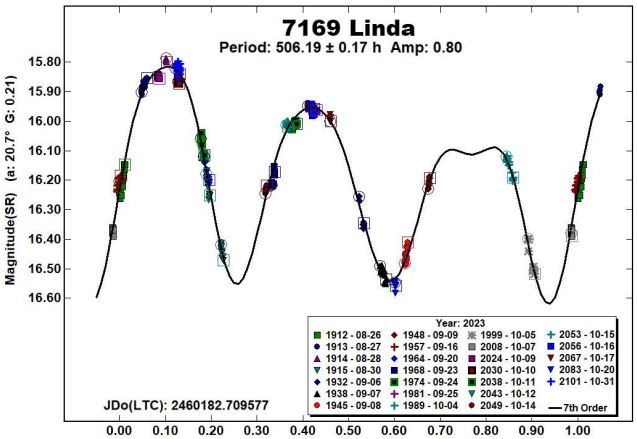

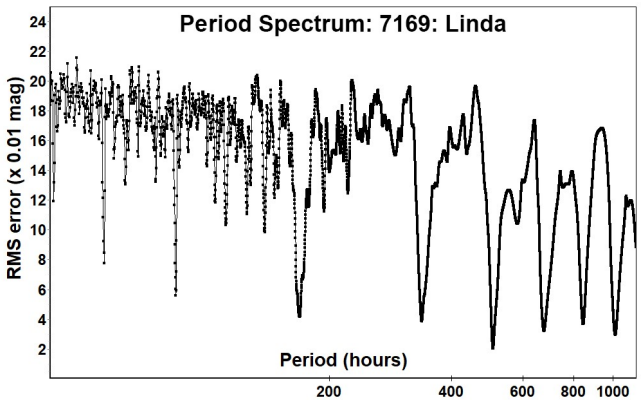

Our 26 nights' observation over nine weeks leads us to report a trimodal lightcurve and best period estimate of 506.19 h ± 0.17 h. Attempts to constrain the fits to monomodal or bimodal models met with frustration; our trimodal result is indeed approximately 1.5 times the duration of the two most recent period reports.

There is little or no evidence of tumbling effect on our lightcurve. Our best *G* value is 0.21, and our Fourier fit RMS error is 20 mmag.

Our lightcurve phase coverage is nearly complete. To cover every minimum, maximum, brightening, and dimming within this complex, high-order lightcurve might require about 50 nights' observation in a single apparition, which suggests a future campaign of observations from multiple locations with largely uncorrelated weather. In compensation, the period is so long that only a few observations need be taken each night. The next promising opportunity is the 2026 apparition, which favors the Southern Hemisphere.

14835 Holdridge. In the previous issue of the *Minor Planet Bulletin*, the author reported a trimodal lightcurve for this Phocaea-family asteroid (Dose, 2023). We have now extended our previous 15 nights of observation to 22 nights (over nine weeks, which is about nine period durations), with an emphasis on long observing sessions whenever possible, to capture brightness changes within each night.

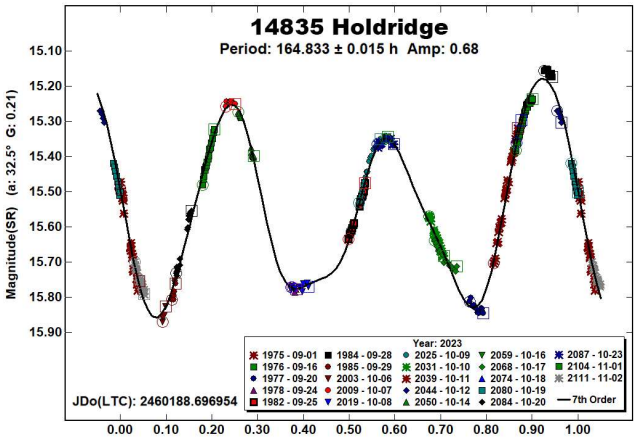

In the end, the trimodal lightcurve shape is strongly confirmed, and a new period estimate of 164.833 ± 0.015 h is little changed from our previous estimate of 164.401 ± 0.029 h; both are consistent with one known period report, a lower limit of 10 h (Prevec et al., 2005web). Each brightness minimum and maximum in the lightcurve is now covered, and we still see no evidence of tumbling effect.

With a best *G* value of 0.21, our updated Fourier fit has RMS error of 16 mmag.

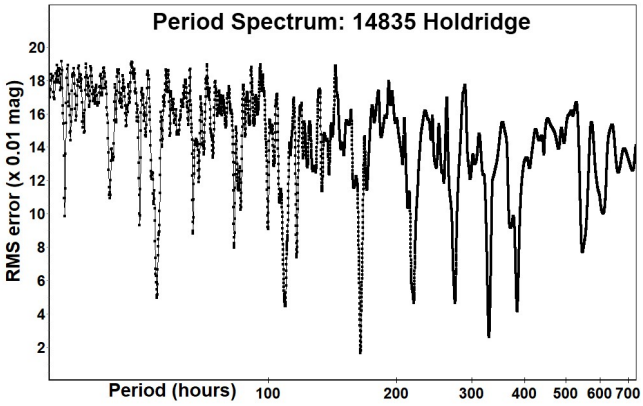

The updated period spectrum is very similar to the previous plot, except that signals other than those at 1× and 2× the proposed period are even weaker.

The next readily accessible apparition will center on 2026 May and will slightly favor the Southern Hemisphere.

(18896) 2000 GN113. We observed this inner main-belt asteroid for four nights rather late in its 2023 apparition. We report a rotation period of 6.634 ± 0.001 h, in agreement with one previous set of reports (6.631 h, 6.633 h, 6.630 h, Waszczak et al., 2015) but differing from another previous report (7.22 h, Behrend, 2005web).

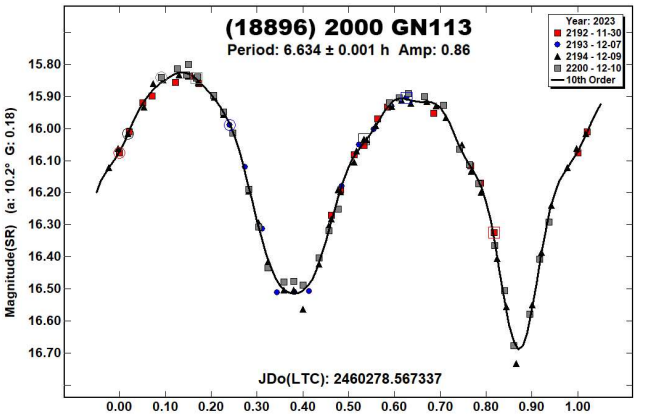

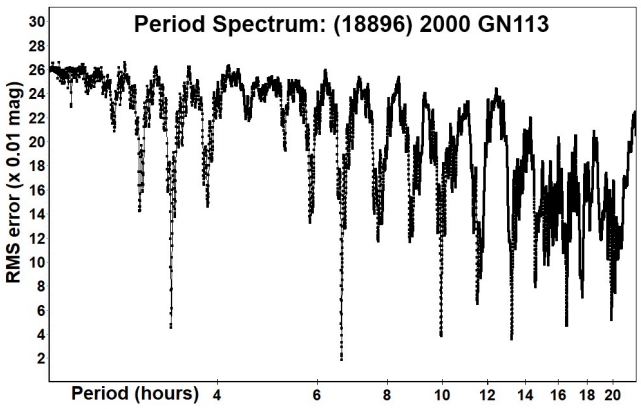

Number	Name	yyyy mm/dd	Phase	L_{PAB}	B_{PAB}	Period(h)	P.E.	Amp	A.E.	Grp
526	Jena	2023 10/23-11/22	*8.0,3.6	50	-3	11.877	0.001	0.24	0.02	THM
549	Jessonda	2023 12/18-12-25	21.7,19.0	125	0	2.971	0.001	0.05	0.01	MB-M
717	Wisibada	2023 10/04-12/18	*8.1,21.4	28	2	609.060	0.490	0.17	0.03	MB-O
722	Frieda	2023 09/28-11/08	*14.5,9.3	29	-3	130.284	0.153	0.54	0.10	MB-I
1112	Polonia	2023 11/01-11/07	10.9,12.8	15	11	18.574	0.011	0.10	0.02	EOS
1408	Trusanda	2023 10/03-10/17	2.3,7.7	5	3	29.357	0.015	0.13	0.03	EOS
1429	Pemba	2023 10/20-12/15	*13.6,17.9	48	0	421.310	0.250	0.74	0.06	MB-I
1604	Tombaugh	2023 10/27-12/06	*12.7,5.2	65	11	7.036	0.001	0.22	0.03	EOS
2122	Pyatiletka	2023 12/04-12/28	4.2,14.0	66	-6	8.902	0.002	0.23	0.04	MB-I
2374	Vladvysotskij	2023 10/15-10/19	8.7,10.3	6	8	5.412	0.001	0.48	0.03	MEL
2967	Vladisvyat	2023 10/15-10/19	11.1,9.7	48	4	8.375	0.001	0.67	0.04	URS
3530	Hammel	2023 11/02-11/15	29.3,30.6	350	1	4.609	0.001	0.95	0.12	HER
3759	Piironen	2023 10/20-12/30	*14.4,18.2	55	14	406.700	0.250	0.59	0.08	MB-O
5740	Toutoumi	2023-4 12/27-01-07	21.2,24.1	55	5	11.681	0.002	0.35	0.04	MB-M
6790	Pingouin	2023 05/31-11/04	*28.4,30.1	311	14	123.851	0.011	0.94	0.10	MB-I
7169	Linda	2023 08/26-10/31	*20.9,18.6	5	8	506.190	0.170	0.80	0.10	MAT
14835	Holdridge	2023 09/01-11/02	*32.5,10.4	30	20	164.833	0.015	0.68	0.06	PHO
18896	2000 GN113	2023 11/30-12/10	10.1,14.8	49	2	6.634	0.001	0.86	0.08	MB-I

Table I. Observing circumstances and results. The phase angle is given for the first and last date. If preceded by an asterisk, the phase angle reached an extrema during the period. L_{PAB} and B_{PAB} are the approximate phase angle bisector longitude/latitude at mid-date range (see Harris et al., 1984). Grp is the asteroid family/group (Warner et al., 2009).

The lightcurve is bimodal, with one unusually sharp and brief minimum (phase 0.8 - 0.95 in our lightcurve plot), before and after which the brightness changes by about 0.4 magnitudes within 15 minutes. Our best *G* value is about 0.18, and our Fourier fit RMS error is 19 mmag.

As for most bimodal lightcurves, this period spectrum is dominated by signals at multiples of one-half the bimodal period, and especially by a signal at the period itself. No major signal occurs at the previously reported period near 7.22 h.

Acknowledgements

The author thanks all contributors to the ATLAS paper (Tonry et al., 2018) for providing openly and without cost the ATLAS refcat2 catalog release. This current work also makes extensive use of the python language interpreter and of several supporting packages (notably: astropy, ccdproc, ephem, matplotlib, pandas, photutils, requests, skyfield, and statsmodels), all made available openly and without cost.

References

Albers, K.; Kragh, K.; Monnier, A.; Pligge, Z.; Stolze, K.; West, J.; Yim, A.; Ditteon, R. (2010). "Asteroid Lightcurve Analysis at the Oakley Southern Sky Observatory: 2009 October thru 2010 April." *Minor Planet Bull*. **37**, 152-158.

Barucci, M.A.; Di Martino, M.; Dotto, E.; Fulchignoni, M.; Rotundi, A.; Burchi, R. (1994). "Rotational Properties of Small Asteroids: Photoelectric Observations of 16 Asteroids." *Icarus* **109**, 267-273.

Behrend, R. (2002web, 2005web, 2008web, 2011web, 2017web, 2018web, 2023web). Observatoire de Genève web site. *http://obswww.unige.ch/~behrend/page_cou.html*

Binzel, R.P. (1987). "A photoelectric survey of 130 asteroids." *Icarus* **72**, 135-208.

Brincat, S.M. (2002web). CALL lightcurve entry for 540 Jessonda. *https://minplanobs.org/MPInfo/php/callsearch.php*

Clark, M. (2007). "Lightcurve Results for 1318 Nerina, 2222 Lermontov, 3015 Candy, 3089 Oujianquan, 3155 Lee, 6410 Fujiwara, 6500 Kodaira, (8290) 1992 NP, 9566 Rykhlova, (42923) 1999 SR18, and 2001 FY." *Minor Planet Bull*. **34**, 19-22.

Clark, M. (2008). "Asteroid Lightcurves from the Chiro Observatory." *Minor Planet Bull*. **35**, 42-43.

Dose, E.V. (2020). "A New Photometric Workflow and Lightcurves of Fifteen Asteroids." *Minor Planet Bull*. **47**, 324-330.

Dose, E.V. (2021a). "Lightcurves of Nineteen Asteroids." *Minor Planet Bull*. **48**, 69-76.

Dose, E.V. (2021b). "Lightcurves of Eighteen Asteroids." *Minor Planet Bull*. **48**, 125-132.

Dose, E.V. (2023). "Lightcurves of Eighteen Asteroids." *Minor Planet Bull*. **51**, 42-49.

Ďurech, J.; Hanuš, J. (2018). "Reconstruction of asteroid spin states from Gaia DR2 photometry." *Astron. Astrophys.* **620**, A91.

Ďurech, J.; Hanuš, J.; Alí-Lagoa, V. (2018). "Asteroid models reconstructed from the Lowell Photometric Database and WISE data." *Astron. Astrophys.* **617**, A57.

Ďurech, J.; Hanuš, J.; Vančo, R. (2019). "Inversion of asteroid photometry from Gaia DR2 and the Lowell Observatory photometric database." *Astron. Astrophys.* **631**, A2.

Ďurech, J.; Tonry, J.; Erasmus, N.; Denneau, L.; Heinze, A.N.; Flewelling, H.; Vančo, R. (2020). "Asteroid models reconstructed from ATLAS photometry." *Astron. Astrophys.* **643**, A59.

Erasmus, N.; McNeill, A.; Mommert, M.; Trilling, D.E.; Sickafoose, A.A.; Paterson, K. (2019). "A Taxonomic Study of Asteroid Families from KMTNET-SAAO Multiband Photometry." *Astrophys. J. Suppl. Series* **242**, 15.

Erasmus, N.; Navarro-Meza, S.; McNeill, A.; Trilling, D.E.; Sickafoose, A.A.; Denneau, L.; Flewelling, H.; Heinze, A.; Tonry, J.L. (2020). "Investigating Taxonomic Diversity within Asteroid Families through ATLAS Dual-band Photometry." *Astrophys. J. Suppl. Series* **247**, 13.

Hamanowa, H.; Hamanowa, H. (2011web). *http://www2.ocn.ne.jp/~hamaten/astlcdata.htm*

Hanuš, J.; Bronž, M.; Ďurech, J.; Warner, B.D.; Brinsfield, J.; Durkee, R.; Higgins, D.; Koff, R.A.; Oey, J.; Pilcher, F.; Stephens, R.; Strabla, L.P.; Ulisse, Q.; Girelli, R. (2013). "An anisotropic distribution of spin vectors in asteroid families." *Astron. Astrophys.* **559**, A134.

Hanuš, J. and 168 colleagues (2016). "New and updated convex shape models of asteroids based on optical data from a large collaboration network." *Astron. Astrophys.* **586**, A108.

Harris, A.W.; Young, J.W.; Scaltriti, F.; Zappala, V. (1984). "Lightcurves and phase relations of the asteroids 82 Alkmene and 444 Gyptis." *Icarus* **57**, 251-258.

Harris, A.W.; Young, J.W.; Bowell, E.; Tholen, D.J. (1999). "Asteroid Lightcurve Observations from 1981 to 1983." *Icarus* **142**, 173-201.

Higgins, D.; Gonçalves, R.M.D. (2007). "Asteroid Lightcurve Analysis at Hunters Hill Observatory and Collaborating Stations – June - September 2006." *Minor Planet Bull.* **34**, 16-18.

Klinglesmith, D.A.; DeHart, A.; Hanowell, J.; Hendrickx, S. (2015). "Etscorn Observatory Lightcurve Results for Asteroids 2245, 3759, 6388, 214088." *Minor Planet Bull*. **42**, 158-159.

Lagerkvist, C.-I. (1978). "Photographic Photometry of 110 Main-Belt Asteroids." *Astrophys. J. Suppl.* **31**, 361-381.

Martikainen, J.; Muinonen, K.; Penttilä, A.; Cellino, A.; Wang, X.-B. (2021). "Asteroid absolute magnitudes and phase curve parameters from Gaia photometry." *Astron. Astrophys.* **649**, A98.

McNeill, A.; Mommert, M.; Trilling, D.E.; Llama, J.; Skiff, B. (2019). "Asteroid Photometry from the Transiting Exoplanet Survey Satellite: A Pilot Study." *Astrophys. J. Suppl. Series* **245**, 29.

Olguin, L.; Saucedo, J.C.; Loera-González, P.; Contreras, M.E.; Valdés, J.R.; Guichard, J.; López-González, R.; Michimani-García, J.; Cerdán-Hernández, G.; Schuster, W.J.; Valdés-Sada, P.; Núñez-López, R.; Ayala-Gómez, S.A. (2020). "The 2019 Mexican Asteroid Photometry Campaign." *Minor Planet Bull*. **47**, 340-342.

Pál, A.; Szakáts, R.; Kiss, C.; Bódi, A.; Bognár, Z.; Kalup, C.; Kiss, L.L.; Marton, G.; Molnár, L.; Plachy, E.; Sárneczky, K.; Szabó, G.M.; Szabó, R. (2020). "Solar System Objects Observed with TESS - First Data Release: Bright Main-belt and Trojan Asteroids from the Southern Survey." *Ap. J. Suppl Ser*. **247**, id. 26.

Pilcher, F. (2020). "Lightcurves and Rotation Periods of 83 Beatrix, 86 Semele, 118 Peitho, 153 Hilda, 527 Euryanthe, and 549 Jessonda." *Minor Planet Bull*. **47**, 192-195.

Polakis, T. (2019). "Photometric Observations of Seventeen Minor Planets." *Minor Planet Bull*. **46**, 400-406.

Polakis, T. (2020a). "Photometric Observations of Thirty Minor Planets." *Minor Planet Bull*. **47**, 177-186.

Polakis, T (2020b). "Photometric Observations of Twenty-Seven Minor Planets." *Minor Planet Bull*. **47**, 314-321.

Pravec, P.; Wolf, M.; Sarounova, L. (2005web). Ondrejov Asteroid Photometry Project. *http://www.asu.cas.cz/~ppravec/neo.htm*

Sárneczky, K.; Szabó, G.; Kiss, L.L. (1999). "CCD observations of 11 faint asteroids." *Astrophys. J. Suppl. Series* **137**, 363-368.

Stephens, R.D. (2015). "Asteroids Observed from CS3: 2014 October - December." *Minor Planet Bull*. **42**, 104-106.

Strabla, L.; Quadri, U.; Girelli, R. (2013). "Asteroid Observed from Bassano Bresciano Observatory 2012 August - December." *Minor Planet Bull*. **40**, 83-84.

Tonry, J.L.; Denneau, L.; Flewelling, H.; Heinze, A.N.; Onken, C.A.; Smartt, S.J.; Stalder, B.; Weiland, H.J.; Wolf, C. (2018). "The ATLAS All-Sky Stellar Reference Catalog." *Astrophys. J.* **867**, A105.

Vander Haagen, G.A. (2007). "Lightcurve of Minor Planet 5740 Toutoumi." *Minor Planet Bull*. **34**, 42.

Warner, B.D. (2006). "Asteroid Lightcurve Analysis at the Palmer Divide Observatory: Late 2005 and Early 2006." *Minor Planet Bull*. **33**, 58-62.

Warner, B.D. (2008). "Asteroid Lightcurve Analysis at the Palmer Divide Observatory: September - December 2007." *Minor Planet Bull*. **35**, 67-71.

Warner, B.D.; Harris, A.W.; Pravec, P. (2009). "The asteroid lightcurve database." *Icarus* **202**, 134-146. *https://minplanobs.org/MPInfo/php/lcdb.php*

Warner, B.D. (2011). "Upon Further Review: VI. An Examination of the Previous Lightcurve Analysis from the Palmer Divide Observatory." *Minor Planet Bull*. **38**, 96-101.

Warner, B.D. (2021). *MPO Canopus* Software, version 10.8.4.11. BDW Publishing. *http://www.bdwpublishing.com*

Waszczak, A.; Chang, C.-K.; Ofeck, E.O.; Laher, R.; Masci, F.; Levitan, D.; Surace, J.; Cheng, Y.-Ch.; Ip, W.-H.; Kinoshita, D.; Helou, G.; Prince, T.A.; Kulkarini, S. (2015). "Asteroid Light Curves from the Palomar Transient Factory Survey: Rotation Periods and Phase Functions from Sparse Photometry." *Astron. J.* **150**, 75-109.

PHOTOMETRIC RESULTS FOR TWENTY MINOR PLANETS

Tom Polakis
Command Module Observatory
121 W. Alameda Dr.
Tempe, AZ 85282
tpolakis@cox.net

Mike Wiles
NAC Observatory (MPC U98)
mikewilesaz@gmail.com

(Received: 2023 December 29)

Photometric measurements were made for 20 main-belt asteroids, based on CCD observations made from 2023 October through 2023 December. Phased lightcurves were created for all twenty asteroids, and an orbital period was computed for one binary asteroid. All the data have been submitted to the ALCDEF database.

CCD photometric observations of 20 main-belt asteroids were performed at Command Module Observatory (MPC V02) in Tempe, AZ and NAC Observatory (MPC U98) in Benson, AZ.

Images were taken at V02 using a 0.32-m f/6.7 Modified Dall-Kirkham telescope, SBIG STXL-6303 CCD camera, and a 'clear' glass filter. Exposure time for the images was either 2 minutes or 1 minute. The image scale after 2×2 binning was 1.76 arcsec/pixel.

Images from U98 were taken through a clear filter using a 0.35-m Corrected Dall-Kirkham telescope operating at f/4.7 and an SBIG CCD47-10 CCD camera, whose image scale with 1×1 binning is 1.60 arcsec/pixel. Exposure times are 1 minute for brighter objects, 2 minutes for all others.

Table I shows the observing circumstances and results. All of the images for these asteroids were obtained between 2023 October and 2023 December.

Images taken at V02 were calibrated using a dozen bias, dark, and flat frames. Flat-field images were made using an electroluminescent panel. Image calibration and alignment was performed using *MaxIm DL* software.

Images taken at U98 were calibrated using bias, dark and flat frames. Flat-field images were made using an electroluminescent panel.

The data reduction and period analysis were done using *MPO Canopus* (Warner, 2023). In these fields, the asteroid and three to five comparison stars were measured. Comparison stars were selected with colors within the range of 0.5 < B-V < 0.95 to correspond with color ranges of asteroids. In order to reduce the internal scatter in the data, the brightest stars of appropriate color that had peak ADU counts below the range where chip response becomes nonlinear were selected. *MPO Canopus* plots instrumental vs. catalog magnitudes for solar-colored stars, which is useful for selecting comp stars of suitable color and brightness.

The clear-filtered images were reduced to Sloan r′ to minimize error with respect to a color term. Comparison star magnitudes were obtained from the ATLAS catalog (Tonry et al., 2018), which is incorporated directly into *MPO Canopus*. The ATLAS catalog derives Sloan *griz* magnitudes using a number of available catalogs. The consistency of the ATLAS comp star magnitudes and color-indices allowed the separate nightly runs to be linked often with no zero-point offset required or shifts of only a few hundredths of a magnitude in a series.

Data reduction for V02 images used a 9-pixel (16 arcsec) diameter measuring aperture for asteroids and comp stars. A 12-pixel (19 arcsec) diameter aperture was used for U98 images. It was typically necessary to employ star subtraction to remove contamination by field stars.

For the asteroids described here, the RMS scatter on the phased lightcurves is noted, which gives an indication of the overall data quality including errors from the calibration of the frames, measurement of the comp stars, the asteroid itself, and the period-fit. Period determination was done using the *MPO Canopus* Fourier-type FALC fitting method (Harris et al., 1989). Phased lightcurves show the maximum at phase zero. Magnitudes in these plots are apparent and scaled by *MPO Canopus* to the first night.

Asteroids were selected from the CALL website (Warner, 2011), either for having uncertain periods or for needing more lightcurves for shape modeling. In this set of observations, eight of the 10 asteroids had U = 2, two were rated as U = 1, and four had no published periods. The Asteroid Lightcurve Database (LCDB; Warner et al. (2009) was consulted to locate previously published results. All the new data for these asteroids can be found in the ALCDEF database.

488 Kreusa was discovered by Max Wolf and Luigi Carnera at Heidelberg in 1902. Stephens (2014) and Pilcher (2019) published similar rotation periods of 32.666 ± 0.003 h and 32.645 ± 0.001 h, while Colazo et al. (2022) obtained 639 ± 5 h. During this apparition, obtaining a clean lightcurve for this asteroid proved to be difficult, possibly due to a pole-on orientation or tumbling. A period similar to that of Stephens and Pilcher does appear in the period spectrum. Observing on 12 nights, 2091 data points were used to determine a period of 32.65 ± 0.02 h, with an amplitude of only 0.06 ± 0.012 mag.

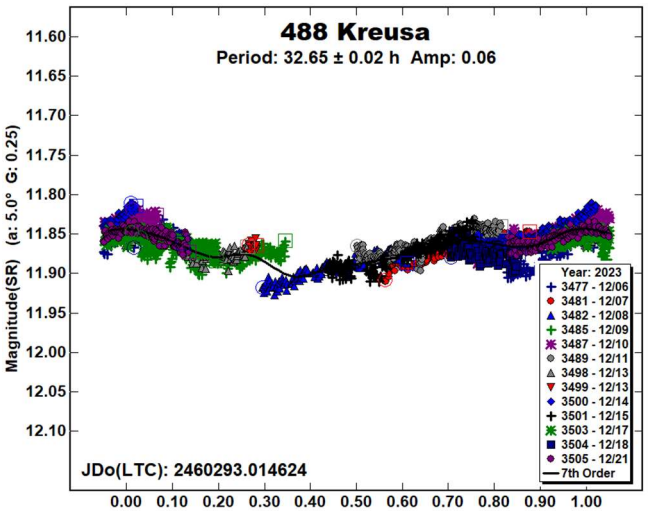

Number	Name	yy/mm/dd	Phase	L_{PAB}	B_{PAB}	Period(h)	P.E.	Amp	A.E.	Grp
488	Kreusa	23/12/06-12/21	*4.9, 1.1	86	1	32.65	0.020	0.06	0.01	MB-O
526	Jena	23/11/11-12/02	1.3, 7.3	50	-3	11.8776	0.0009	0.23	0.02	THM
542	Susanna	23/10/20-10/23	10.6,11.8	6	-10	10.091	0.008	0.28	0.02	MB-O
674	Rachele	23/11/07-11/10	7.6, 8.6	30	-7	30.82	0.07	0.14	0.01	MB-O
717	Wisisbada	23/10/05-10/25	*7.5, 2.8	26	1	480.8	2.2	0.19	0.02	MB-O
1033	Simona	23/10/10-10/20	3.8, 8.1	8	0	136.7	0.9	0.20	0.03	EOS
1048	Feodosia	23/11/02-11/04	3.6, 2.9	49	-2	10.426	0.007	0.27	0.02	MB-O
1112	Polonia	23/10/05-10/07	5.1, 5.0	14	11	18.50	0.08	0.11	0.01	EOS
1332	Marconia	23/10/21-10/24	1.1, 2.4	25	1	31.34	0.12	0.22	0.02	MARC
1372	Haremari	23/12/03-12/05	10.9,10.7	75	21	--	--	--	--	WAT
1429	Pemba	23/11/02-12/11	*5.2,16.5	48	1	836.6	0.7	0.76	0.06	MB-I
1631	Kopff	23/11/05-11/06	4.9, 4.5	47	5	6.880	0.005	0.28	0.02	MB-I
1887	Virton	23/10/05-10/20	*4.2, 4.7	18	6	69.64	0.08	0.31	0.02	EOS
2165	Young	23/10/18-10/20	6.2, 7.1	11	0	6.388	0.003	0.67	0.02	THM
2203	van Rhijn	23/11/02-11/05	2.1, 0.7	44	0	30.72	0.08	0.42	0.03	THM
2244	Tesla	23/12/03-12/07	3.4, 4.0	70	-6	--	--	--	--	MB-O
2967	Vladisvyat	23/11/05-11/06	3.5, 3.3	48	6	8.378	0.006	0.57	0.03	URS
3115	Baily	23/11/05-11/06	5.7, 6.0	38	9	16.172	0.027	0.34	0.02	MB-I
3921	Klement'ev	23/10/18-10/19	11.6,12.1	13	-12	6.740	0.019	0.17	0.04	MB-M
14835	Holdridge	23/10/21-10/29	12.9,10.5	33	14	112.2	0.3	0.56	0.03	PHO

Table I. Observing circumstances and results. The phase angle is given for the first and last date. If preceded by an asterisk, the phase angle reached an extrema during the period. L_{PAB} and B_{PAB} are the approximate phase angle bisector longitude/latitude at mid-date range (see Harris et al., 1984). Grp is the asteroid family/group (Warner et al., 2009).

526 Jena. This Themis-family asteroid was discovered in 1904 by Max Wolf at Heidelberg. Hanus et al. (2016) found a rotation period of 9.51664 ± 0.00005 h, but Erasmus et al. (2020) shows 11.877 ± 0.009 h, and Martikainen (2021) computed a similar period of 11.876510 ± 0.00000601 h. A total of 396 images were taken over the course of three nights, with a three-week wait for the third night to account for its commensurate period with half of an earth rotation. The result is a period of 11.8776 ± 0.0009 h, in agreement with Erasmus and Martikainen. The lightcurve has an amplitude of 0.23 mag, and an RMS error on the fit of 0.023 mag.

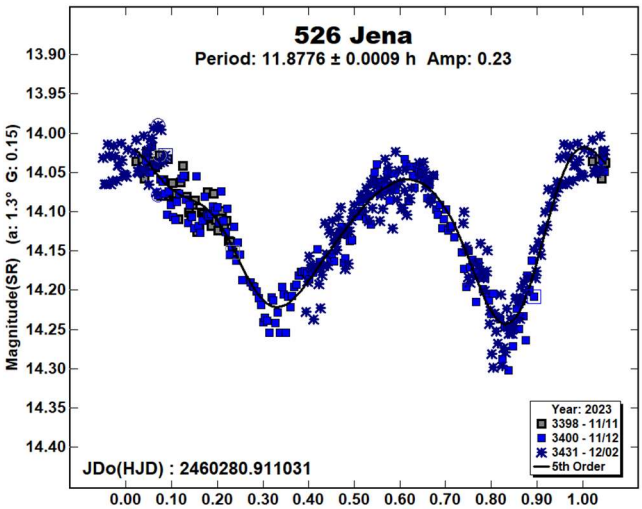

542 Susanna was discovered at Heidelberg in 1904 by Paul Götz and August Kopff. Its rotation period is well known, most recently computed by Pilcher (2022), who obtained 10.089 ± 0.001 h. During four nights, 250 images were used to compute a synodic period of 10.091 ± 0.008 h, in agreement with previous results. The amplitude is 0.28 mag, with an RMS error of 0.021 mag.

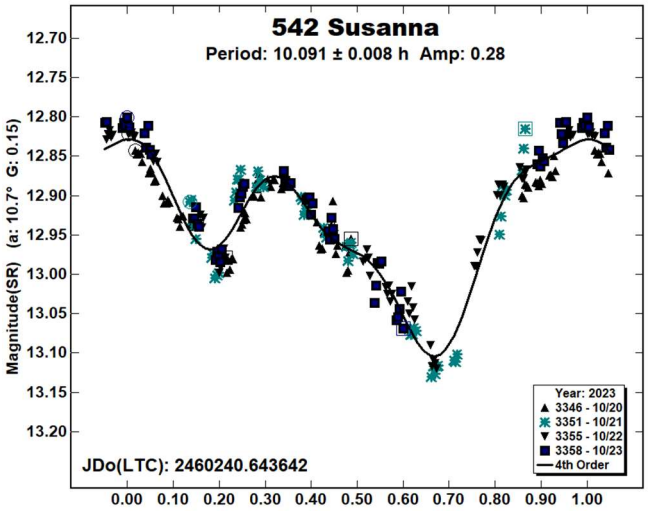

674 Rachele. Hendrik Lorenz discovered this minor planet at Heidelberg in 1904. Again, the period is established, with the most recent value of 30.957 ± 0.005 h coming from Pál et al. (2020). A total of 966 images were gathered in four nights. This analysis produced a period of 30.82 ± 0.07 h, with an amplitude of 0.14 ± 0.008 mag, agreeing with previous values.

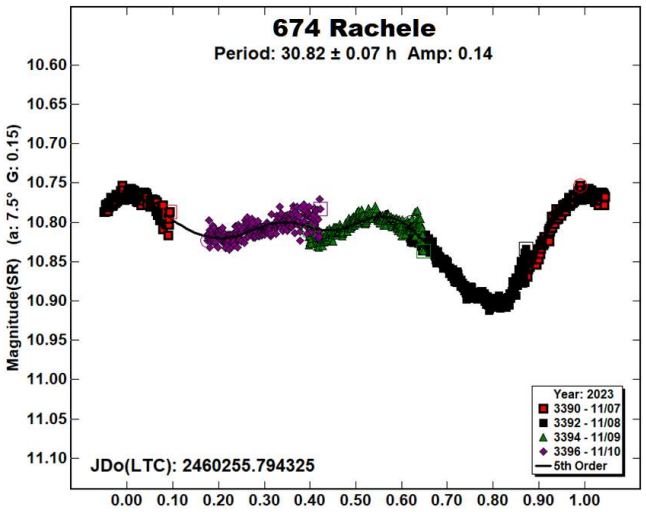

717 Wisibada, an outer main-belt asteroid, was discovered in 1911 at Heidelberg by Frederik Kaiser. No period solutions appear in the LCDB. During 21 consecutive October nights, 813 images were gathered, resulting in a period of 480.8 ± 2.2 h. The amplitude of the lightcurve is 0.19 ± 0.018 h.

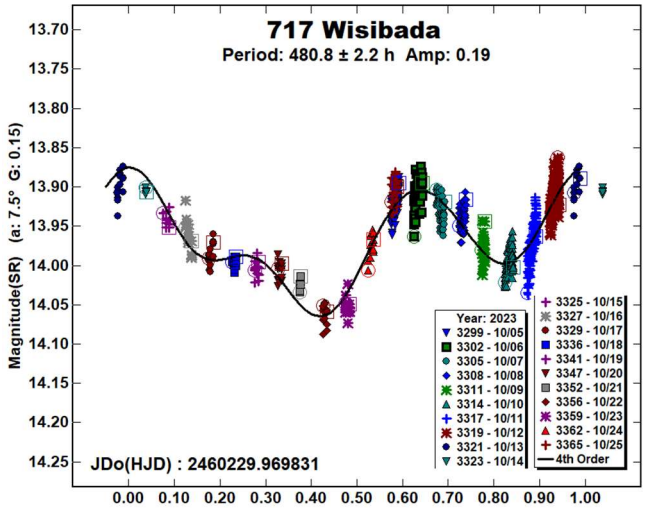

1033 Simona. George Van Biesbroeck discovered this Eos-family asteroid at Williams Bay in 1924. The only period solution in the LCDB belongs to Shipley et al. (2008), 10.07 ± 0.06 h. An 11-night run during which 380 images were taken was used to arrive at a rotation period of 136.7 ± 0.9 h, disagreeing with Shipley's result. The lightcurve has an amplitude of 0.20 mag, with an RMS error of 0.028 mag.

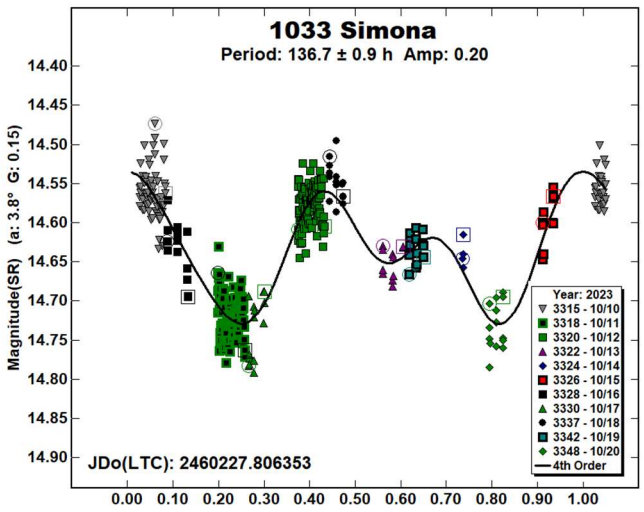

1048 Feodosia is an outer main-belt asteroid, which Karl Reinmuth discovered at Heidelberg in 1924. Polakis (2020) found a period of 10.42 ± 0.02 h, while Franco et al. (2021) computed 10.417 ± 0.001 h. Colazo et al. (2023) found a different period of 15.635 ± 0.006 h. Three nights and 235 images were sufficient to calculate a synodic period of 10.426 ± 0.007 h, in agreement with Polakis and Franco. The amplitude is 0.27 ± 0.019 mag.

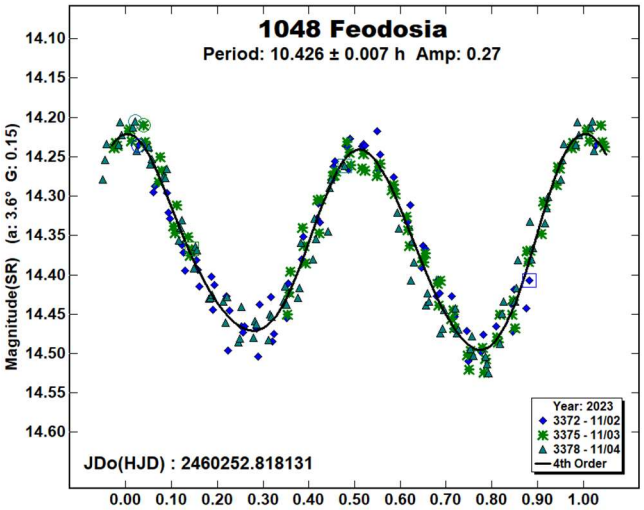

1112 Polonia. Pelageya Shajn discovered this asteroid in in 1928 at Simeis. The period computed by Behrend (2018web) is 18.605 ± 0.002h, while Polakis (2020) shows 18.71 ± 0.04 h. A total of 236 data points were acquired on three nights, resulting in a rotation period of 18.50 ± 0.08 h, agreeing with Behrend and Polakis. The amplitude of the lightcurve is 0.11 mag, with an RMS error of 0.011 mag.

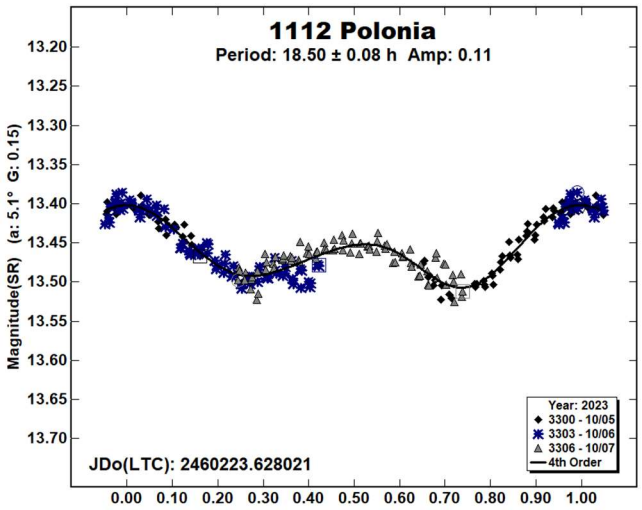

1332 Marconia was discovered in 1934 at Pino Torinese by Allesandro Volta. Durech et al. (2016) published a period solution of 19.2264 ± 0.0001 h, and Devogele et al. (2017) calculated 32.1201 ± 0.0005 h. During four nights, 376 images were gathered, resulting in a period of 31.34 ± 0.12 h, in agreement with Devogele. The amplitude is 0.22 mag., and the RMS error is 0.016 mag.

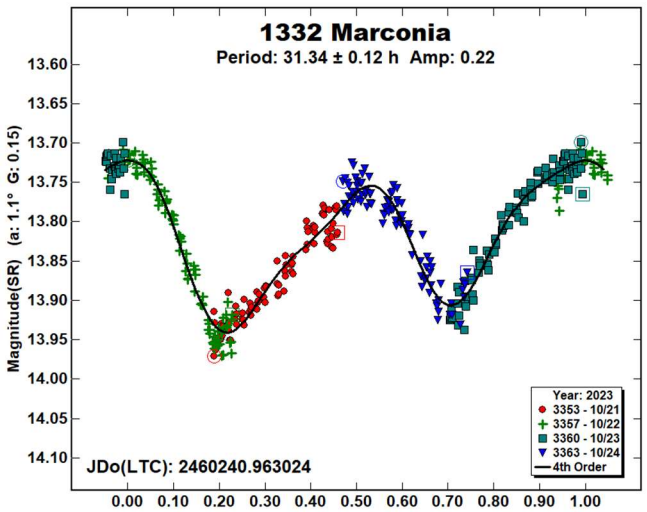

1372 Haremari is a member of the Watsonia asteroid family. Its discovery was made by Karl Reinmuth in 1935, at Heidelberg. Two similar periods appear in the LCDB; Durkee (2010), 15.25 ± 0.03 h, and Devogele et al. (2017), 1524 ± 0.03 h. It was apparent after three nights and 401 images that the amplitude would be too small for a period solution to be obtained. The raw lightcurve is provided.

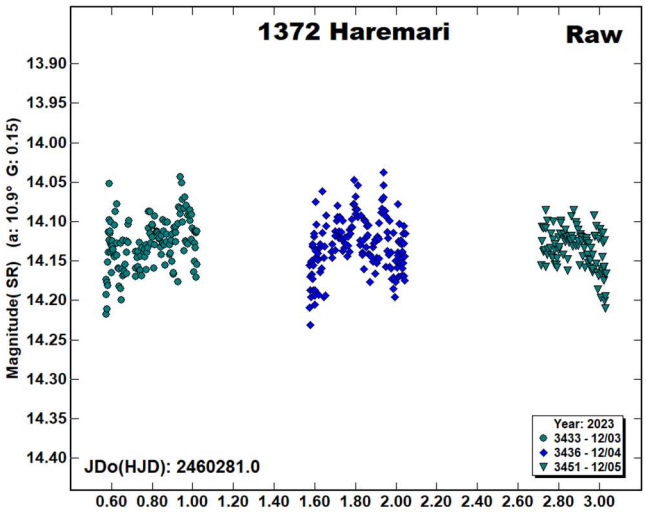

1429 Pemba is an inner main-belt minor planet in a highly eccentric orbit. Cyril Jackson discovered it at Johannesburg in 1937. The only period in the LCDB is Harris et al. (1999), >20 h. The asteroid showed only small changes in brightness, and only after several weeks did a period solution begin to emerge. After completing 38 nights of observing with only one lost to clouds, the period was determined as 836.6 ± 0.7 h, with an amplitude of 0.76 ± 0.056 mag.

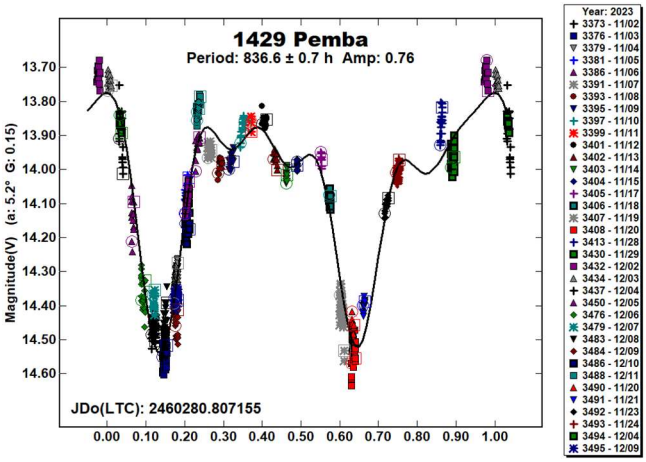

1631 Kopff. Yrjö Väisälä discovered this asteroid in 1936 at Turku, and named it after August Kopff, himself a discoverer of 68 minor planets. Sada et al. (2004) published a period of 6.683 ± 0.001 h, and Durech et al. (2020) calculated 6.68106 ± 0.00005 h. After acquiring 192 images in two nights, a synodic period of 6.680 ± 0.005 h was computed. The amplitude of the lightcurve is 0.28 ± 0.021 h.

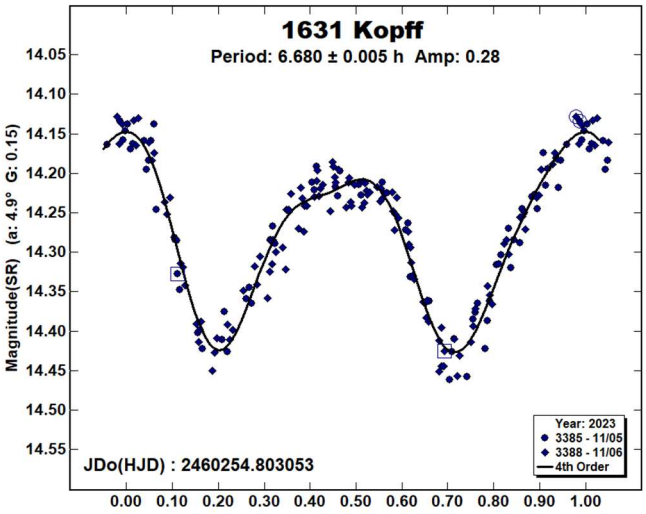

1887 Virton. This Eos-family minor planet was discovered at Uccle by Sylvain Arend in 1950. No period solutions appear in the LCDB. Over the course of nine nights, 455 images were taken. The synodic period is 69.64 ± 0.08 h, with an amplitude of 0.31 ± 0.023 mag.

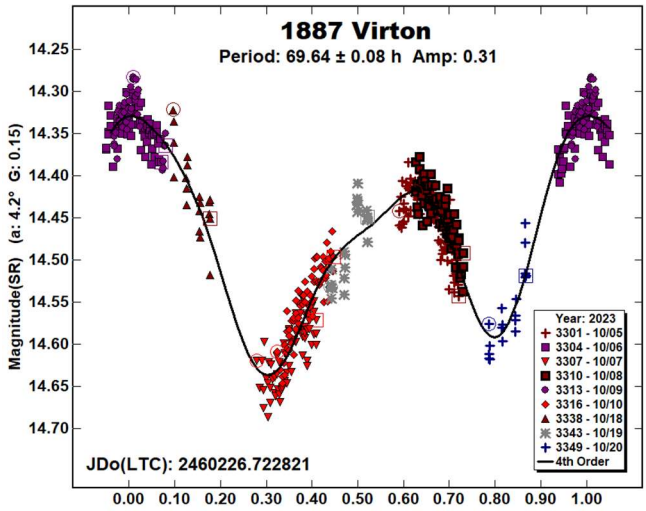

2165 Young was discovered in 1956 at Goethe Link Observatory, near Brooklyn, Indiana USA. Durech et al. (2020) shows a period of 6.39014 ± 0.00002 h, and Erasmus et al. (2020) published a value of 6.389 ± 0.003 h. A total of 247 data points acquired during three nights were used to compute a synodic period of 6.388 ± 0.003 h, in agreement with published values. The amplitude is 0.67 ± 0.055 mag.

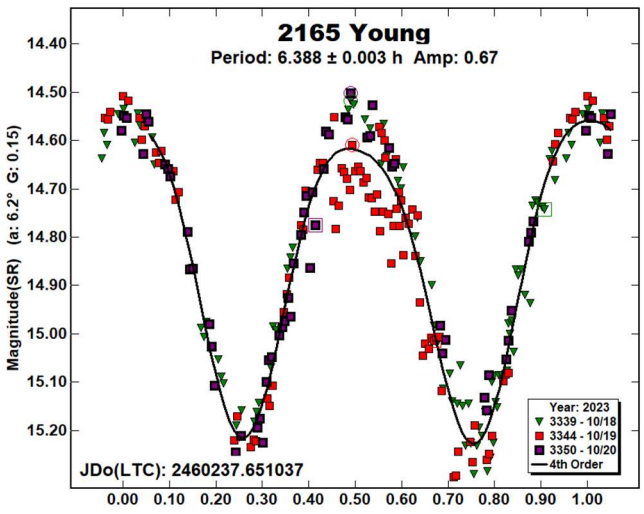

2203 van Rhijn. This member of the Themis family was discovered by Hendrik van Gent at Johannesburg in 1935. The two most recent periods in the LCDB are Durech et al. (2020), 30.6088 ± 0.0008 h, and Erasmus et al. (2020), 30.590 ± 0.067 h. In four nights, 315 data points were gathered, resulting in a period of 30.72 ± 0.08 h, and an amplitude of 0.42 ± 0.030 mag.

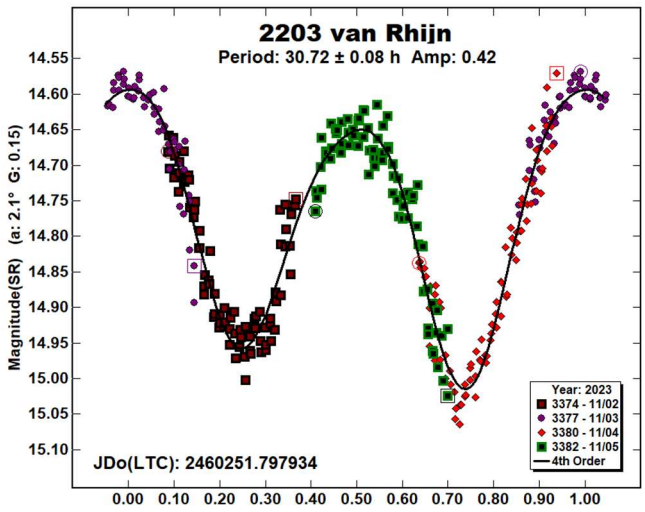

2244 Tesla was discovered at Belgrade in 1952 by Milorad Protitch. No periods appear in the LCDB. After five nights, 486 images were taken, but the amplitude is too small to discern a rotation period. The raw lightcurve is given.

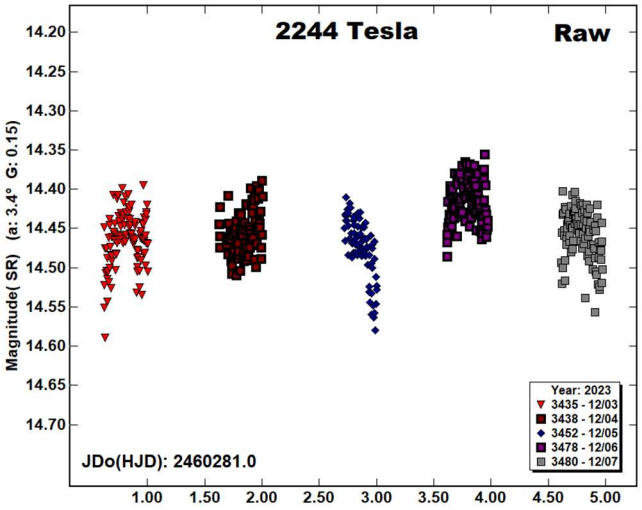

2967 Vladisvyat is a member of the Ursula family. Nikolai Chernykh discovered this minor planet at Nauchnyj in 1977. The LCDB contains no period solutions for it. Two nights and 192 images were sufficient to create a phased lightcurve, which shows a period of 8.378 ± 0.006 h, and an amplitude of 0.57 ± 0.029 mag.

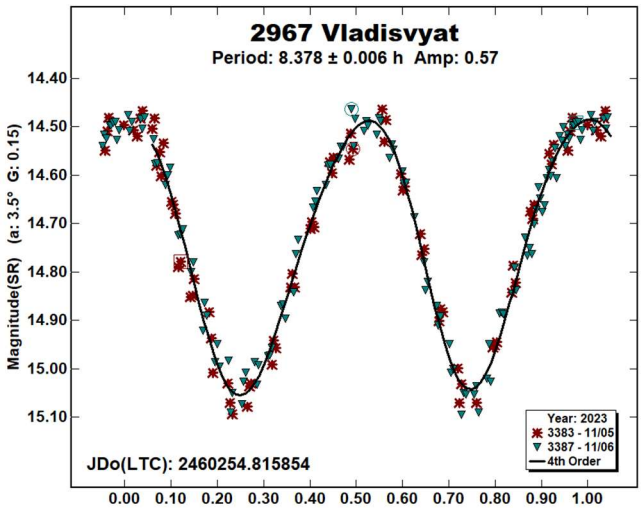

3115 Baily. Ted Bowell discovered this inner main-belt asteroid at Flagstaff in 1981. The two most recent, agreeing periods belong to Aznar et al. (2016), 16.012 ± 0.001 h, and Durech et al. (2020), 16.2414 ± 0.0005 h. During two nights, 172 images were taken, which produced a rotation period of 16.172 ± 0.027 h, and an amplitude of 0.34 ± 0.021 mag.

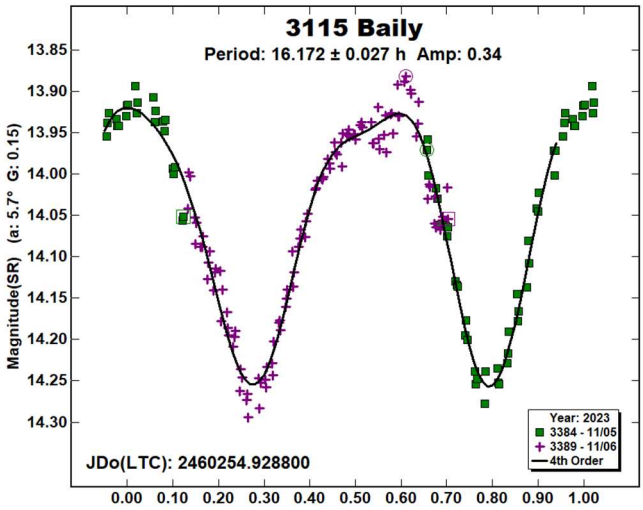

3921 Klement'ev is a member of the inner main-belt, discovered in 1971 by Bella Burnasheva at Nauchnyj. One rotation period appears in the LCDB, belonging to Behrend (2019web), who lists it as 6.754 ± 0.005 h. Two nights and 128 images were enough to determine a period of 6.740 ± 0.019 h, agreeing with Behrend's result. The amplitude is 0.17 mag, with an RMS error on the fit of 0.035 mag.

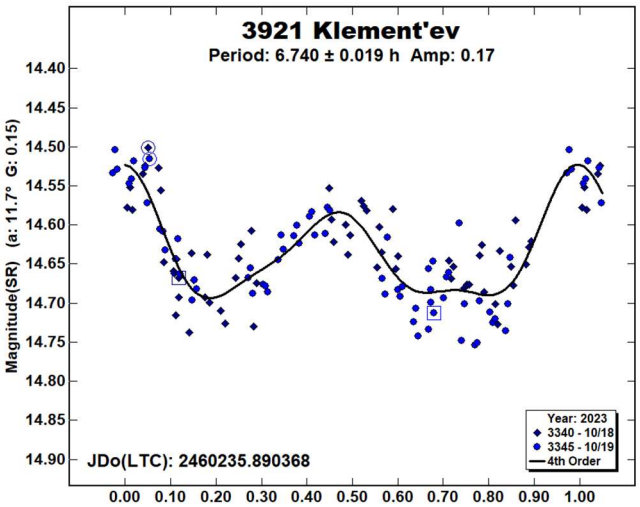

14835 Holdridge lies in a highly eccentric orbit, which brought it to a favorable opposition in 2023. It was discovered by Eugene and Carolyn Shoemaker in 1987. Pravec (2005web) gives a rotation period of >10 h. Eight nights of observing and 709 images produced a period of 112.2 ± 0.3 h, with an amplitude of 0.56 ± 0.033 mag. Some of the fit error could be accounted for by tumbling.

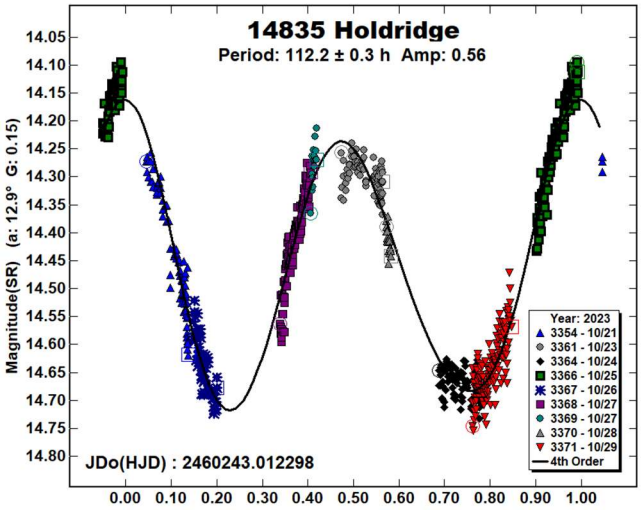

Acknowledgements

The author would like to express his gratitude to Brian Skiff for his indispensable mentoring in data acquisition and reduction. Thanks also go out to Brian Warner for support of his *MPO Canopus* software package.

References

Aznar, A. and 9 co-authors (2016). "Twenty-one Asteroid Lightcurves at Group Observadores de Asteroides (OBAS): Late 2015 to Early 2016." *Minor Planet Bull*. **43**, 257-263.

Behrend, R. (2018web, 2019web). Observatoire de Geneve web site. *http://obswww.unige.ch/~behrend/page_cou.html*

Colazo, M. and 19 co-authors (2022). "Asteroid Photometry and Lightcurve Results for Seven Asteroids." *Minor Planet Bull*. **49**, 189-193.

Colazo, M. and 17 co-authors (2023). "Asteroid Photometry and Lightcurves of Twelve Asteroids - January 2023." *Minor Planet Bull*. **50**, 147-150.

Devogele, M. and 19 co-authors (2017). "Shape and spin determination of Barbarian asteroids." *Astron. & Astrophys*. **607**, 119-141.

Durech, J.; Hanus, J.; Oszkiewicz, D.; Vanco, R. (2016). "Asteroid models from the Lowell photometric database." *Astron. & Astrophys*. **587**, 48-43.

Durech, J. and 6 co-authors (2020). "Asteroid models reconstructed from ATLAS photometry." *Astron. & Astrophys*. **643**, 59-63.

Durkee, R. (2010). "Asteroids Observed from the Shed of Science Observatory: 2009 October - 2010 March." *Minor Planet Bull*. **37**, 125-127.

Erasmus, N. and 8 co-authors (2020). "Investigating Taxonomic Diversity within Asteroid Families through ATLAS Dual-band Photometry." *Astron. & Astrophys. Suppl.* **247**, 13-19.

Franco, L. and 13 co-authors (2021). "Collaborative Asteroid Photometry from UAI: 2021 April-June." *Minor Planet Bull*. **48**, 372-374.

Hanus, J. and 19 co-authors (2016). "New and updated convex shape models of asteroids based on optical data from a large collaboration network." *Astron. & Astrophys*. **586**, 108-131.

Harris, A.W.; Young, J.W.; Scaltriti, F.; Zappala, V. (1984). "Lightcurves and phase relations of the asteroids 82 Alkmene and 444 Gyptis." *Icarus* **57(2)**, 251-258.

Harris, A.W.; Young, J.W.; Bowell, E.; Martin, L.J.; Millis, R.L.; Poutanen, M.; Scaltriti, F.; Zappala, V.; Schober, H.J.; Debehogne, H.; Zeigler, K.W. (1989). "Photoelectric Observations of Asteroids 3, 24, 60, 261, and 863." *Icarus* **77**, 171-186.

Harris, A.W.; Young, J.W.; Bowell, E.; Tholen, D. (1999). "Asteroid Lightcurve Observations from 1981 to 1983." *Icarus* **142**, 173-201.

Martikainen, J.; Muinonen, K.; Penttilä, A.; Cellino, A.; Wanx, X.-B. (2021). "Asteroid absolute magnitudes and phase curve parameters from Gaia photometry." *Astron. & Astrophys.* **649**, 98-105.

Pál, A. and 12 co-authors (2020). "Solar System Objects Observed with TESS - First Data Release: Bright Main-belt and Trojan Asteroids from the Southern Survey." *Ap. J. Supl. Ser.* **247**, 26-34.

Pilcher, F. (2019). "Rotation Period Determinations for 58 Concordia, 384 Burdigala, 464 Megaira, 488 Kreusa, and 491 Carina." *Minor Planet Bull*. **46**, 360-363.

Pilcher, F. (2022). "Lightcurves and Rotation Periods of 233 Asterope, 240 Vanadis 275 Sapientia, 282 Clorinde, 414 Liriope, and 542 Susanna." *Minor Planet Bull.* **49**, 346-349.

Polakis, T. (2020), "Photometric Observations of Thirty Minor Planets." *Minor Planet Bull*. **47**, 177-186.

Pravec, P. (2005web). Ondrejov Asteroid Photometry Project. *https://www.asu.cas.cz/~ppravec/*

Sada, P.; Canizales, E.; Armada, E. (2004). "CCD photometry of asteroids 970 Primula and 1631 Kopff using a remote commercial telescope." *Minor Planet Bull*. **31**, 49-50.

Shipley, H. and 7 co-authors (2008). "Asteroid Lightcurve Analysis at the Oakley Observatory - September 2007." *Minor Planet Bull*. **35**, 99-102.

Stephens, R.D. (2014). "Asteroids Observed from CS3: 2014 April-June." *Minor Planet Bull*. **41**, 226-230.

Tonry, J.L.; Denneau, L.; Flewelling, H.; Heinze, A.N.; Onken, C.A.; Smartt, S.J.; Stalder, B.; Weiland, H.J.; Wolf, C. (2018). "The ATLAS All-Sky Stellar Reference Catalog." *Astrophys. J.* **867**, A105.

Warner, B.D.; Harris, A.W.; Pravec, P. (2009). "The Asteroid Lightcurve Database." *Icarus* **202**, 134-146. Updated 2023 Oct. *http://www.minorplanet.info/lightcurvedatabase.html*

Warner, B.D. (2011). Collaborative Asteroid Lightcurve Link website. *http://www.minorplanet.info/call.html*

Warner, B.D. (2023). MPO Canopus Software. *http://bdwpublishing.com*

PHOTOMETRY AND LIGHTCURVE ANALYSIS OF 26 ASTEROIDS

Rafael González Farfán (Z55)
Observatorio Uraniborg
Écija, (Sevilla, SPAIN)
uraniborg16@gmail.com

Faustino García de la Cuesta (J38)
La Vara, Valdés,
(Asturias, SPAIN)

Esteban Reina Lorenz (232)
Masquefa, Can Parellada
Barcelona, (SPAIN)

Esteban Fernández Mañanes (Y90)
Noelia Graciá Ribes
Observatorio Estelia
Ladines, (Asturias, SPAIN)

José María Fernández Andújar (Z77)
Observatorio Inmaculada del Molino
Sevilla, (SPAIN)

Javier Ruiz Fernández (J96)
Observatorio de Cantabria
Cantabria, (SPAIN)

Jesús Delgado Casal (Z73)
Observatorio Nuevos Horizontes
Camas, (Sevilla, SPAIN)

Javier de Elías Cantalapiedra (L46)
Observatorio Majadahonda
Madrid, (SPAIN)

Pablo de la Fuente
Observatorio en Salamanca
Salamanca, (SPAIN)

Juan Collada
Observatorio en Deva
Deva, (Gijón, SPAIN)

(Received: 2023 November 14)

Based on observations from 2022 January to 2023 September, lightcurves and rotation periods were found for 95 Arethusa (8.705 h), 164 Eva (13.687 h), 303 Josephina (12.454 h), 310 Margarita (12.608 h), 624 Hektor (6.920 h), 631 Philippina (5.899 h), 751 Faina (23.667 h), 771 Libera (5.890 h), 841 Arabella (3.138 h), 885 Ulrique (4.893 h), 904 Rockefelia (5.022 h), 911 Agamemnon (6.592 h), 964 Subamara (6.867 h), 1511 Dalera (3.881 h), 1523 Pieksamaki (5.321 h), 1589 Fanatica (2.580 h), 2004 Lexell (5.442 h), 2965 Surikov (9.076 h), 3223 Forsius (2.460 h), 3698 Manning (3.062 h), 3710 Bogoslosvkij (8.014 h), 4253 Marker (2.397 h), 6137 Johnfletcher (6,932 h), 6147 Straub (10.304 h), 9628 Sendaiotsuna (2.674 h), and (98943) 2001 CC21 (5.023 h).

In many cases, analysis of the data we obtained for the rotation periods of 26 asteroids are in good agreement with those previously published in the literature. However, the shape and amplitudes of the lightcurve were often different because the observations were at different phase angles. We were not able to find a rotation period for 3710 Bogoslosvkij, 4523 Marker, 6137 Johnfletcher, 6147 Straub, or 9628 Sendaiotsuna.

All observations reported here were unfiltered. The images were calibrated in the standard way (bias, darks and flats). Images were measured, and periods analysis were done using *FotoDif* (Castellano, 2021) *Tycho Tracker* (Parrott, 2022) and *Periodos* (Mazzone, 2020) packages. All data were light-time corrected. The results are summarized below. Individual lightcurve plots along with additional comments as required are also presented.

95 Arethusa was previously studied by, among others, Alton (2013) in 2012. Our result of 8.705 h, based on observations in 2022 October-November, confirm Alton's period of 8.705 h. Our lightcurve amplitude is 0.32 ± 0.03 mag.

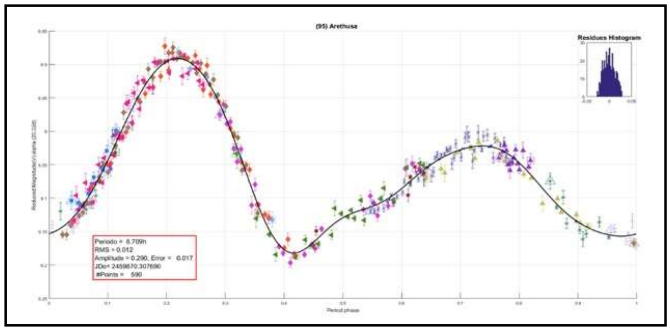

164 Eva. There are several previous results. For example, Behrend (2016web) who found a period of 13.660 h. The shape of our lightcurve is different from Behrend's, but our period is in good agreement with his. Our data, were obtained during the first half of 2023 February, gave a rotation period of 13.687 ± 0.009 hours and an amplitude of 0.09 ± 0.02 mag.

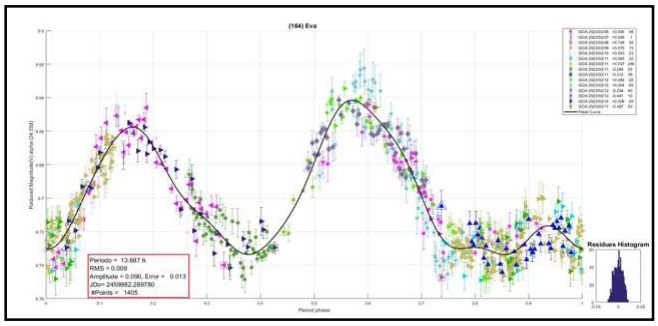

303 Josephina. Discovered in 1891 February at the Collegio Romano observatory in Rome, Italy, the rotation period we found is 12.454 ± 0.006 hours with an amplitude of 0.19 ± 0.01 mag.

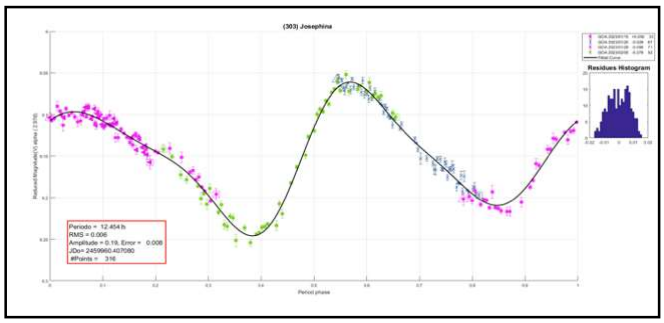

310 Margarita. Pilcher and Oey (2010) found a period of 12.070 h based on observations in 2010. Given that more than a decade had passed, we thought that an update was appropriate. Our data yielded a period of 12.068 ± 0.010 h, as previously published, and an amplitude of 0.36 ± 0.02 mag. The different lightcurve shape and amplitude from Pilcher and Oey (2010) were as expected.

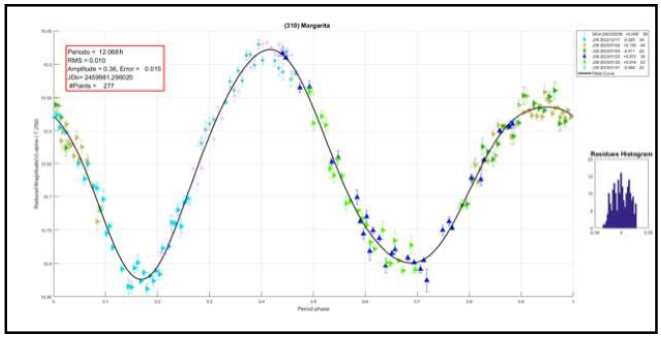

624 Hektor. The latest published reference in the LCDB for this Jupiter Trojan dates back to 2022 (Stephens and Warner, 2022), who proposed a period of 6.923 hours. Our data set of 657 points led to a very similar result of 6.920 ± 0.013 h. The lightcurve amplitude is 0.46 ± 0.02 mag.

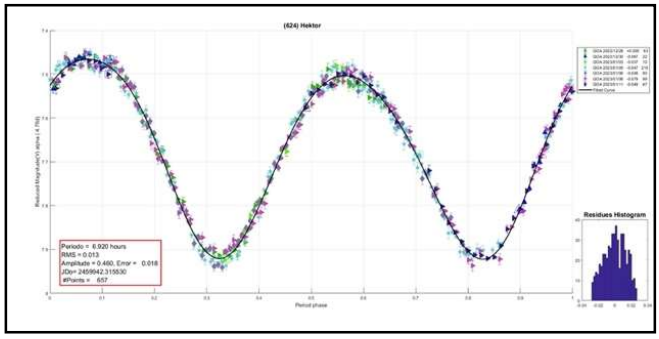

631 Philippina. For this main-belt asteroid, discovered in 1907 from Germany, we obtained results very much in line with those recently published from the Geneva observatory by Behrend (2020web). Our results were a period of 5.899 ± 0.008 hours and an amplitude of 0.20 ± 0.01 mag. There is a 3-D model from Hanuš et al. (2013) found in the DAMIT database (Durech and Jovtech, 2023).

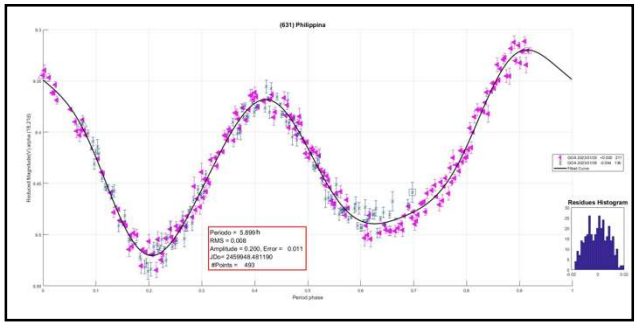

751 Faina. According to the data we obtained for this asteroid, its rotation period is 23.667 ± 0.005 hours with an amplitude of 0.12 ± 0.01 mag. Miles (1989) found almost exactly the same period. Behrend (2019web) reported a period that is one-half of ours.

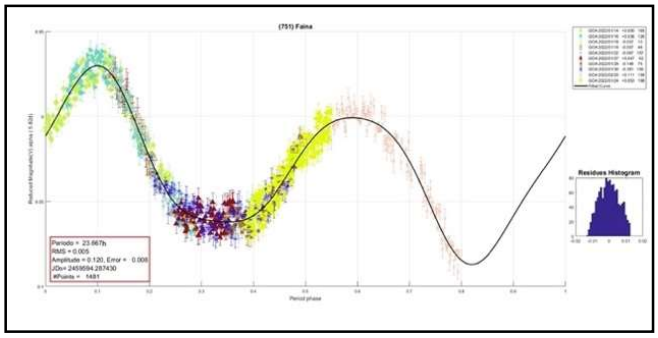

771 Libera. Our lightcurve of 569 points for this asteroid allowed us to conclude a rotation period of 5.890 ± 0.012 hours and an amplitude of 0.34 ± 0.02 mag.

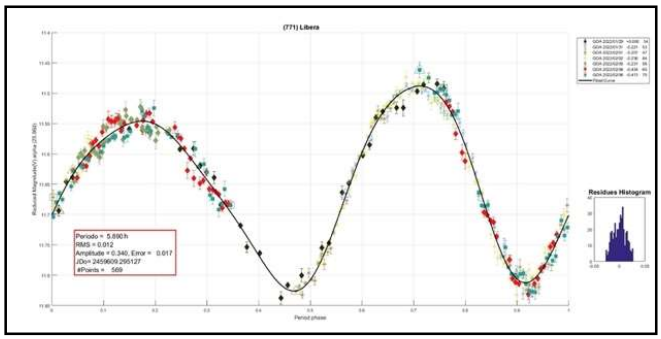

841 Arabella. Our rotation period of 3.138 ± 0.014 h is within 0.002 h of the period reported by Stephens and Warner (2019). Our lightcurve has an amplitude of 0.25 ± 0.02 mag, or about 0.07 smaller than from Stephens and Warner (2019).

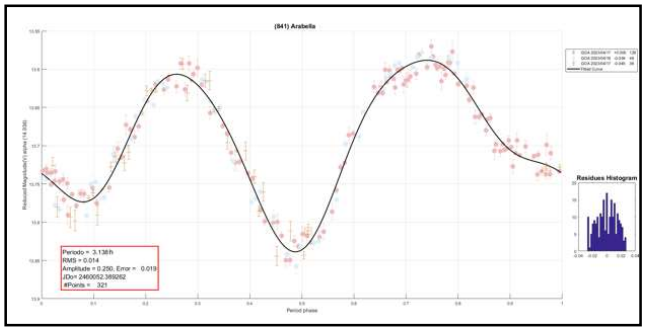

885 Ulrike. Our lightcurve for this asteroid had a total of 436 points, which allowed us to deduce a rotation period of 4.893 ± 0.024 hours and an amplitude of 0.40 ± 0.04 mag. Behrend (2020web) found a period of 4.90567 hours, making the two consistent within the error bars.

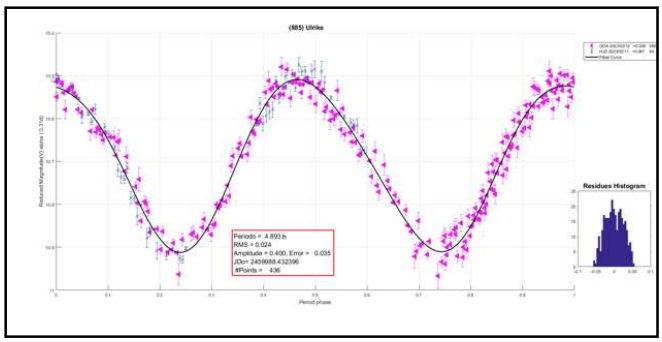

904 Rockefellia is a main-belt asteroid that was discovered on 1918 October 29 by Maximilian Franz Wolf from the observatory of Heidelberg-Königstuhl, Germany. We found a rotation period of 5.022 ± 0.017 hours and an amplitude of 0.10 ± 0.03 mag. Colazo et al. (2013) found a period of 6.823 h. The two periods have a close to 4:3 ratio, which suggests the possibility is an alias of the other.

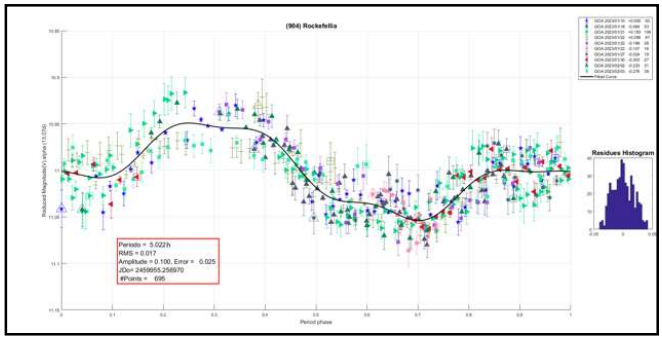

911 Agamemnon is a Trojan asteroid about 170 km in diameter. Its lightcurve and period were studied in 2021 by Stephens and Warner (2021). Our period and theirs of 6.582 hours are in good agreement. Using a data set of 550 points, we found a period of 6.592 ± 0.010 hours and amplitude of 0.17 ± 0.02 mag.

Other studies carried out by Diez Alonso et al. (2023) from the University of Oviedo (ICTEA, Spain) in 2023 suggest that the asteroid may be a binary.

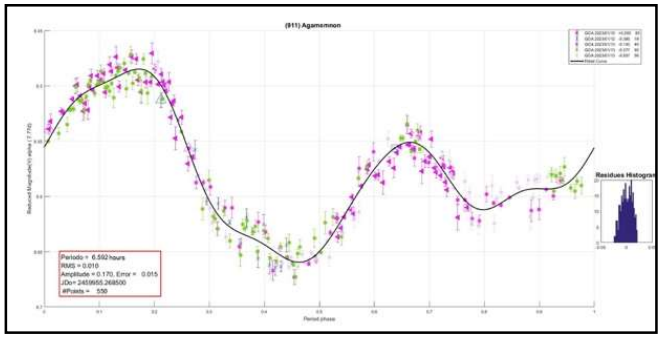

964 Subamara. There are not many references to this asteroid in the specialized literature. The most recent one in the LCDB is from Polakis (2018), who found a period of 6.8695 h. Our results are similar to his. We found a period of 6.867 ± 0.011 hours and an amplitude of 0.13 ± 0.02 mag. There is no 3-D model on DAMIT.

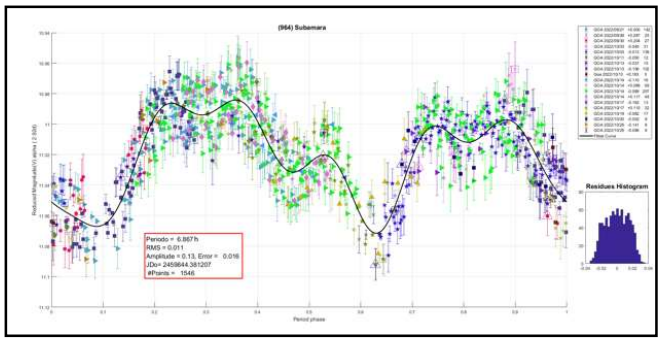

1511 Dalera. The data obtained for this asteroid allowed us to deduce a rotation period of 3.881 ± 0.012 hours, which is in accordance with a sideral period published by Durech et al. (2020). The lightcurve amplitude is 0.13 ± 0.02 mag.

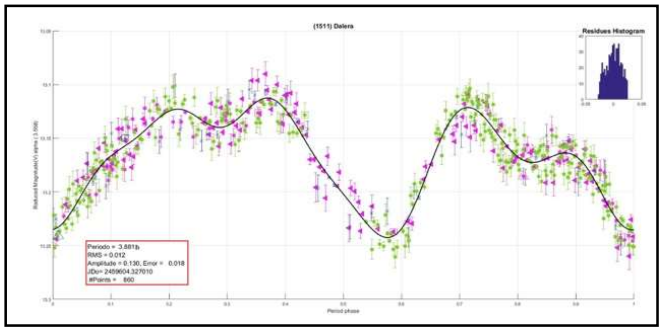

1523 Pieksamaki. Our lightcurve is based on 471 points and has a synodic period 5.321 ± 0.026 hours; its amplitude is 0.52 ± 0.04 mag. Other recent results are from Stephens and Warner (2019; 5.326 h) and Franco et al. (2023; 5.3210 h).

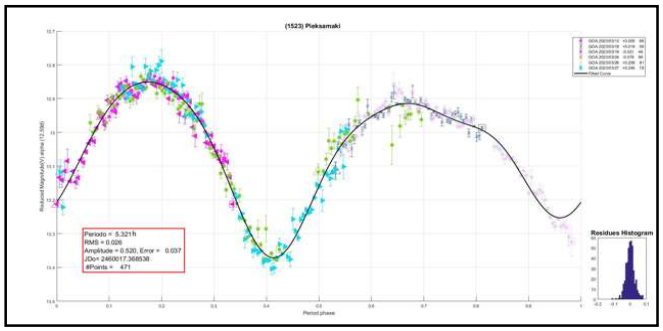

1589 Fanatica. We were able to observe this asteroid in both 2020 and 2023. The results obtained for its rotation period are in agreement with those previously published by Stephens and Warner (2020). We obtained a period of 2.580 ± 0.011 hours and amplitude of 0.17 ± 0.02 mag.

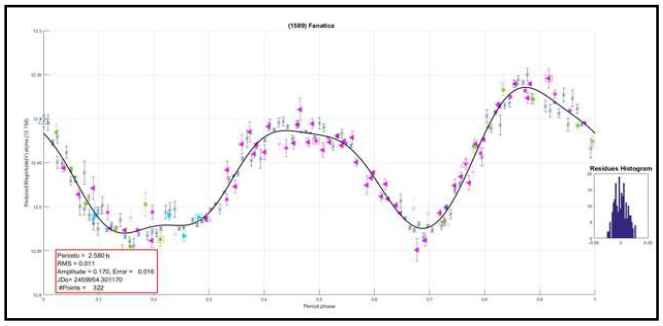

2004 Lexell. The data we obtained for this asteroid in 2023 March and April allowed us to deduce a rotation period of 5.442 ± 0.020 hours with a lightcurve amplitude of 0.48 ± 0.03 mag.

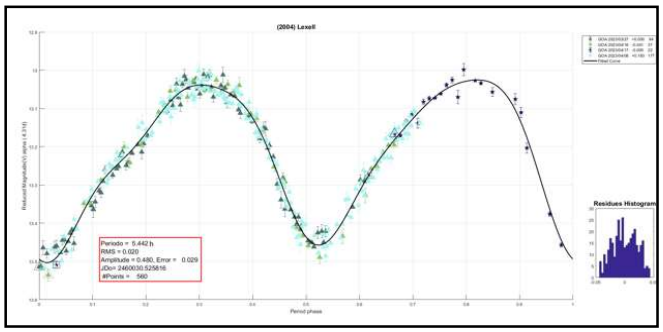

2965 Surikov. Provisionally designated as 1975 BX, this asteroid was discovered in 1975 January by Liudmila Chernyj at the Crimean Astrophysical Observatory. Our rotation period is 9.076 ± 0.019 hours and the amplitude is 0.28 ± 0.03 mag.

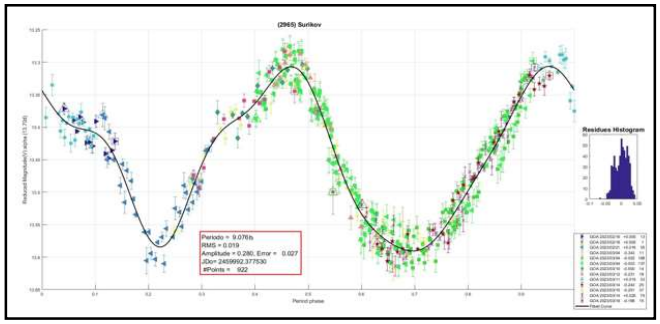

3223 Forsius. The most recent data on this asteroid found in the literature are from (Liu, 2006). Those results are in good agreement our period period of 2.460 ± 0.032 hours. The lightcurve amplitude is 0.23 ± 0.05 mag.

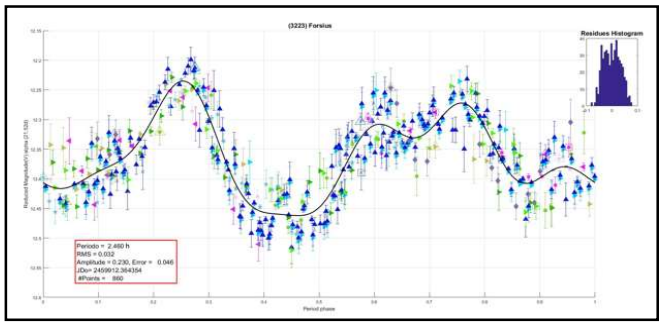

3698 Manning. According to our data, Manning is a fast rotator with P = 3.062 ± 0.034 h with a lightcurve amplitude of 0.27 ± 0.05 mag.

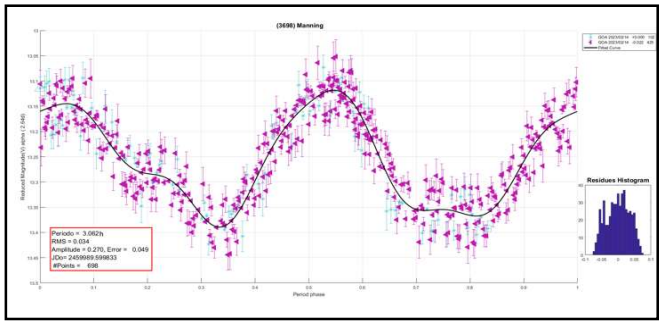

3710 Bogoslovskij. We found no previously reported period for this asteroid, which was discovered on 1978 September 13 by N.S. Chernykh from the Crimean Astrophysical Observatory.

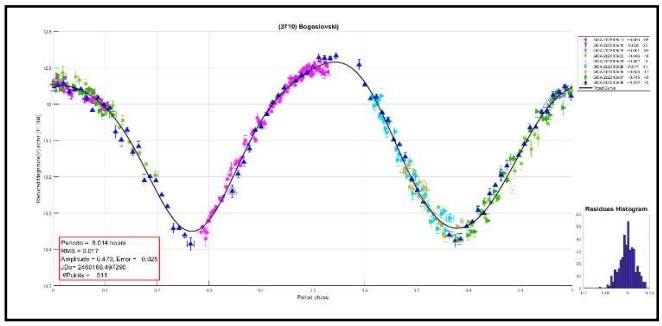

Our studies went from 2023 August to September. The lightcurve with 511 points has a period of 8.014 ± 0.017 hours and amplitude of 0.47 ± 0.03 mag.

4253 Marker. This main-belt asteroid, discovered on 1985 October 11 Carolyn Shoemaker from the Mount Palomar Observatory. Our study of this asteroid was carried out in 2023 September. The result was a short rotation period of 2.397 ± 0.030 hours and amplitude of 0.18 ± 0.04 mag.

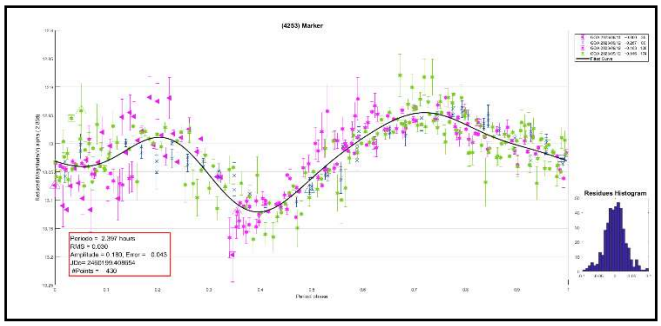

6137 Johnfletcher. We did not find a published period or lightcurve for this 31-km main-belt asteroid. Initially designated 1991 BY, it was discovered on 1991 January 25 by Akira Natori and Takeshi Urata, from Yakiimo Station, Shimizu-ku, in Japan.

Our team of asteroid observers (GOAS) carried out the study of this object in 2023 September, obtaining a result of 6.932 ± 0.013 hours for its rotation period and an amplitude of 0.31 ± 0.02 mag.

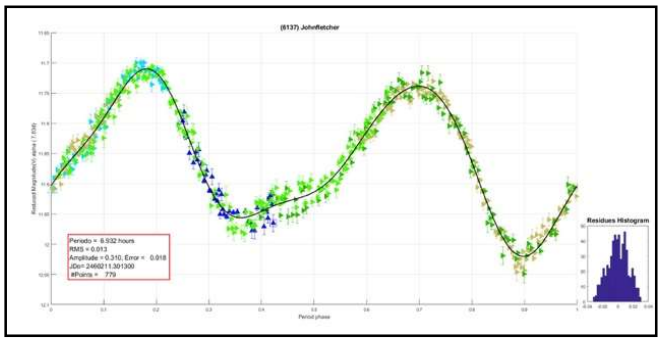

6147 Straub. Our observations of this asteroid were made in 2023 July and August. The data led to a rotation period of 10.304 ± 0.010 hours and amplitude of 0.53 ± 0.02 mag. Behrend (2023web) reported a period of 10.9 ± 0.1 h.

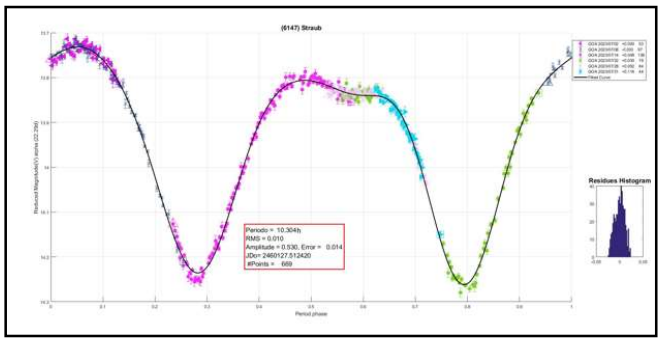

Number	Asteroid	20yy mm/dd	Phase	Period(h)	P.E.	Amp	A.E.
95	Arethusa	22/10/17-11/25	20.0-20.2	8.705	0.012	0.320	0.017
164	Eva	23/02/06-02/14	24.5-24.9	13.687	0.009	0.090	0.013
303	Josephina	23/01/15-02/05	02.9-09.4	12.454	0.006	0.190	0.008
310	Margarita	23/01/02-02/05	01.5-13.7	12.068	0.010	0.360	0.015
624	Hektor	22/12/28-01/11	04.2-06.5	6.920	0.013	0.460	0.018
631	Philippina	23/01/03-01/05	18.3-17.9	5.899	0.008	0.200	0.011
751	Faina	22/01/18-02/06	05.8-18.3	23.667	0.005	0.120	0.008
771	Libera	22/08/12-08/27	06.8-04.8	5.890	0.012	0.340	0.017
841	Arabella	23/04/17-04/18	15.3-15.7	3.138	0.014	0.250	0.019
885	Ulrike	23/02/12-02/12	17.7-17.7	4.893	0.024	0.400	0.035
904	Rockefelia	23/01/10-01/22	13.1-16.0	5.022	0.017	0.100	0.025
911	Agamemnon	23/01/10-01/14	07.8-08.3	6.592	0.010	0.170	0.015
964	Subamara	22/09/21-10/06	08.7-06.9	6.867	0.011	0.130	0.016
1511	Dalera	22/01/04-01/31	05.3-02.3	3.881	0.012	0.130	0.018
1523	Pieksamaki	23/03/14-03/27	13.0-18.0	5.321	0.026	0.520	0.037
1589	Fanatica	23/01/09-01/14	12.1-14.2	2.580	0.011	0.170	0.016
2004	Lexell	23/03/27-04/17	04.0-07.4	5.442	0.031	0.500	0.045
2965	Surikov	23/02/16-03/19	13.6-26.2	9.076	0.019	0.280	0.027
3223	Forsius	22/11/26-23/01/05	21.5-23.0	2.460	0.032	0.230	0.046
3698	Manning	23/02/13-02/14	02.8-02.4	3.062	0.034	0.270	0.049
3710	Bogoslovskij	23/08/11-09/08	11.4-08.8	8.014	0.017	0.470	0.025
4253	Marker	23/09/11-09/13	03.0-02.1	2.397	0.030	0.180	0.043
6137	Johnfletcher	23/09/23-09/30	07.8-06.0	6.932	0.013	0.310	0.018
6147	Straub	23/07/01-07/30	22.4-13.9	10.304	0.010	0.530	0.014
9628	Sendaiotsuna	23/09/09-09/10	18.1-17.8	2.674	0.009	0.080	0.013
98943	2001 CC21	23/01/29-02/01	24.5-27.5	5.020	0.026	0.710	0.037

Table I. Observing circumstances and results. Phase is the solar phase angle given at the start and end of the date range. If preceded by an asterisk, the phase angle reached an extrema during the period.

9628 Sendaiotsuna. The estimated diameter is 8.45 km based on $H = 12.42$. There were no rotation periods found in the LCDB. Our study was carried out during 2023 September. Data analysis of 668 points found a rotation period 2.674 ± 0.009 hours and an amplitude of 0.08 ± 0.02 mag.

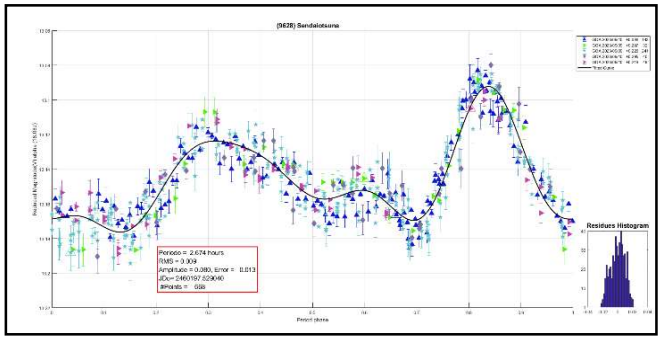

(98943) 2001 CC21. We studied this asteroid in 2023 January and February. Pravec et al. (2022web) reported 5.0247 h while Warner (2023) found 5.0159 h. Our rotation period 5.021 ± 0.020 hours is in good agreement with theirs. The lightcurve amplitude is 0.72 ± 0.02 mag, which is the smallest of the three results.

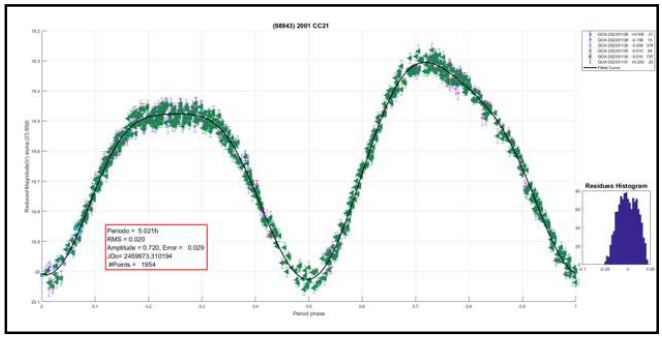

References

ALCDEF (2022). Asteroid Photometry Database. *https://alcdef.org/*

Alton, K.B. (2013). "CCD Lightcurve of 95 Arethusa." *Minor Planet Bulletin* **40**, 87-88.

Behrend, R. (-2016web, -2019web, -2020web, -2023web) Observatoire de Geneve web site. *http://obswww.unige.ch/~behrend/page_cou.html*.

Castellano, J. (2021). *FotoDif* software. *http://astrosurf.com/orodeno/fotodif/index.htm*

Colazo, M.; Fornari, C.; Ciancia, G.; Scotta, D.; Morales, M.; Melia, R.; Wilberger, A.; Suárez, N.; Monteleone, B.; García, A.; Anzola, M.; Santos, F.; Mottino, A.; Colazo, C. (2023). "Asteroid Photometry and Lightcurve Analysis for Eight Asteroids." *Minor Planet Bulletin* **50**, 235-238.

Díez Alonso, E.; Rodríguez Rodríguez, J.; Iglesias Álvarez, S.; Pérez Fernández, S.; Anangonó Tutasig, R.S.; Buendía Roca, A.; Fernández Menéndez, S.; Sánchez Lasheras, F.; de Cos Juez, F.J. (2023). "Shape and spin model for (911) Agamemnon. Hints of its Binarity Using Gaia DATA." Instituto Universitario de Ciencias y Tecnologías Espaciales de Asturias (ICTEA). Universidad de Oviedo, Spain.

Durech, J.; Tonry, J.; Erasmus, N.; Denneau, L.; Heinze, A.N.; Flewelling, H.; Vanco, R. (2020). "Asteroid models reconstructed from ATLAS photometry." *Astron. Astrophys*. **643**, A59.

Durech, J.; Jovtech, S. (2023). DAMIT (Database of Asteroid Models using Inversion Techniques). *https:/astro.troja.mff.cuni.cz/projects/damit/*

Franco, L.; Marchini, A.; Papini, R.; Iozzi, M.; Scarfì, G.; Galli, G.; Fini, P.; Betti, G.; Coffano, A.; Marinello, W.; Bacci, P.; Maestripieri, M.; Ruocco, N.; Mortari, F.; Gabellini, D.; Baj, G.; Lombardo, M.; Aceti, P.; Banfi, M.; Tinelli, L. (2023). "Collaborative Asteroid Photometry from UAI: 2023 January - March." *Minor Planet Bulletin* **50**, 228-232.

Grupo de Observación de Asteroides (GOAS). *https://sites.google.com/view/goas2*

Hanuš, J.; Brož, M.; Ďurech, J.; Warner, B.D.; Brinsfield, J.; Durkee, R.; Higgins, D.; Koff, R.A.; Oey, J.; Pilcher, F.; Stephens, R.; Strabla, L.P.; Ulisse, Q.; Girelli, R. (2013). "An anisotropic distribution of spin vectors in asteroid families." *Astron. Astrophys.* **559**, A134.

Liu, J. (2016). "Rotation Period for 3223 Forsius." *Minor Planet Bulletin* **43**, 299.

Mazzone, F. (2020). *Períodos* software. *http://www.astrosurf.com/salvador/Programas.html*

Miles, R. (1989). "The Rotation Period and Phase Relation of the Asteroid 751 Faina." *Minor Planet Bulletin* **16**, 25-27.

Parrott, D. (2022). *Tycho Tracker* software. *https://www.tycho-tracker.com/*

Pilcher, F.; Oey, J. (2010). "Rotation Period Determination for 310 Magarita." *Minor Planet Bulletin* **37**, 144.

Polakis, T. (2018). "Lightcurve Analysis for Elven Main-belt Asteroids." *Minor Planet Bulletin* **45**, 199-203.

Pravec, P.; Wolf, M.; Sarounova, L. (2022web). *http://www.asu.cas.cz/~ppravec/neo.htm*

Stephens, R.D.; Warner, B.D. (2019). "Main-Belt Asteroids Observed from CS3: 2019 January - March." *Minor Planet Bulletin* **46**, 298-301.

Stephens, R.D.; Warner, B.D. (2020). "Main-Belt Asteroids Observed from CS3: 2020 January - March." *Minor Planet Bulletin* **47**, 224-230.

Stephens, R.D.; Warner, B.D. (2021). "Lightcurve Analysis of L4 Trojan Asteroids at The Center for Solar System Studies: 2020 July to September." *Minor Planet Bulletin* **48**, 13-15.

Stephens, R.D.; Warner, B.D. (2022). "Lightcurve Analysis of L4 Trojan Asteroids at The Center for Solar System Studies: 2021 July to September." *Minor Planet Bulletin* **49**, 51-55.

Warner, B.D.; Harris, A.W.; Pravec, P. (2009). "The Asteroid Lightcurve Database." *Icarus* **202**, 134-146. Updated 2023 Oct. *http://www.minorplanet.info/lightcurvedatabase.html*

Warner, B.D. (2023) "Asteroid Lightcurve Analysis at the Center for Solar System Studies Palmer Divide Station: 2023 January - February." *Minor Planet Bulletin* **50**, 217-221.

PHOTOMETRIC OBSERVATIONS AND ROTATION PERIOD DETERMINATION FOR 14 MINOR PLANETS

Mike Wiles
NAC Observatory (MPC U98)
4126 N. Twilight Cir.
Mesa, AZ 85207
mikewilesaz@gmail.com

(Received: 2023 December 31 Revised: 2024 February 9)

Photometric measurements of fourteen main-belt asteroids were conducted from 2023 September through 2023 November. Phased lightcurves and rotation periods for each one are presented here. Six of the asteroids have no prior published period solutions. All lightcurve data has been submitted to the ALCDEF database.

CCD observations of fourteen main-belt asteroids were performed at NAC Observatory (MPC U98) in Benson, AZ. Images were taken using a 0.35m f/4.7 Corrected Dall-Kirkham telescope. Images were captured using an SBIG CCD47-10 CCD camera. It utilizes a back-illuminated Teledyne E2V CCD47-10 AIMO sensor and is operated at 1×1 binning with a scale of 1.60 arc seconds per pixel. Table I shows observing circumstances and results. All images for these observations were obtained between 2023 September and 2023 November.

Data reduction and period analysis were done using *Tycho* (Parrott, 2023). The CCD camera provides a 27'×27' field of view. The asteroid and five or more comparison stars were measured. Comparison stars were selected with colors within the range of 0.5 < B - V < 0.95 to correspond with color ranges of asteroids.

Comparison star magnitudes were obtained from the ATLAS catalog (Tonry et al., 2018), which is incorporated directly into Tycho. The ATLAS catalog derives Sloan griz magnitudes using a number of available catalogs. The consistency of the ATLAS comp star magnitudes and color indices allowed the separate nightly runs to be linked often with no zero-point offset required. The measuring aperture diameter for asteroids and comp stars was set to a value equal to the average FWHM of the session data set multiplied by four. Interference from field stars necessitated the exclusion of affected observations. Period determination was done using Tycho.

Asteroids were selected from the CALL website (Warner, 2011), either for having uncertain periods (U <= 2) or no reported period at all**.** In this set of observations, six of the fourteen asteroids had no previous period analysis listed. The Asteroid Lightcurve Database (LCDB; Warner et al., 2009) was consulted to locate previously published results. All new data for these asteroids has been submitted to the ALCDEF database.

1109 Tata is a Hygiea family asteroid with two reported periods in the LCDB. Behrend (2005web) reported a period of 8.277 ± 0.002 h and Polakis (2020) reported a differing period of 55.50 ± 0.12 h. During this apparition 402 observations were made over six nights in 2023 September. The best period fit 33.03 ± 0.01 h with an amplitude of 0.102 ± 0.011 mag. This result disagrees with those of both Behrend and Polakis.

Number	Name	yy/mm/dd	Phase	L_{PAB}	B_{PAB}	Period(h)	P.E.	Amp	A.E.	Grp
1109	Tata	23/09/24-10/05	2.3, 5.5	357	+5.0	33.03	0.01	0.102	0.011	Hygie
1887	Virton	23/11/07-11/22	11.3,15.9	19	7.3	69.65	0.01	0.373	0.018	Eos
2122	Pyatiletka	23/11/07-11/13	11.3, 8.8	66	-7.3	8.898	0.001	0.233	0.015	MB-I
2360	Volgo-Don	23/10/03-10/11	6.3, 2.1	20	-1.7	3.125	0.001	0.080	0.018	MB-M
2521	Heidi	23/09/15-10/05	*4.9, 5.8	0	+9.4	41.70	0.01	0.172	0.024	MB-I
2886	Tinkaping	23/11/02-11/12	6.0, 1.1	49	-1.7	108.0	0.1	0.919	0.018	MB-I
3476	Dongguan	23/10/12-10/31	8.7, 1.6	37	-4.5	7.019	0.001	0.287	0.017	MB-O
3803	Tuchkova	23/10/12-10/24	8.3,11.2	0	14.3	6.065	0.001	0.151	0.021	MB-O
4177	Kohman	23/10/12-10/22	11.5,14.9	359	9.9	10.831	0.001	0.069	0.022	MB-O
5147	Maruyama	23/09/15-10/20	*6.4, 9.4	5	+3.6	286.59	0.01	0.191	0.019	MB-M
9262	Bordovitsyna	23/11/08-11/23	9.4,15.3	32	11.5	15.59	0.01	0.141	0.018	Maria
15127	2000 EN45	23/11/01-11/06	11.4,13.5	22	12.5	12.85	0.01	0.283	0.013	MB-O
30598	2001 QA117	23/09/15-09/25	3.2, 7.3	347	+4.9	8.922	0.001	0.143	0.033	Eunom
30980	1995 QU3	23/09/27-10/11	22.1,21.2	22	+33	8.659	0.001	0.210	0.054	MB-O

Table I. Observing circumstances and results. The phase angle is given for the first and last date. If preceded by an asterisk, the phase angle reached an extrema during the period. LPAB and BPAB are the approximate phase angle bisector longitude/latitude at mid-date range (see Harris et al., 1984). Grp is the asteroid family/group (Warner et al., 2009).

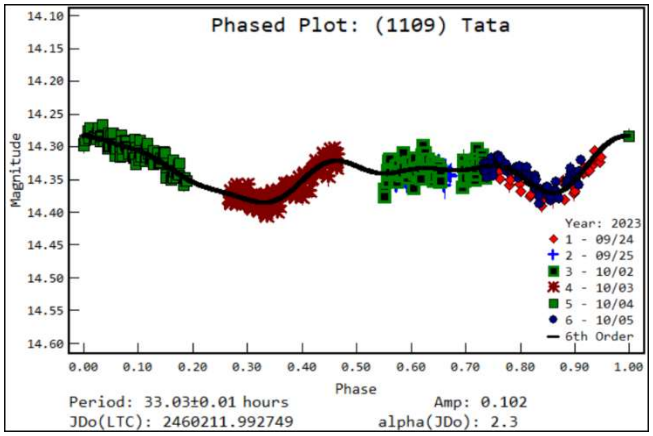

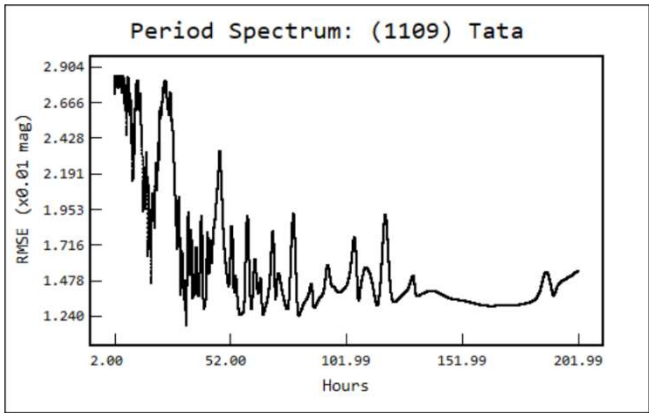

1887 Virton was discovered in 1950 by S. Arend at Uccles. No period solutions appear in the LCDB. A total of 464 data points obtained during ten nights were used to calculate a period solution of 69.65 ± 0.01 h. The amplitude of the lightcurve is 0.373 ± 0.018 mag.

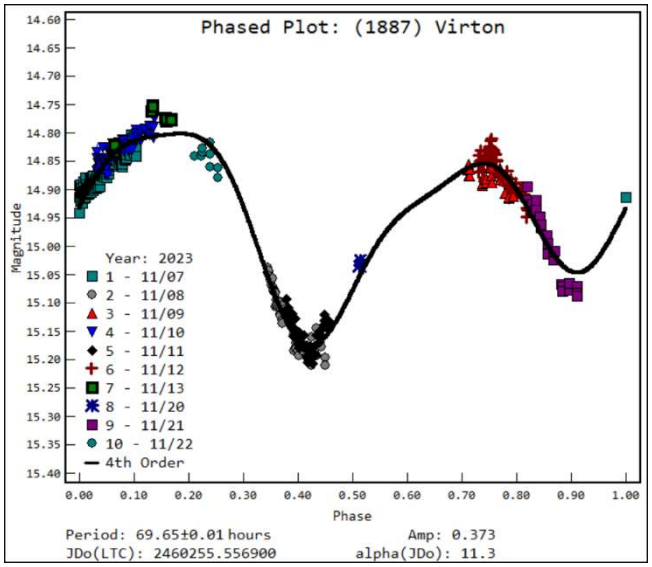

2122 Pyatiletka is an inner main-belt asteroid discovered at the Crimean Astrophysical Observatory in 1971 by T.M. Smirnova. Waszcak et al. (2015) reported a period of 8.899 ± 0.0053 h and Durech et al. (2020) reported a similar period of 8.90167 ± 0.00003 h. Observing over six nights during the 2023 November, 347 observations were made. A period solution of 8.898 ± 0.001 h was calculated with an amplitude of 0.233 ± 0.015 mag. This is also in close agreement with the results of Durech et al. and Waszcak et al.

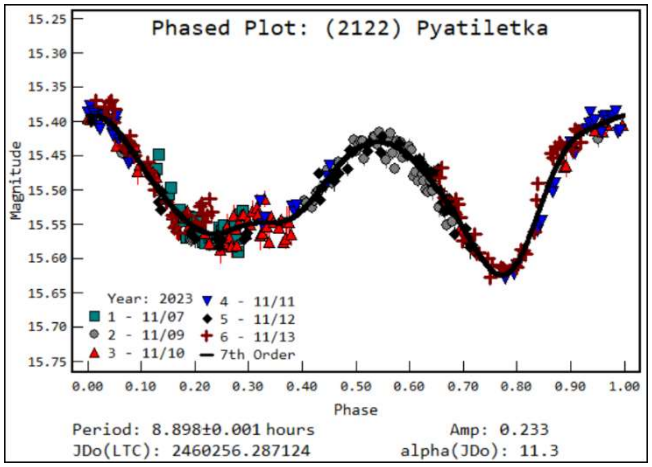

2360 Volgo-Don is a main belt asteroid discovered by T. Smirnova at Nauchnyj in 1975. No period solutions have been identified in the LCDB. Over 5 nights in 2023 October, 247 observations were obtained to calculate a rotational period of 3.125 ± 0.001 h. The amplitude of the light curve is 0.080 ± 0.018 mag.

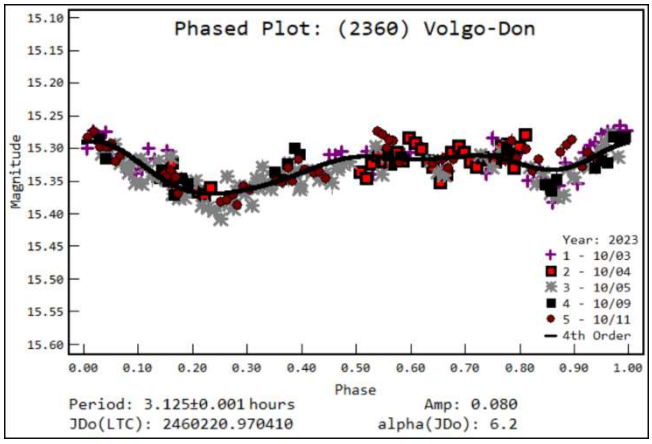

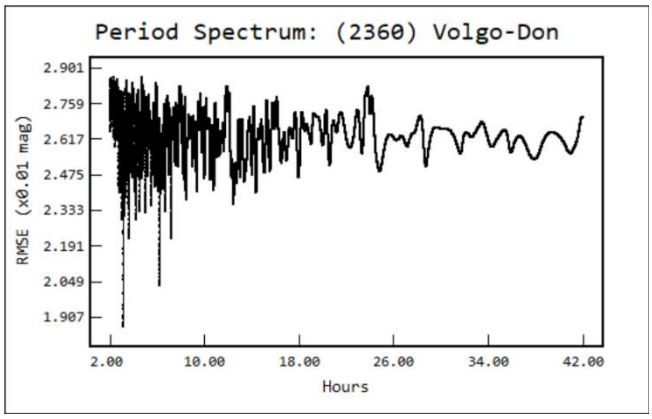

2521 Heidi was discovered in 1979 by Paul Wild at Zimmerwald. Behrend (2004web) reported a period solution of 12 hours but noted that it was a meaningless solution due to a low amplitude/uncertainty ratio. Durech et al. (2019) reported a period solution of 41.5665 ± 0.0002 h. During a 20-day period, 528 observations were made on 12 nights. A period solution of 41.70 ± 0.01 h was calculated from the observations. The amplitude of the light curve is 0.172 ± 0.024 mag.

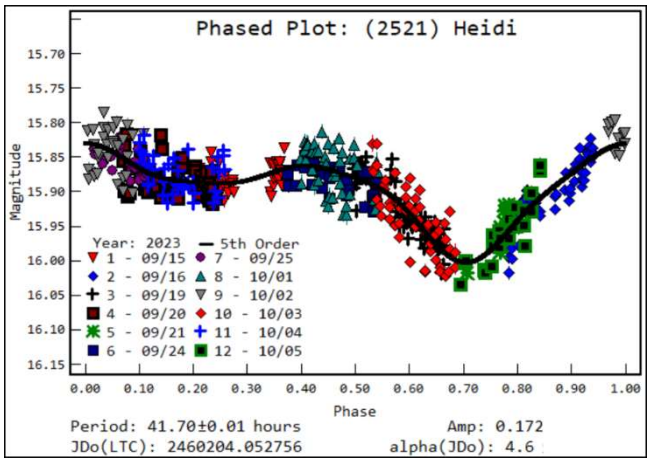

2886 Tinkaping is an inner main-belt asteroid discovered by Purple Mountain Observatory at Nanking in 1965. Wisniewski et al. (1997) published a period of 12 ± 6 h. Also found in the LCDB is a published period of 107.116 ± 0.007 h by Durech et al. (2020). Observations for the 2023 apparition were obtained on 11 consecutive nights providing 446 data points for a light curve. The period determined from those observations is 108.0 ± 0.1 h, in agreement with the period from Durech et al. The amplitude of the light curve is 0.919 ± 0.018 mag.

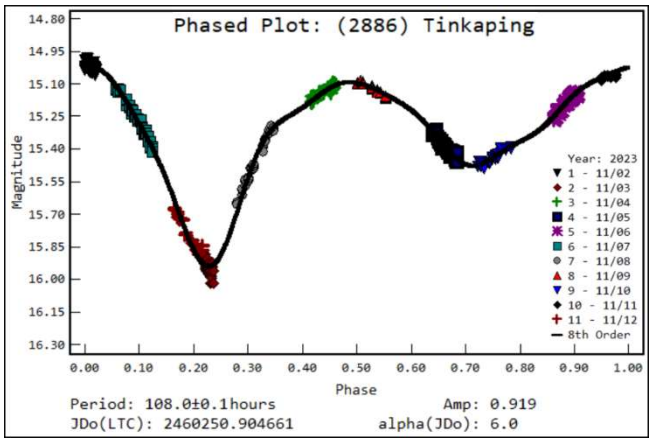

3476 Dongguan is an outer main-belt asteroid discovered in 1978 by Purple Mountain Observatory at Nanking. No periods are shown in the LCDB. During eight nights in 2023 October, 421 images were gathered, producing a period solution of 7.019 ± 0.001 h. The amplitude is 0.287 mag., and the RMS error on the fit is 0.017 mag.

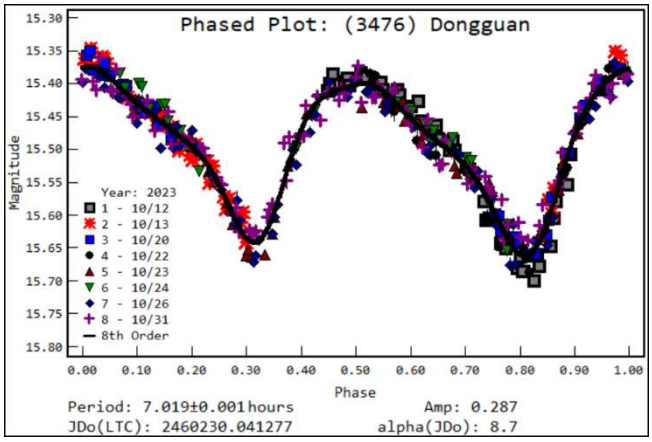

3803 Tuchkova is an outer main-belt asteroid discovered at Nauchnyj by L. Zhuravleva in 1981. Durech et al (2020) reported a period of 6.07014 ± 0.00003 h for this body. The author conducted a campaign of 320 observations in 2023 October and calculated a rotation period of 6.065 ± 0.001 h. This is in agreement with Durech et al.'s observations from 2020. The amplitude of the light curve is 0.151 mag and the RMS error on the fit is 0.021 mag.

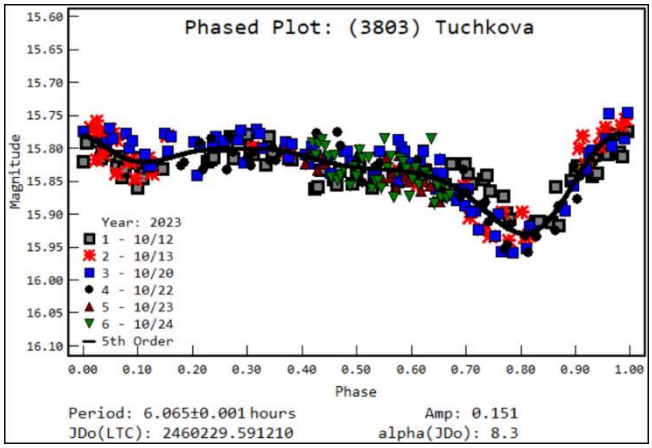

4177 Kohman was discovered at Lowell Observatory's Anderson Mesa Station near Flagstaff by E. Bowell in 1987. There are no reported solutions for the period in the LCDB. A total of 234 data points obtained during four nights were used to calculate a period solution of 10.831 ± 0.001 h. The amplitude of the lightcurve is 0.069 ± 0.022 mag.

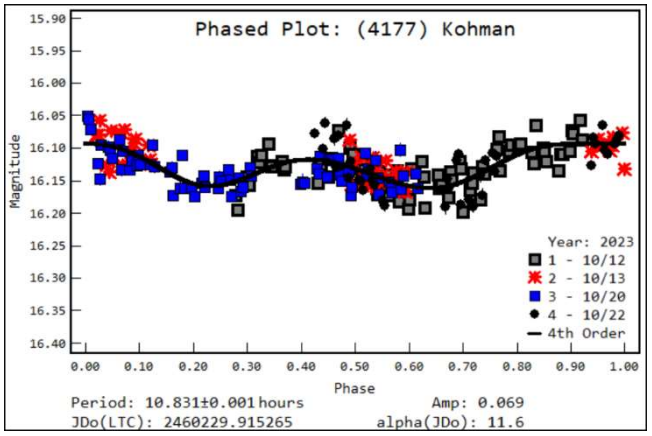

5147 Maruyama is a main-belt asteroid with an estimated diameter of 7.655 km. It was discovered in 1992 by S. Ueda and H. Kaneda at Kushiro. Hayes-Gehrke et al. (2023) reported a period solution of 50.9 ± 0.1h, but noted in their observations that the period should considered provisional and that more data was needed. This author collected 439 images observing on 16 nights of a 35- day interval during the 2023 apparition. Observations were used to calculate a rotational period of 286.59 ± 0.01 h disagreeing with the period reported by Hayes-Gehrke et al. The amplitude of the light curve is 0.191 ± 0.019 mag.

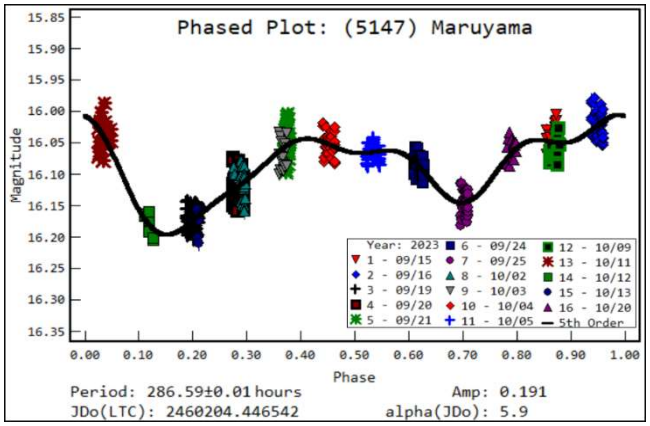

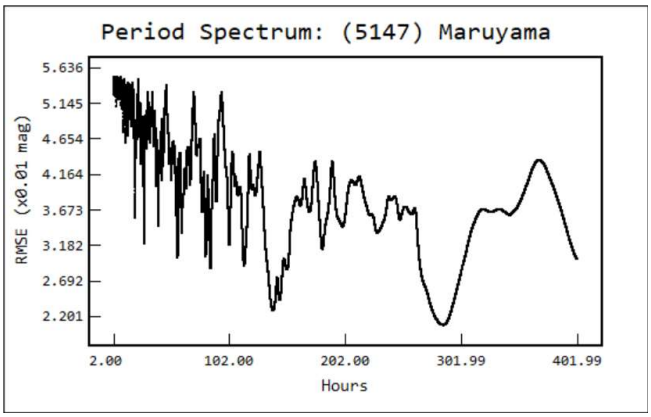

9262 Bordovitsyna was discovered in 1973 by T.M. Smirnova at Crimean Astrophysical Observatory. Sárneczky et al. (1999) reported an estimated period of 9 hours based on a data set consisting of less than a full period. During 2023 November the asteroid was observed on ten nights in a fifteen-night interval. A total of 669 images were taken and reduced to calculate a period solution of 15.59 ± 0.01 h with an amplitude of 0.141 ± 0.018 mag. The calculated period is in disagreement with the Sárneczky et al. period.

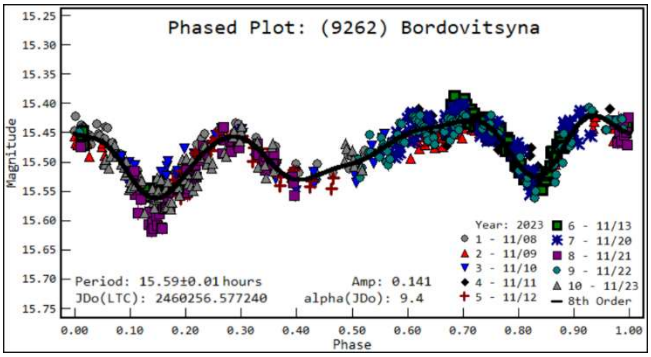

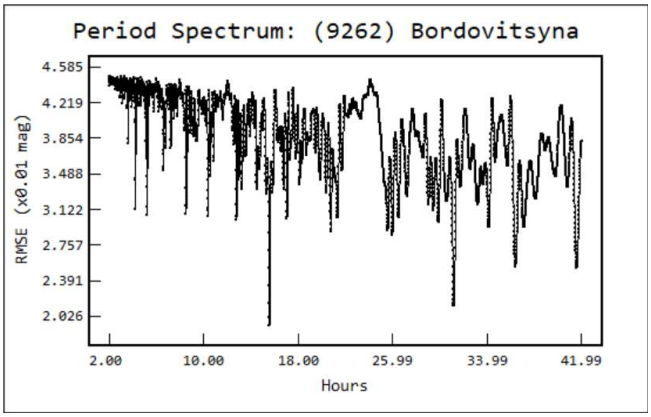

15127 2000 EN45 was discovered in 2000 by LINEAR at Socorro. It has a 20-degree inclined orbit, and was passing through the plane of the ecliptic near its closest approach to Earth (1.2 AU) during the 2023 apparition. This presented a favorable observing opportunity compared to future upcoming apparitions. 688 images were captured on six consecutive nights to establish a rotation period, as no published periods are listed in the LCDB. Those observations produced a light curve indicating a period of 12.85 ± 0.01 h with an amplitude of 0.283 ± 0.013 mag.

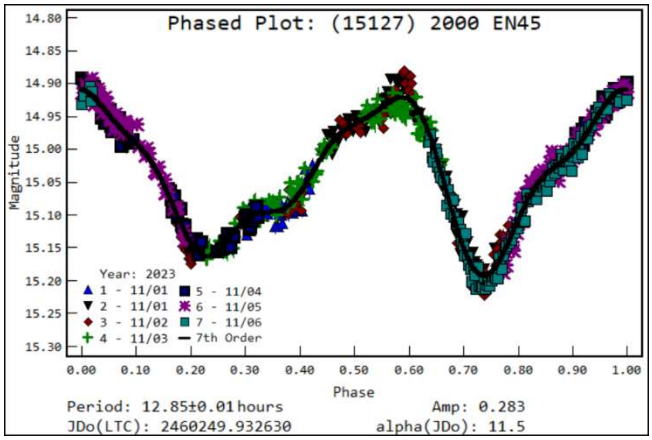

30598 2001 QA117 was reported to have a period of 8.709 ± 0.0031 h by Wasczak et al. (2015). In 2023 September the author observed the asteroid on 7 nights of a 10 night period, capturing 256 images in the process. A rotational period of 8.922 ± 0.001 h with an amplitude of 0.143 ± 0.033 mag was calculated from the observations. Though the notes on the Wasczak et al. observations mentioned a low confidence in the period, the author's results are in agreement.

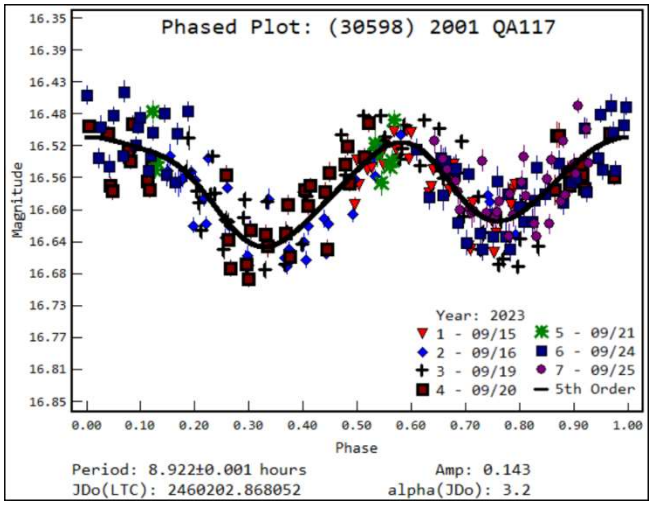

30980 1995 QU3 is an outer main belt asteroid with an orbit inclined 24º to the plane of the ecliptic. There are no reported periods for this asteroid in the LCDB. 324 data points were obtained during five nights to calculate a period solution of 8.659 ± 0.001 h. The fit is poor with an RMS error of 0.054 mag.

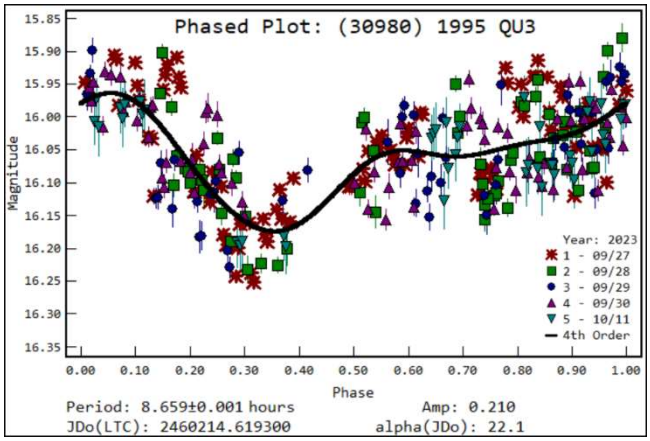

Acknowledgements

The author would like to thank Tom Polakis for his many years of encouragement and mentorship. Thanks also go out to Daniel Parrott for his responsive support of the *Tycho* software package.

References

Behrend, R. (2004web, 2005web). Observatoire de Geneve web site. *http://obswww.unige.ch/~behrend/page4cou.html*

Durech, J.; Hanus, J.; Vanco, R. (2019). "Inversion of asteroid photometry from Gaia DR2 and the Lowell Observatory photometric database." *Astron. Astrophys.* **631**, A2.

Durech, J.; Tonry, J.; Erasmus, N.; Denneau, L.; Heinze, A.N.; Flewelling, H.; Vančo, R. (2020). "Asteroid models reconstructed from ATLAS photometry." *Astron. Astrophys.* **643**, A59.

Harris, A.W.; Young, J.W.; Scaltriti, F.; Zappala, V. (1984). "Lightcurves and phase relations of the asteroids 82 Alkmene and 444 Gyptis." *Icarus* **57(2)**, 251-258.

Hayes-Gehrke, M.; Arcilesi, C.; Batres, J.; Byrne, W.; Devan, J.; Eichenwald, V.; Goodwin, N.; Huang, B.; Joshi, S.; Karafotias, C.; Maxwell, N.; Pereyra, N.; Brincat, S.M.; Galdies, C. (2023). "Lightcurve Analysis and Rotation Period for Asteroid 5147 Maruyama." *Minor Planet Bulletin* **50**, 15

JPL (2022). Small-Body Database Browser. *https://ssd.jpl.nasa.gov/sb/orbits.html*

Parrot, D. (2023). Tycho software. *https://www.tycho-tracker.com*

Polakis, T. (2020). "Photometric Observations of Thirty Minor Planets." *Minor Planet Bulletin* **47**, 177.

Sárneczky, K.; Szabó, Gy.; Kiss, L.L. (1999). "CCD Observations of 11 faint asteroids." *Astron. Astrophys. Suppl.* **137**, 363.

Tonry, J.L.; Denneau, L.; Flewelling, H.; Heinze, A.N.; Onken, C.A.; Smartt, S.J.; Stalder, B.; Weiland, H.J.; Wolf, C. (2018). "The ATLAS All-Sky Stellar Reference Catalog." *Astrophys. J.* **867**, A105.

Warner, B.D.; Harris, A.W.; Pravec, P. (2009). "The Asteroid Lightcurve Database." *Icarus* **202**, 134-146. Updated 2023 Apr. *https://www.minorplanet.info/php/lcdb.php*

Warner, B.D. (2011). Collaborative Asteroid Lightcurve Link website. *https://www.minorplanet.info/php/call.php*

Waszczak, A.; Chang, C.; Ofek, E.; Laher, R.; Masci, F.; Levitan, D.; Surace, J.; Cheng, Y.; Ip, W.; Kinoshita, D.; Helou, G.; Prince, T.; Kulkarni, S. (2015). "Asteroid Light Curves from the Palomar Transient Factory Survey: Rotation Periods and Phase Functions from Sparse Photometry." *Astron. J.* **150**, A75.

Wisniewski, W.Z.; Michalowski, T.M.; Harris, A.W.; McMillan, R.S. (1997). "Photometric Observations of 125 Asteroids." *Icarus* **126**, 395.

ASTEROID PHOTOMETRY OF EIGHT ASTEROIDS

Milagros Colazo
Astronomical Observatory Institute, Faculty of Physics,
Adam Mickiewicz University,
ul. Słoneczna 36, 60-286 Poznań, Poland.
Grupo de Observadores de Rotaciones de Asteroides (GORA),
Argentina, https://aoacm.com.ar/gora/index.php
milirita.colazovinovo@gmail.com

Bruno Monteleone
Osservatorio Astronomico "La Macchina del Tempo" (MPC M24)
Ardore Marina (Reggio Calabria - Italia)

Francisco Santos
Observatorio Astronómico Giordano Bruno (MPC G05)
Piconcillo (Córdoba - España)

Alberto García
Observatorio Río Cofio (MPC Z03)
Robledo de Chavela (Madrid - España)

Giuseppe Ciancia
CapoSudObservatory (GORA CS1)
Palizzi Marina (Reggio Calabria - Italia)
CapoSudObservatory (GORA CS2)
Palizzi Marina (Reggio Calabria - Italia)
Specola "Giuseppe Pustorino 3" (GORA GC3)
Palizzi Marina (Reggio Calabria - Italia)

Mario Morales
Observatorio de Sencelles (MPC K14)
Sencelles (Mallorca - Islas Baleares - España)

Raúl Melia
Observatorio de Raúl Melia Carlos Paz (GORA RMC)
Carlos Paz (Córdoba - Argentina)

Tiago Speranza, Axel Ortiz
Observatorio Astronómico Municipal Reconquista (GORA OMR)
Reconquista (Santa Fe - Argentina)

Damián Scotta
Observatorio de Damián Scotta 1 (GORA ODS)
San Carlos Centro (Santa Fe - Argentina)

Néstor Suárez
Observatorio Antares (MPC X39)
Pilar (Buenos Aires - Argentina)

Paolo Aldinucci
Osservatorio Astronomico di Orciatico (OAL)
Lajatico (Pisa - Italia)

Nicola Montecchiari
Elijah Observatory (MPC M27)
Lajatico (Pisa - Italia)

Aldo Wilberger
Observatorio Los Cabezones (MPC X12)
Santa Rosa (La Pampa - Argentina)

Marcos Anzola
Observatorio Astronómico Vuelta por el Universo (GORA OMA)
Córdoba (Córdoba - Argentina)

Carlos Colazo
Observatorio Astronómico El Gato Gris (MPC I19)
Tanti (Córdoba - Argentina)

(Received: 2023 December 11 Revised: 2024 February 6)

Synodic rotation periods and amplitudes are reported for: 343 Ostara, 366 Vincentina, 892 Seeligeria, 914 Palisana, 1112 Polonia, 1237 Genevieve, 1332 Marconia, and 1496 Turku.

The periods and amplitudes of asteroid lightcurves presented in this paper are the product of collaborative work by the GORA (Grupo de Observadores de Rotaciones de Asteroides) group. In all the studies, we have applied relative photometry assigning *V* magnitudes to the calibration stars.

The image acquisition was performed without filters and with exposure times of a few minutes. All images used were corrected using dark frames and, in some cases, bias and flat-field corrections were also used. Photometry measurements were performed using *FotoDif* software and for the analysis, we employed *Períodos* software (Mazzone, 2012).

Below, we present the results for each asteroid studied. The lightcurve figures contain the following information: the estimated period and period error and the estimated amplitude and amplitude error. In the reference boxes, the columns represent, respectively, the marker, observatory MPC code, or - failing that - the GORA internal code, session date, session offset, and several data points.

Targets were selected based on the following criteria: 1) those asteroids with magnitudes accessible to the equipment of all participants, 2) those with favorable observation conditions from Argentina or Spain, i.e., with negative or positive declinations δ, respectively, and 3) objects with few periods reported in the literature and/or with Lightcurve Database (LCDB) (Warner et al., 2009) quality codes (U) of less than 3.

In this work, we present measurements of periods corresponding to asteroids previously analyzed by our team. These light curves display improved results and are part of a new long-term project that we are initiating.

343 Ostara. This asteroid was discovered in 1892 by M. Wolf. In the literature, we found two rather different periods calculated for this object: P = 6.42 h (Binzel, 1987) and P = 110.027 ± 0.001 h (Martikanien et al., 2021). The results we obtained, P = 109.35 ± 0.01 h with Δm = 0.55 ± 0.01 mag, are consistent with the longer period proposed by Martikanien.

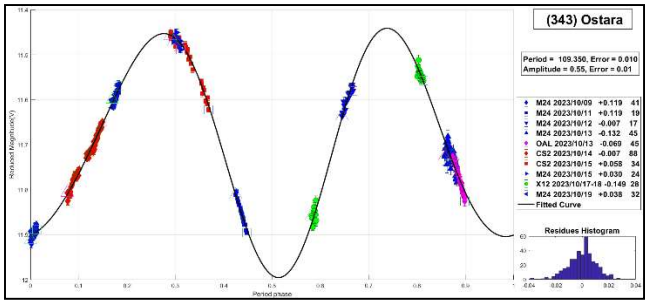

366 Vincentina. This asteroid was discovered in 1893 by A. Charlois. Two different periods were reported in the literature. Robinson (2002) found a period of 15.5 ± 0.1 h, whereas Benishek (2013) measured a period of P = 12.7365 ± 0.0005 h. In this work, we provide similar results and propose P= 17.348 ± 0.0009 h and Δm = 0.11 ± 0.01 mag. This diagram validates our previous result (Colazo et al., 2021).

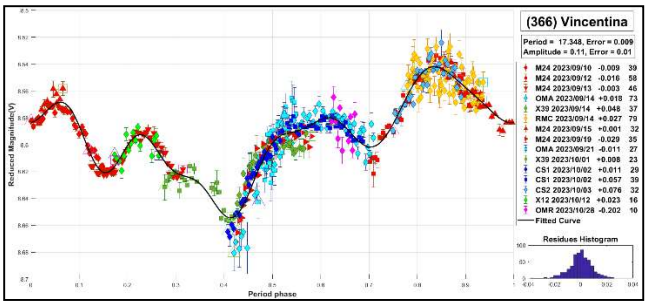

892 Seeligeria. This asteroid was discovered in 1918 by M. Wolf. Several periods were measured for this asteroid with the following results: $P = 41.40 \pm 0.02$ h (Behrend, 2007web), $P = 15.78 \pm 0.04$ h (Shipley et al., 2008), and $P = 16.693 \pm 0.008$ h (Colazo et al., 2023). We have determined a period of 16.692 ± 0.017 h with $\Delta m = 0.14 \pm 0.02$ mag, which is consistent with our previous result.

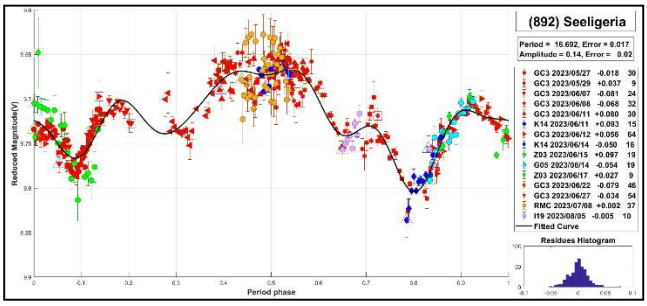

914 Palisana. This asteroid was discovered in 1919 by M. Wolf. The more recent period published in the literature corresponds to $P = 8.681 \pm 0.010$ h (Colazo et al., 2022). We have determined a period of 8.684 ± 0.007 h with $\Delta m = 0.25 \pm 0.01$ mag, which is consistent with our previous result. This diagram was derived from high-quality curves, and the ephemerides were covered as expected.

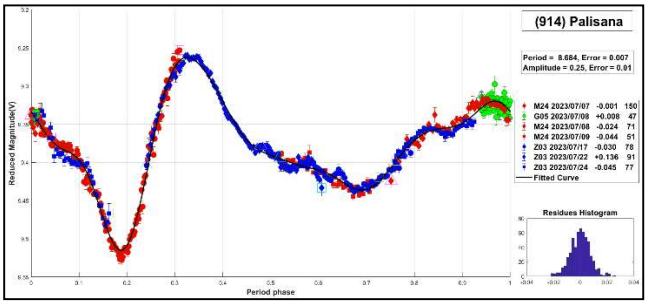

1112 Polonia. This asteroid was discovered in 1928 by P. Shajn. We found in the literature two rather different periods calculated for this object: $P = 82.5 \pm 0.5$ h (Warner, 2008) and $P = 18.71 \pm 0.04$ h (Polakis, 2020). The results we obtained are $P = 18.606 \pm 0.008$ h and $\Delta m = 0.10 \pm 0.01$ mag. Our period well agrees with the one measured by Polakis.

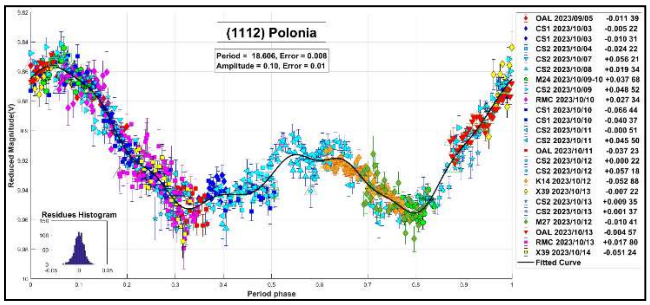

1237 Genevieve. This asteroid was discovered in 1931 by G. Reiss. The two more recent periods published in the literature correspond to $P = 24.82 \pm 0.07$ h (Behrend, 2005web) and $P = 16.31 \pm 0.04$ h (Polakis, 2022). We have determined a period of 24.712± 0.013 h, which is consistent with the longer period proposed by Beherend.

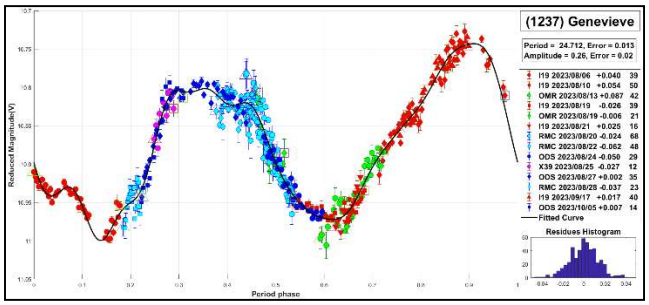

1332 Marconia. This asteroid was discovered in 1934 by L. Vorta. The more recent period published in the literature corresponds to $P = 19.16 \pm 0.01$ h (Stephens, 2013). In this work, we provide rather different results and propose a longer period of $P = 32.029 \pm 0.009$ h and $\Delta m = 0.21 \pm 0.01$ mag.

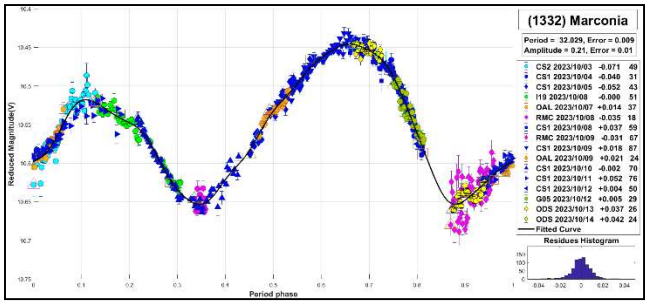

1496 Turku. This asteroid was discovered in 1938 by Y. Vaisala. The more recent period published in the literature corresponds to $P = 6.47375 \pm 0.00001$ h (Ďurech et al., 2016). We have determined a period of 6.473 ± 0.028 h with $\Delta m = 0.54 \pm 0.04$ mag, which is consistent with the one proposed by Ďurech.

Number	Name	yy/ mm/dd- yy/ mm/dd	Phase	L_{PAB}	B_{PAB}	Period(h)	P.E.	Amp	A.E.	Grp
343	Ostara	23/10/09-23/10/27	13.3,02.4	35	-1	109.270	0.012	0.52	0.02	MB-I
366	Vincentina	23/09/10-23/10/29	01.4,16.3	343	1	17.348	0.009	0.11	0.01	MB-O
892	Seeligeria	23/05/27-23/08/06	*08.7,15.1	257	25	16.692	0.017	0.14	0.02	MB-O
914	Palisana	23/07/07-23/07/27	22.4,20.4	310	29	8.684	0.007	0.25	0.01	MB-I
1112	Polonia	23/09/05-23/10/14	*13.7,05.6	14	11	18.606	0.008	0.10	0.01	Eos
1237	Genevieve	23/08/06-23/10/05	06.5,22.2	311	-12	24.712	0.013	0.26	0.02	MB-M
1332	Marconia	23/10/03-23/10/12	07.0,03.1	25	0	32.029	0.009	0.21	0.01	Marc
1496	Turku	23/08/21-23/10/07	*03.8,21.5	334	3	6.473	0.028	0.54	0.04	MB-I

Table I. Observing circumstances and results. The phase angle is given for the first and last date. If preceded by an asterisk, the phase angle reached an extremum during the period. LPAB and BPAB are the approximate phase angle bisector longitude/latitude at mid-date range (see Harris et al., 1984). Grp is the asteroid family/group (Warner et al., 2009). MB-I: main-belt inner; MB-O: main-belt outer; Eos: 221 Eos; MB-M: main-belt middle; Marc: 1332 Marconia.

Observatory	Telescope	Camera
G05 Obs.Astr.Giordano Bruno	SCT (D=203mm; f=6.3)	CCD Atik 420 m
I19 Obs.Astr.El Gato Gris	SCT (D=355mm; f=10.6)	CCD SBIG STF-8300M
K14 Obs.Astr.de Sencelles	Newtonian (D=250mm; f=4.0)	CCD SBIG ST-7XME
M24 Oss.Astr.La Macchina del Tempo	RCT (D250mm; f=8.0)	CMOS ZWO ASI 1600MM
X12 Obs.Astr.Los Cabezones	Newtonian (D=200mm; f=5.0)	CMOS QHY 174M
M27 Elijah Observatory	RCT (D250mm; f=6.0)	CCD QSI 683
X39 Obs.Astr.Antares	Newtonian (D=250mm; f=4.72)	CCD QHY9 Mono
Z03 Obs.Astr.Río Cofio	SCT (D=254mm; f=6.3)	CCD SBIG ST-8XME
CS1 CapoSudObservatory	RCT (D=400mm; f=5.7)	CCD Atik 383L+Mono
CS2 CapoSudObservatory	Newtonian (D=254mm; f=4.7)	CCD Atik 420 Mono
GC3 Specola Giuseppe Pustorino 3	RCT (D=400mm; f=5.7)	CCD Atik 383L+Mono
OAL Osservatorio Astronomico di Orciatico	SCT (D=355mm; f=7.4)	CCD SBIG ST10XME
ODS Obs.Astr.de Damián Scotta 1	Newtonian (D=300mm; f=4.0)	CMOS QHY 174M
OMA Obs.Astr.Vuelta por el Universo	Newtonian (D=150mm; f=5.0)	CMOS POA Neptune-M
OMR Obs.Astr.Municipal Reconquista	Newtonian (D=254mm; f=4.0)	Player One Ceres-M
RMC Obs.Astr.de Raúl Melia Carlos Paz	Newtonian (D=254mm; f=4.7)	CMOS QHY 174M

Table II. List of observatories and equipment.

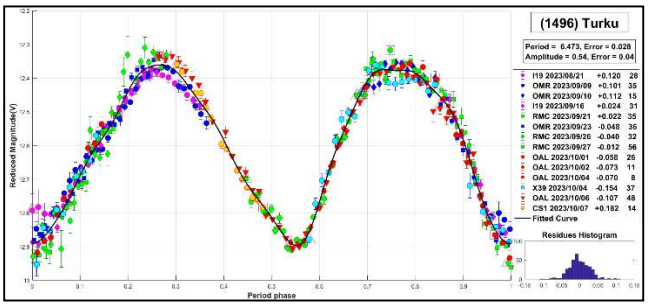

Acknowledgements

We want to thank Julio Castellano as we used his *FotoDif* program for preliminary analyses, Fernando Mazzone for his *Periods* program, which was used in final analyses, and Matías Martini for his *CalculadorMDE_v0.2* used for generating ephemerides used in the planning stage of the observations. This research has made use of the Small Bodies Data Ferret (*http://sbn.psi.edu/ferret/*), supported by the NASA Planetary System. This research has made use of data and/or services provided by the International Astronomical Union's Minor Planet Center.

References

Behrend, R. (2005web, 2007web). Observatoire de Geneve web site. *http://obswww.unige.ch/~behrend/page4cou.html*

Benishek, V. (2013). "Lightcurves for 366 Vincentina, 592 Bathseba, and 1544 Yugoslavia from Belgrade Astronomical Observatory." *The Minor Planet Bulletin* **40(2)**, 100-101.

Binzel, R.P. (1987). "A photoelectric survey of 130 asteroids." *Icarus* **72(1)**, 135-208.

Castellano, J. FotoDif software. *http://www.astrosurf.com/orodeno/fotodif/*

Colazo, M.; Fornari, C.; Wilberger, A.; Morales, M.; Bellocchio, E.; Pulver, E.; Scotta, D.; Suárez, N.; Melia, R.; Santos, F.; Mottino, A.; Stechina, A.; García, A.; Chapman, A.; Colazo, C. (2021). "Asteroid Photometry and Lightcurve Analysis at GORA'S Observatories Part V." *The Minor Planet Bulletin* **48(4)**, 363-365.

Colazo, M.R.; Scotta, D.; Monteleone, B.; Morales, M.; Ciancia, G.; García, A.; Melia, R.; Suárez, N.; Wilberger, A.; Fornari, C.; Nolte, R.; Bellocchio, E.; Mottino, A.; Colazo, C. (2022). "Asteroid Photometry and Lightcurve Analysis for Six Asteroids." *The Minor Planet Bulletin*, **49(4)**, 304-306.

Colazo, M.; Scotta, D.; Melia, R.; Ciancia, G.; Fornari, C.; Morales, M.; Wilberger, A.; Santos, F.; García, A.; Suárez, N.; Bellocchio, E.; Chapman, A.; Nolte, R.; Martini, M.; Mottino, A.; Colazo, C. (2023). "Asteroid Photometry and Lightcurve." *The Minor Planet Bulletin*, **50(1)**, 51-53.

Ďurech, J.; Hanuš, J.; Oszkiewicz, D., Vančo, R. (2016). "Asteroid models from the Lowell photometric database." *Astronomy & Astrophysics* **587**, A48.

Harris, A.W.; Young, J.W.; Scaltriti, F.; Zappala, V. (1984). "Lightcurves and phase relations of the asteroids 82 Alkmene and 444 Gyptis." *Icarus* **57(2)**, 251-258.

Martikainen, J.; Muinonen, K.; Penttilä, A.; Cellino, A.; Wang, X.B. (2021). "Asteroid absolute magnitudes and phase curve parameters from Gaia photometry." *Astronomy & Astrophysics* **649**, A98.

Martini, M. Calculador de Magnitud Diferencial Estandarizada. *https://www.observatorioomega.com.ar/2020/11/calculador-de-magnitud-diferencial.html*

Mazzone, F.D. (2012). Periodos software. Version 1.0. *http://www.astrosurf.com/salvador/Programas.htm*

Polakis, T. (2020). "Photometric Observations of Thirty Minor Planets." *The Minor Planet Bulletin* **47(3)**, 177-186.

Polakis, T. (2022). "Lightcurves for Sixteen Minor Planets." *The Minor Planet Bulletin* **49(4)**, 298-303.

Robinson, L.E. (2002). "Photometry of Five Difficult Asteroids: 309 Fraternitas, 366 Vincentina 421 Zahringia, 578 Happelia, 959 Anne." *The Minor Planet Bulletin* **29**, 30-31.

Shipley, H.; Dillard, A.; Kendall, J.; Reichert, M.; Sauppe, J.; Shaffer, N.; Kleeman, T.; Ditteon, R. (2008). "Asteroid Lightcurve Analysis at the Oakley Observatory -September 2007." *The Minor Planet Bulletin* **35(5)**, 99-102.

Stephens, R.D. (2013). "Asteroids Observed from Santana and CS3 Observatories: 2012 July - September." *The Minor Planet Bulletin* **40(1)**, 34-35.

Warner, B.D. (2008). "Asteroid Lightcurve Analysis at the Palmer Divide Observatory: September - December 2007." *The Minor Planet Bulletin* **35(2)**, 67-71.

Warner, B.D.; Harris, A.W.; Pravec, P. (2009). "The Asteroid Lightcurve Database." *Icarus* **202**, 134-146. Updated 2021 April. *https://www.minorplanet.info/php/lcdb.php*

LIGHTCURVES ANALYSIS OF 1677 TYCHO BRAHE, 1802 ZHANG HENG, AND 18151 LICCHELLI

Lorenzo Franco
Balzaretto Observatory (A81), Rome, ITALY
lor_franco@libero.it

Domenico Licchelli
R. P. Feynman Observatory (M63), Gagliano del Capo, ITALY

(Received: 2023 December 31)

Photometric observations of three main-belt asteroids were carried out at the R. P. Feynman Observatory on year 2017. The synodic period and lightcurve amplitude were found for 1677 Tycho Brahe, 1802 Zhang Heng, and 18151 Licchelli.

CCD observations of three main-belt asteroids were carried out at the R. P. Feynman Observatory on year 2017 using an Orion 0.30-m newtonian reflector equipped with a CCD Atik 460EX (bin 2×2), as part of an educational project involving high school students. Lightcurves analysis was done by the authors with *MPO Canopus* (Warner, 2023). All the images were calibrated with dark and flat frames and converted to standard magnitudes using solar colored field stars from CMC15 catalogue.

1677 Tycho Brahe is a medium albedo middle main-belt asteroid. Observations were made over four nights using a SR filter. The period analysis shows a synodic period of $P = 3.858 \pm 0.001$ h with an amplitude $A = 0.41 \pm 0.05$ mag. The period is close to the previously published results in the asteroid lightcurve database (LCDB; Warner et al., 2009) referred to hereinafter as "LCDB".

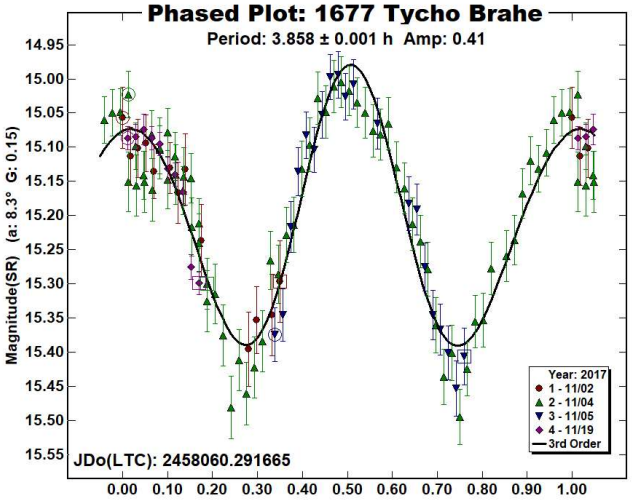

Number	Name	2017 mm/dd	Phase	L_{PAB}	B_{PAB}	Period(h)	P.E.	Amp	A.E.	Grp
1677	Tycho Brahe	11/02-11/19	8.3, 9.9	44	18	3.858	0.001	0.41	0.05	MB-M
1802	Zhang Heng	11/01-11/11	1.4, 4.6	39	-3	3.161	0.001	0.30	0.03	MB-O
18151	Licchelli	10/08-10/28	10.0, 1.5	34	-3	10.680	0.003	0.26	0.03	MB-O

Table I. Observing circumstances and results. The first line gives the results for the primary of a binary system. The second line gives the orbital period of the satellite and the maximum attenuation. The phase angle is given for the first and last date. If preceded by an asterisk, the phase angle reached an extrema during the period. L_{PAB} and B_{PAB} are the approximate phase angle bisector longitude/latitude at mid-date range (see Harris et al., 1984). Grp is the asteroid family/group (Warner et al., 2009).

1802 Zhang Heng is a medium albedo outer main-belt asteroid. Unfiltered observations were made over three nights. The period analysis shows a synodic period of P = 3.161 ± 0.001 h with an amplitude A = 0.30 ± 0.03 mag. The period is close to the previously published results in the LCDB.

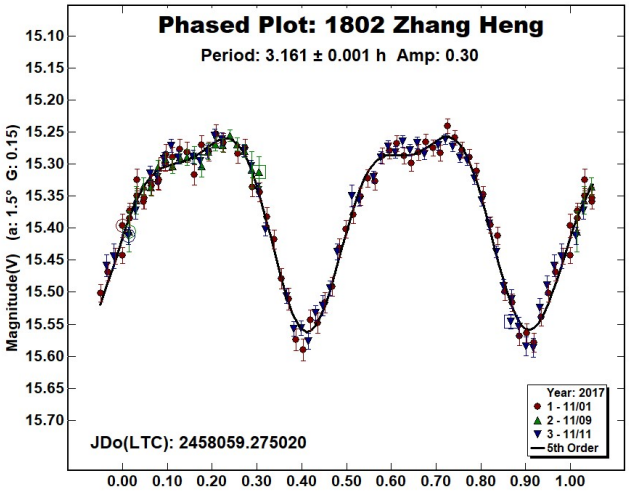

18151 Licchelli is an outer main-belt asteroid. We started observing this asteroid after a photometric session dedicated to exoplanets, so the observations were conducted with an Astrodon Exoplanet-BB filter. To maintain consistency, the same filter was used for all subsequent observations, which were carried out over eleven nights. The period spectrum shows a deeper minimum close to 10 hours and the split halves plot shows that the two halves are quite different, so we prefer the bimodal solution of P = 10.680 ± 0.003 h with an amplitude A = 0.26 ± 0.03 mag. For this asteroid, no periods were found in the LCDB.

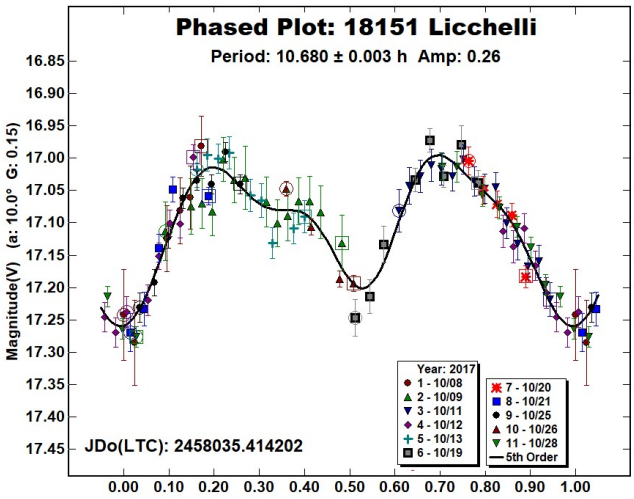

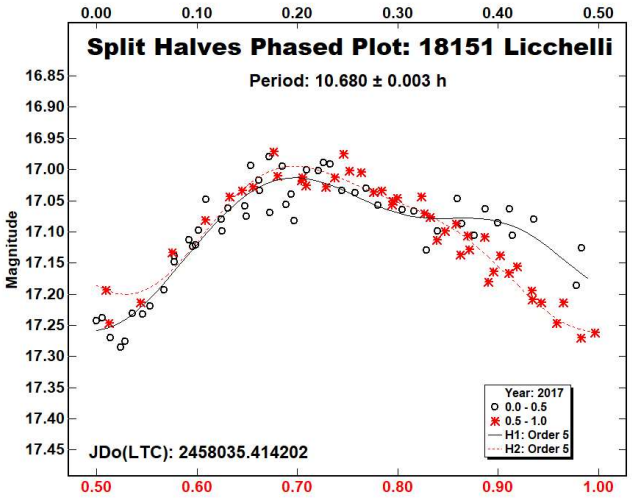

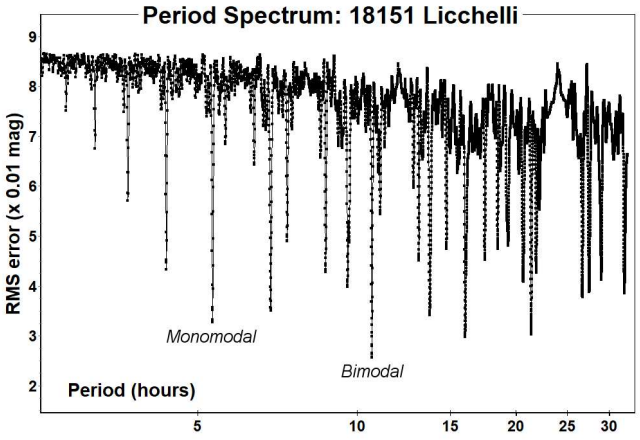

References

Harris, A.W.; Young, J.W.; Scaltriti, F.; Zappala, V. (1984). "Lightcurves and phase relations of the asteroids 82 Alkmene and 444 Gyptis." *Icarus* **57**, 251-258.

Warner, B.D.; Harris, A.W.; Pravec, P. (2009). "The asteroid lightcurve database." *Icarus* **202**, 134-146. Updated 2023 Sep 27. *https://minplanobs.org/alcdef/index.php*

Warner, B.D. (2023). MPO Software, MPO Canopus v10.8.6.20. Bdw Publishing. *http://minorplanetobserver.com*

COLLABORATIVE ASTEROID PHOTOMETRY FROM UAI: 2023 OCTOBER-DECEMBER

Lorenzo Franco
Balzaretto Observatory (A81), Rome, ITALY
lor_franco@libero.it

Alessandro Marchini
Astronomical Observatory, University of Siena (K54)
Via Roma 56, 53100 - Siena, ITALY

Marco Iozzi
HOB Astronomical Observatory (L63)
Capraia Fiorentina, ITALY

Giorgio Baj
M57 Observatory (K38), Saltrio, ITALY

Luciano Tinelli
GAV (Gruppo Astrofili Villasanta), Villasanta, ITALY

Giulio Scarfi
Iota Scorpii Observatory (K78), La Spezia, ITALY

Albino Carbognani
Virgil Observatory (M60), Loiano; ITALY

Gianni Galli
GiaGa Observatory (203), Pogliano Milanese, ITALY

Pietro Aceti, Massimo Banfi
Seveso Observatory (C24), Seveso, ITALY

Paolo Fini, Guido Betti
Blessed Hermann Observatory (L73), Impruneta, ITALY

Nello Ruocco
Osservatorio Astronomico Nastro Verde (C82), Sorrento, ITALY

Matteo Lombardo
Zen Observatory (M26), Scandicci, ITALY

(Received: 2024 January 11)

Photometric observations of six asteroids were made to acquire lightcurves for shape/spin axis modeling. Lightcurves were produced for 363 Padua, 815 Coppelia, 1204 Renzia, 1675 Simonida, 3819 Robinson, and (139622) 2001 QQ142.

Collaborative asteroid photometry was done inside the Italian Amateur Astronomers Union (UAI, 2023) group. The targets were selected mainly in order to acquire lightcurves for shape/spin axis modeling. Table I shows the observing circumstances and results.

The CCD observations were made in 2023 October-December using the instrumentation described in the Table II. Lightcurve analysis was performed at the Balzaretto Observatory with *MPO Canopus* (Warner, 2023). All the images were calibrated with dark and flat frames and converted to standard magnitudes using solar colored field stars from CMC15 and ATLAS catalogues, distributed with *MPO Canopus*. For brevity, "LCDB" is a reference to the asteroid lightcurve database (Warner et al., 2009).

363 Padua is a X-type (Bus and Binzel, 2002) middle main-belt asteroid. Multiband photometry was made by G. Baj and M. Iozzi on 2023 November 16, 21, and 24. We found B-V = 0.71 ± 0.02 and V-R = 0.43 ± 0.02 after averaging three pairs of values. These are consistent with an M-type asteroid (Shevchenko and Lupishko, 1998).

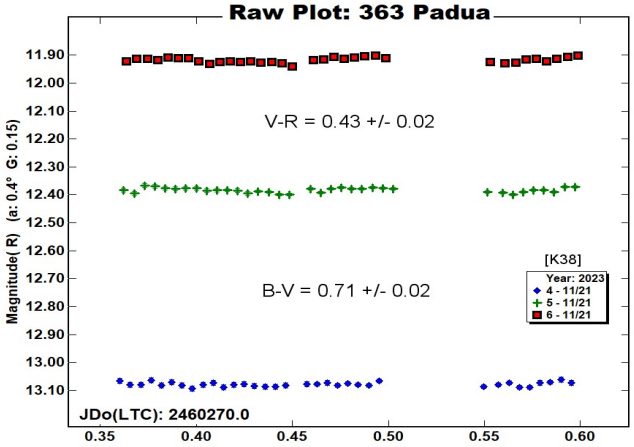

815 Coppelia is an Xe-type (Bus and Binzel, 2002) middle main-belt asteroid. Collaborative data from six nights produced a synodic period of 4.4202 ± 0.0003 h, close to other LCDB results, and an amplitude 0.25 ± 0.02 mag. Multiband photometry by G. Baj on 2023 Dec 17 found B-V = 0.78 ± 0.04 and V-R = 0.49 ± 0.04. The latter is consistent with an Xe-type asteroid (Pravec et al., 2012).

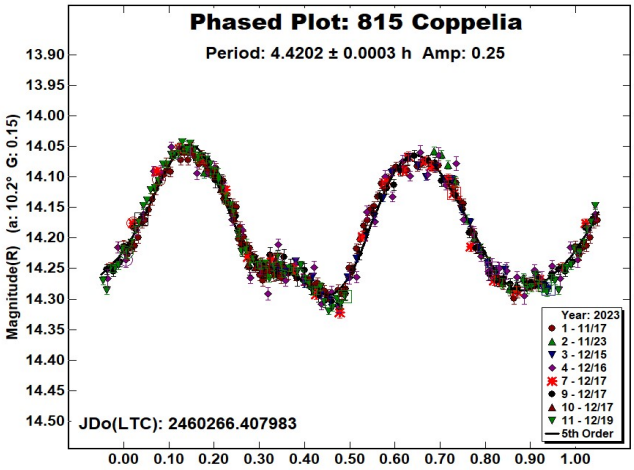

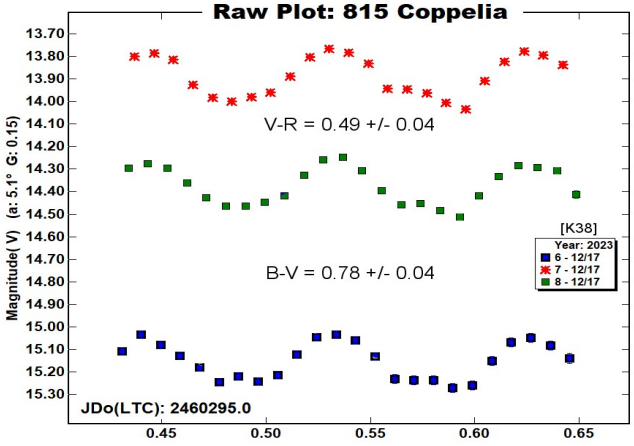

1204 Renzia is an S-type (Bus and Binzel, 2002) inner main-belt asteroid. Analysis of observations by L. Tinelli during four nights showed a synodic period of P = 7.885 ± 0.001 h, close to other LCDB results, with an amplitude A = 0.43 ± 0.03 mag.

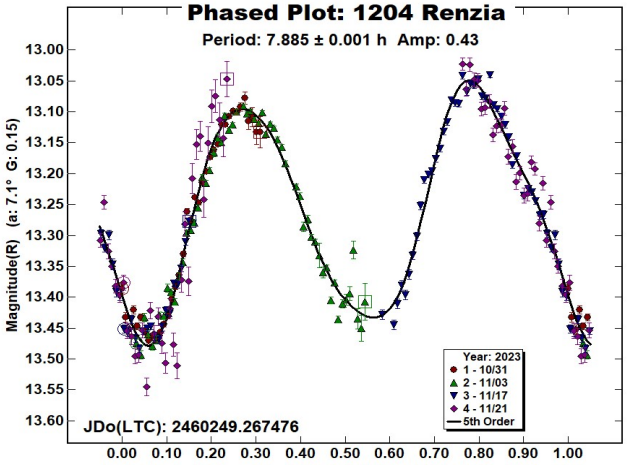

1675 Simonida is an inner main-belt asteroid. Collaborative observations over two nights led to a synodic period of P = 5.290 ± 0.005 h, close to other LCDB results, and A = 0.29 ± 0.02 mag.

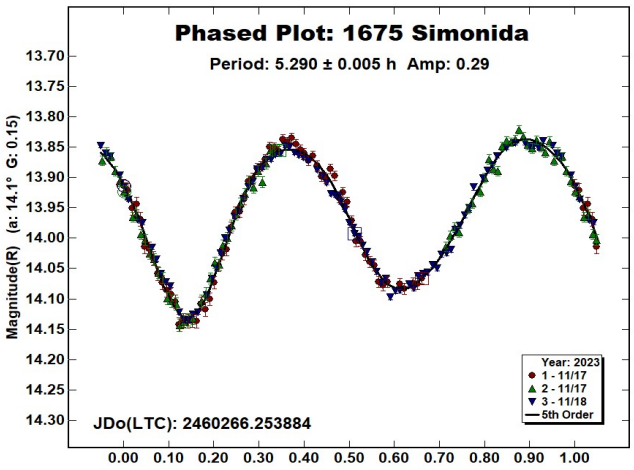

3819 Robinson is an Sr-type (Bus and Binzel, 2002) middle main-belt asteroid.

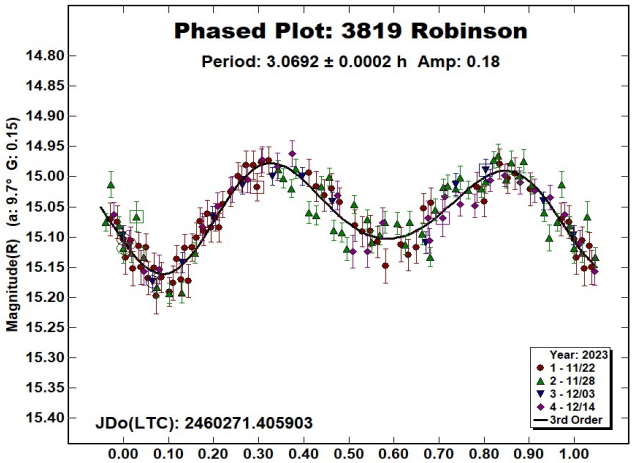

Analysis of collaborative observations over four nights found a synodic period of P = 3.0692 ± 0.0002 h, also close to other LCDB results, with an amplitude A = 0.18 ± 0.03 mag.

(139622) 2001 QQ142 is an Sq-type (Bus and Binzel, 2002) Apollo Near-Earth asteroid, classified as Potentially Hazardous Asteroid (PHA). Collaborative observations were made over seven nights, following its close approach to the Earth. The period spectrum shows a deeper minimum with a bimodal solution of P = 16.99 ± 0.01 h with an amplitude A = 0.38 ± 0.08 mag. No others periods were found in the LCDB.

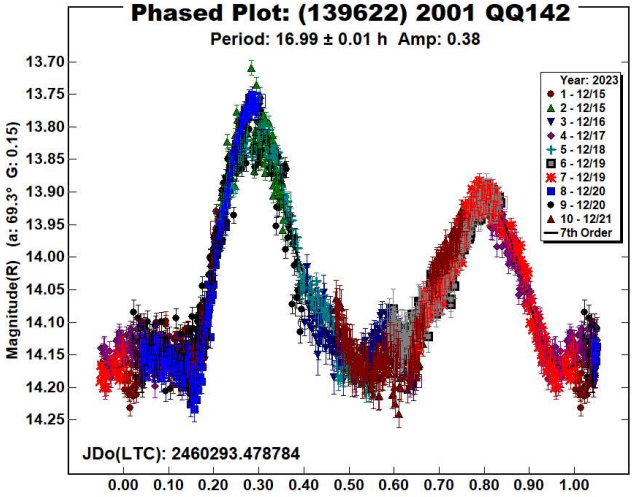

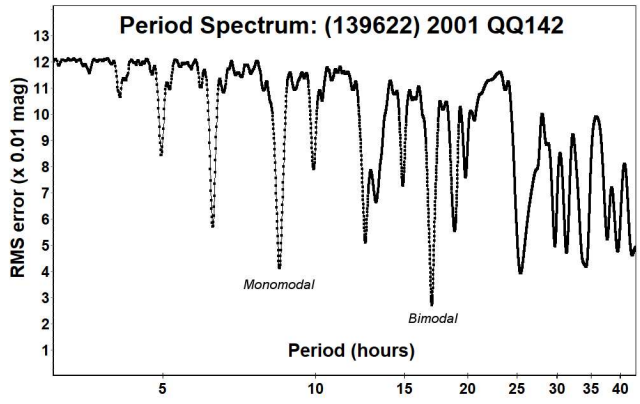

References

Bus S.J.; Binzel R.P. (2002). "Phase II of the Small Main-Belt Asteroid Spectroscopic Survey - A Feature-Based Taxonomy." *Icarus* **158**, 146-177.

Harris, A.W.; Young, J.W.; Scaltriti, F.; Zappala, V. (1984). "Lightcurves and phase relations of the asteroids 82 Alkmene and 444 Gyptis." *Icarus* **57**, 251-258.

Pravec, P.; Harris, A.W.; Kušnirák, P.; Galád, A.; Hornoch, K. (2012) "Absolute magnitudes of asteroids and a revision of asteroid albedo estimates from WISE thermal observations." *Icarus* **221**, 365-387.

Shevchenko V.G.; Lupishko D.F. (1998). "Optical properties of Asteroids from Photometric Data." *Solar System Research*, **32**, 220-232.

Number	Name	2023 mm/dd	Phase	L_{PAB}	B_{PAB}	Period(h)	P.E.	Amp	A.E.	Grp
363	Padua	11/16-11/24	*2.2,1.5	59	-1					MB-M
815	Coppelia	11/17-12/19	*10.2,6.2	77	6	4.4202	0.0003	0.25	0.02	MB-M
1204	Renzia	10/31-11/21	7.1,17.8	29	1	7.885	0.001	0.43	0.03	MB-I
1675	Simonida	11/17-11/18	14.1,14.6	32	2	5.290	0.005	0.29	0.02	MB-I
3819	Robinson	11/22-12/14	9.6,17.9	42	1	3.0692	0.0002	0.18	0.03	MB-M
139622	2001 QQ142	12/15-12/21	69.3,61.3	120	10	16.99	0.01	0.38	0.08	NEA

Table I. Observing circumstances and results. The phase angle is given for the first and last date. If preceded by an asterisk, the phase angle reached an extrema during the period. L_{PAB} and B_{PAB} are the approximate phase angle bisector longitude/latitude at mid-date range (see Harris et al., 1984). Grp is the asteroid family/group (Warner et al., 2009).

Observatory (MPC code)	Telescope	CCD	Filter	Observed Asteroids (#Sessions)
Astronomical Observatory, University of Siena (K54)	0.30-m MCT f/5.6	SBIG STL-6303e (bin 2×2)	C	139622(6)
HOB Astronomical Observatory (L63)	0.20-m SCT f/6.0	ATIK 383L+	C,B, V,R_c	363(1), 815(1), 3819(2)
M57 (K38)	0.35-m RCT f/5.5	SBIG STT1603ME	B,V, R_c	363(3), 815(1)
GAV	0.20-m SCT f/7.0	SXV-H9	R_c	1204(4)
Iota Scorpii(K78)	0.40-m RCT f/8.0	SBIG STXL-6303e (bin 2×2)	R_c	815(2), 3819(1)
Virgil Observatory (M60)	0.30-m NRT f/4.0	ASI 533 MM	C	139622(3)
GiaGa Observatory (203)	0.36-m SCT f/5.8	Moravian G2-3200	R_c	815(1), 1675(1)
Seveso Observatory (C24)	0.30-m SCT f/10.0	Moraviann KAF 8300 (bin 3×3)	R	815(1), 3819(1)
Blessed Hermann Observatory (L73)	0.30-m SCT f/6.0	QHY 174MGPS (bin 2×2)	R_c	363(2)
Osservatorio Astronomico Nastro Verde (C82)	0.35-m SCT f/6.3	SBIG ST10XME (bin 2×2)	C	1675(1)
Zen Observatory (M26)	0.30-m RCT f/7.4	ATIK 383L+	C	815(1)

Table II. Observing Instrumentations. MCT: Maksutov-Cassegrain, NRT: Newtonian Reflector, RCT: Ritchey-Chretien, SCT: Schmidt-Cassegrain.

UAI (2023), "Unione Astrofili Italiani" web site. *https://www.uai.it*

Warner, B.D. (2023). MPO Software, MPO Canopus v10.8.6.20. Bdw Publishing. *http://minorplanetobserver.com*

Warner, B.D.; Harris, A.W.; Pravec, P. (2009) "The asteroid lightcurve database." *Icarus* **202**, 134-146. Updated 2024 January. *https://minplanobs.org/alcdef/index.php*

LIGHTCURVES AND SYNODIC ROTATION PERIODS FOR 30 ASTEROIDS FROM SOPOT ASTRONOMICAL OBSERVATORY: 2023 APRIL – DECEMBER

Vladimir Benishek
Belgrade Astronomical Observatory
Volgina 7, 11060 Belgrade 38, SERBIA
vlaben@yahoo.com

(Received: 2024 January 15)

The results of lightcurve and synodic rotation period determinations for 30 asteroids obtained from CCD photometric observations carried out at the Sopot Astronomical Observatory in the time span 2023 April - December are summarized in this paper.

Photometric observations of 30 asteroids were conducted at Sopot Astronomical Observatory (SAO) from 2023 April through 2023 December in order to determine the asteroids' synodic rotation periods. For this purpose, two 0.35-m *f*/6.3 Meade LX200GPS Schmidt-Cassegrain telescopes were employed. The telescopes are equipped with a SBIG ST-8 XME and a SBIG ST-10 XME CCD cameras. The exposures were unfiltered and unguided for all targets. Both cameras were operated in 2×2 binning mode, which produces image scales of 1.66 arcsec/pixel and 1.25 arcsec/pixel for ST-8 XME and ST-10 XME cameras, respectively. Prior to measurements, all images were corrected using dark and flat field frames.

Photometric reduction was conducted using *MPO Canopus* (Warner, 2018). Differential photometry with up to five comparison stars of near solar color ($0.5 \leq$ B-V ≤ 0.9) was performed using the Comparison Star Selector (CSS) utility. This helped ensure a satisfactory quality level of night-to-night zero-point calibrations and correlation of the measurements within the standard magnitude framework. Field comparison stars were calibrated using standard Cousins R magnitudes derived from the Carlsberg Meridian Catalog 15 (VizieR, 2022) Sloan r' magnitudes using the formula: R = r' - 0.22 in all cases presented in this paper. In some instances, small zero-point adjustments were necessary in order to achieve the best match between individual data sets in terms of achieving the most favorable statistical indicators of Fourier fit goodness.

Lightcurve construction and period analysis was performed using *Perfindia* custom-made software developed in the R statistical programming language (R Core Team, 2020) by the author of this paper. The essence of its algorithm is reflected in finding the most favorable solution for rotational period by minimizing the *residual standard error* of the lightcurve Fourier fit.

The lightcurve plots presented in this paper show so-called 2% error for rotational periods, i.e. an error that would cause the last data point in a combined data set by date order to be shifted by 2% (Warner, 2012) and represented by the following formula:

$$\Delta P = (0.02 \cdot P^2) / T$$

where P and T are the rotational period and the total time span of observations, respectively. Both of these quantities must be expressed in the same units.

Some of the targets presented in this paper were observed within the Photometric Survey for Asynchronous Binary Asteroids (*BinAstPhot Survey*) under the leadership of Dr Petr Pravec from Ondřejov Observatory, Czech Republic.

Table I gives the observing circumstances and results summary.

Observations and Results

985 Rosina. According to the Asteroid Lightcurve Database (LCDB; Warner et al., 2009) several results for this Mars-crossing asteroid were obtained from the year 2002 onwards. Some of these are as follows: 3.0126 h (Behrend, 2002web), 3.012 h (Martinez et al., 2010), 3.015 h (Skiff et al., 2019), 3.01263 h (Pál et al., 2020). These previous results are in very good agreement with the newly found rotation period values from the SAO observations performed in two different viewing geometries, and therefore established from two separate lightcurves. A period value of $P = 3.013 \pm 0.001$ h was found from the first dataset obtained over 6 nights in late 2023 August, while the second dataset acquired in late 2023 September gave a fairly similar value of $P = 3.010 \pm 0.007$ h.

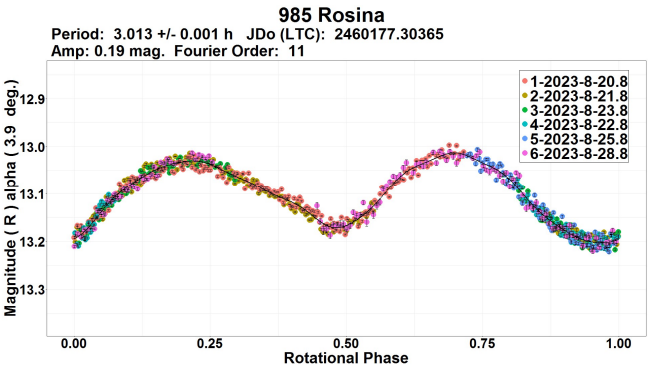

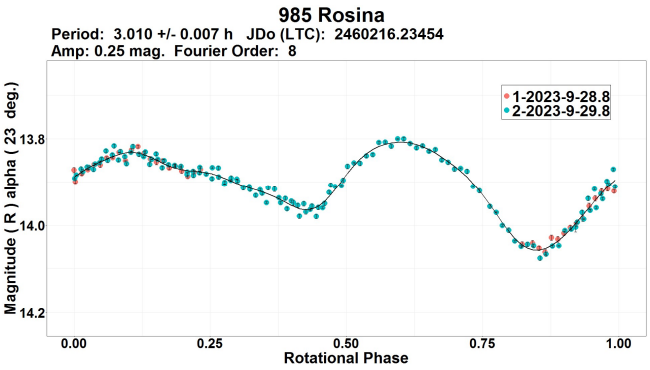

2213 Meeus. A period of $P = 2.9815 \pm 0.0006$ h determined from the dense photometric data obtained at SAO on 5 nights in 2023 September differs somewhat from the only previously reported result by Tomassini et al. (2014, 2.651 h), which is established from a highly scattered combined dataset relating to a rotational cycle containing a gap in data coverage.

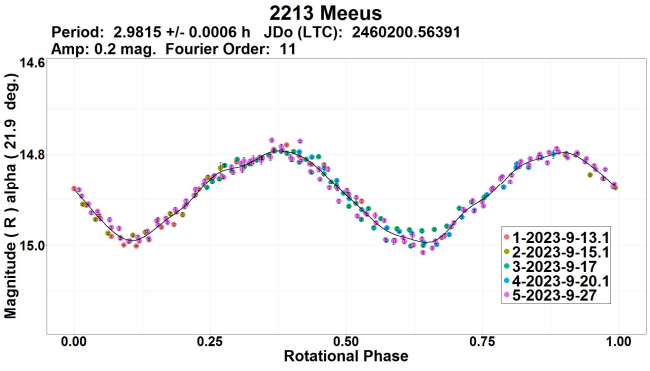

3225 Hoag. A period result of P = 2.3725 ± 0.0002 h, found from the data obtained on 11 nights in 2023 July - August for this Hungaria family asteroid fits very good with the multitude of a previously found period results (in the time span 2007 - 2023) listed in the LCDB (Warner et al., 2009), which are almost all statistically equal to the value of 2.37 hours.

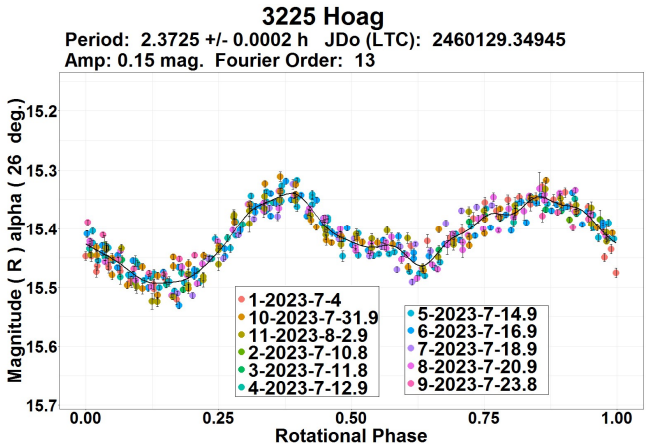

3879 Machar. Dense photometric datasets obtained in 2 temporally quite distant nights at the end of 2023 September and beginning of 2023 November show no noticeable change in the lightcurve shape and yield a bimodal rotation period result of P = 4.1378 ± 0.0004 h. Some of the earlier results shown in the LCDB are: 4.131 h (Behrend, 2012web), 4.14 h (Chang et al., 2015), 4.137 h (Waszczak et al., 2015), and 4.13843 h (Pál et al., 2020).

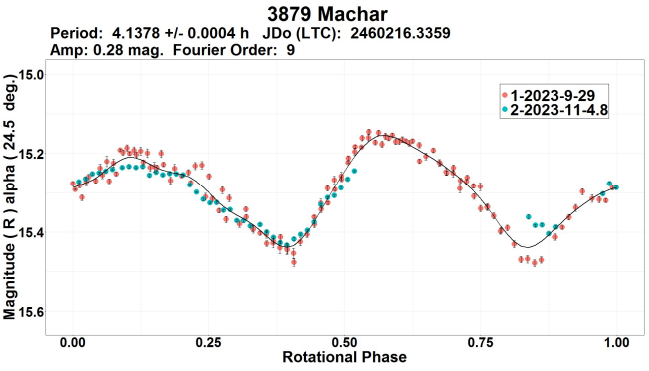

4175 Billbaum. Two consecutive nights data from 2023 December indicate a rotation period solution of P = 2.743 ± 0.006 h. Two previously known periods of 2.7425 h (Ditteon and West, 2011) and 2.730 h (Megna, 2011web) agree well with the new result, but it is slightly different from the value by Aymami (2011, 2.908 h) found from the highly scattered combined dataset.

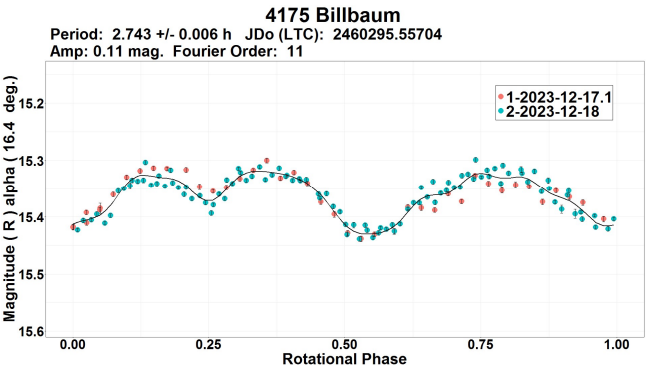

4621 Tambov. No results for previous rotation period determinations were found for this asteroid. Photometric observations carried out in 2023 July - August indicate a period of P = 5.3170 ± 0.0009 h, as statistically the most favorable one.

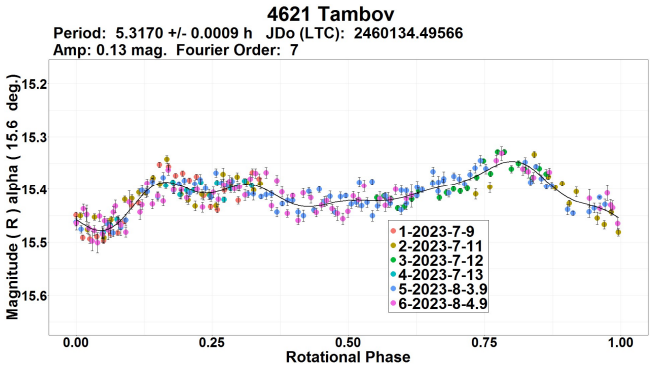

4671 Drtikol. Another asteroid without a previously known rotation period determination results. A bimodal period solution of P = 3.83 ± 0.02 h results from the data obtained on two consecutive nights in 2023 September.

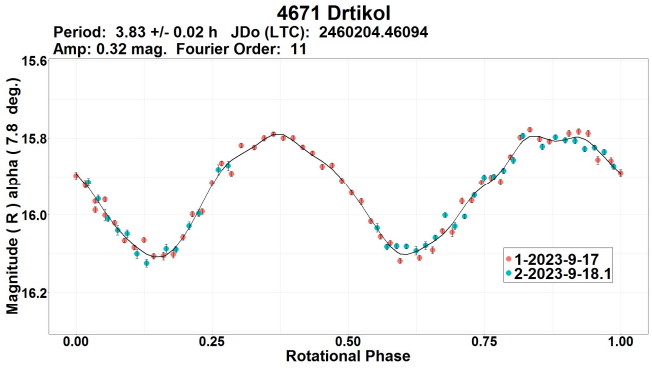

4839 Daisetsuzan. A bimodal period solution (P = 3.3839 ± 0.0005 h) found from the 2023 August - September data strongly corroborates the only prior period determination by Yeh et al. (2020, 3.38 h).

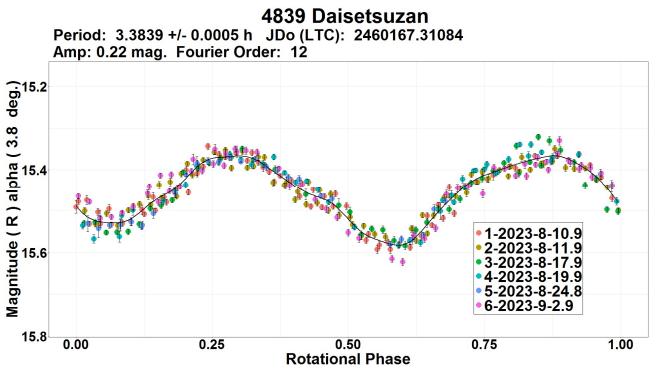

5111 Jacliff. Photometric observations performed at SAO in 2023 August show a bimodal rotation period solution of P = 2.840 ± 0.004 h, which is in accordance with the previously established values listed in the LCDB (Warner et al., 2009), and all of them are in a narrow interval of 2.839 - 2.840 h.

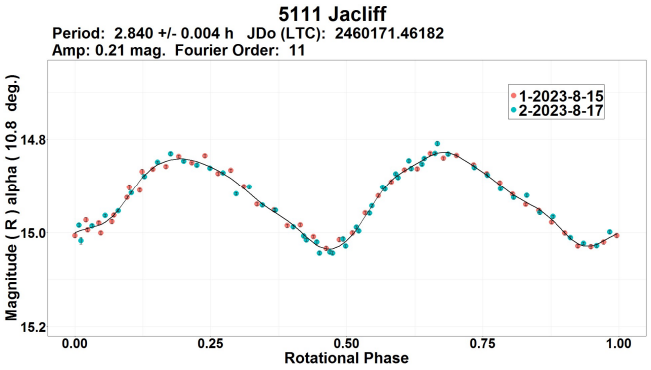

(5787) 1992 FA1. Prior results for period by Ditteon et al. (2010, 4.0176 h), Waszczak et al. (2015, 4.018 h), and Erasmus et al. (2020, 4.017 h) are well supported with the new bimodal period of P = 4.018 ± 0.002 h, obtained from the SAO data collected on 6 nights in late 2023 August and early 2023 September.

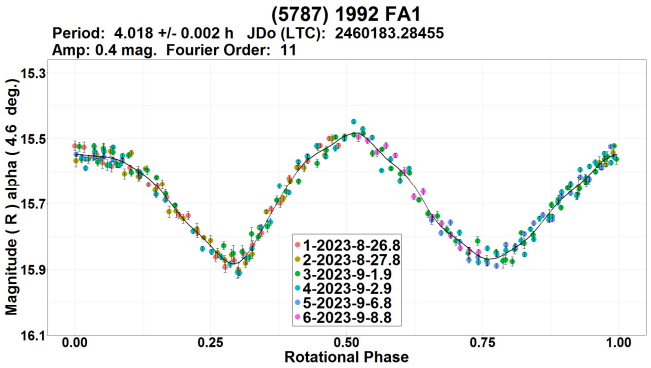

6108 Glebov. Period analysis made upon a combined dataset obtained in 2023 July - August led to an unequivocal solution for period of P = 2.8301 ± 0.0005 h, which is consistent with previously known period determinations by Higgins (2011web, 2.8310 h), and Behrend (2020web, 2.85 h).

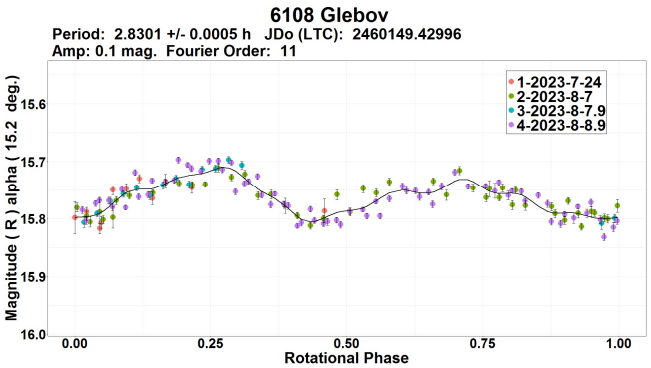

(6872) 1993 CN1. An inspection of the LCDB has not revealed any results for previous rotation period determinations. A bimodal rotational lightcurve of rather large amplitude (0.49 mag.) phased to a period of P = 3.8201 ± 0.0005 h emerges as an unambiguous solution from the period analysis conducted on the dataset obtained in 2023 August - September.

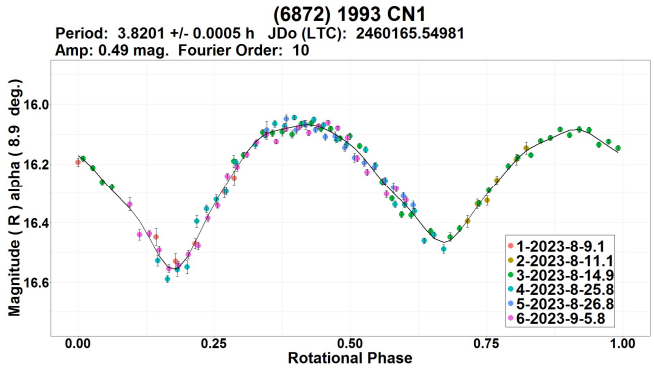

12071 Davykim. Observations conducted over 4 nights in 2023 October - November yielded a bimodal lightcurve phased to a period value of P = 3.5473 ± 0.0005 h, which confirms the previous result found by Higgins (2011web, 3.5483 h).

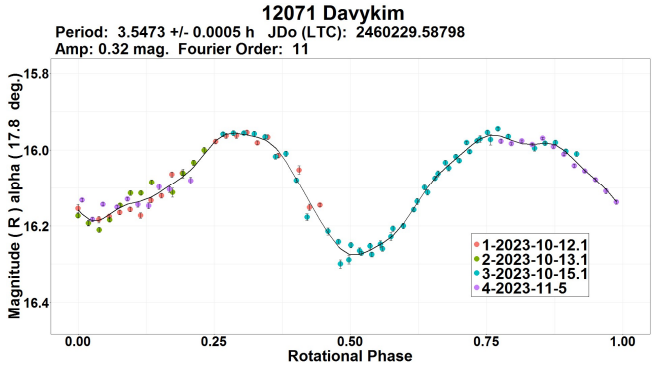

(12724) 1991 PZ14. With no prior references in the LCDB (Warner et al., 2009) this appears to be the first lightcurve and rotation period determination result for this asteroid. A bimodal period solution of P = 3.000 ± 0.004 h was found from the SAO photometric data obtained on 3 consecutive nights in late 2023 July.

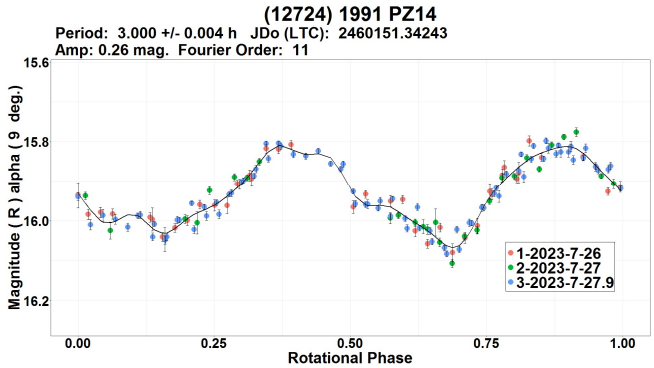

(13081) 1992 EW9. There are no LCDB records of previous lightcurve and rotation period determinations in this case as well. 2023 August data obtained over two consecutive nights reveal a bimodal period of P = 5.41 ± 0.03 h as the most likely solution.

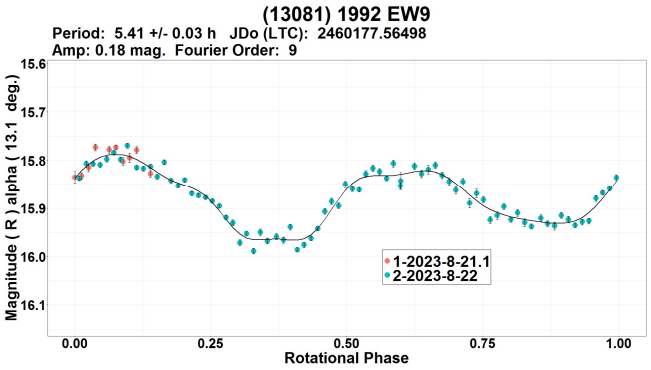

14031 Rozyo. A dense single night photometric dataset from late 2023 September indicates a bimodal rotational period of P = 2.89 ± 0.03 h. Regardless of the fact that the collected amount of data may call into question reliability of the newly derived result, it matches well with the only previously derived (sidereal) rotation period by Ďurech et al. (2016, 2.900652 h).

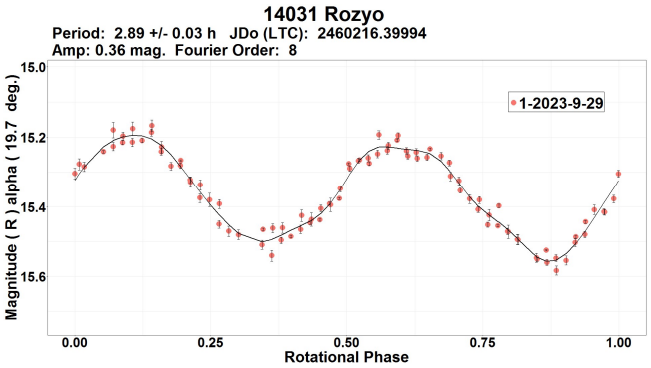

15007 Edoardopozio. Previous lightcurve and rotation period determinations are not known for this asteroid. Observations at SAO over two consecutive nights in 2023 October indicate a bimodal lightcurve phased to a period of P = 4.30 ± 0.02 h as the statistically most favorable solution.

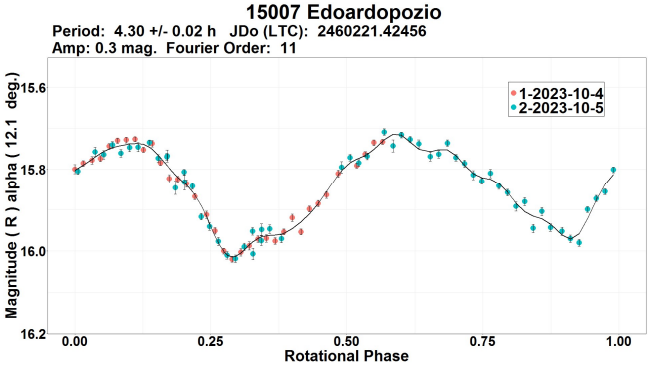

(16591) 1992 SY17. The result for rotation period of P = 2.7372 ± 0.0006 h derived from the data obtained in 2023 June - July is highly consistent with the two previously found values: 2.73728 h (Pravec, 2013web) and 2.73624 h (Pál et al., 2020).

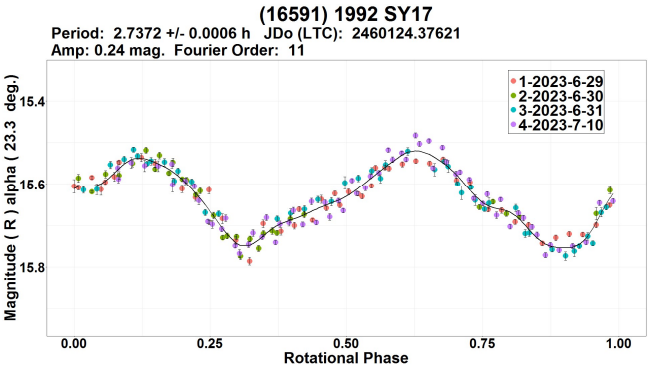

(17204) 2000 AR75. No records on previous rotation period determinations were found in the LCDB. The statistically best solution for the rotation period established from data taken on 3 nights in late 2023 August is: P = 2.845 ± 0.003 h.

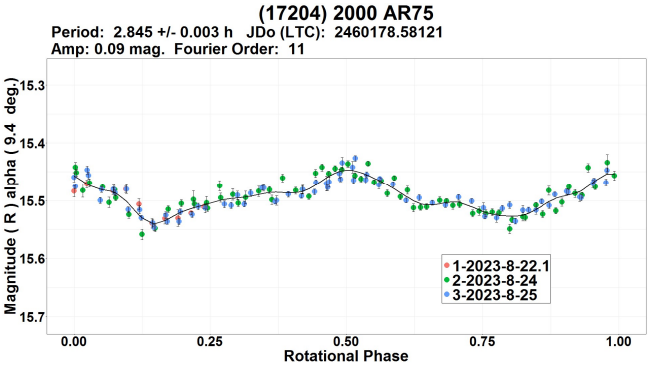

(24417) 2000 BK5. According to the LCDB records this is the first rotation period determination for this asteroid. A bimodal solution for period found from the 2023 October - November photometric data is: P = 3.7830 ± 0.0004 h.

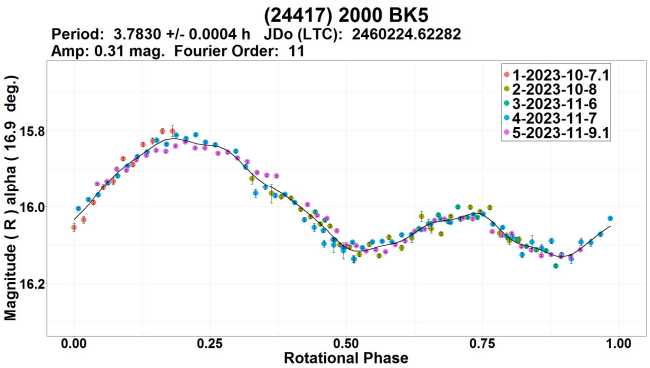

24643 MacCready. Period result (P = 2.828 ± 0.005 h) obtained from observations conducted over 2 consecutive nights in late 2023 September is in very good accordance with the previous result found by Skiff et al. (2019, 2.8291 h).

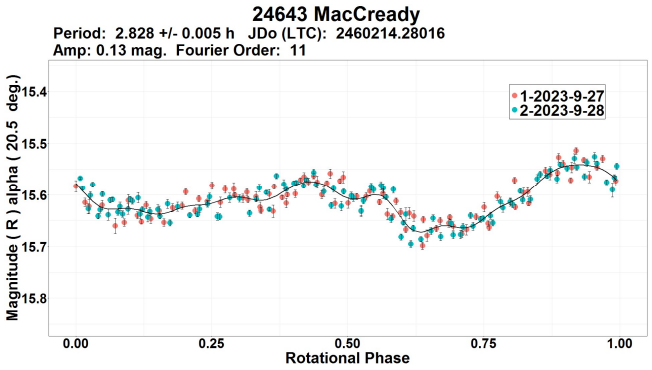

(36360) 2000 OH3. Rotation period found analyzing photometric data obtained at SAO on 5 nights in 2023 October is $P = 2.4620 \pm 0.0004$ h. The LCDB records suggest that this represents the first lightcurve and rotation period determination to date.

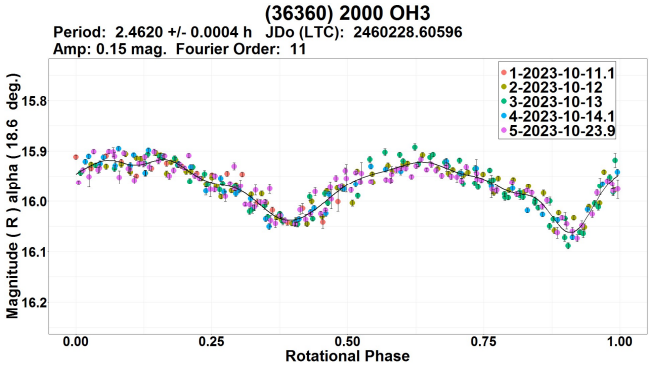

(41044) 1999 VW6. Warner (2013) found a rotation period of 2.734 h. Analysis of the SAO observations obtained in late 2023 July resulted in a very similar rotation period of $P = 2.731 \pm 0.002$ h.

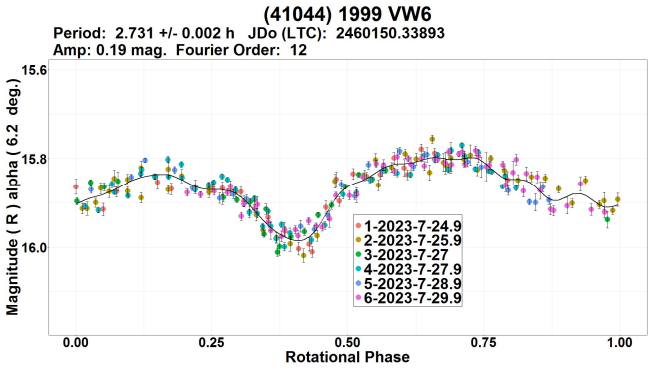

(48601) 1995 BL. In the three apparitions, during 2010, 2014, and in 2015 Warner (2011, 2014, 2016) finds the following values for the rotation period of this Hungaria family member: 4.590 h, 4.60 h, and 4.598 h, respectively. The SAO observations on two consecutive nights carried out in 2023 August at low solar phase angles led to a bimodal lightcurve of rather large amplitude (0.41 mag.) and a corresponding period value of $P = 4.63 \pm 0.02$ h.

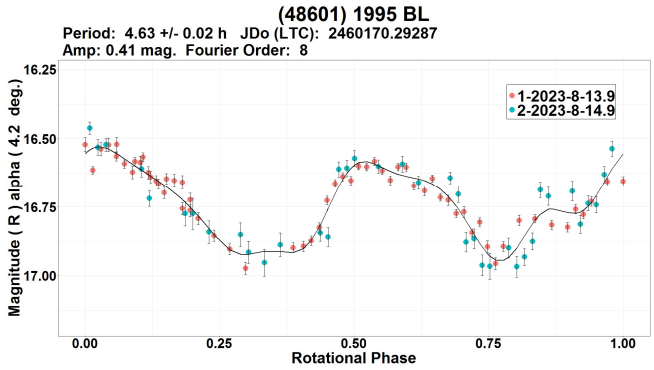

(50403) 2000 CB114. A *BinAstPhot Survey* target observed at SAO on 5 nights in 2023 September - October. A period of $P = 2.5669 \pm 0.0005$ h found from these observations is highly consistent with the period result of 2.5671 h found within the same *Survey* during the 2016 apparition.

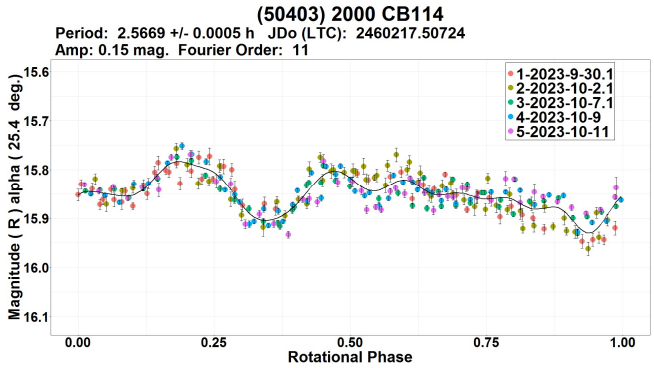

(53523) 2000 AC153. Waszczak et al. (2015) found a rotation period of 2.172 h. The 2023 April - May observations resulted in a rotation period of $P = 2.8309 \pm 0.0006$ h.

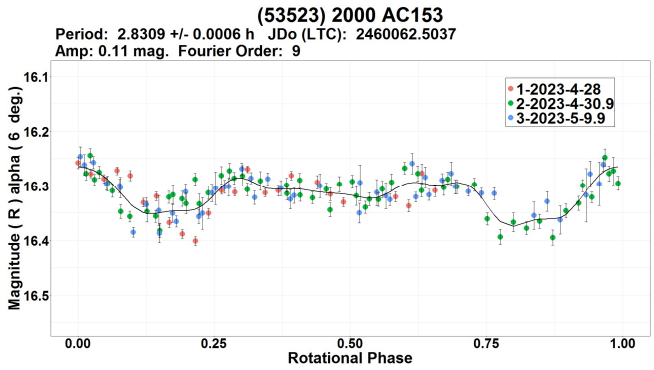

(60300) 1999 XV176. No previous rotation period determination results were found in the LCDB. The 2023 September SAO data revealed a period of $P = 2.7083 \pm 0.0007$ h as the statistically most favorable solution resulting from the period analysis.

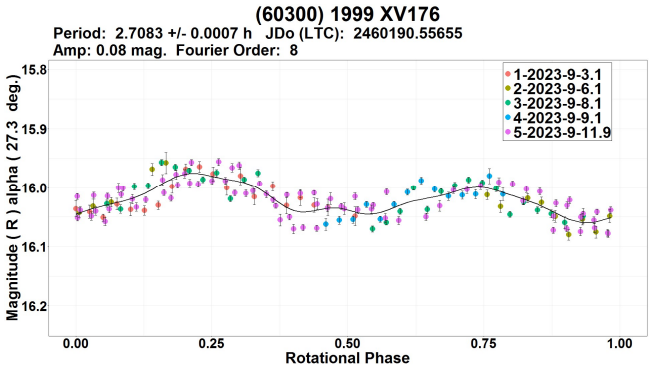

(64676) 2001 XE68. A rotation period of P = 2.4340 ± 0.0003 h was found from the SAO data acquired in 2023 October - November over 5 nights. This is the first ever rotation period determination for this asteroid.

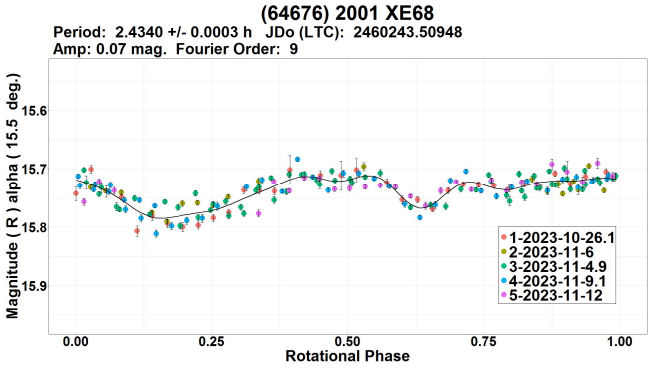

(81300) 2000 GW2. Previous rotation period determinations are not known in this case either. Period analysis performed on dense photometric dataset obtained in 2023 July at SAO indicate a favorable bimodal solution for a synodic rotation period of P = 2.9629 ± 0.0004 h.

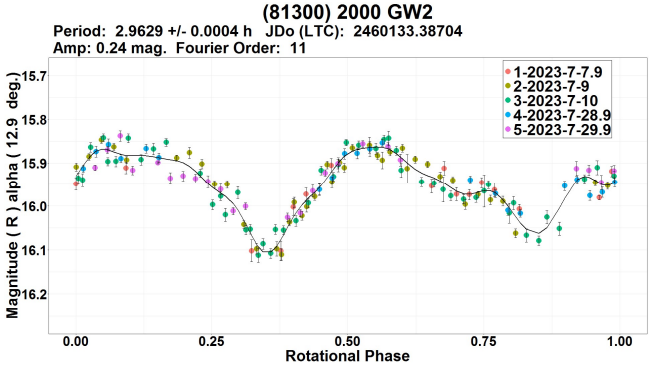

(154244) 2002 KL6. The two new rotation period results of P_1 = 4.605 ± 0.005 h and P_2 = 4.61 ± 0.02 h are derived from two independent groups of data obtained at SAO in the time span 2023 July 31 - 2023 August 05 (first group) and on two consecutive nights in early 2023 September (second group), corresponding to two different viewing geometries. These results fit very well in the entire series of previously determined rotation periods (from 2009 through 2023) ranging in a narrow interval of values from 4.605 h to 4.6101 h, as specified in the LCDB (Warner et al., 2009).

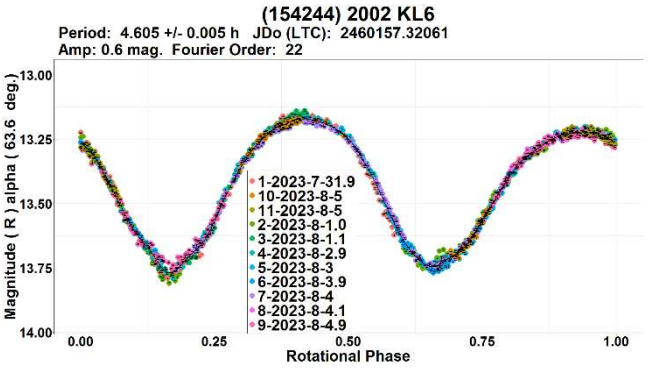

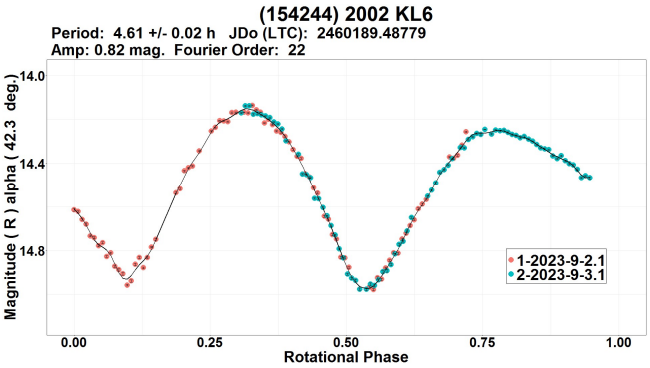

Acknowledgements

Observational work at Sopot Astronomical Observatory is generously supported by Gene Shoemaker NEO Grants awarded by the Planetary Society in 2018 and 2022.

References

Aymami, J.M. (2011). "CCD Photometry and Lightcurve Analysis of 1318 Nerina, 4175 Billbaum and 5168 Jenner from Observatori Carmelita (MPC B20) in Tiana." *Minor Planet Bull.* **38**, 158-159.

Behrend, R. (2002web, 2012web, 2020web). Observatoire de Geneve web site. *http://obswww.unige.ch/~behrend/page_cou.html*

Chang, C.; Ip, W.; Lin, H.; Cheng, Y.; Ngeow, C.; Yang, T.; Waszczak, A.; Kulkarni, S.; Levitan, D.; Sesar, B.; Laher, R.; Surace, J.; Prince, T.A. (2015). "Asteroid Spin-rate Study Using the Intermediate Palomar Transient Factory." *Astrophys. J. Suppl. Ser.* **219**, A27.

Ditteon, R.; Kirkpatrick, E.; Doering, K. (2010). "Asteroid Lightcurve Analysis at the Oakley Southern Sky Observatory: 2009 April - May." *Minor Planet Bull.* **37**, 1-3.

Ditteon, R.; West, J. (2011). „Asteroid Lightcurve Analysis at the Oakley Southern Observatory: 2011 January thru April." *Minor Planet Bull.* **38**, 214-217.

Ďurech, J.; Hanuš, J.; Oszkiewicz, D.; Vančo, R. (2016). "Asteroid models from the Lowell photometric database." *A&A* **587**, id. A48.

Erasmus, N.; Navarro-Meza, S.; McNeill, A.; Trilling, D.E.; Sickafoose, A.A.; Denneau, L.; Flewelling, H.; Heinze, A.; Tonry, J.L. (2020). "Investigating Taxonomic Diversity within Asteroid Families through ATLAS Dual-band Photometry." *Ap. J. Suppl. Ser.* **247**, A13.

Number	Name	20yy/mm/dd	Phase	L_{PAB}	B_{PAB}	Period (h)	P.E.	Amp	A.E.	Grp
985	Rosina	23/08/20-23/08/28	*3.9, 6.0	329	5	3.013	0.001	0.19	0.01	MC
985	Rosina	23/09/28-23/09/29	23.0,23.5	337	6	3.010	0.007	0.25	0.02	MC
2213	Meeus	23/09/13-23/09/27	21.9,14.6	19	-8	2.9815	0.0006	0.20	0.02	MB-I
3225	Hoag	23/07/03-23/08/03	26.0,29.4	276	37	2.3725	0.0002	0.15	0.03	HUN
3879	Machar	23/09/28-23/11/04	24.5, 9.6	43	13	4.1378	0.0004	0.28	0.05	MB-I
4175	Billbaum	23/12/17-23/12/18	16.4,16.0	112	-16	2.743	0.006	0.11	0.02	MB-M
4621	Tambov	23/07/08-23/08/05	*15.6, 3.1	310	4	5.3170	0.0009	0.13	0.02	MB-I
4671	Drtikol	23/09/16-23/09/18	7.8, 7.2	7	2	3.83	0.02	0.32	0.02	MB-I
4839	Daisetsuzan	23/08/10-23/09/02	*3.8, 11.5	319	6	3.3839	0.0005	0.22	0.03	MB-I
5111	Jacliff	23/08/14-23/08/17	10.8, 9.9	337	8	2.840	0.004	0.21	0.02	V
5787	1992 FA1	23/08/26-23/09/08	4.6,10.3	329	6	4.018	0.002	0.40	0.03	FLOR
6108	Glebov	23/07/23-23/08/09	15.2, 5.9	321	4	2.8301	0.0005	0.10	0.02	MB-I
6872	1993 CN1	23/08/09-23/09/05	*8.9, 7.4	331	5	3.8201	0.0005	0.49	0.02	MB-I
12071	Davykim	23/10/12-23/11/05	17.8, 3.7	46	-1	3.5473	0.0005	0.32	0.02	FLOR
12724	1991 PZ14	23/07/25-23/07/28	9.0, 8.1	315	8	3.000	0.004	0.26	0.03	MB-I
13081	1992 EW9	23/08/21-23/08/22	13.1,12.6	351	-4	5.41	0.03	0.18	0.03	MAR
14031	Rozyo	23/09/28-23/09/29	19.7,19.6	36	-17	2.89	0.03	0.36	0.03	EUN
15007	Edoardopozio	23/10/03-23/10/05	12.1,11.6	28	10	4.30	0.02	0.30	0.02	MB-I
16591	1992 SY17	23/06/28-23/07/10	23.3,19.0	305	12	2.7372	0.0006	0.24	0.03	MC
17204	2000 AR75	23/08/22-23/08/25	9.4, 7.6	340	-2	2.845	0.003	0.09	0.02	MB-I
24417	2000 BK5	23/10/07-23/11/09	16.9, 1.0	47	0	3.7830	0.0004	0.31	0.03	MB-I
24643	MacCready	23/09/26-23/09/28	20.5,19.7	26	15	2.828	0.005	0.13	0.03	PHO
36360	2000 OH3	23/10/11-23/10/24	18.6,13.3	43	13	2.4620	0.0004	0.15	0.03	MB-I
41044	1999 VW6	23/07/24-23/07/30	*6.2, 5.8	305	10	2.731	0.002	0.19	0.03	MB-I
48601	1995 BL	23/08/13-23/08/14	4.2, 4.9	315	4	4.63	0.02	0.41	0.04	HUN
50403	2000 CB114	23/09/30-23/10/11	25.4,21.1	52	-1	2.5669	0.0005	0.15	0.03	PHO
53523	2000 AC153	23/04/28-23/05/10	*6.0, 6.2	223	7	2.8309	0.0006	0.11	0.02	FLOR
60300	1999 XV176	23/09/03-23/08/12	27.3,25.5	17	29	2.7083	0.0007	0.08	0.02	PHO
64676	2001 XE68	23/10/26-23/11/12	15.5, 5.4	52	-7	2.4340	0.0003	0.07	0.02	MB-I
81300	2000 GW2	23/07/07-23/07/29	*12.9, 4.6	301	7	2.9629	0.0004	0.24	0.03	MB-I
154244	2002 KL6	23/07/31-23/08/05	*63.6,63.0	305	35	4.605	0.005	0.60	0.03	NEA
154244	2002 KL6	23/09/01-23/09/03	42.3,41.1	2	13	4.61	0.02	0.82	0.02	NEA

Table I. Observing circumstances and results. Phase is the solar phase angle given at the start and end of the date range. If preceded by an asterisk, the phase angle reached an extrema during the period. L_{PAB} and B_{PAB} are the average phase angle bisector longitude and latitude. Grp is the asteroid family/group (Warner et al., 2009): EUN = Eunomia, MB-I/M = main-belt inner/middle, NEA = near-Earth asteroid, MAR = Maria, V = Vestoid, HUN = Hungaria, MC = Mars Crosser, V = Vestoid, FLOR = Flora, PHO = Phocaea.

Higgins, D.J. (2011web). No longer active. *http://www.david-higgins.com/Astronomy/asteroid/lightcurves.htm*

Martinez, J.; Aymami, J.M.; Bosque, R.; Martin, J. (2010). "CCD Photometry and Lightcurve Analysis of 985 Rosina and 990 Yerkes from Grup D'Astronomica de Tiana (G.A.T.) Observatory." *Minor Planet Bull.* **37**, 42-43.

Megna, R. (2011web). Posting on the CALL web site. *https://minplanobs.org/MPInfo/php/callsearch.php*

Pál, A.; Szakáts, R.; Kiss, C.; Bódi, A.; Bognár, Z.; Kalup, C.; Kiss, L.L.; Marton, G.; Molnár, L.; Plachy, E.; Sárneczky, K.; Szabó, G.M.; Szabó, R. (2020). "Solar System Objects Observed with TESS - First Data Release: Bright Main-belt and Trojan Asteroids from the Southern Survey." *Ap. J. Supl. Ser.* **247**, 26-34.

Pravec, P. (2013web). Photometric Survey for Asynchronous Binary Asteroids web site. *http://www.asu.cas.cz/~ppravec/newres.txt*

R Core Team (2020). R: A language and environment for statistical computing. R Foundation for Statistical Computing. Vienna, Austria. *https://www.R-project.org/*

Skiff, B.A.; McLelland, K.P.; Sanborn, J.J.; Pravec, P.; Koehn, B.W. (2019). "Lowell Observatory Near-Earth Asteroid Photometric Survey (NEAPS): Paper 4." *Minor Planet Bull.* **46**, 458-503.

Tomassini, A.; Cervoni, M.; Scardella, M. (2014). "Rotational Period and H-G Parameters for Asteroid 2213 Meeus." *Minor Planet Bull.* **41**, 19.

VizieR (2022). *http://vizier.u-strasbg.fr/viz-bin/VizieR*

Warner, B.D.; Harris, A.W.; Pravec, P. (2009). "The Asteroid Lightcurve Database." *Icarus* **202**, 134-146. Updated 2023 Oct 01. *http://www.minorplanet.info/lightcurvedatabase.html*

Warner, B.D. (2011). "Asteroid Lightcurve Analysis at the Palmer Divide Observatory: 2010 September - December." *Minor Planet Bull.* **38**, 82-86.

Warner, B.D. (2012). *The MPO Users Guide: A Companion Guide to the MPO Canopus/PhotoRed Reference Manuals*. BDW Publishing, Eaton, CO.

Warner, B.D. (2013). "Asteroid Lightcurve Analysis at the Palmer Divide Observatory: 2013 January - March." *Minor Planet Bull.* **40**, 137-145.

Warner, B.D. (2014). "Asteroid Lightcurve Analysis at CS3-Palmer Divide Station: 2014 January - March." *Minor Planet Bull.* **41**, 144-155.

Warner, B.D. (2016). "Asteroid Lightcurve Analysis at CS3-Palmer Divide Station: 2015 June - September." *Minor Planet Bull.* **43**, 57-65.

Warner, B. D. (2018). MPO Canopus software, version 10.7.11.3. *http://www.bdwpublishing.com*

Waszczak, A.; Chang, C.-K.; Ofek, E.O.; Laher, R.; Masci, F.; Levitan, D.; Surace, J.; Cheng, Y.-C.; Ip, W.-H.; Kinoshita, D.; Helou, G.; Prince, T.A.; Kulkarni, S. (2015). "Asteroid Light Curves from the Palomar Transient Factory Survey: Rotation Periods and Phase Functions from Sparse Photometry." *Astron. J.* **150**, A75.

Yeh, T.-S.; Li, B.; Chang, C.-K.; Zhao, H.-B.; Ji, J.-H.; Lin, Z.-Y.; Ip, W.-H. (2020). "The Asteroid Rotation Period Survey Using the China Near-Earth Object Survey Telescope (CNEOST)." *Astron. J.* **160**, id. 73.

PHOTOMETRIC OBSERVATIONS OF ASTEROIDS 1631 KOPFF, 2244 TESLA, 2967 VLADISVYAT AND 9628 SENDAIOTSUNA

Alessandro Marchini, Riccardo Papini
Astronomical Observatory, University of Siena (K54)
Via Roma 56, 53100 - Siena, ITALY
marchini@unisi.it

(Received: 2024 January 6)

Photometric observations of four main-belt asteroids were conducted to determine their synodic rotation periods. We found: for 1631 Kopff, P = 6.682 ± 0.002 h with A = 0.28 ± 0.02 mag; for 2244 Tesla, P = 24.65 ± 0.04 h with A = 0.13 ± 0.03 mag; for 2967 Vladisvyat, P = 8.374 ± 0.001 h with A = 0.59 ± 0.02 mag, for 9628 Sendaiotsuna, P = 2.664 ± 0.001 h with A = 0.07 ± 0.02 mag.

CCD photometric observations of four main-belt asteroids were carried out in October - December 2023 at the Astronomical Observatory of the University of Siena (K54). We used a 0.30-m *f*/5.6 Maksutov-Cassegrain telescope, SBIG STL-6303E NABG CCD camera, and clear filter; the pixel scale was 2.30 arcsec when binned at 2×2 pixels and all exposures were 300 seconds.

Data processing and analysis were done with *MPO Canopus* (Warner, 2018). All images were calibrated with dark and flat-field frames and the instrumental magnitudes converted to R magnitudes using solar-colored field stars from a version of the CMC-15 catalogue distributed with *MPO Canopus*. Table I shows the observing circumstances and results.

1631 Kopff (1936 UC) was discovered on 1936 October 11 by Y. Vaisala at Turku and named in memory of August Kopff (1882-1960), who as Wolf's assistant in Heidelberg discovered and observed many minor planets. It is an inner main-belt asteroid with a semi-major axis of 2.236 AU, eccentricity 0.214, inclination 7.491°, and an orbital period of 3.34 years. Its absolute magnitude is H = 12.29 (JPL, 2023). The NEOWISE satellite infrared radiometry survey (Mainzer et al., 2019) found a diameter D = 8.636 ± 0.395 km using an absolute magnitude H = 12.10.

Observations were conducted over two nights and collected 78 data points. The period analysis shows a rotational period of P = 6.682 ± 0.002 h with an amplitude A = 0.28 ± 0.02 mag, in good agreement with the previously results published in the LCDB (Sada et al., 2004; Ďurech et al., 2020).

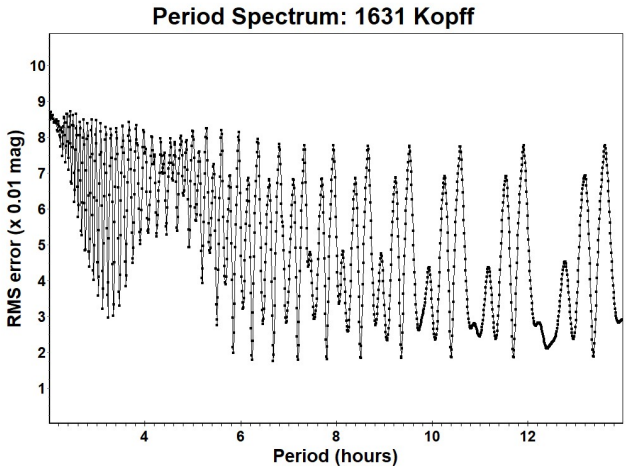

Number	Name	2023/mm/dd	Phase	L_{PAB}	B_{PAB}	Period(h)	P.E.	Amp	A.E.	Grp
1631	Kopff	11/07-11/11	*4.0,3.8	48	6	6.682	0.002	0.28	0.02	MB-I
2244	Tesla	12/03-12/19	3.4,9.0	70	-6	24.65	0.04	0.13	0.03	MB-O
2967	Vladisvyat	11/07-11/18	*3.0,4.3	48	6	8.374	0.001	0.59	0.02	URS
9628	Sendaiotsuna	10/03-10/14	*11.2,10.8	16	17	2.664	0.001	0.07	0.02	EUN

Table I. Observing circumstances and results. The phase angle is given for the first and last date. If preceded by an asterisk, the phase angle reached an extremum during the period. L_{PAB} and B_{PAB} are the approximate phase angle bisector longitude/latitude at mid-date range (see Harris et al., 1984). Grp is the asteroid family/group (Warner et al., 2009).

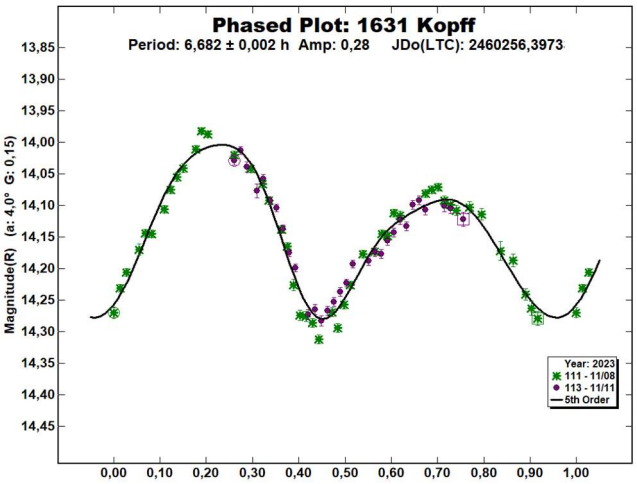

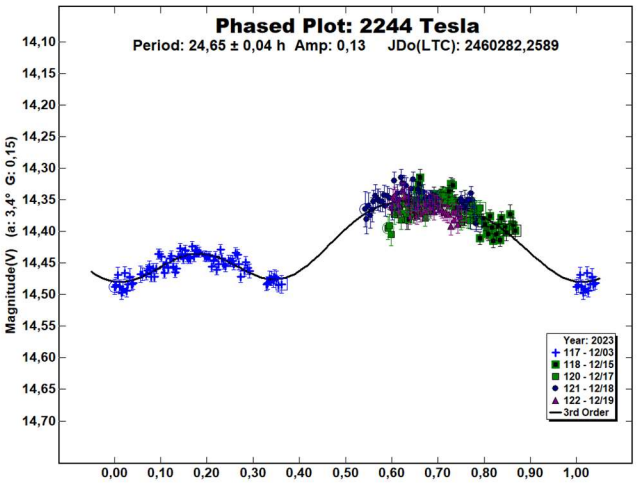

2244 Tesla (1952 UW1) was discovered on 1952 October 22 by M.B. Protitch at Belgrade and named in memory of Nikola Tesla (1856-1943), the famous Yugoslav-born physicist well known for his numerous scientific researches and discoveries in the field of multi-phase and high frequency currents and radio electrocommunications. It is an outer main-belt asteroid with a semi-major axis of 2.812 AU, eccentricity 0.182, inclination 7.822°, and an orbital period of 4.72 years. Its absolute magnitude is $H = 11.99$ (JPL, 2023). The NEOWISE satellite infrared radiometry survey (Mainzer et al., 2019) found a diameter $D = 24.377 \pm 0.030$ km using an absolute magnitude $H = 11.9$.

Observations during the period of visibility, conducted over six nights and collecting 277 data points, do not cover the entire rotation and do not allow us to identify an unambiguous solution. Although the period spectrum shows a few possible alternative solutions, we have selected the slightly stronger one that is associated with a bimodal lightcurve. We suggest that the most likely value of the synodic rotational period is P = 24.65 ± 0.04 hours with an amplitude of A = 0.13 ± 0.03 mag. Further observations will be necessary to nail down the actual period of this slow rotating asteroid.

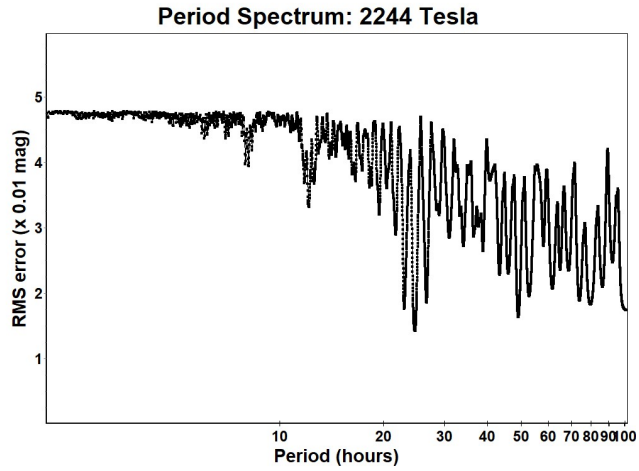

2967 Vladisvyat (1977 SS1) was discovered on 1977 September 19 by N.S. Chernykh at Nauchnyj and named for Vladimir Svyatoslavich (ca. 950-1015), Kiev Grand Prince who worked for the consolidation of Kiev and introduced Christianity into Russia in 988-989. It is a main-belt asteroid with a semi-major axis of 3.203 AU, eccentricity 0.137, inclination 18.003°, and an orbital period of 5.73 years. Its absolute magnitude is $H = 11.31$ (JPL, 2023). The NEOWISE satellite infrared radiometry survey (Mainzer et al., 2019) found a diameter $D = 32.879 \pm 0.553$ km using an absolute magnitude $H = 11.0$.

Observations were conducted over three nights and collected 219 data points. The period analysis shows a rotational period of $P = 8.374 \pm 0.001$ h with an amplitude $A = 0.59 \pm 0.02$ mag.

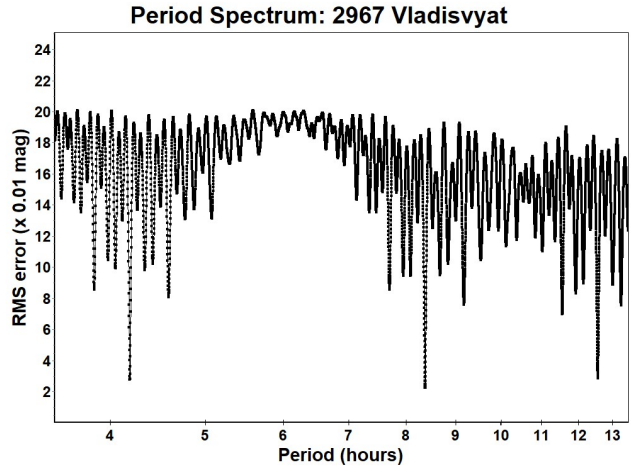

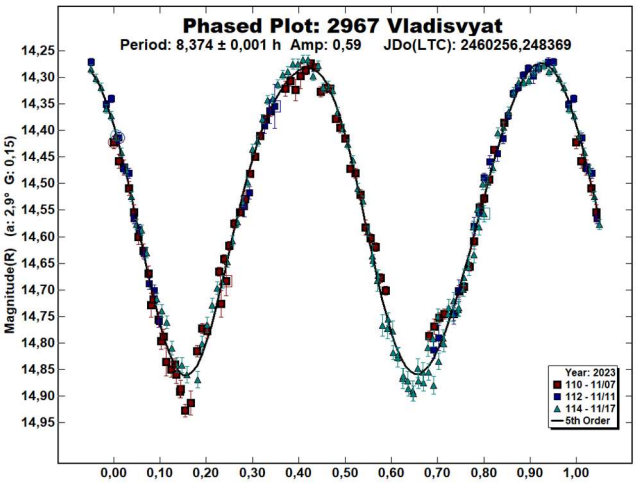

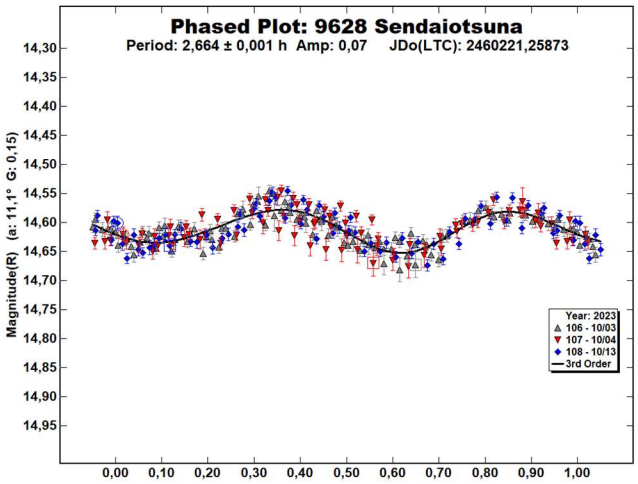

9628 Sendaiotsuna (1993 OB2) was discovered on 1993 July 16 by E.F. Helin at Palomar and named for Sendai Otsunahiki, a 400-year-old tug-of-war festival held in Satsumasendai City in the evening of the day before the Autumnal Equinox. Japan's biggest tug-of-war rope, "Sendai Otsuna," 365 meters in length and six tons in weight, is used for the festival. It is a main-belt asteroid with a semi-major axis of 2.610 AU, eccentricity 0.203, inclination 12.418°, and an orbital period of 4.22 years. Its absolute magnitude is H = 12.42 (JPL, 2023). The NEOWISE satellite infrared radiometry survey (Mainzer et al., 2019) found a diameter D = 9.208 ± 0.243 km using an absolute magnitude H = 12.1.

Observations were conducted over three nights and collected 255 data points. The period analysis shows a rotational period of P = 2.664 ± 0.001 h with an amplitude A = 0.07 ± 0.02 mag. The rotation is quite close to the spin limit barrier; because of the slight possible attenuation of light between phase 0.30 and phase 0.55 during the session of October 5, further observations are strongly encouraged to investigate the possibility of a satellite.

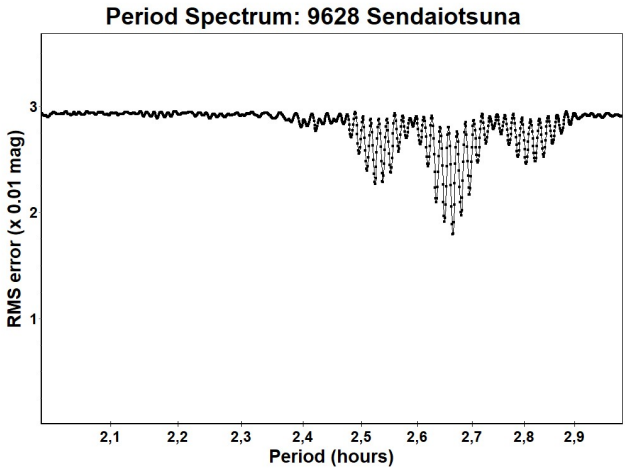

Acknowledgements

The authors want to thank a group of high school students from Liceo "Sacro Cuore di Gesù" (Siena), involved in an interesting vocational guidance project about astrophysics at the Astronomical Observatory of the University of Siena. With their teacher, Sara Mancino, they attended some observing sessions and participated in data analysis: L. Ahmed, G. Ciabatti, C. Giglia, G. Marino, E. Marra, M. Perozzi, V. Vanzi, M. Vegni, W. Zheng.

References

Ďurech, J.; Tonry, J.; Erasmus, N.; Denneau, L.; Heinze, A.N.; Flewelling, H.; Vančo, R. (2020). "Asteroid models reconstructed from ATLAS photometry." *Astron. Astrophys.* **643**, A59.

Harris, A.W.; Young, J.W.; Scaltriti, F.; Zappala, V. (1984). "Lightcurves and phase relations of the asteroids 82 Alkmene and 444 Gyptis." *Icarus* **57**, 251-258.

JPL (2023). Small Body Database Search Engine. *https://ssd.jpl.nasa.gov*

Mainzer, A.K.; Bauer, J.M.; Cutri, R.M.; Grav, T.; Kramer, E.A.; Masiero, J.R.; Sonnett, S.; Wright, E.L. (2016). "NEOWISE Diameters and Albedos V1.0." *NASA Planetary Data System. https://doi.org/10.26033/ddgd-9m07*

Sada, P.V.; Canizales, E.D.; Armada, E.M. (2004). "CCD photometry of asteroids 970 Primula and 1631 Kopff using a remote commercial telescope." *Minor Planet Bull.* **31**, 49-50.

Warner, B.D.; Harris, A.W.; Pravec, P. (2009). "The Asteroid Lightcurve Database." *Icarus* **202**, 134-146. Updated 2023 Oct 1. *https://minplanobs.org/mpinfo/php/lcdb.php*

Warner, B.D. (2018). MPO Software, MPO Canopus v10.7.7.0. Bdw Publishing. *http://bdwpublishing.com/*

PHOTOMETRIC OBSERVATIONS AND ANALYSIS OF EIGHT ASTEROIDS FROM MALTA, SLOVAKIA AND ESTONIA

Stephen M. Brincat
Flarestar Observatory (MPC: 171)
Fl.5 George Tayar Street
San Gwann SGN 3160, MALTA
stephenbrincat@gmail.com

Marek Bucek
Luckystar Observatory (MPC: M55)
Dr. Lučanského 547,
Važec, 032 61, SLOVAKIA

Charles Galdies
Znith Observatory
Armonie, E. Bradford Street,
Naxxar NXR 2217, MALTA

Martin Mifsud
Manikata Observatory
51, Penthouse 7, Sky Blue Court
Dun Manwel Grima Street
Manikata MLH 5013, MALTA

Winston Grech
Antares Observatory
76/3, Kent Street,
Fgura FGR 1555, MALTA

Tõnis Eenmäe
Tartu Observatory, Estonia

(Received: 2023 December 20)

We report the results of our photometric observations of eight main-belt asteroids from six observatories in Malta, Slovakia, and Estonia. We obtained the lightcurves for the following asteroids, which can facilitate future analysis of these objects at different oppositions: 894 Erda; 914 Palisana; 2286 Fesenkov; 2360 Volgo-Don; 3710 Bogoslovskij; 3852 Glennford; 6898 Saint-Marys; and (23552) 1994 NB.

We conducted photometric observations of eight main-belt asteroids from four observatories located on the Maltese mainland, one at Važec, Slovakia and another at Tartu, Estonia. Through these observatories listed in Table 1, we have observed the following asteroids: 894 Erda, 914 Palisana, 2286 Fesenkov, 2360 Volgo-Don, 3710 Bogoslovskij, 3852 Glennford, 6898 Saint-Marys, and (23552) 1994 NB. Except for the images gathered at Tartu Observatory for which a Cousins R-filter was used, we employed a clear filter (unfiltered) with PR (Pan-STARRS r) zero point for all other images. All of our images were calibrated through dark-frame subtraction and flat-field division.

We remotely controlled all of our equipment over the Internet or from a nearby location for each telescope. Operations at Tartu Observatory were performed through direct control on site by C. Galdies. We used *Sequence Generator Pro* (Binary Star Software) for image acquisition by all Maltese Observatories. Luckystar Observatory used the *NINA* image acquisition software (Berg, 2023) while at Tartu Observatory, *Maxim DL* software was employed. We used *MPO Canopus* software (Warner, 2017) for our image analysis, to obtain differential aperture photometry, and to construct lightcurves. Table I displays the details of the instrumentation and observation tuns for each target. We selected near-solar color comparison stars using the Comparison Star Selector (CSS) feature of *MPO Canopus*. We based all brightness measurements on the Asteroid Terrestrial-impact Last Alert System (ATLAS) catalogue (Tonry et al., 2018).

Observatory Country	Ap (m) Type	Camera	Asteroids (#Runs)
Antares MALTA	0.28 SCT	SBIG ST-11	2360 (5)
Flarestar (171) MALTA	0.25 SCT	Moravian G2-1600	894 (7) 914 (5) 2360 (4)
Luckystar (M55) SLOVAKIA	0.25 SCT	Atik 460EX	3710 (3) 6898 (6) 23552 (3)
Manikata MALTA	0.20 SCT	SBIG ST-9	2286 (3)
Tartu (L75) ESTONIA	0.60 Zeiss 600 L	Andor iKon-L 936	894 (1)
Znith Obs. MALTA	0.20 SCT	Moravian G2-1600	3852 (4)

Table I. Instrumentation and Observation Runs. SCT: Schmidt-Cassegrain Telescope; L: Reflector. Observatory column gives the MPC code.

894 Erda is an outer main-belt asteroid that was discovered on 1918 Jun 4 by M. Wolf at Heidelberg. This asteroid was named for the Norse goddess, incarnation of the nature and a seer who knows the origin and the destination of all things (Schmadel, 2003). It has an estimated diameter of 28.3 ± 1.5 km diameter, based on *H* of 9.87. It orbits the Sun with a semi-major axis of 3.117 au with an eccentricity of 0.11 and period of 5.5 years (JPL, 2023).

This asteroid was previously observed by Behrend (2023web); Stephens (2002); Higgins and Goncalves (2007); and Benishek (2022).

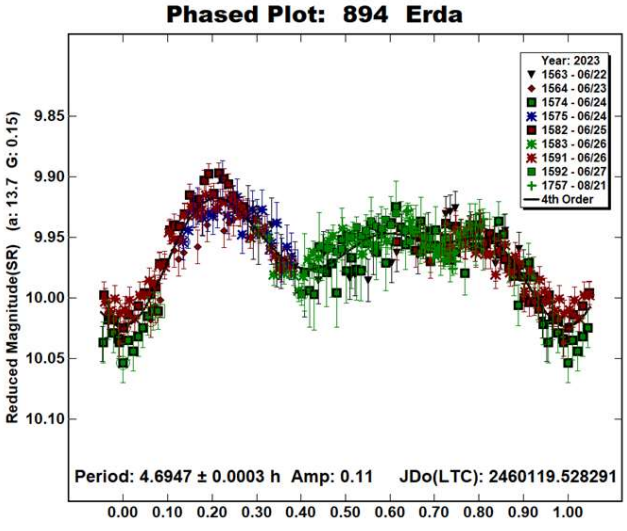

During this observing campaign, Flarestar Observatory observed this target for a period of seven nights from 2023 June 22-27. Tartu Observatory in Estonia also contributed to the data by conducting another observation run of this asteroid on 2023 August 21using a 0.6-m reflector Zeiss 600. The data obtained from Tartu Observatory merged effectively with the data acquired from Flarestar Observatory.

From our analysis, we derived a synodic period of 4.6947 ± 0.0003 h with an amplitude of 0.11 ± 0.02 magnitude. The period is consistent with the previously published results.

914 Palisana is a carbonaceous asteroid that is taxonomic CU under the Tholen Classification. The letter U is assigned when an object possesses an unusual spectrum for its type. This makes Palisana an interesting object because type CU objects are uncommon. It was discovered on 1919 July 4 by M. Wolf at Heidelberg and is named in honor of the well-known Austrian astronomer Johann Palisana (1848-1925), who was an observer at the Marine Observatory in Pola (now Pula, Croatia) (Schmadel, 2003).

The Small-Body database and JPL (2023) list the asteroid as having a diameter of 76.190 ± 0.486 km by NEOWISE (Masiero et al., 2014) and orbits the Sun with a semi-major axis of 2.457 au. Its orbit has an eccentricity of 0.214 and a period of 3.853 years (JPL, 2023).

Palisana was observed from Flarestar Observatory on five nights. Our results yielded a synodic period of 8.685 ± 0.001 h with an amplitude of 0.27 ± 0.02 mag, which is consistent with the previously published results by Colazo et al. (2022) and Stephens and Warner's (2020) period 1 of 8.686 ± 0.03 h.

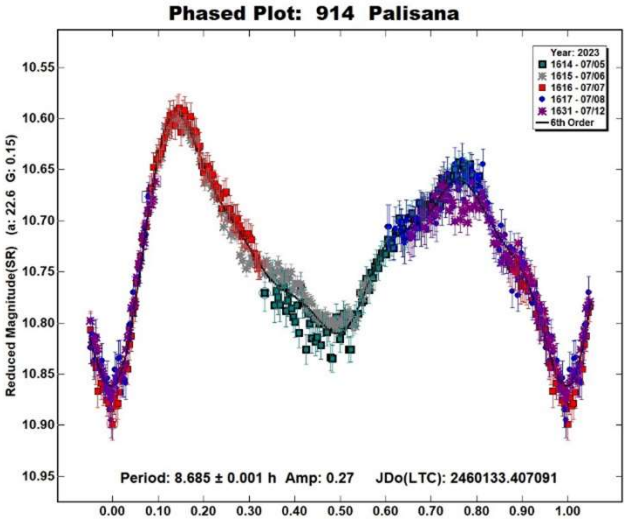

2286 Fesenkov is a main-belt asteroid that was discovered by N.S. Chernykh at the Crimean Astrophysical Observatory on 1977 July 14. The asteroid was named in memory of Vasilej Grigor'evich Fesenkov (1889-1972), one of the founders of the study of astrophysics in the former Soviet Union (Schmadel, 2003). Notably, he served as the editor of the Astronomicheskij Zhurnal from 1924 to 1964 and assumed the role of Chairman of the Committee on Meteorites of the U.S.S.R. Academy of Sciences from 1945 onward.

Based on NEOWISE data (Masiero et al., 2012), the estimated diameter is 6.691 ± 0.103 km. The absolute magnitude is H = 13.11. This minor planet orbits the Sun with a semi-major axis of 2.193 au, eccentricity of 0.093, and period of 3.25 years (JPL, 2023).

With the aim to improve the quality of the published period by Waszczak et al. (2015) of 5.404 ± 0.0025 h (U=2), observations of Fesenkov were acquired from Manikata Observatory over three nights from 2023 November 14 to 20. Our results are consistent with those obtained by Waszczak et al., our synodic period being 5.402 ± 0.001 h with an amplitude of 0.53 ± 0.03 mag.

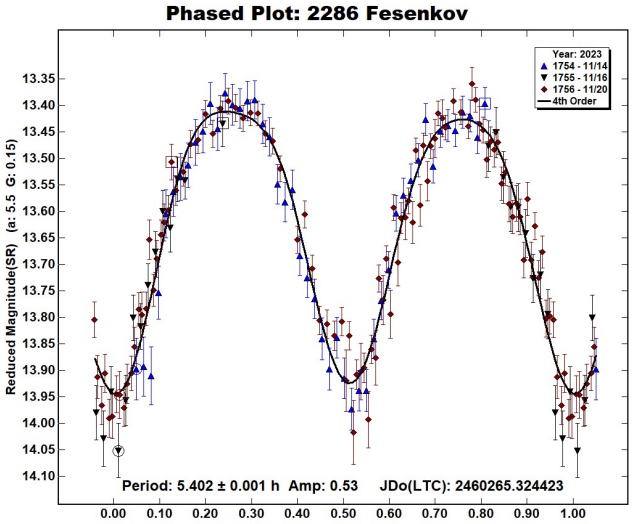

2360 Volgo-Don (1975 VD3) is a middle main-belt asteroid that was discovered on 1975 November 2 by T. Smirnova at Nauchnyj (Schmadel, 2003). It was named on the occasion of the 30th anniversary of the construction of the Volgo-Don Navigation Canal, which connects the Volga and Don rivers at their closest approach.

NEOWISE data gives an estimated diameter of 9.692 ± 0.071 km (Masiero et al., 2014). This absolute magnitude is H = 13.05. The orbit has a semi-major axis of 2.672 au with an eccentricity of 0.196. The orbital period is 3.19 years (JPL, 2023).

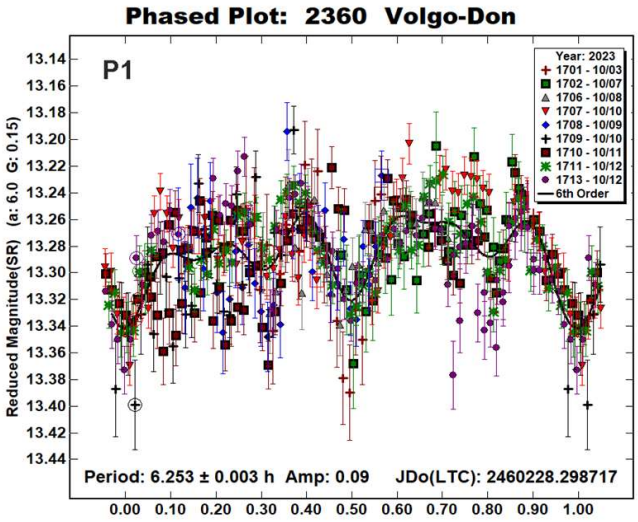

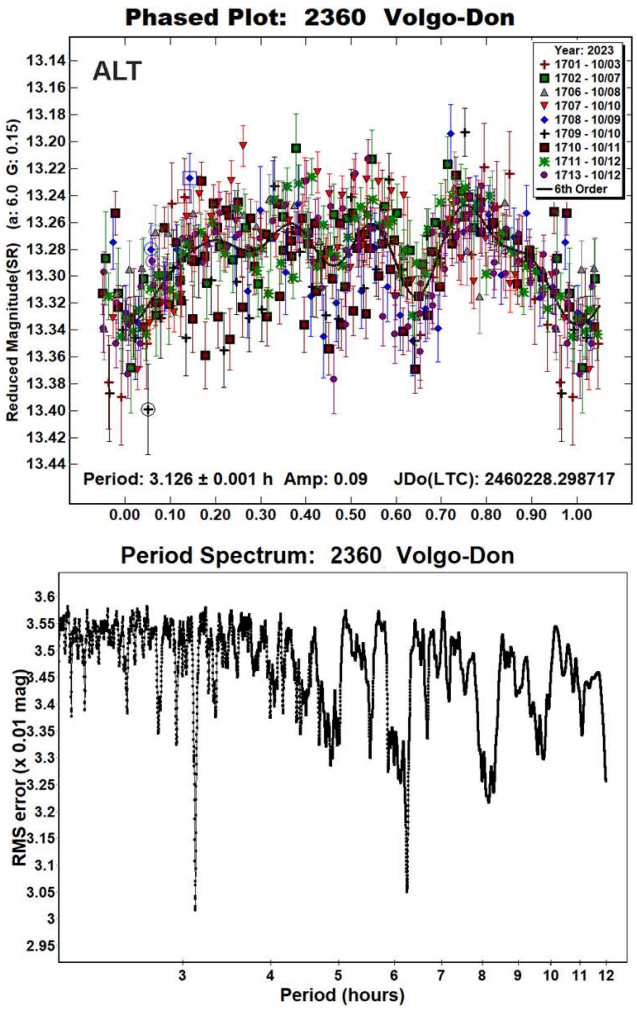

Because the asteroid had no published period that we could find, it was picked for observation by Flarestar and Antares Observatories. Our results produced two possible lightcurve solutions, with the preferred one (P_1) being 6.253 ± 0.003 h (A = 0.09 ± 0.04 mag). The alternate solution of 3.126 ± 0.001 h (amp. 0.09 ± 0.04 mag.) is the half-period. Both solutions share a similar RMS with the shorter period having slightly lower residuals.

In our opinion, close inspection of the lightcurve reveals that the 6.253 h period is more likely due to a more coherent fitting to a somewhat symmetrical bi-modal solution. Additional follow-up for this asteroid is encouraged to uncover its true period.

3710 Bogoslovskij (1978 RD6) is a main-belt asteroid that was discovered on 1978 September 13 by N. Chernykh at Nauchnyj. It is named in honor of Nikita Bogoslovskij, a well-known contemporary composer and writer, on the occasion of his eightieth birthday (Schmadel, 2003).

The estimated diameter is 11.625 ±0.196 km (Masiero et al., 2012) The absolute magnitude is listed as H = 12.76. The semi-major axis is 2.74 au and the orbital eccentricity is 0.159. A year for the asteroid is equivalent to 3.17 Earth-years (JPL, 2023).

3710 Bogoslovskij was observed from Luckystar Observatory on three nights from 2023 August 19 to September 7. Our result is consistent with Behrend (2023web), who observed the asteroid around the same time. He reported the rotation period to be 8.0138 ± 0.0004 h. Our solution was 8.016 ± 0.008 h with an amplitude of 0.49 ± 0.02 mag.

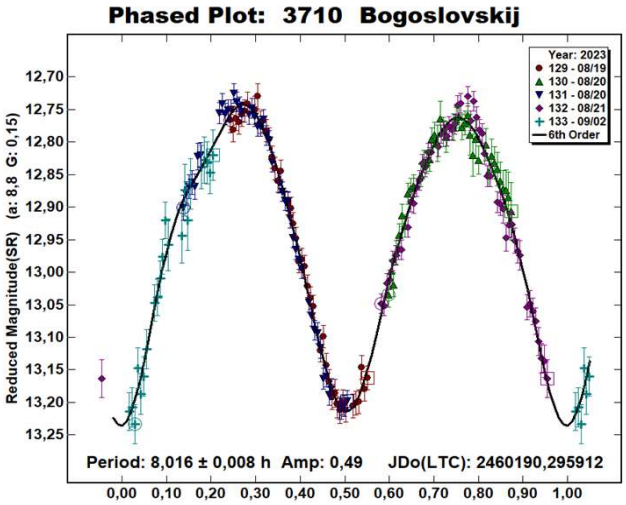

3852 Glennford is a main-belt asteroid that was discovered on 1987 February 24 by H. Debehogne at the European Southern Observatory. The diameter of this asteroid is estimated to be 18.510 ± 0.179 km (Masiero et. al, 2011) and has an absolute magnitude of H = 12.37. The semi-major axis is 3.105 au, which yields an orbital period of 3.71 years. 3852 Glennford is named after the Canadian-born actor Glenn Ford (1916-2006), who appeared in more than 100 movies covering virtually every genre, from westerns to science fiction (Schmadel, 2003).

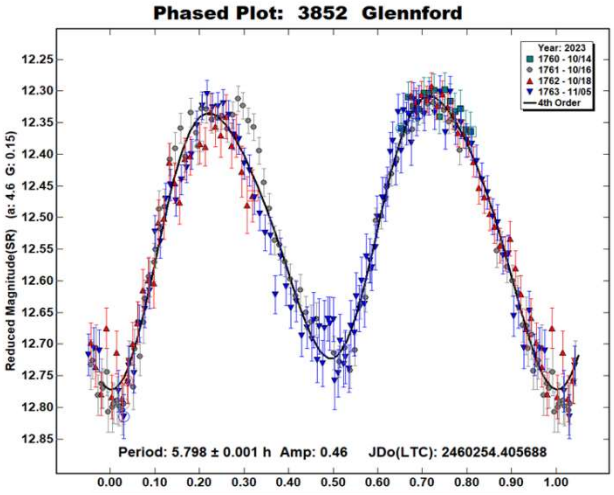

We observed on four nights from Znith Observatory, where we derived the synodic period to be 5.798 ± 0.001 h with an amplitude of 0.46 ± 0.03 mag. Our result is consistent with that published by Ďurech et al. (2019).

6898 Saint-Marys (1998 LE) is a main-belt asteroid that belongs to the 502 Eunomia family (Nesvorny et al., 2015). It was discovered on 1988 June 8 by C.S. Shoemaker at Palomar. Its estimated diameter is 8.447 ± 0.130 km (Masiero et al., 2014). It orbits the Sun with a semi-major axis of 2.665 au and has an eccentricity of 0.123. The asteroid completes one orbit around the sun every 4.35 years (JPL, 2023).

We observed 6898 from Luckystar Observatory on six nights from 2023 May 10-21. Based on these observations, we determined the synodic period to be 5.778 ± 0.001 hours, with an amplitude of 0.13 ± 0.02 mag. The shape of the lightcurve for that period is bimodal. Close inspection of the lightcurve reveals two bumps prior to the peak brightness. Although it is possible that these are real features, this prompted us to check whether or not the half-period was the correction solution.

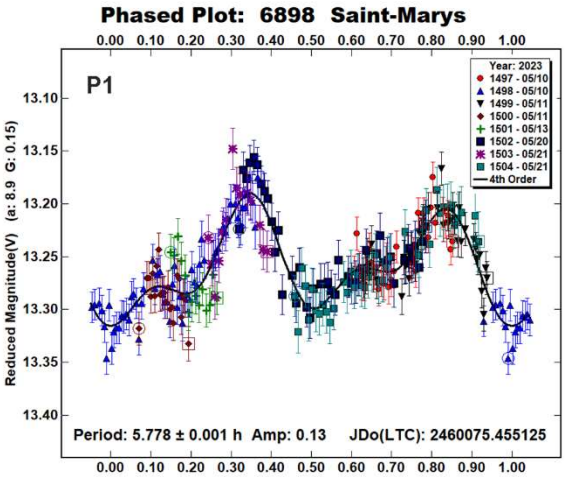

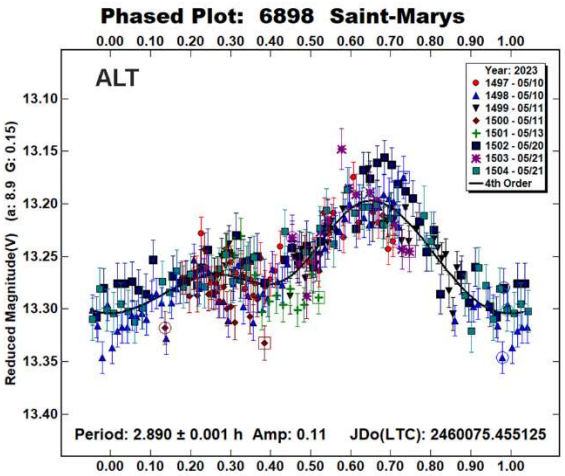

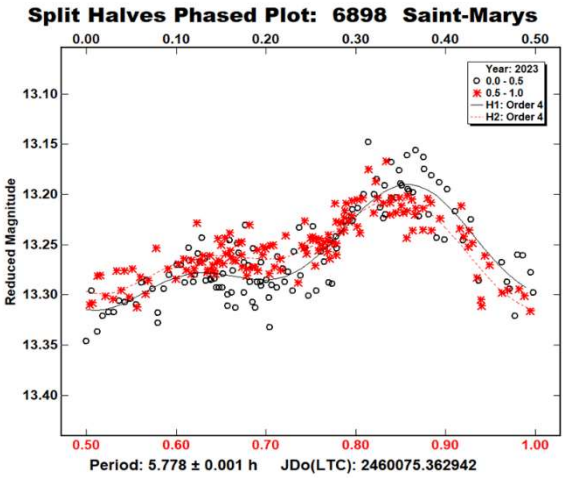

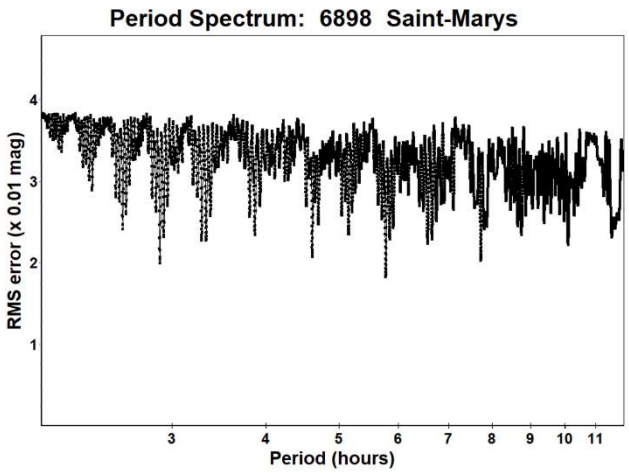

The split-halves plot showed a similar distribution with some deviations that did not allow us to confidently determine its true period. Hence, we cannot rule out the alternative period (ALT) of 2.890 ± 0.001 h with an amplitude of 0.11 ± 0.03 mag. The LCDB database did not contain any previous results.

(23552) 1994 NB is a main-belt asteroid that belongs to the Phocaea family. This asteroid was discovered on 1994 July 3 by E.F. Helin, at Palomar Observatory. The absolute magnitude is H =13.68. The orbit has a semi-major axis of 2.364 au and eccentricity of 0.277. The orbital period is 3.63 years (JPL, 2023).

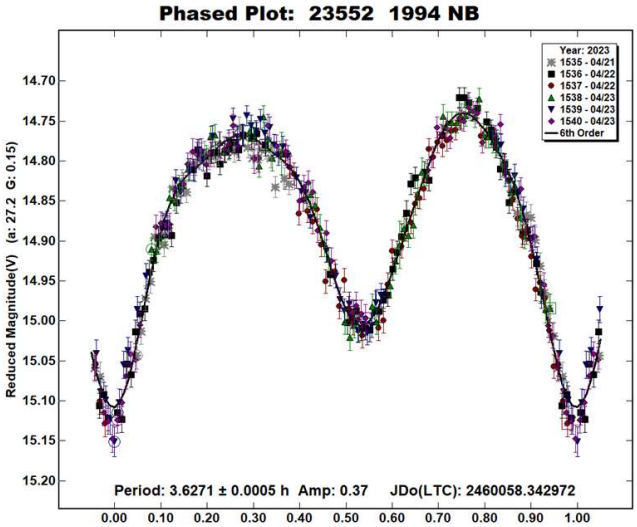

(23552) 1994 NB was observed from Luckystar Observatory over three nights from 2023 April 21-23. Our synodic period of 3.6271 ± 0.0005 h is consistent with results from Loera-González et al. (2023) and Skiff et al. (2023). The amplitude is 0.37 ± 0.03 mag.

Number	Name	2023 mm/dd	Phase	L_{PAB}	B_{PAB}	Period(h)	P.E.	Amp	A.E.	Grp
894	Erda	06/22-08/21	14.0,12.0	302	15	4.6947	0.0003	0.11	0.02	MB
914	Palisana	07/05-07/12	22.8,21.6	309	27	8.685	0.001	0.27	0.02	MB
2286	Fesenkov	11/14-11/20	6.0,2.5	61	0	5.402	0.001	0.53	0.03	MB
2360	Volgo-Don	10/03-10/12	6.5,1.8	20	-2	6.253	0.003	0.09	0.04	MB
						3.126	0.001	0.09	0.04	
3710	Bogoslovskij	08/19-09/02	9.1,7.5	335	14	8.016	0.008	0.49	0.02	MB
3852	Glennford	10/14-11/05	4.6,5.8	30	1	5.798	0.001	0.46	0.03	Themis
6898	Saint-Marys	05/10-05/21	8.8,11.3	223	15	5.778	0.001	0.13	0.02	Eunomia
						2.890	0.001	0.11	0.03	
23552	1994 NB	04/21-04/23	27.0,27.4	197	36	3.6271	0.0005	0.37	0.02	Phocaea

Table II. Observing circumstances and results. The phase angle is given for the first and last date. L_{PAB} and B_{PAB} are the approximate phase angle bisector longitude and latitude at mid-date range (see Harris et al., 1984). Grp is the asteroid family/group (Warner et al., 2009).

Acknowledgements

We are grateful to Tartu Observatory for the organization of the Asteroid Research Training Workshop held at Tartu Observatory, which was financed by European Regional Development Fund Project Development of space research ground infrastructure in Estonia (KosEST) and the European Commission HORIZON 2020 project EUROPLANET 2024 Research Infrastructure. Europlanet 2024 Research Infrastructure has received funding from the European Union's Horizon 2020 research and innovation programme under grant agreement No. 871149. We would like to thank Brian Warner for his work in the development of *MPO Canopus* and for his efforts in maintaining the CALL website (Warner, 2009; 2016). This research made use of the JPL's Small-Body Database (JPL, 2023).

References

Behrend, R. (2023web). Observatoire de Geneve web site. *http://obswww.unige.ch/~behrend/page_cou.html*

Benishek, V. (2022). "CCD Photometry of 29 Asteroids at Sopot Astronomical Observatory: 2020 July - 2021September." *Minor Planet Bull.* **49**, 38-44.

Berg, S. (2023). "Nightime Imaging 'N' Astronomy (NINA)" web site. *https://nighttime-imaging.eu/.* Last accessed: 29 June 2023.

Colazo, M.; Scotta, D.; Monteleone, B.; Morales, M.; Ciancia, G.; García, A.; Melia, R.; Suárez, N.; Wilberger, A.; Fornari, C.; Nolte, R.; Bellocchio, E.; Mottino, A.; Colazo, C. (2022). "Asteroid Photometry and Lightcurve Analysis for Six Asteroids." *Minor Planet Bull.* **49**, 304-306.

Ďurech, J.; Hanus, J.; Vanco, R. (2019). "Inversion of asteroid photometry from Gaia DR2 and the Lowell Observatory photometric database." *Astron & Astrophys.* **631**, id. A2.

Harris, A.W.; Young, J.W.; Scaltriti, F.; Zappala, V. (1984). "Lightcurves and phase relations of the asteroids 82 Alkmene and 444 Gyptis." *Icarus* **57(2)**, 251-258.

Higgins, D.; Goncalves, R. (2007). "Asteroid Lightcurve Analysis at Hunters Hill Observatory and Collaborating Stations - June-September 2006." *Minor Planet Bull.* **34**, 16-18.

JPL (2023). Small-Body Database Browser (2023 July 11). *https://ssd.jpl.nasa.gov/tools/sbdb_lookup.html#/*

Loera-González, P.A.; Olguín, L.; Saucedo, J.C.; Contreras, M.E.; Nuñez-López, R.; Domínguez-González, Rafael; Cortez, R.A. (2023). "Rotation Periods for 2707 Ueferji and (23552) 1994 NB." *Minor Planet Bull.* **50**, 258.

Masiero, J.R.; Mainzer, A.K.; Grav, T.; Bauer, J.M.; Cutri, R.M.; Dailey, J.; Eisenhardt, P.R.M.; McMillan, R.S.; Spahr, T.B.; Skrutskie, M.F.; Tholen, D.; Walker, R.G.; Wright, E.L.; DeBaun, E.; Elsbury, D.; Gautier, T.; IV, Gomillion, S.; Wilkins, A. (2011). "Main Belt Asteroids with WISE/NEOWISE. I. Preliminary Albedos and Diameters." *Ap. J.* **741**, A68.

Masiero, J.R.; Mainzer, A.K.; Grav, T.; Bauer, J.M.; Cutri, R.M.; Nugent, C.; Cabrera. (2012). "Preliminary Analysis of WISE/NEOWISE 3-Band Cryogenic and Post-Cryogenic Observations of Main Belt Asteroids." *Ap. J. Letters* **759**, L8.

Masiero, J.R.; Grav, T.; Mainzer, A.K.; Nugent, C.R.; Bauer, J.M.; Stevenson, R.; Sonnett, S. (2014). "Main-belt asteroids with WISE/NEOWISE: Near-infrared albedos." *Ap. J.* **791**, 121.

Nesvorny, D.; Broz, M.; Carruba, V. (2015). "Identification and Dynamical Properties of Asteroid Families." In *Asteroids IV* (P. Michel, F. DeMeo, W.F. Bottke, R. Binzel, Eds.). Univ. of Arizona Press, Tucson, also available on astro-ph.

Schmadel, L.D. (2003). "Catalogue of Minor Planet Names and Discovery Circumstances." In *Dictionary of Minor Planet Names*. Springer, Berlin, Heidelberg.

Skiff, B.A.; McLelland, K.P.; Sanborn, J.J.; Koehn, B.W. (2023). "Lowell Observatory Near-Earth Asteroid Photometric Survey (NEAPS): Paper 5." *Minor Planet Bull.* **50**, 74-101.

Stephens, R.D. (2002). "Photometry of 866 Fatme, 894 Erda, 1108 Demeter, and 3443 Letungdao." *Minor Planet Bull.* **29**, 2-3.

Stephens, R.D.; Warner, B.D. (2020). "Main-belt Asteroids Observed from CS3: 2020 January to March." *Minor Planet Bull*. **47**, 224-229.

Tonry, J.L.; Denneau, L.; Flewelling, H.; Heinze, A.N.; Onken, C.A.; Smartt, S.J.; Stalder, B.; Weiland, H.J.; Wolf, C. (2018). "The ATLAS All-Sky Stellar Reference Catalog." *Ap. J.* **867**, A105.

Warner, B.D. (2016). Collaborative Asteroid Lightcurve Link website. *http://www.minorplanet.info/call.html* Last accessed: 2018 September 26.

Warner, B.D. (2017). MPO Software, *MPO Canopus* version 10.7.10.0. Bdw Publishing. *http://www.minorplanetobserver.com/*

Warner, B.D. (2021). Asteroid Lightcurve Data Exchange Format (ALCDEF) web site. *https://minplanobs.org/alcdef/index.php*

Warner, B.D.; Harris, A.W.; Pravec, P. (2009). "The asteroid lightcurve database." *Icarus* **202**, 134-146. Updated 2023 Apr. *http://www.minorplanet.info/lightcurvedatabase.html*

Waszczak, A.; Chang, C.; Ofek, E.; Laher, R.; Masci, F.; Levitan, D.; Surace, J.; Cheng, Y.; Ip, W.; Kinoshita, D.; Helou, G.; Prince, T.; Kulkarni, S. (2015). "Asteroid Light Curves from the Palomar Transient Factory Survey: Rotation Periods and Phase Functions from Sparse Photometry." *Astron. J.* **150**, A75.

LIGHTCURVE AND ROTATION PERIOD ANALYSIS OF 1887 VIRTON AND 4099 WIGGINS

W. Hawley
Old Orchard Observatory (Z09)
The Old Orchard House, Church Road
Fiddington, UK, TA5 1JG
hawley.wayne@gmail.com

R. Miles
Asteroids and Remote Planets Section
British Astronomical Association

P. Wiggins
University of Utah
Tooele Observatory (718)

J. McCormick
Farm Cove Observatory (E85)
24 Rapallo Place, Farm Cove,
Auckland 2012, New Zealand

A.Watkins
T21 iTelescope (U94)

J.D. Armstrong
University of Hawaii Institute for Astronomy,
34 Ohia Ku Street,
Pukalani, HI 96768 USA

E. Kardasis
Pelagia-Eleni Observatory
Glyfada-Athens, Greece

F. Pilcher
Organ Mesa Observatory (G50)
4438 Organ Mesa Loop
Las Cruces, NM 88011 USA

S. Arnold
NNHS Observatory (Z34)
Stable Lane, Pitsford
Northamptonshire, UK

(Received: 2023 November 20 Revised: 2024 February 7)

Photometric observations of two main-belt asteroids were obtained between 2023 July 13 and 2023 November 11. The following rotational periods were determined: 1887 Virton, 70.165 ± 0.003 h; 4099 Wiggins, 10.985 ± 0.001 h.

Photometric images obtained for this report were obtained from observatories around the globe. Several of the co-authors used their own equipment and some used the iTelescope or Las Cumbres Observatory facilities.

Photometry analysis and period determination were carried out using *TychoTracker Pro* Version 10.8.5. (TT), easily performing both functions. Photometric analysis was done using standard differential techniques on images. The TT software has the facility to allow the user to choose comparison stars, for which the default color range of $+0.50 < (B\text{-}V) < +0.90$ was employed. The ATLAS catalog (Tonry et al., 2018) was used as the source of reference stars for both asteroids. TT's period determination operates by finding model light curves - comprising a user-defined number of Fourier components which best fit the asteroid photometric data. The program lists the candidate periods found within a user-defined period range and sampling frequency, based on minimizing Root Mean Square Errors (RMSE), i.e. using the difference between modelled and photometric magnitudes. The candidate periods are listed in increasing RMSE value and the entire suite of RMSE values is plotted as a "periodogram" for quality control.

In these periodograms both objects yielded clear 'best-fit' period solutions having well-defined 'stalactites' as shown in the following Figures. Neither asteroid has a value for its rotational period listed in the current issue of the LCDB (Warner et al., 2009).

Periodograms often exhibit several possible candidate periods, in which case an examination of the rotational phase plot for each of these is then conducted looking for a credible lightcurve. Where the object shape is the dominant factor in producing the observed magnitude changes, (typically having lightcurve amplitudes of >0.2 mag), the rotational phase plot often has two peaks and two troughs (bimodal) and this is usually chosen as the most likely for such asteroids.

In this paper there is no attempt to find an absolute magnitude for any of the asteroids and a value of $G = 0.15$ has been used throughout the calculations. Time-series from different nights and observing locations using a variety of imaging equipment were offset in magnitude to bring them into alignment when producing the raw and rotational-phase plots. The same offset was used for each instance of an individual imaging setup. When this paper is accepted for publication all the observations will be loaded into the ALCDEF database. Some individual datapoints have been combined by stacking during period analysis to improve the signal-to-noise ratio.

The results are summarized in the table below. Column 3 gives the span of dates over which the observations were made. Column 4 is the range of phase angles for each date range, if this is preceded by an asterisk this means the asteroid passed through minimum phase

angle during the observing period. Columns 5 and 6 give the range of values for the Phase Angle Bisector (PAB) longitude and latitude respectively, for the mid date of the observation set. Column 7 gives the period and Column 8 the minimum possible formal error in hours given by *TychoTracker Pro*. Columns 9 and 10 give the amplitude and its associated uncertainty in magnitude. Dips in the results from the period analysis have been checked to see if they are monomodal or bimodal and bimodal periods have been chosen for the best-fit period for each asteroid. Information given below for each of the objects is taken from the JPL Small-Body Database Lookup webpage.

Observatory	Telescope	CCD/CMOS	Filter	Asteroid (Sessions)
Old Orchard (Z09, Hawley)	0.25-m SCT f/10	SX694 Trius Pro (2×2)	SR	(1887)(8)
University of Utah, Tooele (718, Wiggins)	0.35-m SCT f/5.5	ST-10XME (3×3)	C	(1887)(24)
Farm Cove (E85, McCormick)	0.35-m SCT f/10	ST-8XME (2×2)	C	(4099)(9)
Siding Spring LCO-A (Q63, Miles)	1.0-m f/8	Sinistro (1×1)	SR/V	(4099)(1)/(2)
Siding Spring Faulkes Telescope South (E10, Miles)	2.0-m f/10	Spectral (2×2)	SR/V	(1887)(2)/(2) (4099)(16)/(3)
Siding Spring LCO-B (Q64, Miles)	1.0-m f/8	Sinistro (1×1)	SR/V	(4099)(3)
Siding Spring LCO-Clamshell #2 (Q59, Armstrong)	0.4-m f/8	SBIG STL6303 (1×1)	W	(4099)(1)
Sutherland LCO-Aqawan A (L09, Armstrong)	0.4-m f/8	SBIG STL6303 (1×1)	W	(4099)(2)
Cerro Tololo-LCO Aqawan B #1 (W79, Armstrong)	0.4-m f/8	SBIG STL6303 (1×1)	SR	(1887)(1)
Sutherland LCO-C (K93, Miles)	1.0-m f/8	Sinistro (1×1)	SR	(4099)(2)
Haleakala-LCO Clamshell #2 (T03, Armstrong)	0.4-m f/8	SBIG STL6303 (1×1)	W	(4099)(1)
Haleakala-LCO Clamshell #1 (T04, Armstrong)	0.4-m f/8	SBIG STL6303 (1×1)	W	(4099)(1)
McDonald LCO Aqawan A #1 (V38, Miles)	0.4-m f/8	SBIG STL6303 (1×1)	SR/V	(1887)(1) (1)
Tenerife Observatory-LCO B (Z24, Miles)	1.0-m f/8	Sinistro (1×1)	SR	(4099)(1)
Tenerife Observatory-LCO A (Z31, Miles)	1.0-m f/8	Sinistro (1×1)	SR	(4099)(1)
Pelagia-Eleni Observatory Glyfada-Athens Greece (247, Kardasis)	0.28-m SCT, f/10	ASI183MM PRO (4×4)	V	(1887)(1) (4099)(2)
T21 iTelescope Observatory, Beryl Junction (Sato) (U94, Watkins)	0.43-m f/6.8	FLI-PL16803	V	(1887)(3) (4099)(1)
Organ Mesa, Las Cruces (G50, Pilcher)	0.35-m SCT f/10	SBIG STL-1001E (1×1)	C	(1887)(8)
NNHS Observatory (Z34, Arnold)	0.3-m Reflector f/3.8	SX694 (1×1)	C	(1887)(3)

1887 Virton. A main belt asteroid and a member of the Eos family. Discovered on 1950 October 05 by S. Arend, observing from Uccle, Belgium. It has an approximate diameter of 21 km. Although no rotation period has been published to our knowledge, the LCDB does list a value of 0.5 mag for the amplitude of its lightcurve, i.e., greater than the value reported here. The lightcurve period and amplitude results reported here are based on 54 observing sessions (a total of 3870 exposures) during 2023 September–November (70.165 ± 0.003 h, 0.381 ± 0.02 mag).

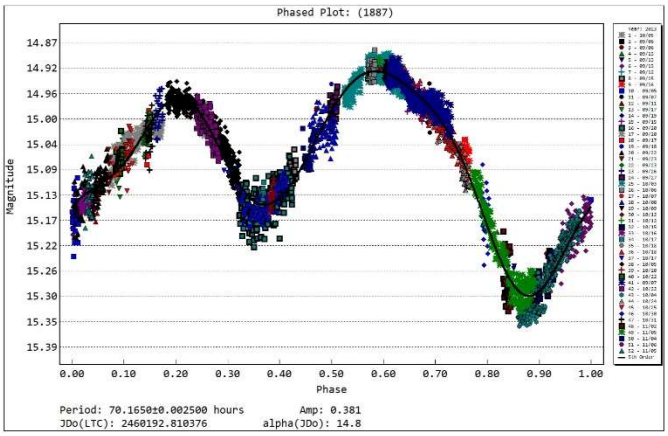

Number	Name	yyyy mm/dd	Phase	L_{PAB}	B_{PAB}	Period (h)	P.E.	Amp	A.E.	Grp
1887	Virton	2023 09/05-11/11	*2.9,14.8	18	6	70.165	0.003	0.381	0.025	606
4099	Wiggins	2023 07/13-11/02	*2.8,22.0	332	-6	10.985	0.001	0.335	0.031	506

Table I. Observing circumstances and results. The phase angle is given for the first and last date. If preceded by an asterisk, the phase angle reached a minimum during the period. L_{PAB} and B_{PAB} are the approximate phase angle bisector longitude/latitude at mid-date range (see Harris et al., 1984). Grp is the asteroid family/group (Warner et al., 2009).

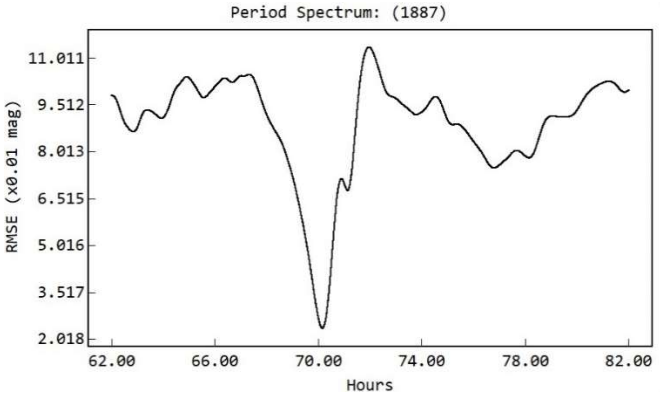

4099 Wiggins. A main belt asteroid and a member of the Maria family. Discovered on 1988 January 13 by H. Debehogne at the European Southern Observatory. It is a relatively small object having an approximate diameter of 7.5 km. This object is named after one of the co-authors of this paper. No previously published rotation period has been found. Lightcurve period and amplitude results from 51 sessions (541 exposures) are reported for 2023 July - November (10.985 ± 0.001 h, 0.335 ± 0.03 mag).

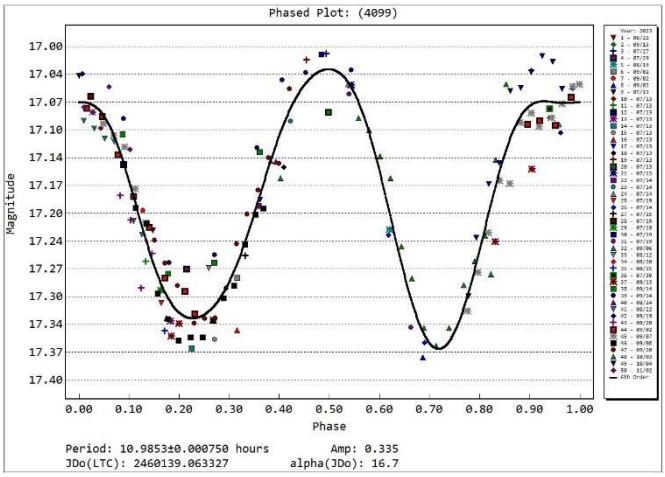

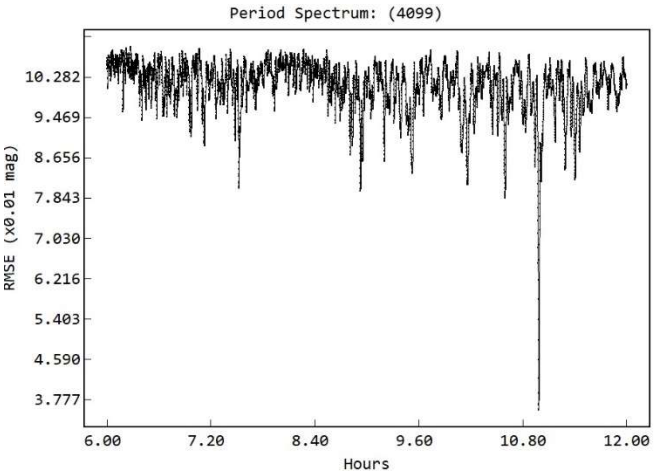

Acknowledgements

Our thanks are extended to Daniel Parrott, author of *TychoTracker Pro*.

This work has made use of data from the Asteroid Terrestrial-impact Last Alert System (ATLAS) project. ATLAS is primarily funded to search for near earth asteroids through NASA grants NN12AR55G, 80NSSC18K0284, and 80NSSC18K1575; byproducts of the NEO search include images and catalogs from the survey area. The ATLAS science products have been made possible through the contributions of the University of Hawaii Institute for Astronomy, the Queen's University Belfast, the Space Telescope Science Institute, and the South African Astronomical Observatory. The ATLAS Catalog makes use of the formulae to convert Pan-STARRS gri to BVRI. (Kostov and Bonev, 2017).

References

JPL Small-Body Database Lookup webpage. *https://ssd.jpl.nasa.gov/tools/sbdb_lookup.html*

Harris, A.W.; Young, J.W.; Scaltriti, F.; Zappala, V. (1984). "Lightcurves and phase relations of the asteroids 82 Alkmene and 444 Gyptis." *Icarus* **57**, 251-258.

Kostov, A.; Bonev, T. (2017) "Transformation of Pan-STARRS1 gri to Stetson BVRI magnitudes. Photometry of small bodies observations." *Bulgarian Astron. J.* **28**, 3 (ArXiv:1706.06147v2).

Tonry, J.L.; Denneau, L.; Flewelling, H.; Heinze, A.N.; Onken, C.A.; Smartt, S.J.; Stadler, B.; Weiland, H.J.; Wolf, C. (2018). "The ATLAS All-Sky Stellar Reference Catalog." *Astrophys. J.* **867**, A105.

Warner, B.D.; Harris, A.W.; Pravec, P. (2009). "The Asteroid Lightcurve Database." *Icarus* **202**, 134-146. Updated 2023 Oct 1. *https://minorplanet.info/php/lcdb.php*

LIGHTCURVE ANALYSIS FOR EIGHT MAIN-BELT AND THREE NEAR-EARTH ASTEROIDS

Gonzalo Fornas, AVA - J57, CAAT
Centro Astronómico del Alto Turia, SPAIN
gon@iicv.es

Fernando Huet, AVA - Z93

Enrique Arce, AVA - J67

Rafael Barberá, AVA - J57, CAAT
Centro Astronómico del Alto Turia, SPAIN

Álvaro Fornas AVA - J57, CAAT
Centro Astronómico del Alto Turia, SPAIN

Gonzalo Fornas Jr.

Vicente Mas, AVA - J57, CAAT,
Centro Astronómico del Alto Turia, SPAIN

(Received: 2024 January 9)

Photometric observations of eight main-belt asteroids and three NEAs were obtained between 2023/8 - 2023/12. We derived the following rotational synodic periods: 353 Ruperto-Carola, 2.7389 ± 0.000016 h; 452 Hamiltonia, 2.88119 ± 0.00007 h; 914 Palisana, 8.68062 ± 0.00017 h; 1554 Yugoslavia, 3.8873 ± 0.0002 h; 2729 Urumqi, 3.127840 ± 0.000024 h; 4917 Yurilvovia, 10.169 ± 0.018 h; 8142 Zolotov, 4.32388 ± 0.00005 h; (6037) 1988 EG, 2.75724 ± 0.00036 h; 15817 Lucianotesi, 12.687 ± 0.005 h; (41437) 2000 GT122, 2.99011 ± 0.00035 h; (154244) 2002 KL6, 4.60721 ± 0.00002 h. And the following sidereal periods: 452 Hamiltonia: 2.881314 ± 0.000002 h; 1554 Yugoslavia: 3.88762 ± 0.000003; 8142 Zolotov: 4.323410 ± 0.000003 h.

We report on the photometric analysis results for eight main-belt and three NEAs by Asociación Valenciana de Astronomía (AVA). The data were obtained during the last months of 2023. We present graphic results of data analysis, mainly lightcurves, with the plot phased to a given period. We managed to obtain a number of accurate and complete lightcurves and calculating as accurately as possible their rotation periods.

Observatory	Telescope (meters)	CCD
C.A.A.T. J57	43 cm DK	QHY- 600
C.A.A.T. J57	200 mm NW	ZWO ASI 1600
Z93	SC 8”	SBIG ST8300
J67	SC 10”	SBIG ST7

Table I. List of instruments used for the observations.

We focused on asteroids with no reported period and those where the reported period was poorly established and needed confirmation. All the targets were selected from the Collaborative Asteroid Lightcurve (CALL) website (*http://www.minorplanet.info/call.html)* and the Minor Planet Center (*http://www.minorplanet.net*). The Asteroid Lightcurve Database (LCDB; Warner et al., 2009) was consulted to locate previously published results.

Work Methods

Images were measured using *MPO Canopus* (Bdw Publishing) with the differential photometry technique. The comparison stars were restricted to near solar-color to minimize color dependencies, especially at larger air masses. The lightcurves show the synodic rotation period. The amplitude (peak-to-peak) that is shown is that for the Fourier model curve and not necessarily the true amplitude.

If we have enough data in ALCDEF in addition to our own data, we can try a second step with the software *LC INVERT* (Bdw Publishing), which uses the inversion method described by Kaasalainen (2001). This software uses the code written by J. Durech based on the original FORTRAN code written by Kaasalainen: “Period Scan”. The advantage of this method is that it allows the use of "dense" data such as the ones we have obtained in our measurements together with "sparse" data type, available in databases from Catalina, USNO, Atlas, Palomar, etc.

This is an iterative method that, based on an initial estimate of the period given by the lightcurve, finds the local minimum of χ^2 and gives the corresponding solution. The procedure starts with six initial poles for each trial period and selects the period that gives the lowest χ^2. If there is a clear minimum in χ^2 when plotted as a function of the period, we can assume it as a correct solution. Not always we get a clear solution. We have referenced only those asteroids with an unambiguous calculation.

When calculating we use weighting coefficients to take into account the density of the data. We assign to "dense" data a value of 1 and to "sparse" data a value of 0.3 as an empiric rule.

Error estimates for inversion method are not obvious. The smallest separation ΔP of local minima (Kaasalainen and Torppa, 2001; Kaasalainen et al., 2001), in the period parameter space is roughly given by

$$\Delta P \approx 0.5 * P^2/\Delta t$$

where Δt is the full epoch range of the data set. This derives from the fact that the maxima and minima of a double sinusoidal lightcurve for periods P and $P \pm \Delta P$ are at the same epochs after Δt time.

As we can read at M. Kaasalainen and Torppa (2001), “The period error is mostly governed by the epochs of the lightcurves. If the best local χ^2minimum of the period spectrum is clearly lower than the others, one can obtain an error estimate of, say, a hundredth part of the smallest minimum width ΔP since the edge of a local minimum ravine always lies much higher than its bottom.”

J. Durech proposes an estimate of error of

$$\Delta P \approx (1/10 * 0.5) * P^2/\Delta t$$

The factor 1/10 means that the period accuracy is 1/10 of the difference between local minima in the periodogram.

In case we get an unambiguous result with the inversion Method, we can check our result with the calculation method given by Slivan (2012, 2013; Eqs. 3-5), as implemented in *http://www.koronisfamily.com*). With this method, from the maximum lux of different apparitions, we try to delimit the error intervals to know an exact number of rotations of the asteroid, which univocally leads us to know its sidereal period. This is a valid method for data of the "dense" type, obtained continuously during an entire observation session.

Results

353 Ruperto-Carola. This middle main-belt asteroid was discovered on 1893 Jan 16 by M.F. Wolf at Heidelberg. We made observations from 2023 Nov 23 - Dec 23. From our data we derive a rotation period of 2.7389 ± 0.000016 h and an amplitude of 0.27 mag. Our result matches with Behrend (2020web) who got 2.7396 h, Warner (2006) with 2.73898 h, Hanus et al. (2016) and Durech et al. (2016) with the result of 2.73896 h. Pal et al. (2020) got 2.73912 h and Martikainen et al. (2021) got 2.738970 h.

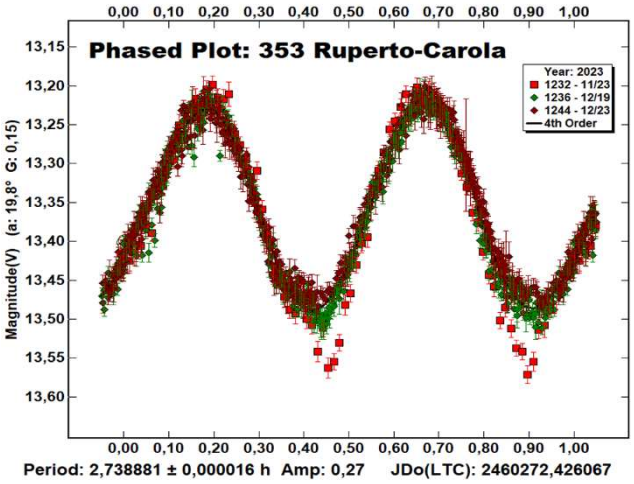

452 Hamiltonia. This outer main-belt asteroid was discovered on 1899 Dec 6 by J.E. Keeler at Mount Hamilton. We made observations from 2023 Oct 1 to Nov 7. From our data we derive a rotation period of 2.88119 ± 0.00007 h and an amplitude of 0.22 mag. Our result matches with Pilcher (2010) who found a period of 2.8813 h and Aznar et al. (2018), who found 2.88 h. Beherend (2011web) found 3.8 h.

We use data from LCDB, Pilcher (2010), in conjunction with our own dense data and sparse data from ATLAS (672 points: 2017/6/15 - 2022/2/28), Catalina (383 points: 2006/12/1 - 2023/5/29), LONEOS (20 points: 1999/8/12 - 2007/6/10), Palomar (128 points: 2018/1/20 - 2022/7/16) and USNO (124 points: 1998/4/21 - 2011/2/23). With the inversion method we calculate a sidereal rotation period of 2,881314 ± 0.000002 h. For the error estimation we have used the interval 2005-2023. In the lower graph we show the χ^2 value as a function of the period, which clearly shows the convergence of the iterative method used.

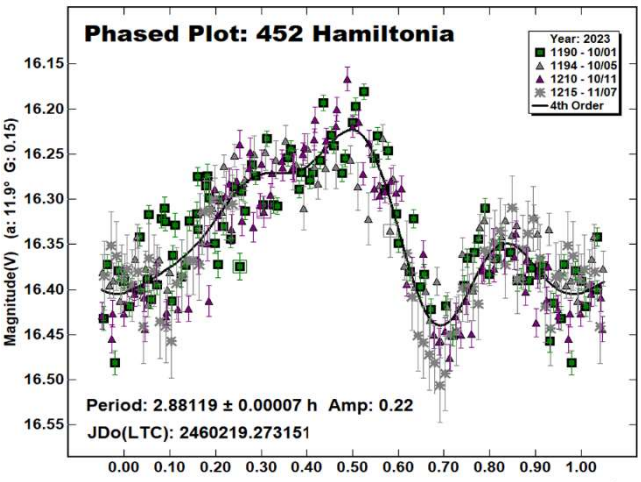

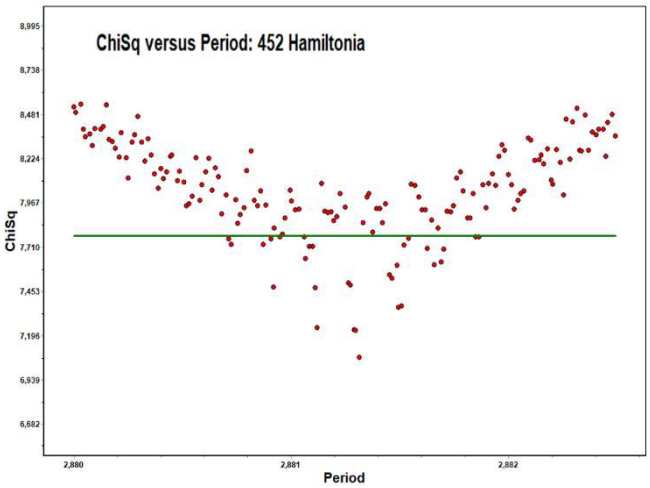

914 Palisana. This inner main-belt asteroid was discovered on 1919 Jul 4 by M.F. Wolf at Heidelberg We made observations on 2023 from Aug 8 to Oct 4. From our data, we derive a rotation period of 8.68062 ± 0.00017 h and an amplitude of 0.12 mag. This is consistent with Behrend (2019web) who got 8.68113 h and Stephens and Warner (2020) with 8.686 h. Colazo et al. (2022) got too 8.681 h. In the other side, Riccioli et al. (1995) got a period of 15.62 h and Warner (2009) got 15.922 h.

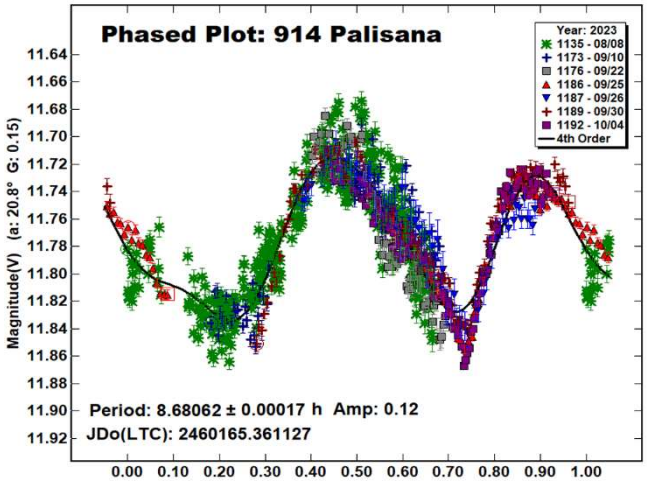

1554 Yugoslavia. This middle main-belt asteroid of the Eumonia family was discovered on 1940 Sep 6 by M.B. Protic at Belgrade. We made observations on 2023 April 5-16. From our data we derive a rotation period of 3.8873 ± 0.0002 h and an amplitude of 0.7 mag.

The asteroid 1554 Yugoslavia has already been studied and there are several calculations of its synodic period in the LCDB. It is worth highlighting the data available in ALCDEF: Higgins (2008), 2007/04/9-15 who got a period of 3.8879 h; Benishek (2013) 2012/08/28-09/08, with a period of 3.8876 h; Brines et al. (2017), 2016/07/04, with a period of 3.8876 h; J. Delgado 2021/12/3-6; S. Hopkings 2021/12/22-31.

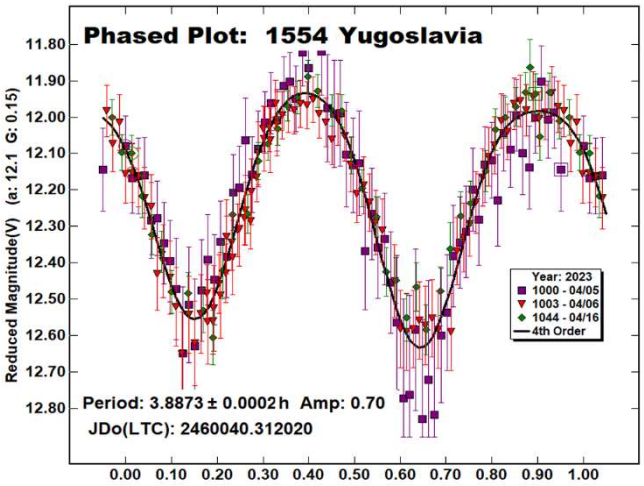

We use this data from LCDB in conjunction with our own dense data and sparse data from ATLAS (934 points: 2017/10/19 - 2023/3/25), Catalina (382 points: 2005/12/2 - 2023/4/9), Palomar (73 points: 2014/5/18 - 2022/2/19) and USNO (97 points: 1999/5/31 - 2013/12/30). With the inversion method we calculate a sidereal rotation period of 3.887673 ± 0.000003 h. For the error estimation we have used the interval 2005-2023. In the lower graph we show the χ^2 value as a function of the period, which clearly shows the convergence of the iterative method used.

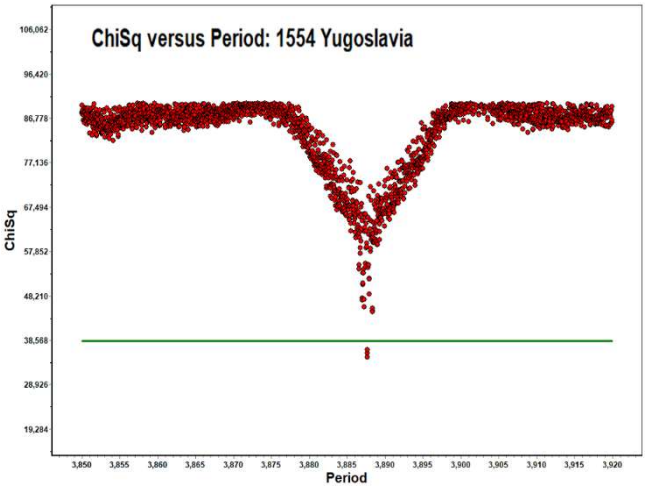

We use the calculation method given by Slivan. The times of the maximum values in the lightcurves are:

2023/4/06: JD 2460041.3475
2021/4/12: JD 2459570.8182

With an error estimation of .00001 h, we do get an ambiguous solution: 3.887682 ± $7*10^{-6}$ h with an amplitude of 0.24 mag. Martikainen et al. (2021) found a period of 3.887670 h.

2729 Urumqi. This outer main-belt asteroid was discovered on 1979 Oct 19 by the Purple Mountain Obs. at Nanking. We made observations on 2023 Oct 2 to Nov 14. From our data we derive a rotation period of 3.127840 ± 0.000024 h and an amplitude of 0.25 mag. Slivan et al. (2008) and Gao and Tan (2020) got a period of 3.127 h, Liu (2016) got 3.1274 h.

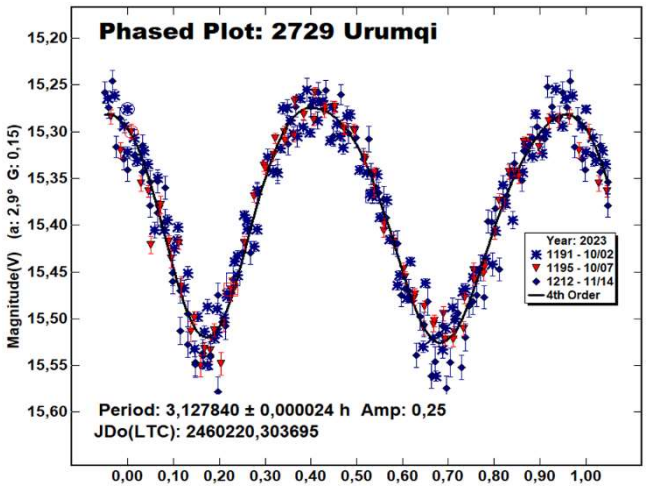

4917 Yurilvovia. This middle main-belt asteroid was discovered on 1973 Sep 28 by the Crimean Astrophysical Obs. at Nauchnij. We made observations on 2023 Oct 8-12. From our data we derive a rotation period of 10.169 ± 0.018 h and an amplitude of 0.09 mag. Hanus et al. (2016) got a sidereal period of 4.17744 h with the inversion method.

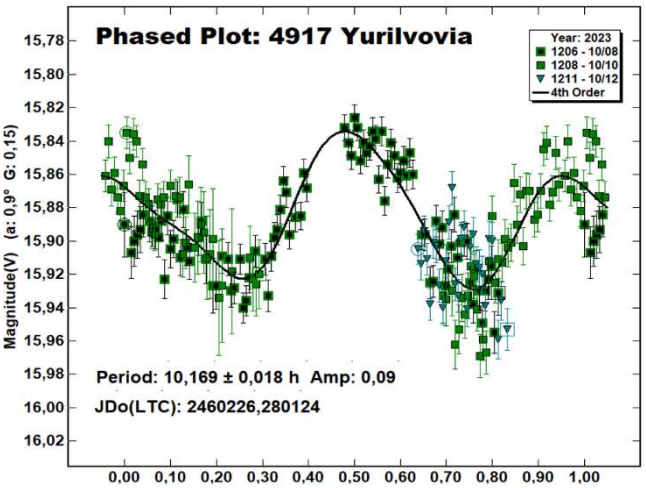

8142 Zolotov. This inner main-belt asteroid was discovered on 1982 Oct 20 by L.G. Karachkina at Nauchnij. We made observations on 2023 Oct 8 to Nov 15. From our data we derive a rotation period of 4.32388 ± 0.00005 h and an amplitude of 0.66 mag. Erasmus et al. (2020) got a period of 4.323 h.

We use our dense data and sparse data from ATLAS (469 points: 2018/3/29 - 2023/9/10), Catalina (415 points: 2003/4/22 - 2023/6/19), Palomar (80 points: 2016/11/7 - 2022/7/2) and LONEOS (28 points: 1999/3-/19 - 207/5/16). With the inversion method we calculate a sidereal rotation period of 4.323410 ± 0.000003 h. For the error estimation we have used the interval 2003 - 2023. In the lower graph we show the χ^2 value as a function of the period, which clearly shows the convergence of the iterative method used.

We haven't data from previous observations to try the Slivan method with this asteroid.

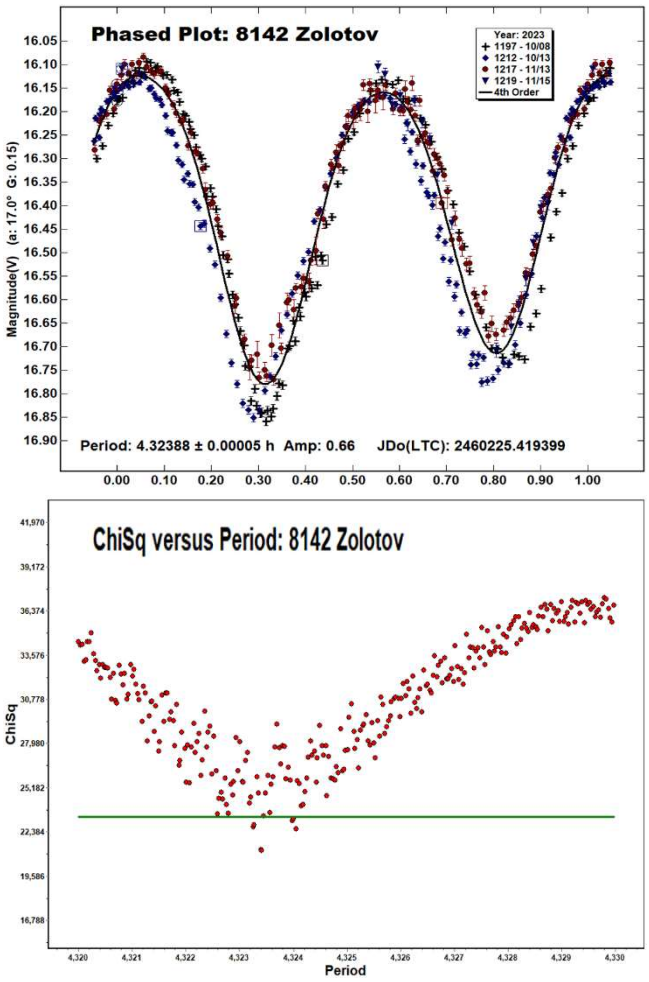

(6037) 1988 EG. This near-Earth object was discovered on 1988 March 22 by J. Alu at Palomar. We made observations on 2023 Jul 30 to Aug 9. Data analysis found a rotation period of 2.75724 ± 0.00036 h and an amplitude of 0.15 mag. Pravec et al. (1998web and 2021web) got 2.76 h and 2.7602 h.

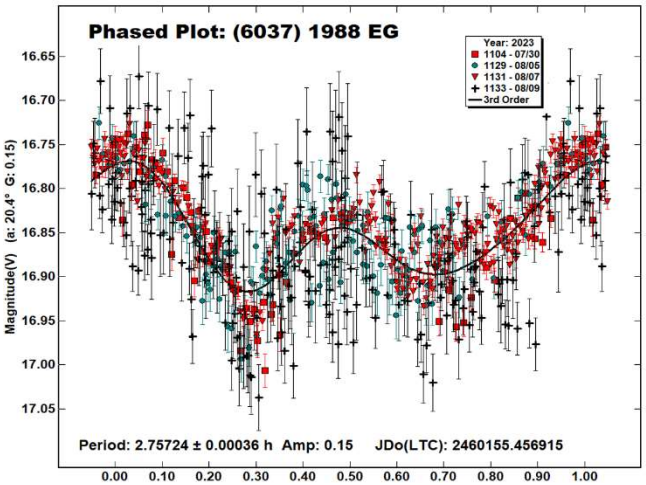

15817 Lucianotesi. This near-Earth object was discovered on 1994 Aug 28 by A. Boattini and M. Tombelli at San Marcello. We made observations on 2023 Sep 11 to 23. From our data we derive a rotation period of 12.687 ± 0.005 h and an amplitude of 0.57 mag. We have not previous information about its rotation period.

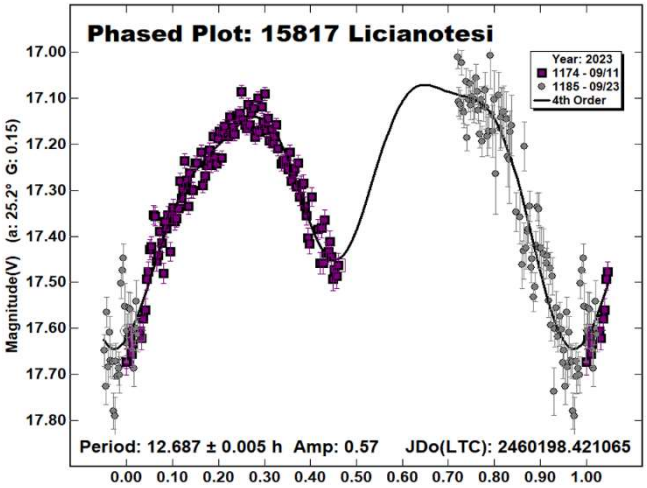

(41437) 2000 GT122. This middle main-belt asteroid was discovered on 2000 Apr 11 by C.J. Juels at Fountain Hills. We made observations on 2023 Oct 6 to11. From our data we derive a rotation period of 2.99011 ± 0.00035 h and an amplitude of 0.15 mag. Waszczak et al. (2015) got a period of 2.991 h.

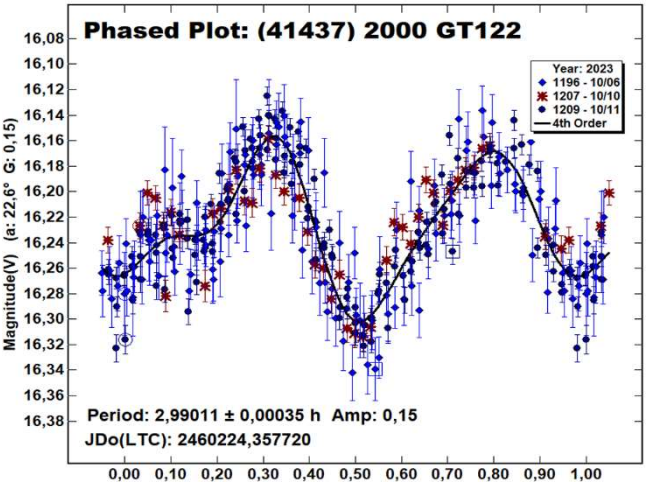

(154244) 2002 KL6. This near-Earth object was discovered on 2002 May 27 by NEAT at Haleakala. We made observations in 2023 Aug 8-21. In LCDB there are observations from Benishek, 2023 Jul 31 to Aug 5 and from Warner, 2023 Jun 13 to Jun 15. We use all of the 2023 data to get a rotation period of 4.60721 ± 0.00002 h and an amplitude of 0.57 mag. Our calculation is compatible with data from LCDB.

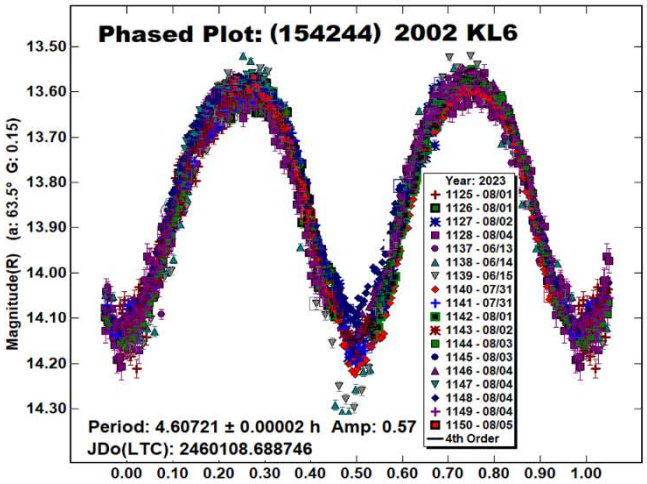

Number	Name	Sidereal Period (h)	P. Error (h)
452	Hamiltonia	2.881314	0.000002
1554	Yugoslavia	3.887682	0.000003
8142	Zolotov	4.323401	0.000003

Table II. Sidereal rotation period obtained from LCINVERT, when available

Acknowledgements

We would like to express our gratitude to Brian Warner for supporting the CALL web site and his suggestions. To Dr. Stephen Slivan for his advice.

References

Aznar, A.M.; Cornea, R.; Suciu, O. (2018). "Photometric Analysis and Physical Parameters for Six Mars-crossing and Ten Main-belt Asteroids from APT Observatory Group: 2017 April- September." *Minor Planet Bull.* **45**, 92-96.

Behrend, R. (2011web, 2019web, 2020web). Observatoire de Geneve web site. *http://obswww.unige.ch/~behrend/page_cou.html*

Benishek, V. (2013). "Lightcurves for 366 Vincentina, 592 Bathseba, and 1544 Yugoslavia from Belgrade Astronomical Observatory." *Minor Planet Bull.* **40**, 100-101.

Brines, P.; Lozano, J.; Rodrigo, O.; Fornas, A.; Herrero, D.; Mas, V.; Fornas, G.; Carreño, A.; Arce, E. (2017). "Sixteen Asteroids Lightcurves at Asteroids Observers (OBAS) - MPPD: 2016 June - November.". *Minor Planet Bull.* **44**, 145-149.

Colazo, M.; Damián, S.; Montelenoe, B.; Morals, M.; Ciancia, G.; García, A.; Melia, R.; Suárez, N.; Wilberger, A.; Fornari, C.; Nolte, R.; Bellocchio, E.; Mottino, A.; Colazo, C. (2022). "Asteroid Photometry and Lightcurve Analysis for Six Asteroids." *Minor Planet Bull.* **49**, 304-306.

Durech, J.; Hanus, J.; Oszkiewsicz, D.; Vanco, R. (2016). "Asteroid models from the Lowell photometric database." *Astron. Astrophys*. **587**, A48.

Erasmus, N.; Navarro-Meza, S.; McNeill, A.; Trilling, D.E.; Sickafoose, A.A.; Denneau, L.; Flewelling, H.; Heinze, A.; Tonry, J.L. (2020). "Investigating Taxonomic Diversity within Asteroid Families through ATLAS Dual-band Photometry." *Ap. J. Suppl. Ser.* **247**, A13.

Gao, X.; Tan, H. (2020). "Photometry of 2729 Urumqi at the Xingming Observatory in Urumqi City." *Minor Planet Bull.* **47**, 151.

Hanus, J.; Durech, J.; Oszkiewicz, D.A.; Behrend, R.; and 165 colleagues (2016). "New and updated convex shape models of asteroids based on optical data from a large collaboration network." *Astron. Astrophys*. **586**, A108.

Harris, A.W.; Young, J.W.; Scaltriti, F.; Zappala, V. (1984). "Lightcurves and phase relations of the asteroids 82 Alkmene and 444 Gyptis." *Icarus* **57(2)**, 251-258.

Higgins, D. (2008). "Asteroid Lightcurve Analysis at Hunters Hill Observatory and Collaborating Stations: April 2007 - June 2007." *Minor Planet Bull.* **35**, 30-32.

Kaasalainen, M. (2001). "Interpretation of lightcurves of precessing Asteroids." *Astron. and Astrophysics* **376**, 302-309. doi:10.1051/0004-6361:20010935.

Kaasalainen, M.; Torppa, J. (2001). "Optimization Methods for Asteroid Lightcurve Inversion. I Shape detemination." *Icarus* **143**, 24-36.

Number	Name	mm/dd	Phase	L_{PAB}	B_{PAB}	Period(h)	P.E.	Amp	A.E.	Grp
353	Ruperto-Carola	2023/11/23-12/23	20.2,15.2	91.9	-2.8	2.7389	0.000016	0.27	0.05	MB-M
452	Hamiltonia	2023/10/1-11/7	9.5,18.4	345.1	-3.7	2.88119	0.00007	0.22	0.05	MB-O
914	Palisana	2023/8/8-10/4	20.6,27.7	318.3	32.0	8.68062	0.00017	0.12	0.02	MB-I
1554	Yugoslavia	2023/4/5-16	12.1,14.6	160.7	-10.8	3.8873	0.0002	0.7	0.05	MB-M
2729	Urumqi	2023/10/02-11/14	2.8,14.7	4.0	-3.3	3.127840	0.000024	0.25	0.05	MB-O
4917	Yurilvovia	2023/10/8-12	3.3, 5.3	7.6	-0.8	10.169	0.018	0.09	0.02	MB-M
8142	Zolotov	2023/10/8-11/15	16.5, 6.3	40.2	-0.6	4.32388	0.00005	0.66	0.05	MB-I
6037	1988 EG	2023/7/30-8/9	20.0,21.0	318.0	11.1	2.75724	0.00036	0.15	0.02	NEA
15817	Lucianotesi	2023/9/11-23	10.2,11.9	354.8	-7.0	12.687	0.005	0.57	0.05	NEA
41437	2000 GT122	2023/10/6-11	11.6, 9.2	31.4	6.7	2.99011	0.00035	0.15	0.02	MB-M
154244	2002 KL6	2023/8/8-21	62.1,53.8	336.2	27.5	4.60721	0.00002	0.57	0.05	NEA
	(From Benishek, V.)	2023/7/31-8/05								
	(From Warner, B.)	2023/6/13-7/15								

Table III. Synodic Periods. Observing circumstances and results. The phase angle values are for the first and last date. L_{PAB} and B_{PAB} are the approximate phase angle bisector longitude and latitude at mid-date range (see Harris et al., 1984). Grp is the asteroid family/group (Warner et al., 2009). MB-I/O: Main-belt inner/outer; NEA: Near Earth Asteroid.

Kaasalainen, M.; Torppa, J.; Muinonen, K. (2001). "Optimization Methods for Asteroid Lightcurve Inversion. II The complete Inversion Problem." *Icarus* **153**, 37-51.

Liu, J. (2016). "Rotation Period Analysis for 2729 Urumqi." *Minor Planet Bull.* **43**, 204.

Martikainen, J.; Muinonen, K.; Penttila, A.; Cellino, A.; Wang, X.-B. (2021). "Asteroid absolute magnitudes and phase curve parameters from Gaia photometry." *Astron. & Astrophys.* **649**, A98.

Pal, A.; Szakáts, R.; Kiss, C.; Bódi, A.; Bognár, Z.; Kalup, C.; Kiss, L.L.; Marton, G.; Molnár, L.; Plachy, E.; Sárneczky, K.; Szabó, G.M.; Szabó, R. (2020). "Solar System Objects Observed with TESS - First Data Release: Bright Main-belt and Trojan Asteroids from the Southern Survey." *Ap. J. Suppl Ser*. **247**, id. 26.

Pilcher, F. (2010). "Rotation Period Determinations for 81 Terpsichore, 419 Aurelia, 452 Hamiltonia, 610 Valeska, 649 Josefa, and 652 Jubilatrix,". *Minor Planet Bull.* **37**, 45-46.

Pravec, P.; Wolf, M.; Sarounova, L. (1998web, 2021web). Ondrejov Asteroid Photometry Project. *http://www.asu.cas.cz/~ppravec/neo.htm*

Riccioli, D.; Blanco, C.; Di Martino, M.; De Sanctis, G. (1995). "Lightcurves and rotational periods of main belt asteroids. III." *Astron. Astrophys. Suppl. Ser.* **111**, 297-303.

Slivan, S.M.; Binzel, R.P.; Boroumand, S.C.; Pan, M.W.; Simpson, C.M.; Tanabe, J.T.; Villastrigo, R.M.; Yen, L.L.; Ditteon, R.P.; Pray, D.P.; Stephens, R.D. (2008). "Rotation rates in the Koronis family, complete to H≈11.2." *Icarus* **195**, 226-276.

Slivan, S.M. (2012). "Epoch Data in Sidereal Period Determination. I. Initial Constraint from Closest Epochs." *Minor Planet Bull.* **39**, 204-206.

Slivan, S.M. (2013). "Epoch Data in Sidereal Period Determination II. combining Epochs from Different Apparitions." *Minor Planet Bull.* **40**, 45-48.

Stephens, R.D.; Warner, B.D. (2020). "Main-belt Asteroids Observed from CS3: 2020 January to March." *Minor Planet Bull.* **47**, 224-230.

Warner, B.D. (2006). "Asteroid lightcurve analysis at the Palmer Divide Observatory - February - March 2006." *Minor Planet Bull.* **33**, 82-84.

Warner, B.D. (2009). "Asteroid Lightcurve Analysis at the Palmer Divide Observatory: 2008 September – December." *Minor Planet Bull.* **36**, 70-73.

Warner, B.D.; Harris, A.W.; Pravec, P. (2009). "The Asteroid Lightcurve Database." *Icarus* **202**, 134-146. *https://minplanobs.org/alcdef/index.php*

Waszczak, A.; Chang, C.; Ofek, E.; Laher, R.; Masci, F.; Levitan, D.; Surace, J.; Cheng, Y.; Ip, W.; Kinoshita, D.; Helou, G.; Prince, T.; Kulkarni, S. (2015). "Asteroid Light Curves from the Palomar Transient Factory Survey: Rotation Periods and Phase Functions from Sparse Photometry." *Astron. J.* **150**, A75.

SYNODIC ROTATION PERIOD FOR KORONIS FAMILY OBJECT (452) HAMILTONIA

Francis P. Wilkin, Joseph J. Maier
Union College, Department of Physics and Astronomy,
807 Union St., Schenectady, NY 12308
wilkinf@union.edu

(Received: 2024 January 15)

We present new lightcurves for (452) Hamiltonia in 2023. Observations of Hamiltonia were made at the Union College Observatory and two remote facilities. We derived a single apparition period 2.8813±0.0001 h.

Previously measured periods for (452) Hamiltonia include 2.8813 ± 0.0001 h (Pilcher, 2010), and 2.88 ± 0.01 h (Aznar Macías et al., (2018). We observed (452) Hamiltonia as part of our project at the Union College Observatory (UCO) to characterize Koronis family asteroids (e.g. Wilkin et al., 2022; Crowley and Wilkin, 2023) and to extend the sample completeness (Slivan et al., 2003; Slivan et al., 2024). Specifically, our goal for (452) Hamiltonia is to lengthen the overall time span of observations during the 2023 apparition, so that when combined with earlier observations of Slivan et al. (2023) in July and August, we obtain a more precise synodic rotation period than those previously available.

Observational planning was done using the *Koronisfamily.com* web tool (Slivan, 2003). We recorded lightcurves on a total of five nights using telescopes at three observatories. Telescope and camera properties are given in Table I. All observing runs had similar spans of 2.8-3.8 h. The final run on CHI-1 used exposure time 300 s, in distinction to those listed in Table I. Bias, dark, and twilight-flat field corrections were performed in *AstroImage J* (AIJ; Collins et al., 2017) for the UCO images, and photometry was performed on all images in AIJ. Corrections for light-travel time were applied using ephemerides from the NASA Horizons app (NASA, 2024).

Similar lightcurve shapes were obtained on all nights, although some variation is seen (Fig. 1). To determine a period value, we used the final run, on Oct 20, and the two runs on Sep 17, which as seen in Fig. 1, have considerably higher quality than the earliest run, at UCO. Relative magnitude values of each night were shifted in brightness to produce a self-consistent composite (Fig. 2). Based upon our observations spanning 44 nights, we obtain period 2.8813±0.0001 h and amplitude 0.19±0.02 mag. Note that the datapoints for both figures are identical. Observations reported here are further analyzed by Slivan et al. (2024) together with lightcurves that they recorded earlier in the apparition, to determine the improved synodic period needed for sidereal period determination.

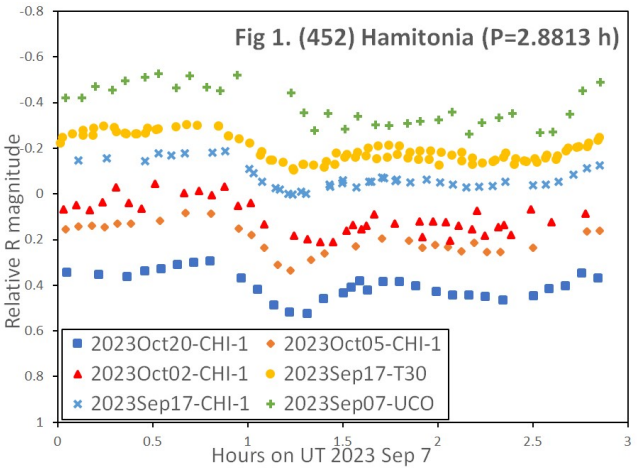

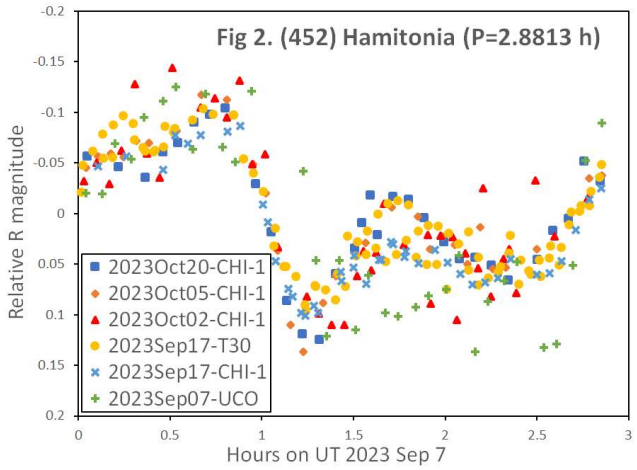

Acknowledgments

We thank the Union College Faculty Research Fund (to F.P.W.), the Student Research Grant (to J.J.M.), along with the Physics & Astronomy Department funding this project. S. Slivan provided encouragement and the suggestion to study this object. We thank D.V. Zora for the use of his lightcurve plotting template.

References

Aznar Macías, A.; Cornea, R.; Suciu, O. (2018). "Photometric Analysis and Physical Parameters for Six Mars-Crossing and Ten Main-belt Asteroids from APT Observatory Group: 2017 April-September." *Minor Planet Bull*. **45**, 92-96.

Collins, K.A.; Kielkopf, J.F.; Stassun, K.G.; Hessman, F.V. (2017). "AstroImageJ: Image Processing and Photometric Extraction for Ultra-precise Astronomical Light Curves." *Astron. J.* **153**, 77-89.

Crowley, E.M.; Wilkin, F.P. (2023). "Lightcurve of Koronis Family Member (993) Moultona." *Minor Planet Bull*. **50**, 6.

NASA, (2024). "Horizons System." *https://ssd.jpl.nasa.gov/horizons/app.html#/*

Pilcher, F. (2010). "Rotation Period Determinations for 81 Terpsichore, 419 Aurelia, 452 Hamiltonia, 610 Valeska, 649 Josefa, and 652 Jubilatrix." *Minor Planet Bull.* **37**, 45-46.

Slivan, S.M. (2003). "A Web-based tool to calculate observability of Koronis program asteroids." *Minor Planet Bull.* **30**, 71-72.

Slivan, S.M.; Binzel, R.P.; Crespo de Silva, L.D.; Kaasalainen, M; Lyndaker, M.M.; Krčo, M. (2003). "Spin vectors in the Koronis family: comprehensive results from two independent analyses of 213 rotation lightcurves." *Icarus* **162**, 285-307.

Slivan, S.M.; Hosek Jr., M.; Kurzner, M.; Sokol, A.; Maynard, S.; Payne, A.V.; Radford, A.; Springmann, A.; Binzel, R.P.; Wilkin, F.P.; Mailhot, E.A.; Midkiff, A.H.; Russell, A.; Stephens, R.D.; Gardiner, V.; Reichart, D.E.; Haislip, J.; LaCluyze, A.; Behrend, R.; Roy, R. (2023). "Spin vectors in the Koronis family: IV. Completing the sample of its largest members after 35 years of study." *Icarus* **394**, A115397.

Slivan, S.M.; Barrea, K.; Colclasure, A.M.; Cusson, E.M.; Larsen, S.S.; McLellan-Cassivi, C.J.; Moulder, S.A.; Nair, P.R.; Namphy, P.D.; Neto, O.S.; Noto, M.I.; Redden, M.S.; Rhodes, S.J.; Youssef, M.S. (2024). "Lightcurves and Derived Results for Koronis Family Member (452) Hamiltonia." *Minor Planet Bull*. **51**, 176-179.

Wilkin, F.P.; Bromberg, J.; AlMassri, Z.; Beauchaine, L.; Nguyen, M. (2022). "Lightcurve for Koronis Family Member (1363) Herberta." *Minor Planet Bull*. **49**, 253.

Name	Site	Telescope	Camera	Bin	T_exp(s)	Filter	FOV(')	Scale ("/pix)
UCO	Schenectady, NY	0.51-m RC f/8.1	SBIG STXL-11002	2×2	240	R	30×20	0.93
CHI-1	Rio Hurtado, Chile	0.61-m RC f/6.8	QHY 600M Pro	2×2	240	r′	31.8×31.8	1.22
T30	Coonabarabran, Aus	0.50-m RC f/6.8	ML16200	1×1	180	R	27.8×41.6	0.81

Table I. Telescopes and Cameras. T30=Sliding Spring Observatory; Chi-1=El Sauce Observatory; UCO = Union College Observatory

Number	Name	yyyy mm/dd	Phase	L_{PAB}	B_{PAB}	Period(h)	P.E.	Amp	A.E.	Grp
452	Hamiltonia	2023 09/07-10/20	4.0,0.5	2	1	2.8813	0.0001	0.19	0.02	KOR

Table II. Observing circumstances and results. The phase angle is given for the first and last dates. L_{PAB} and B_{PAB} are the approximate phase angle bisector longitude/latitude at mid-date range. Grp is the asteroid family/group.

LIGHTCURVES AND DERIVED RESULTS FOR KORONIS FAMILY MEMBER (452) HAMILTONIA

Stephen M. Slivan, Kaylee Barrera, Abigail M. Colclasure,
Erin M. Cusson, Skylar S. Larsen, Claire J. McLellan-Cassivi,
Summer A. Moulder, Prajna R. Nair, Paola D. Namphy,
Orisvaldo S. Neto, Maurielle I. Noto, Maya S. Redden,
Spencer J. Rhodes, Sandra A. Youssef
Massachusetts Institute of Technology,
Dept. of Earth, Atmospheric, and Planetary Sciences,
77 Mass. Ave. Rm. 54-424, Cambridge, MA 02139
slivan@mit.edu

(Received: 2024 January 15)

Lightcurves of (452) Hamiltonia recorded during three apparitions are presented with derived results for synodic rotation period, and analyzed together with data from other apparitions for spin vector and model shape.

Koronis family member (452) Hamiltonia was observed as a smaller target of opportunity during the study of larger Koronis members described by Slivan et al. (2008; 2023). Lightcurves have been reported by Pilcher (2010), who derived a rotation period of about 2.88 h from data spanning 23 nights in 2009, and by Aznar Macías et al. (2018) who observed lightcurves two nights apart in 2017 for a period consistent with the earlier result. The present paper begins by reporting new lightcurve observations from three apparitions, then in combination with data from Wilkin and Maier (2024), a single-apparition synodic period precise enough to count sidereal rotations is determined. Finally, a combined analysis with lightcurves from other apparitions is presented to determine the sidereal rotation period, spin vector orientation, and a convex model shape.

Lightcurves of Hamiltonia were recorded during a total of three apparitions at Whitin Observatory (WhO) in Wellesley, MA, and at the George R. Wallace Astrophysical Observatory (WAO) in Westford, MA. Observing circumstances are presented in Table I, and information about the telescopes and cameras appears in Table II. Observing and data reduction procedures were as previously described by Slivan et al. (2008); the 2022 and 2023 data were measured using synthetic aperture sizes informed by Howell (1989). Lightcurves were reduced for light-time, and standard-calibrated brightnesses were reduced to unit distances. Composite lightcurves are shown in Fig. 1, where nights of relative photometry have been shifted in brightness for best fit to their respective composites.

2006 apparition: (Fig. 1, top) Although these data at a previously unobserved aspect span 45 nights, partial lightcurves on the first two nights do not meaningfully constrain the period. Thus, the period error determination is based on a span of only 24 nights, yielding a composite lightcurve that is doubly periodic in 2.8813 ± 0.0004 h. Observations of Landolt (1983) standard star SA099-367 were used to calibrate the lightcurves to standard system *R*.

2022 apparition: (Fig. 1, center) The data span 28 nights, at a viewing aspect similar to that of the published data from 2017, for a derived period of 2.8812 ± 0.0004 h.

2023 apparition: (Fig. 1, bottom) These data span 23 nights at a previously unobserved aspect, for a derived period of 2.8816 ± 0.0003 h.

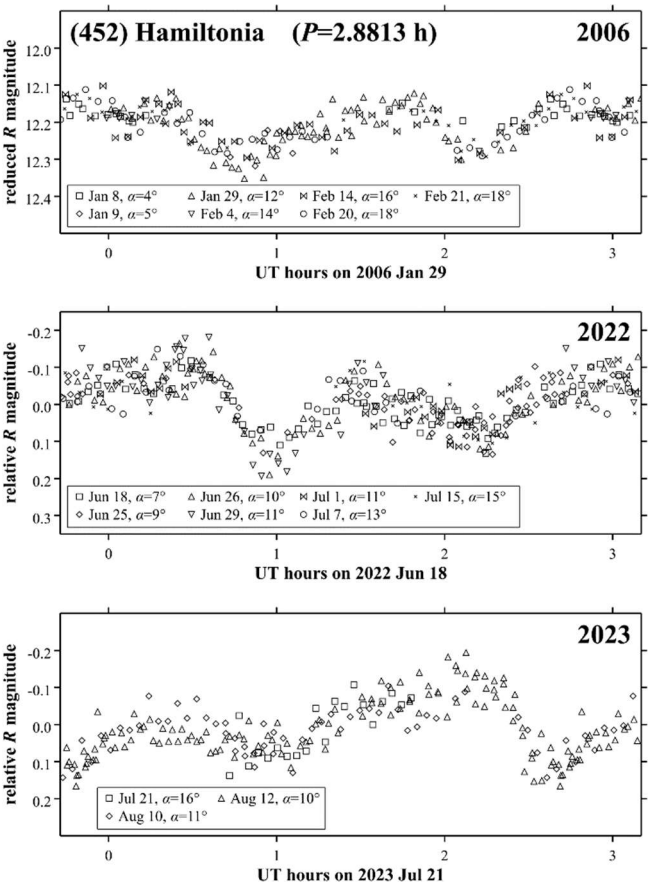

Figure 1. Folded composite lightcurves during apparitions in 2006 (top), 2022 (center), and 2023 (bottom), light-time corrected with the earliest and latest 10% of rotation repeated. Legends give UT dates of observations and solar phase angles α.

The rotation periods derived from the three independent data sets each are consistent with the previously published periods.

In 2023 Hamiltonia also was observed by Wilkin and Maier (2024), to increase the precision of the derived synodic period by extending the length of the time interval spanned by the data during the apparition. Combined, the 2023 data span 92 nights over four lunations and yield a derived synodic rotation period of 2.88130 ± 0.00006 h, which is precise enough to unambiguously count rotations between the consecutive apparitions in 2022 and 2023 (Slivan, 2012; Eqs. 3-5).

The observations reported here, together with those recorded in 2009 (Pilcher, 2010) and in 2017 (Aznar Macías et al., 2018), comprise dedicated lightcurves from a total of five apparitions. The amplitudes do not exceed 0.25 mag, and the lightcurve shapes exhibit significant asymmetric departures from sinusoids. Slivan (2013) discusses constraining an asteroid's sidereal rotation period by combined analysis of observations from multiple apparitions; in favorable cases epochs from five aspects can be sufficient to isolate a sidereal rotation count.

The epochs presented in Table III were measured from the lightcurves using the filtered Fourier series model approach described by Slivan et al. (2024). Estimating the epoch errors here was a bit more involved, because the Hamiltonia lightcurves are asymmetric with significantly different maximum slopes between

each pair of extrema. For that reason, the maximum slope in each unfiltered model at mid-brightness was used in estimating the corresponding epoch error, instead of the slope from the filtered model.

It is noted that the 2017 lightcurve data values used in the present work were estimated from the graph figure presented in Aznar Macías et al. (2018) and are incomplete, because of the 85 points indicated in the text only 72 are distinguishable on the graph, and the original measurements are unavailable.

Applying the sidereal rotation-counting sieve algorithm (Slivan, 2013) to the intervals among all five epochs finds an unambiguous integer count of half-rotations, with the unknown direction of spin yielding a pair of candidate sidereal periods (Fig. 2). Analysis of the same epochs using sidereal photometric astrometry (SPA) (Slivan, 2014; Drummond et al., 1988) indicates that the pole does not lie near the ecliptic plane (Fig. 3), but it does not otherwise distinguish the direction of spin.

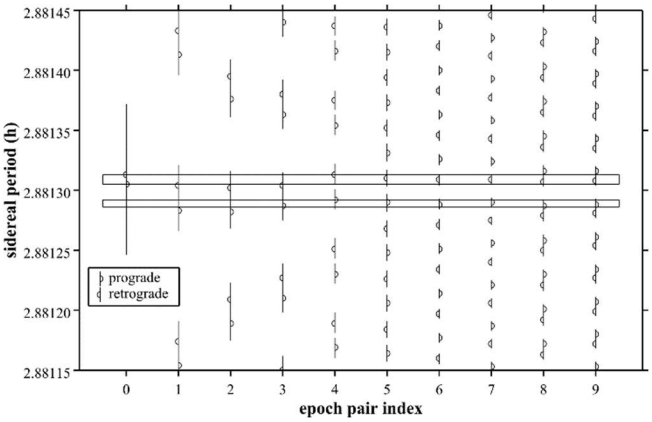

Figure 2. Sieve algorithm output for the five epochs in Table III, Part A. The number of rotations that elapsed during the longest interval spanning 2006 to 2023, excluding the fraction of a rotation induced by the aspect change, is unambiguously 53159.5 rotations. The two ranges of periods indicated by thin horizontal rectangles represent the non-overlapping constraints for the two possible directions of spin. Candidate ranges of periods for each epoch interval were calculated using epoch range half-widths of 2.5 times the epoch errors.

To test whether including epochs from additional apparitions might distinguish the spin direction, the MPC Orbits/Observations Database was checked for suitable additional photometry to fill in gaps in the dedicated lightcurves' aspect coverage (Fig. 4). Observations from the ATLAS sky survey (Tonry et al., 2018) recorded during the 2019 and 2021 apparitions (Fig. 5) supply data from aspects that reduce two of the three largest gaps (Table III, Part B). Including these two epochs does not significantly change the results, which suggests that in this case the aspect coverage is not a limiting factor. Instead, it is plausible that the combined low amplitude and asymmetry of the lightcurves are interfering with measuring the epochs accurately enough to distinguish the direction of spin. Thus, the outcome of the epochs analyses is a pair of derived candidate sidereal periods: 2.8812885 ± 0.0000018 h for prograde spin, and 2.8813078 ± 0.0000018 h for retrograde spin.

With its good aspect coverage over seven apparitions, and having already yielded an unambiguous sidereal rotation count, this data set is a good candidate for convex inversion (CI) (Kaasalainen et al., 2001). The lightcurves were analyzed using CI as described by Slivan et al. (2023), here including the sky survey data as standard-calibrated photometry. The analysis identifies a symmetric pair of retrograde pole regions (Fig. 6) whose ambiguity is a consequence of the small 3° orbit inclination of Hamiltonia; the corresponding spin vector results are summarized in Table IV. Lightcurve fits and model shape renderings for pole solution P_3 are shown in Figs. 7 and 8, respectively. The spin vector lies near the short-period end of the spin rate vs. obliquity distribution of retrograde poles in the Koronis family, close to that of larger member (321) Florentina (Slivan et al., 2023).

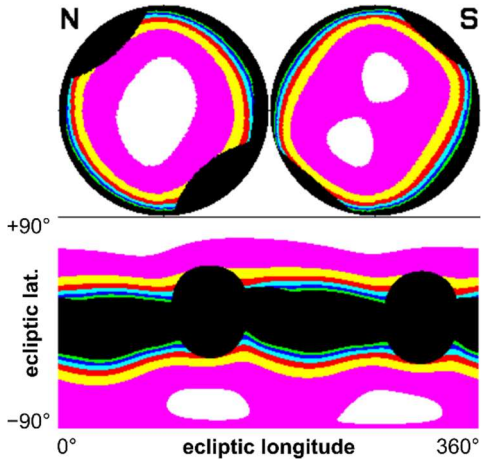

Figure 3. Contour graphs of RMS error of trial poles for the SPA analyses of the five epochs in Table III, Part A. The lower half of the figure represents the celestial sphere as a rectangular grid of ecliptic longitude and latitude; the same data in a polar format undistorted near the ecliptic poles appear in the upper half of the graph, where north and south hemispheres are plotted separately. Best-fit regions are colored white. Here the poorest-fit region (black) rules out pole locations near the ecliptic plane.

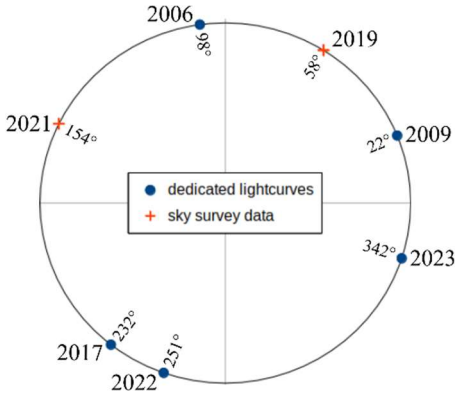

Figure 4. Angular distribution of ecliptic longitudes of phase angle bisectors (PABs) for epochs in Table III. Each apparition of sky survey data is represented by a single longitude calculated for the "median date" of the UT dates of observations.

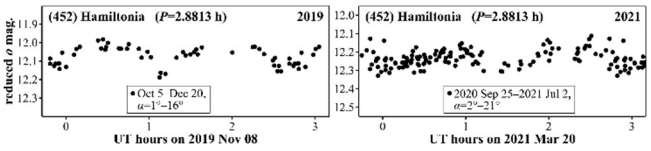

Figure 5. Photometry from the ATLAS sky survey (Tonry et al., 2018) during the 2019 and 2021 apparitions, each composited to the median date of the data. The slope parameter G = 0.23 for S-type objects (Lagerkvist and Magnusson, 1990) was used to reduce for changing solar phase angle.

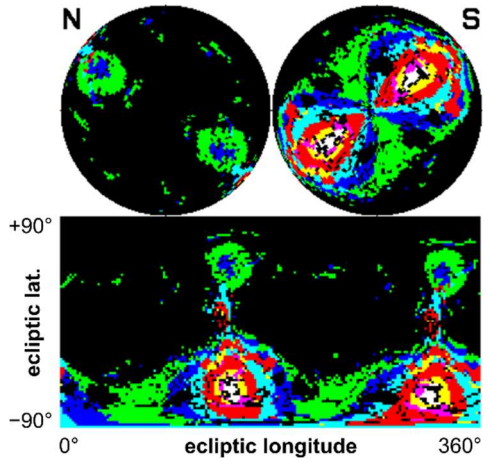

Figure 6. Similar to Fig. 3 but for the CI analysis of the seven apparitions of lightcurve data, locating a symmetric pair of retrograde pole regions.

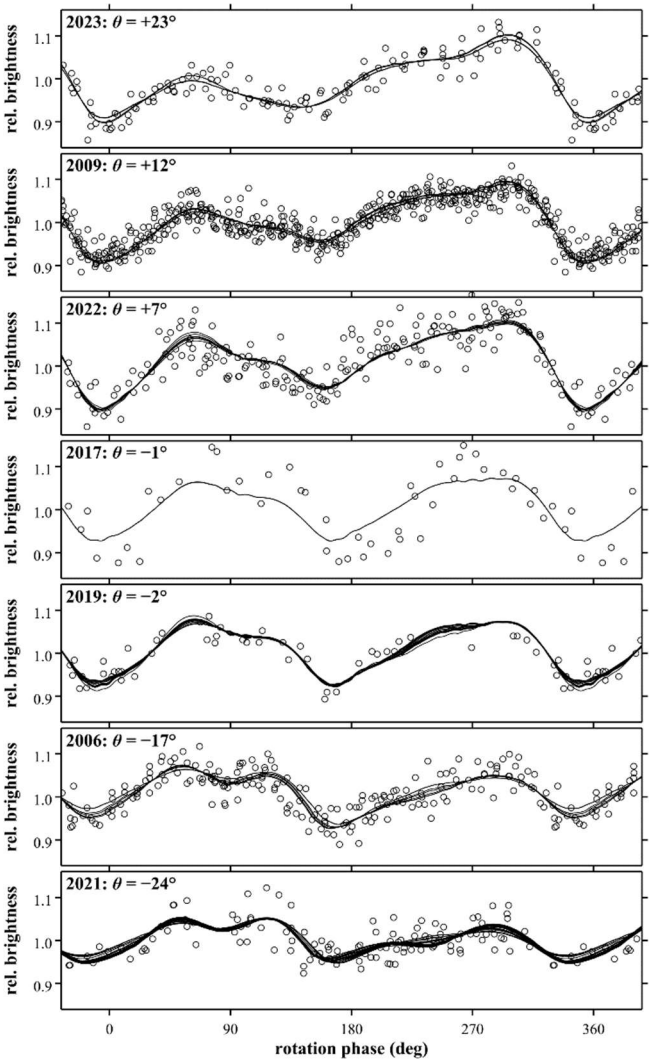

Figure 7: CI model lightcurve fits for pole P_3 as brightness vs. sidereal rotation phase. Changes in lightcurve shape during the apparition appear as non-overlapping model curves. The graphs are presented in order of decreasing sub-PAB latitude θ. The RMS error of the fit to the combined data set corresponds to 0.035 mag.

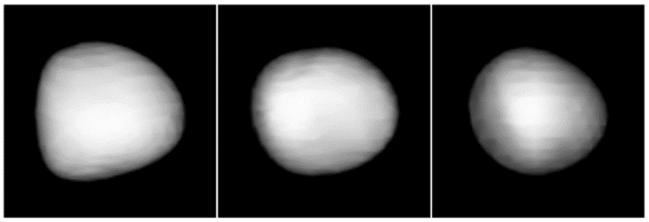

Figure 8. Renderings of convex model for pole P_3. (left) Polar aspect, showing the rounded triangular profile that contributes to low-order asymmetry of the lightcurves. (center and right) Equatorial aspects for side-on (lightcurve maximum) and end-on (lightcurve minimum) views, respectively. The model for the symmetric pole P_4 is essentially a mirror image.

UT date	α (°)	Tel. ID	Filter	Integration time (s)
2006 Jan 08.1	4.2	WhO	*R*	240
2006 Jan 09.0	4.6	WhO	*R*	240
2006 Jan 29.1	12.1	WhO	*R*	240
2006 Feb 04.1	14.0	WhO	*R*	240
2006 Feb 14.1	16.5	WhO	*R*	240
2006 Feb 20.2	17.7	WhO	*R*,c	240
2006 Feb 21.0	17.9	WhO	c	240
2022 Jun 18.1	6.8	WAO-P24	*R*	180
2022 Jun 25.1	9.4	WAO-P24	*R*	500
2022 Jun 25.2	9.4	WAO-3,4	*R*	180
2022 Jun 26.1	9.7	WAO-3	*R*	180
2022 Jun 29.1	10.8	WAO-3	*R*	180
2022 Jul 01.1	11.4	WAO-3	*R*	180
2022 Jul 07.1	13.3	WAO-4	*R*	240
2022 Jul 15.1	15.4	WAO-4	*R*	300
2023 Jul 21.3	16.2	WAO-4	*R*	200
2023 Aug 10.3	10.7	WAO-4	*R*	200
2023 Aug 12.3	10.0	WAO-3,4	*R*	200

Table I: Nightly observing information, rows grouped by apparition. Columns are: UT date at lightcurve mid-time, solar phase angle α, telescope ID (Table II), filter used (*R*, Cousins *R*; c, colorless), and image integration time.

Tel. ID	Dia. (m)	CCD camera	FOV (′)	Bin	Scale (″/pix)
WhO	0.61	Photometrics TK 1K	16×16	2×2	1.84
WAO-3	0.36	FLI ML1001	20×20	1×1	1.18
WAO-4	0.36	SBIG STL-1001	21×21	1×1	1.25
WAO-P24	0.61	FLI PL16803	32×32	1×1	0.46

Table II: Telescopes and cameras information. Columns are: telescope ID (WhO, Sawyer Boller & Chivens 24-in; WAO-3 and WAO-4, shed piers #3 and #4 Celestron Classic C14; WAO-P24, Elliot PlaneWave 24-in CDK), telescope diameter, CCD camera, detector field of view, image binning used, and binned image scale.

UT date	Epoch (UT h)	PAB λ,β(°)	Data ref.
Part A: Dedicated lightcurves			
2006 Jan 29	0.10 ± 0.07	97.9,+0.8	a
2009 Sep 26	1.29 ± 0.04	22.0,-3.9	b
2017 May 17	1.33 ± 0.07	231.9,+2.6	c
2022 Jun 18	0.20 ± 0.06	250.6,+1.3	a
2023 Jul 21	0.46 ± 0.05	342.1,-3.4	a,d
Part B: Sky survey lightcurves sparse-in-time			
2019 Nov 08	0.48 ± 0.11	58.0,-2.5	e,f
2021 Mar 20	0.83 ± 0.12	153.9,+3.7	e,f

Table III: Summary of lightcurve epochs, in each case locating a maximum from the second harmonic of a Fourier series model fit to the lightcurves. PAB λ,β are the J2000.0 ecliptic longitude and latitude of the phase angle bisector. Data references are: a, this work; b, Pilcher (2010); c, Aznar Macías et al. (2018); d, Wilkin and Maier (2024); e, ATLAS-MLO *o*-band; f, ATLAS-HKO *o*-band.

Sidereal period: 2.8813085 ± 0.0000005 h

Spin poles	λ0	σ(λ0)	β0	σ(β0)	ε
P3:	148°	5	-62°	5	155°
P4:	315°	5	-68°	5	156°

Model axial ratios: *a*/*b*: 1.1 *b*/*c*: 1.1

Table IV: Spin vector results. *λ*0 and *β*0 are the pole solutions' ecliptic longitudes and latitudes, respectively; *σ* are the estimated pole errors in degrees of arc; *ε* are the spin obliquities. The axial ratios are very coarse estimates with uncertainties of at least ± 0.1.

Acknowledgments

At Wallace Observatory we thank Dr. Michael Person and Timothy Brothers for allocation of telescope time, and for observer instruction and support. We also thank F. Wilkin and J. Maier for providing their lightcurve data prior to publication. The student observers at Wallace were supported by grants from MIT's Undergraduate Research Opportunities Program. This work uses data obtained from the Asteroid Lightcurve Data Exchange Format (ALCDEF) Asteroid Lightcurve Photometry Database, which is supported by funding from NASA grant 80NSSC18K0851. This work has made use of data and services provided by the International Astronomical Union's Minor Planet Center; specifically, the brightnesses accompanying astrometry from the Asteroid Terrestrial-impact Last Alert System (ATLAS) survey observing program.

References

Aznar Macías, A.; Cornea, R.; Suciu, O. (2018). "Photometric Analysis and Physical Parameters for Six Mars-crossing and Ten Main-belt Asteroids from APT Observatory Group: 2017 April-September." *Minor Planet Bull.* **45,** 92-96.

Drummond, J.D.; Weidenschilling, S.J.; Chapman, C.R.; Davis, D.R. (1988). "Photometric geodesy of main-belt asteroids. II. Analysis of lightcurves for poles, periods, and shapes." *Icarus* **76**, 19-77.

Howell, S.B. (1989). "Two-dimensional Aperture Photometry: Signal-to-noise Ratio of Point-source Observations and Optimal Data-extraction Techniques." *PASP* **101**, 616-622.

Kaasalainen, M.; Torppa, J.; Muinonen, K. (2001). "Optimization methods for asteroid lightcurve inversion. II. The complete inverse problem." *Icarus* **153**, 37-51.

Lagerkvist, C.I.; Magnusson, P. (1990). "Analysis of asteroid lightcurves. II. Phase curves in a Generalized HG-system." *Astron. Astrophys. Suppl. Ser.* **86**, 119-165.

Landolt, A.U. (1983). "*UBVRI* Photometric Standard Stars Around the Celestial Equator." *Astron. J.* **88**, 439-460.

Pilcher, F. (2010). "Rotation Period Determinations for 81 Terpsichore, 419 Aurelia, 452 Hamiltonia, 610 Valeska, 649 Josefa, and 652 Jubilatrix." *Minor Planet Bull.* **37**, 45-46.

Slivan, S.M.; Binzel, R.P.; Boroumand, S.C.; Pan, M.W.; Simpson, C.M.; Tanabe, J.T.; Villastrigo, R.M.; Yen, L.L.; Ditteon, R.P.; Pray, D.P.; Stephens, R.D. (2008). "Rotation rates in the Koronis family, complete to *H*≈11.2." *Icarus* **195**, 226-276.

Slivan, S.M. (2012). "Epoch Data in Sidereal Period Determination. I. Initial Constraint from Closest Epochs." *Minor Planet Bull.* **39**, 204-206.

Slivan, S.M. (2013). "Epoch Data in Sidereal Period Determination. II. Combining Epochs from Different Apparitions." *Minor Planet Bull.* **40**, 45-48.

Slivan, S.M. (2014). "Sidereal Photometric Astrometry as Efficient Initial Search for Spin Vector." *Minor Planet Bull.* **41**, 282-284.

Slivan, S.M.; Hosek Jr., M.; Kurzner, M.; Sokol, A.; Maynard, S.; Payne, A.V.; Radford, A.; Springmann, A.; Binzel, R.P.; Wilkin, F.P.; Mailhot, E.A.; Midkiff, A.H.; Russell, A.; Stephens, R.D.; Gardiner, V.; and 5 colleagues (2023). "Spin vectors in the Koronis family: IV. Completing the sample of its largest members after 35 years of study." *Icarus* **394**, A115397.

Slivan, S.M.; Barrera, K.; Colclasure, A.M.; Cusson, E.M.; Larsen, S.L.; McLellan-Cassivi, C.J.; Moulder, S.A.; Nair, P.R.; Namphy, P.D.; Neto, O.S.; Noto, M.I.; Redden, M.S.; Rhodes, S.J.; Youssef, S.A. (2024). "Lightcurves and Derived Results for Koronis Family Member (5139) Rumoi, Including a Discussion of Measurements for Epochs Analysis." *Minor Planet Bull.* **51**, 6-10.

Tonry, J.L.; Denneau, L.; Heinze, A.N.; Stalder, B.; Smith, K.W.; Smartt, S.J.; Stubbs, C.W.; Weiland, H.J.; Rest, A. (2018). "ATLAS: A High-cadence All-sky Survey System." *PASP* **130**, 064505.

Wilkin, F.P.; Maier, J.J. (2024). "Synodic Rotation Period for Koronis Family Object (452) Hamiltonia." *Minor Planet Bull.* **51**, 174-175.

Number	Name	yyyy mm/dd	Phase	L_{PAB}	B_{PAB}	Period(h)	P.E.	Amp	A.E.
452	Hamiltonia	2006 01/08-02/21	4.2,17.9	98	1	2.8813	0.0004	0.14	0.04
452	Hamiltonia	2022 06/18-07/15	6.8,15.4	251	1	2.8812	0.0004	0.23	0.06
452	Hamiltonia	2023 07/21-08/12	16.2,10.0	343	-4	2.8816	0.0003	0.23	0.06
452	Hamiltonia					2.88130	0.00006		

Table V. Observing circumstances and results. The first three lines give the results derived from only the lightcurves reported in the present paper. Solar phase angles are given for the first and last dates, and L_{PAB} and B_{PAB} are the approximate phase angle bisector longitude/latitude at mid-date range. The last line gives the synodic rotation period derived from analysis of a combined single-apparition data set, comprised of the 2023 lightcurves reported here together with data reported by Wilkin and Maier (2024).

LIGHTCURVES FOR THREE KORONIS FAMILY ASTEROIDS

Francis P. Wilkin, Eduardo Castro, Micaela Magno,
Ryan Petrauskas, Dimitrios Vasileios Zora
Union College
Department of Physics and Astronomy
807 Union St
Schenectady, NY 12308
wilkinf@union.edu

(Received: 2024 January 15)

We present photometry for three Koronis family asteroids, with new synodic rotation periods for two objects with no previously published dense lightcurves: (2470) Agematsu: 2.7952 ± 0.0007 h; and (3856) Lutskij: 7.992 ± 0.0002 h. The lightcurve for (1497) Tampere is consistent with the previously published period.

Members of the Koronis family have been shown to possess strongly anisotropic spin vectors clustered in two directions (Slivan, 2002). Thermal radiation torques by the YORP mechanism (Rubincam, 2000) may dominate collisional evolution of asteroid spins for sufficiently small objects of diameter $\lesssim$ 30 km in the main asteroid belt. Because YORP torques are more relevant for smaller objects, we continue our project (Wilkin et al., 2022; Wilkin et al., 2023) to increase the sample of known spins for koronis family objects (Slivan et al., 2003; Slivan et al., 2023b). Targets were chosen using the Koronis family web tool (Slivan, 2003), specifically, from the shape/spin list: (1497) Tampere, and from the quality Q < 3 list needing more accurate periods: (2470) Agematsu and (3856) Lutskij.

Imaging observations were obtained using four telescopes including the Union College Observatory (UCO) and remote access through the networks iTelescope.net (T11, T21) and Telescope.Live (SPA-2; see Table I). Observation dates and telescopes used are given by the figure legends. All observations used a red filter but specific filters varied by observatory due to availability. Exposure times were 240s and binning 2×2 on all cameras. Images were processed for bias, dark, and twilight flat field corrections. We used *AstroImageJ* software (Collins et al., 2017) to process the Union College images and to perform photometry on all images. NASA Horizons ephemerides (NASA, 2024) were used to apply light-time corrections and to obtain parameter values for phase and phase angle bisector appearing in Table II.

1497 Tampere. Rotation period and lightcurves were published by Slivan et al. (2023a), who obtained synodic period of 3.30237 ± 0.00015 h. Our single night in 2019 yielded a lightcurve consistent with the previous period and amplitude 0.45 ± 0.06 mag in R.

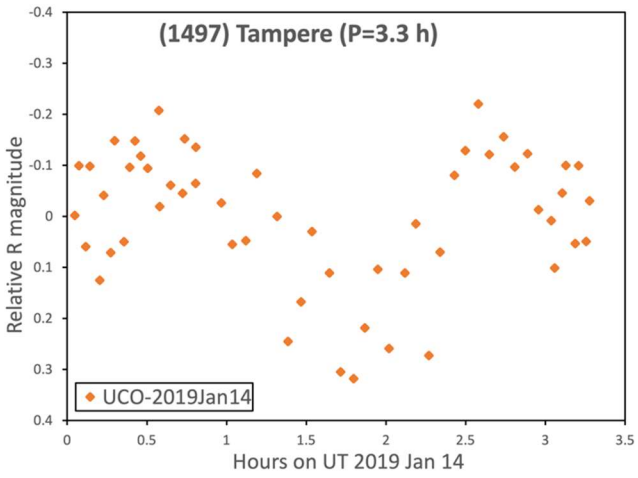

2470 Agematsu. No published periods or lightcurves were found in the lightcurve database (LCDB, Warner et al., 2009). We performed imaging observations on two telescopes and four nights in April, 2023. Relative magnitudes for a given night were shifted to produce a self-consistent composite. The composite lightcurve results in an estimated period of 2.7952 ± 0.0007 h.

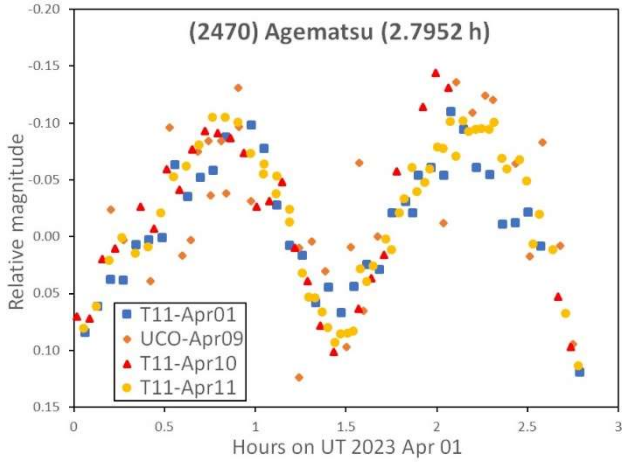

3856 Lutskij. No published periods or lightcurves were found in the lightcurve database (LCDB, Warner et al., 2009). We observed remotely on three nights in early 2022 using two telescopes. Relative magnitudes for a given night were shifted to produce a self-consistent composite. The lightcurve is doubly-periodic at a period of 7.992 ± 0.002 h. The amplitude, 0.42 ± 0.03 mag, is sufficiently large that we may exclude the possibility of a singly-periodic lightcurve at one half that period, or a quadruply-periodic lightcurve at double the given period (Harris et al., 2014). Recently, a sparse-survey period has been given by Ďurech and Hanuš (2023) using GAIA DR3 photometry. Their result, 7.9934 h, with unspecified error, is consistent with ours.

Name	Site	Telescope	Camera	Array	Filter	FOV(')	Scale ("/pix)
UCO	Schenectady, NY	0.51-m RC f/8.1	SBIG STXL-11002	2004×1336x9µm	R	30×20	0.93
T11	Beryl Junction, UT	0.50-m CDK f/6.8	FLI-PL11002M	4008×2672×9µm	R	36×54	0.81
T21	Mayhill, NM	0.43-m CDK f/6.8	FLI-PL6303E	3072×2048x9µm	R	33×49	1.92
SPA-2	Oria, Spain	0.70-m RC f/8	FLI-PL16803	2048×2048x9µm	r'	29×29	0.86

Table I. Telescopes and Cameras. UCO = Union College Observatory; RC=Ritchey-Chrétien; CDK = Planewave Corrected Dall-Kirkham Astrograph. The primary and secondary mirrors of UCO were shifted in early 2021 along with a resurfacing, yielding a slightly altered image scale. Prior to 2021, the image scale was 0.87"/pix.

Number	Name	yyyy mm/dd	Phase	L_{PAB}	B_{PAB}	Period(h)	P.E.	Amp	A.E.	Grp
1497	Tampere	2019 01/14-01/29	1.7	118	0	3.3	0.3	0.45	0.06	Kor
2470	Agematsu	2023 04/01-04/11	*2.6, 2.6	196	4	2.7952	0.0007	0.15	0.02	Kor
3856	Lutskij	2022 01/01-01/29	4.7,14.7	90	2	7.992	0.002	0.42	0.03	Kor

Table II. Observing circumstances and results. The phase angle is given for the first and last dates. If preceded by an asterisk, the phase angle reached an extremum during the period. LPAB and BPAB are the approximate phase angle bisector longitude/latitude at mid-date range.

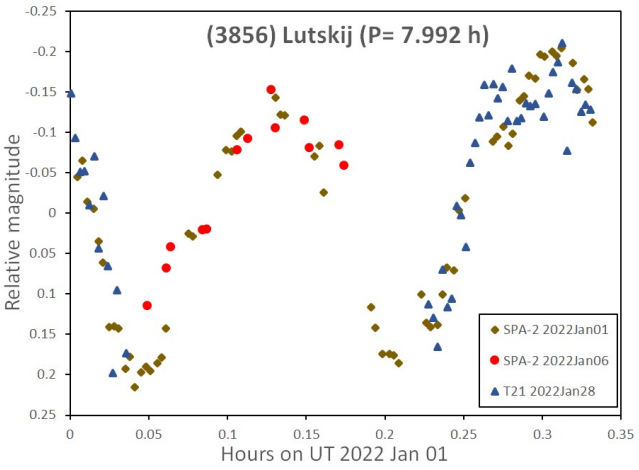

Acknowledgments

FPW received funding from the Union College Faculty Research Fund. We are grateful to S. Slivan for helpful suggestions. Student researchers were funded by the Union College Research Assistant work-study program. We thank T. Jordan of the Scholars Program and R. Morgan of the Department of Physics and Astronomy for making this opportunity available. We thank J. Sindoni for taking the Tampere images.

References

Collins, K.A.; Kielkopf, J.F.; Stassun, K.G.; Hessman, F.V. (2017). "AstroImageJ: Image Processing and Photometric Extraction for Ultra-precise Astronomical Light Curves." *Astron. J.* **153**, 77-89.

Ďurech, J.; Hanuš, J. (2023). "Reconstruction of asteroid spin states from Gaia DR3 photometry." *Astron. Astrophys.* **675**, A24.

Harris, A.W.; Pravec, P.; Gálad, A.; Skiff, B.A.; Warner, B.D.; Világi, J.; Gajdoš, Š.; Carbognani, A.; Hornoch, K.; Kušnirák, P.; Cooney Jr., W.R.; Gross, J.; Terrell, D.; Higgins, D.; Bowell, E.; Koehn, B.W. (2014). "On the maximum amplitude of harmonics of an asteroid lightcurve." *Icarus* **235**, 55-59.

NASA, (2024). "Horizons System." *https://ssd.jpl.nasa.gov/horizons/app.html#/*

Rubincam, D.P. (2000). "Radiative spin-up and spin-down of small asteroids." *Icarus* **148**, 2-11.

Slivan, S.M. (2002). "Spin vector alignment of Koronis family asteroids." *Nature* **419**, 49-51.

Slivan, S.M. (2003). "A Web-based tool to calculate observability of Koronis program asteroids." *Minor Planet Bull.* **30**, 71-72.

Slivan, S.M.; Binzel, R.P.; Crespo de Silva, L.D.; Kaasalainen, M; Lyndaker, M.M.; Krčo, M (2003). "Spin vectors in the Koronis family: comprehensive results from two independent analyses of 213 rotation lightcurves." *Icarus* **162**, 285-307.

Slivan, S.M.; Brothers, T.C.; Colclasure, A.M.; Larsen, S.S.; McLellan-Cassivi, C.J.; Neto, O.S.; Noto, M.I.; Redden, M.S.; Wilkin, F.P.; Das, N. (2023a). "Rotation Period of Koronis Family Member (1497) Tampere." *Minor Planet Bull.* **50**, 125.

Slivan, S.M.; Hosek Jr., M.; Kurzner, M.; Sokol, A.; Maynard, S.; Payne, A.V.; Radford, A.; Springmann, A.; Binzel, R.P.; Wilkin, F.P.; Mailhot, E.A.; Midkiff, A.H.; Russell, A.; Stephens, R.D.; Gardiner, V.; Reichart, D.E.; Haislip, J.; LaCluyze, A.; Behrend, R.; Roy, R. (2023b). "Spin vectors in the Koronis family: IV. Completing the sample of its largest members after 35 years of study." *Icarus* **394**, A115397.

Warner, B.D.; Harris, A.W.; Pravec, P. (2009). "The asteroid lightcurve database." *Icarus* **202**, 134-146. Updated 2024 Jan 15. *http://www.MinorPlanet.info/php/lcdb.php*

Wilkin, F.P.; AlMassri, Z.; Bowles, P.; Pargiello, M.; Sindoni, J. (2022). "Lightcurves for Three Koronis Family Asteroids from the Union College Observatory." *Minor Planet Bull.* **49**, 267-268.

Wilkin, F.P.; Djoroeva, A.; Qureshi, S.; Wright, G. (2023). "Lightcurves for Koronis Family Objects (2498) Tsesevich and (2742) Gibson." *Minor Planet Bull.* **50**, 262-263.

ASTEROID LIGHTCURVE ANALYSIS AT THE CENTER FOR SOLAR SYSTEM STUDIES PALMER DIVIDE STATION: 2023 SEPTEMBER-OCTOBER

Brian D. Warner
Center for Solar System Studies (CS3)
446 Sycamore Ave.
Eaton, CO 80615 USA
brian@MinPlanObs.org

(Received: 2023 December 30)

CCD photometric observations of three Hungaria asteroids were made at the Center for Solar System Studies Palmer Divide Station in 2023 September and October. 10737 Bruck and (48470) 1991 TC2 were found to be new binary discoveries. Bruck has a primary rotation period of 2.3446 h and orbital period of 15.39 h. The estimated effective diameter ratio (Ds/Dp) of the satellite vs. primary is 0.22. (48470) 1991 TC2 has a primary rotation period of 2.5141 h and orbital period of 11.179 h. The estimated Ds/Dp is 0.28.

CCD photometric observations of three Hungaria asteroids were carried out at the Center for Solar System Studies Palmer Divide Station (CS3-PDS) during 2023 September to October as part of an ongoing general study of asteroid rotation periods with a concentration on near-Earth, Hungaria, and Hilda group/family asteroids.

Telescope	Camera
0.30-m *f*/6.3 SCT	SBIG STL-1001E
0.35-m *f*/9.1 SCT (×3)	FLI Microline 1001E
0.50-m *f*/8.1 Ritchey-Chrétien	FLI Proline 1001E

Table I. List of available telescopes and CCD cameras at CS3-PDS. The exact combination for each telescope/camera pair can vary due to maintenance or specific needs.

Table I lists the five telescope/CCD camera pairs available at CS3-PDS. All the cameras use CCD chips from the KAF 1001 blue-enhanced family and so have essentially the same response. The pixel scales ranged from 1.24-1.60 arcsec/pixel. All lightcurve observations were made with no or a clear filter. The exposures varied depending on the asteroid's brightness.

To reduce the number of times and amounts of adjusting nightly zero-points, the ATLAS catalog r´ magnitudes on the Pan-STARRS photometric system (SR; Tonry et al., 2018) are used. Those adjustments are usually ≤ ±0.03 mag. The rare larger corrections may have been related in part to using unfiltered observations, poor centroiding of the reference stars, and not correcting for second-order extinction. Another cause may be selecting what appears to be a single star but is actually an unresolved pair.

The Y-axis values are ATLAS SR "sky" (catalog) magnitudes. The values in the parentheses give the phase angle(s), *a*, along with the value of *G* used to normalize the data to the comparison stars and asteroid phase angle used in the earliest session. This, in effect, adjusts all the observations so that they seem to have been made at a single fixed date/time and phase angle. Presumably, any remaining variations are due only to the asteroid's rotation and/or albedo changes.

There can be up to three phase angles If two, the values are for the first and last night of observations. If three, the middle value is the extrema (maximum or minimum) reached between the first and last observing runs. The X-axis shows rotational phase from -0.05 to 1.05. If the plot includes the amplitude, e.g., "Amp: 0.65," this is the amplitude of the Fourier model curve and *not necessarily the adopted amplitude for the lightcurve*.

For brevity, only some of the previous results are referenced. A more complete listing is in the asteroid lightcurve database (Warner et al., 2009; "LCDB" from here on).

10737 Bruck. Observations of this Hungaria were made form 2023 Oct 4-10. The phase angle decreased from 10.6° to 9.0° while the phase angle bisector longitude and latitude were about 21° and -11°, respectively. The "NoSub" plot shows clear indications of a secondary lightcurve. Dual-period analysis using *MPO Canopus* determined the asteroid to be a binary with an orbital period of 15.39 h and effective diameter ratio *Ds/Dp* ≥ 0.28 ± 0.02. The asymmetric spacing of the events warrants confirmation.

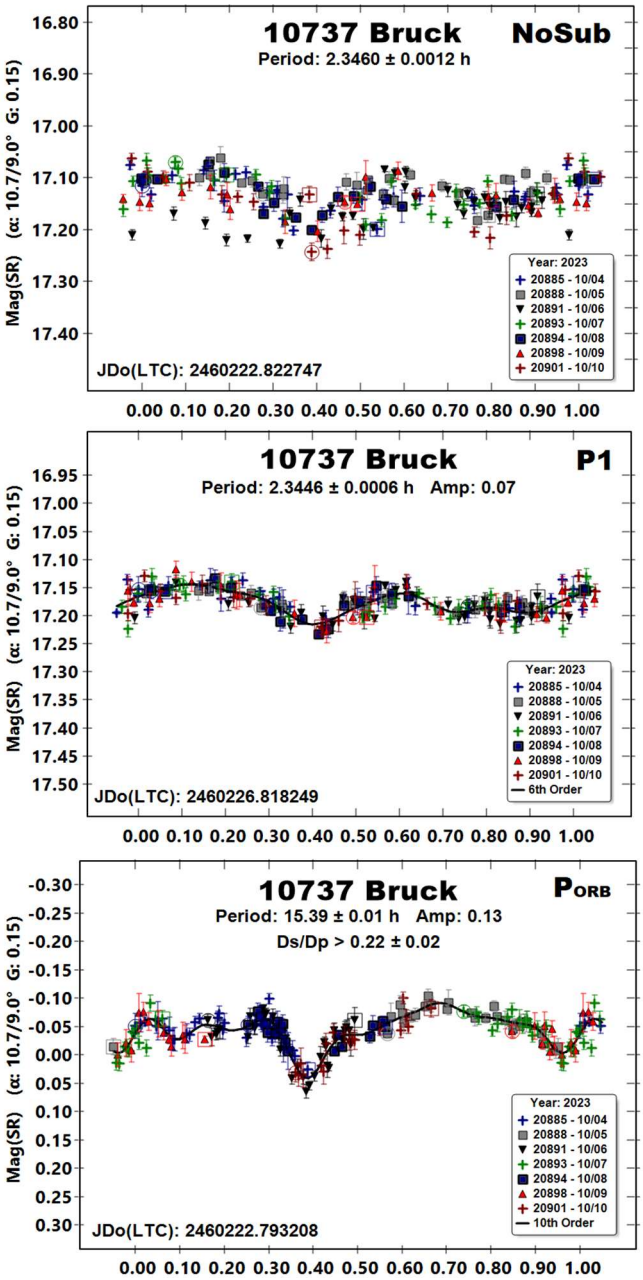

Number	Name	2023/mm/dd	Phase	L_{PAB}	B_{PAB}	Period(h)	P.E.	Amp	A.E.	Grp Ds/Dp
10737	Bruck	10/04-10/10	10.6,9.0	21	-11	[B]2.3446	0.0006	0.07	0.01	H
						15.39	0.01	0.13	0.01	0.22
48470	1991 TC2	09/27-10/09	12.0,6.3	15	-9	[B]2.5141	0.0002	0.11	0.01	H
						11.179	0.004	0.10	0.01	0.28
52748	1998 JJ1	10/04-10/05	14.3,14.0	19	17	4.243	0.005	0.71	0.03	H

Table II. Observing circumstances and results. [B]Period of primary with one or more confirmed or suspected satellites. If a confirmed or suspected binary with mutual events, the second line gives the secondary (or orbital) period and the effective diameter ratio (*Ds/Dp*) based on the shallower (if unequal) event. The amplitude is the maximum amplitude of the secondary lightcurve. The phase angle is given for the first and last date. If preceded by an asterisk, the phase angle reached an extremum during the period. L_{PAB} and B_{PAB} are the approximate phase angle bisector longitude/latitude at mid-date range (see Harris et al., 1984). The Grp column gives the asteroid family or group (Nesvorny, 2015; Nesvorny et al., 2015). H = Hungaria.

Several previous observations of the asteroid, e.g., Warner (2016), Stephens (2017), Stephens and Warner (2020), did not indicate any signs of the asteroid being binary.

(48470) 1991 TC2. Observations of this Hungaria were made between 2023 Sep 27 – Oct 9.

The phase angle decreased from 12.0° to 6.3° while the phase angle bisector longitude and latitude were about 15° and -9°, respectively. The "NoSub" plot shows clear indications of a secondary lightcurve. Dual-period analysis using *MPO Canopus* determined the asteroid to be a binary with an orbital period of 11.179 h and effective diameter ratio $Ds/Dp \geq 0.28 \pm 0.02$.

Observations by Warner (2011; 2014) and Stephens (2016) did not apparently show signs of the asteroid having a satellite.

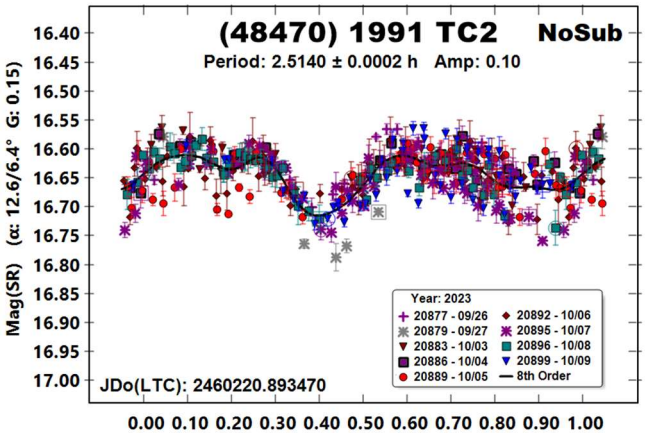

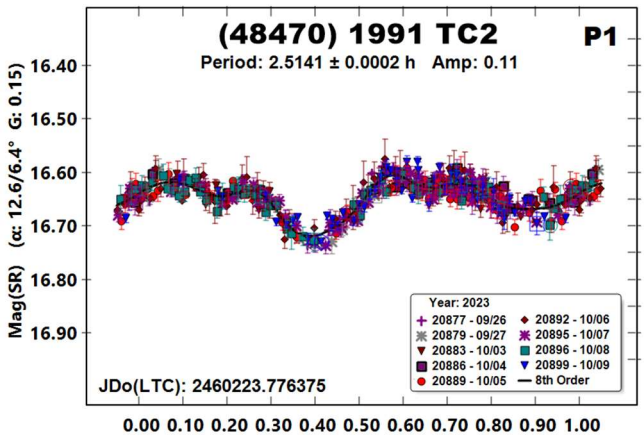

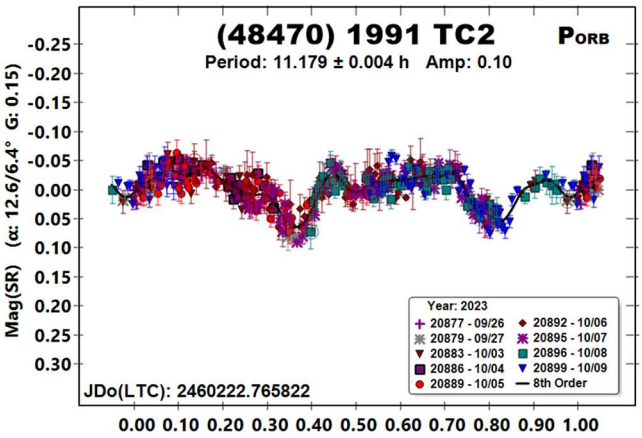

(52748) 1998 JJ1. Clark (2016) reported a period of 4.3260 h while Stephens (2016) found 4.258 h. Durech et al. (2020) used wide-field survey data to find a *sidereal* period of 4.25749 h and ecliptic pole solution $(\lambda, \beta)_{J2000} = (323 \pm 2°, -4 \pm 11°)$.

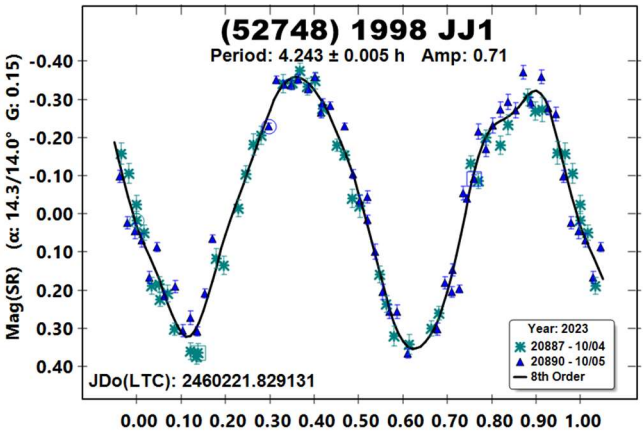

Acknowledgements

This work includes data from the Asteroid Terrestrial-impact Last Alert System (ATLAS) project. ATLAS is primarily funded to search for near earth asteroids through NASA grants NN12AR55G, 80NSSC18K0284, and 80NSSC18K1575; byproducts of the NEO search include images and catalogs from the survey area. The ATLAS science products have been made possible through the contributions of the University of Hawaii Institute for Astronomy, the Queen's University Belfast, the Space Telescope Science Institute, and the South African Astronomical Observatory.

The author gratefully acknowledges a Shoemaker NEO Grants from the Planetary Society (2007). This was used to purchase some of the equipment used in this research.

References

Clark, M. (2016). "Asteroid Photometry from the Preston Gott Observatory." *Minor Planet Bull*. **43**, 132-135.

Durech, J.; Tonry, J.; Erasmus, N.; Denneau, L.; Heinze, A.N.; Flewelling, H.; Vanco, R. (2020). "Asteroid Models reconstructed from ATLAS photometry." *Astron. Astrophys*. **643**, A59.

Harris, A.W.; Young, J.W.; Scaltriti, F.; Zappala, V. (1984). "Lightcurves and phase relations of the asteroids 82 Alkmene and 444 Gyptis." *Icarus* **57**, 251-258.

Nesvorny, D. (2015). "Nesvorny HCM Asteroids Families V3.0." NASA Planetary Data Systems, id. EAR-A-VARGBET-5-NESVORNYFAM-V3.0.

Nesvorny, D.; Broz, M.; Carruba, V. (2015). "Identification and Dynamical Properties of Asteroid Families." In *Asteroids IV* (P. Michel, F. DeMeo, W.F. Bottke, R. Binzel, Eds.). Univ. of Arizona Press, Tucson, also available on astro-ph.

Stephens, R.D. (2016). "Asteroids Observed from CS3: 2015 October - December." *Minor Planet Bull.* **43**, 158-159.

Stephens, R.D. (2017). "Asteroids Observed from CS3: 2017 January - March." *Minor Planet Bull*. **43**, 257-258.

Stephens, R.D.; Warner, B.D. (2020). "Main-Belt Asteroids Observed from CS3: 2020 April to June." *Minor Planet Bull*. **47**, 275-284.

Tonry, J.L.; Denneau, L.; Flewelling, H.; Heinze, A.N.; Onken, C.A.; Smartt, S.J.; Stalder, B.; Weiland, H.J.; Wolf, C. (2018). "The ATLAS All-Sky Stellar Reference Catalog." *Astrophys. J.* **867**, A105.

Warner, B.D.; Harris, A.W.; Pravec, P. (2009). "The asteroid lightcurve database." *Icarus* 2**02**, 134-146. Updated 2023 Oct. *http://www.minorplanet.info/lightcurvedatabase.html*

Warner, B.D. (2011). "Asteroid Lightcurve Analysis at the Palmer Divide Observatory: 2010 December - 2011 March." *Minor Planet Bull*. **38**, 142-149.

Warner, B.D. (2014). "Asteroid Lightcurve Analysis at CS3-Palmer Divide Station: 2014 March - June" *Minor Planet Bull*. **41**, 235-241.

Warner, B.D. (2016). "Asteroid Lightcurve Analysis at CS3-Palmer Divide Station: 2015 June - September." *Minor Planet Bull*. **43**, 57-65.

LIGHTCURVE ANALYSIS FOR NINE NEAR-EARTH ASTEROIDS OBSERVED BETWEEN 2009 - 2023

Peter Birtwhistle
Great Shefford Observatory
Phlox Cottage, Wantage Road
Great Shefford, Berkshire, RG17 7DA
United Kingdom
peter@birtwhistle.org.uk

(Received: 2023 December 31)

Lightcurves and amplitudes for 9 near-Earth asteroids observed from Great Shefford Observatory during close approaches between 2009 - 2019 and August - November 2023 are reported. All are fast or superfast rotators, seven having periods less than 4 minutes, with 2023 TC7 having a period of 12.7 seconds. One has a reliably detected tumbling rotation and another is a possible tumbler.

Photometric observations of near-Earth asteroids during close approaches to Earth in 2009 - 2019 and August - November 2023 were made at Great Shefford Observatory using a 0.40-m Schmidt-Cassegrain and Apogee Alta U47+ CCD camera. All observations were made unfiltered and with the telescope operating with a focal reducer at f/6. The 1K×1K, 13-micron CCD was binned 2×2 resulting in an image scale of 2.16 arc seconds/pixel. All the images were calibrated with dark and flat frames and *Astrometrica* (Raab, 2023) was used to measure photometry using APASS Johnson V band data from the UCAC4 catalogue (Zacharias et al., 2013). *MPO Canopus* (Warner, 2023), incorporating the Fourier algorithm developed by Harris (Harris et al., 1989) was used for lightcurve analysis.

No previously reported results have been found in the Asteroid Lightcurve Database (LCDB) (Warner et al., 2009), from searches via the Astrophysics Data System (ADS, 2023) or from wider searches unless otherwise noted. All size estimates are calculated using H values from the Small-Body Database Lookup (JPL 2023b), using an assumed albedo for NEAs of 0.2 (LCDB readme.pdf file) and are therefore uncertain and offered for relative comparison only.

2009 DO111. This Apollo made a very favourable approach to 1.2 Lunar Distances (LD) from Earth on 2009 Mar 20.2 UTC, nearly 1 month after discovery (Tubbiolo et al., 2009) and will not come closer before 2146. It was followed on four nights, observations starting on 2009 Mar 16.07, 16.94, 18.81 and 19.80 UTC as it brightened from 15th to 12th magnitude on its approach. Reductions from each night produced very similar period spectra, period determinations of 0.04889 h = 176 s and trimodal lightcurves. A representative period spectrum is given from the night of 2009 Mar 18.81, all the minima are related, either integer multiples or small integer fractions (3/2, 4/3, 2/3, 1/2, 1/3) of the best fit period. Independent lightcurves are given for the four nights, for each the Y-axis has been forced to 1.4 magnitudes to aid comparison of the changing amplitude (increasing from 0.37 to 1.29 magnitudes) as the phase angle increased from 16° to 73°. Small zero-point corrections have been made to sessions in the individual lightcurves to minimise scatter in the curves, RMS values of the adjustments for the four nights Mar 16.1, 16.9, 18.8 and 19.8 are 0.01, 0.04, 0.07 and 0.05 respectively. A 'Lightcurve Evolution' plot is given, aligning the deepest minima apparent on each separate night and displacing each night by 0.5 magnitudes vertically to avoid overlap. The key indicates the dates and range of phase angles each covers.

A number of other results for 2009 DO111 have been published previously and are listed here together with the dates covered by the respective lightcurves: 2009 Mar 19.9 (Behrend, 2009web), 2009 Mar 16-18 (Koehn et al., 2014), 2009 Mar 17.0 (Vaduvescu et al., 2017) and 2009 Mar 17.31 & Mar 18.27 (Skiff et al., 2019). The lightcurves presented here are in good agreement with these earlier works for their respective dates of coverage. Behrend notes that tumbling may be present, to be re-analysed. Koehn notes that their result suffers from lightcurve smoothing. The same data was then re-analysed and refined in the Skiff paper. Vaduvescu provides a well-defined lightcurve but remarks that their coverage is insufficient to test the tumbling supposition. There is no evidence of tumbling in the four lightcurves presented in the current paper.

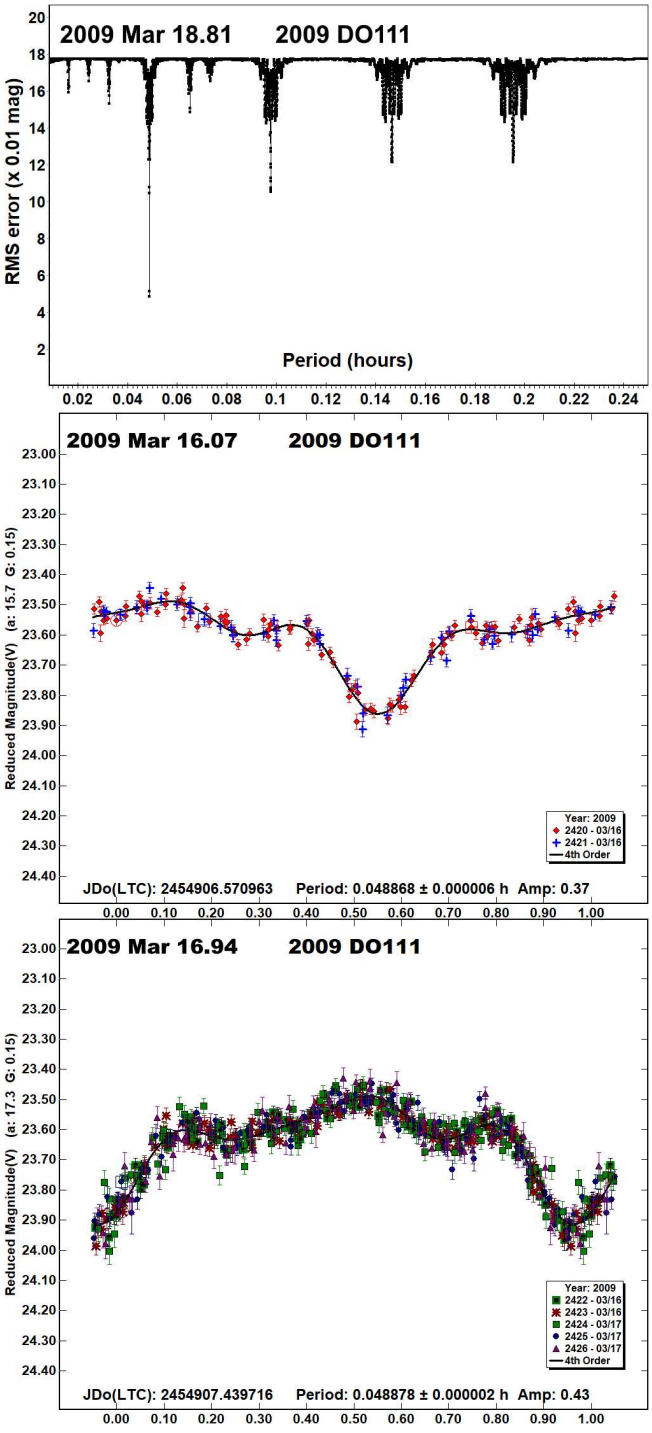

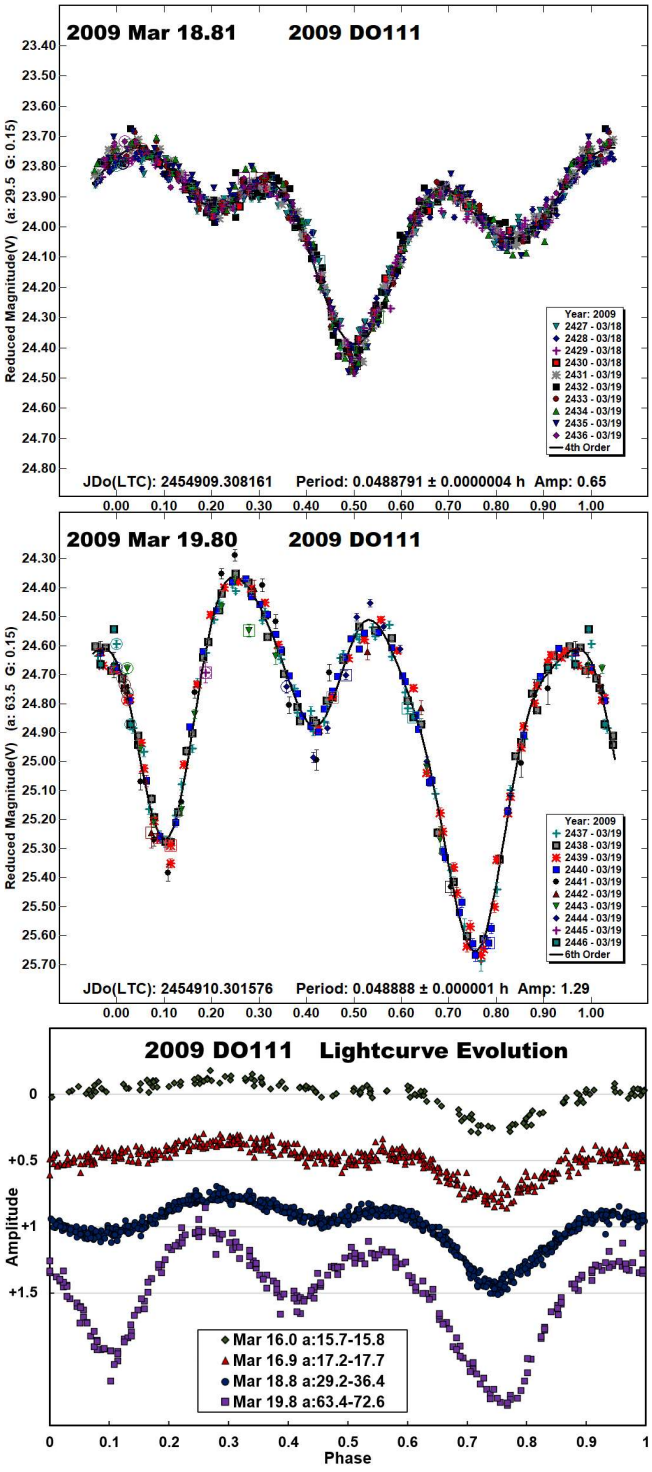

A summary of the data collection circumstances is given in Table I.

Start date 2009 Mar	Exp. len (s)	Data points	Span (h)	Observed for (h)
Mar 16.07	12	150	2.2	0.64
Mar 16.94	4,6	498	4.5	1.31
Mar 18.81	4,6	783	8.8	1.94
Mar 19.80	1.5,2	249	2.9	0.60

Table I. 2009 DO111 data collection circumstances, listing for each date the exposure lengths used (seconds), number of data points, the number of hours from the first to last data point and the number of hours of continuous observation.

2011 PE2. This is an Apollo, discovered by the La Sagra Sky Survey team in Spain on 2011 Aug 8 (Wiggins et al., 2011), some 8 days after it had passed Earth at 3.5 LD when it would have been 15th magnitude. With H = 23.1 it has an estimated dia. of ~71 m. It was observed for 2.9 h starting on 2011 Aug 9.01 UTC and large variations in brightness were obvious within 10 minutes. It was relatively faint for the equipment, especially at minimum, varying from mag 18 - 19.5 and so the 348 usable 20-second exposures were stacked into 68 images for measurement, each stack comprising 4 - 6 images, with the longest effective exposure length (from the start of the first to the end of the last exposure) being 172 s. Analysis with *MPO Canopus* determined the best fit period to be 0.740 ± 0.04 h and amplitude 1.3 magnitudes.

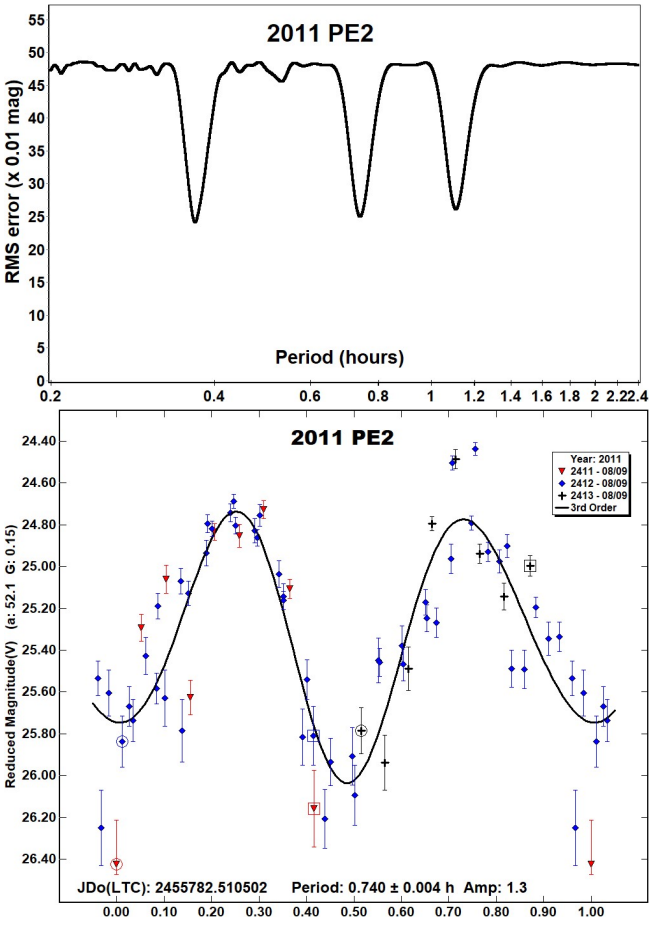

2012 TV. This Apollo with H = 25.2 and an estimated diameter of ~27 m was discovered at the Tenagra II Observatory on 2012 Oct. 5.3 UTC at mag 17 (Boattini et al., 2012). On 2012 Oct. 7.63 UTC it passed Earth within 0.7 Lunar Distances (LD) and it is listed by Sentry (JPL 2023a) and NEODyS (NEODyS, 2023) as a virtual impactor, with a number of low probability potential impacts starting in 2070. It was observed for 1.6 hours starting at 2012 Oct. 6.90 UTC, then after a gap of 2.2 h was observed for a further 2.0 h. It was 14th mag throughout the period of observation and its speed accelerated from 45 to 94 arcsec/min. as its distance reduced from 2.8 to 1.9 LD. 790 measurable images were obtained and a period spectrum from an analysis using *MPO Canopus* shows four RMS minima equating to monomodal to quadrimodal lightcurves, with the best fit solution being a bimodal asymmetric lightcurve of period 0.052611 ± 0.000001 h and amplitude 0.72 ± 0.05. The telescope was repositioned 6 times during the first period of observation and 8 times during the second. There was a slight zero-pointing difference between the two sets of measurements, possibly due to changes in aspect or conditions in the intervening 2.2 h and small adjustments to the 14 sessions have been made to reduce the overall scatter in the lightcurve, the RMS of the adjustments being 0.06 mag. 2012 TV completed 30 rotations during the first observing period and 38 during the second.

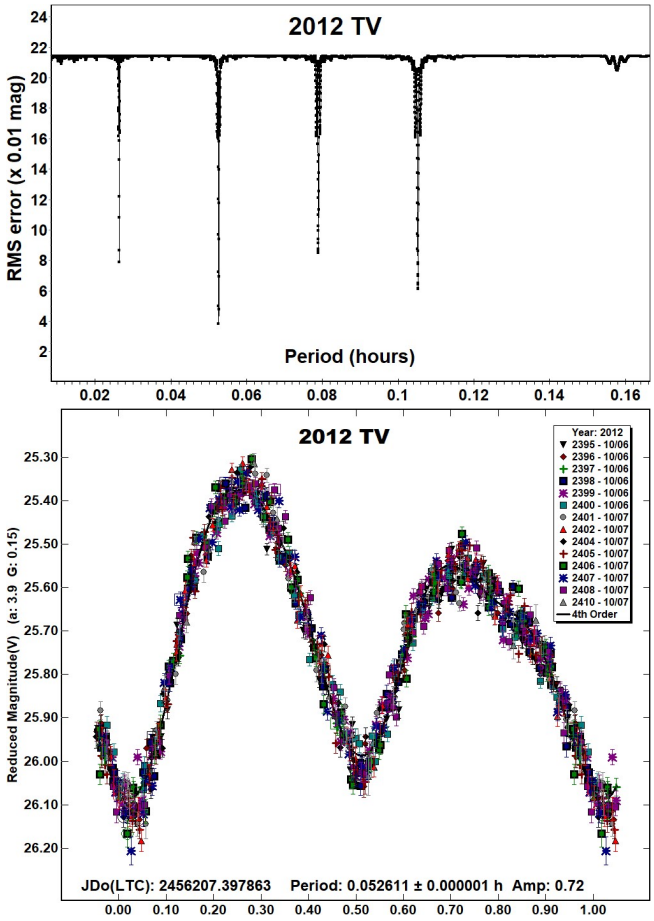

Franco et al., (2013) determined a lightcurve for 2012 TV from observations made on 2012 Oct. 6.3 and Oct. 6.8 and it is in good agreement with this result, with P = 0.0525 ± 0.0001 h and amplitude 0.57 ± 0.04.

2017 OM1. Discovered at magnitude 17 from Mauna Loa by the ATLAS team on 2017 Jul 22.5 UTC, it passed Earth at 2.3 LD three days later on 2017 Jul 25.49 UTC (Hoegner et al., 2017). 2017 OM1 is listed with H = 23.4 in the SBDB, inferring a dia. of ~ 62 m and was recovered at magnitude 23 in July 2018 but now does not approach within 19 LD of Earth for at least the next 100 years. It was observed for 74 minutes starting on 2017 Jul 25.05 UTC when it was 15th mag, moving at 150 arcsec/min and at a relatively large phase angle of 85°. A total of 607 measurable images were obtained and analysis using *MPO Canopus* determined the best fit lightcurve to be 0.05903 ± 0.00003 h and the amplitude to be 0.3 mags, relatively small considering the large phase angle and implying 2017 OM1 may be nearly spherical, or was presented pole-on to Earth at that time.

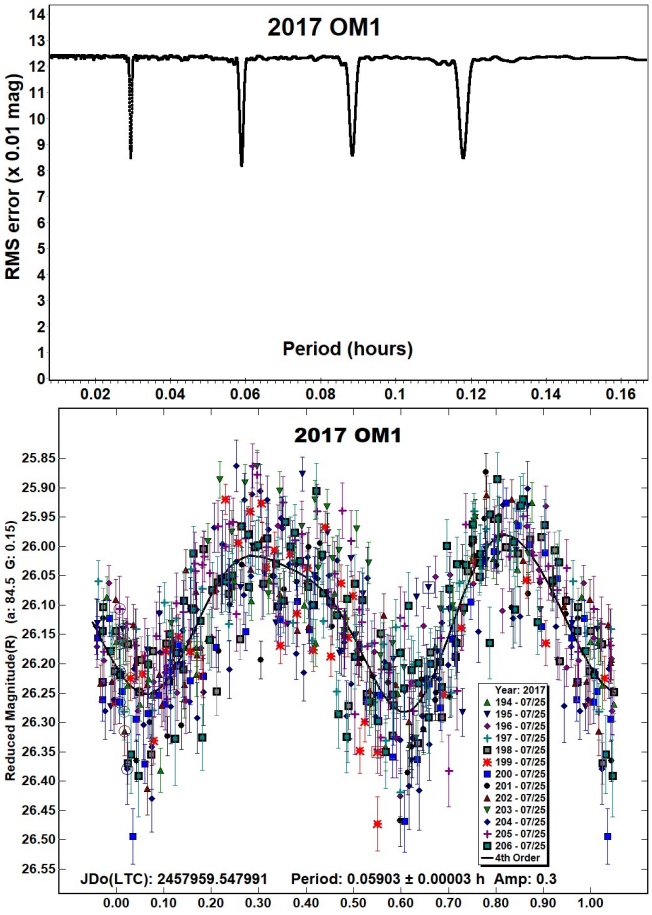

2019 UM12. This Apollo was discovered by the Mt. Lemmon Survey on 2019 Oct 29, 10 days before it passed Earth at 1.3 LD (Bulger et al., 2019). It is listed in the SBDB with H = 24.7, suggesting a dia. of ~34 m. It was observed for 1.9 h while it was still inbound, starting on 2019 Nov 7.91 UTC when it was 15th mag and large variations in magnitude were obvious within a few minutes. A raw plot of the measurements shows maxima approximately every 10 minutes, suggesting a ~20-minute bimodal period. However, maxima and minima vary in height and attempts to determine the lightcurve with *MPO Canopus* are unsatisfactory, systematic trends indicating that 2019 UM12 is probably tumbling.

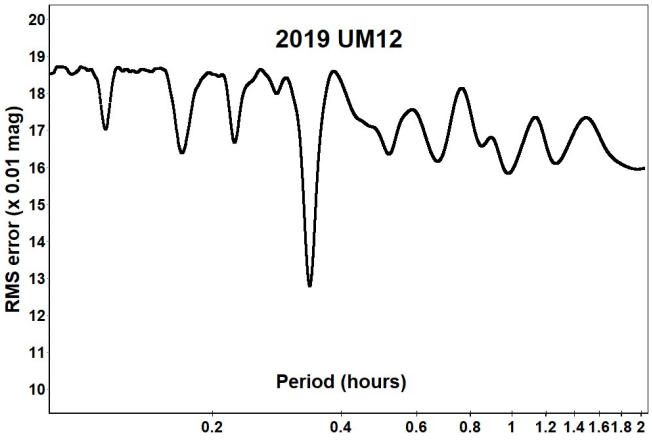

The period spectrum locates the dominant period around 0.339 h = 20.3 minutes but also indicates a number of less well-defined minima but no coherent solution for tumbling or non-principal axis rotation can be found.

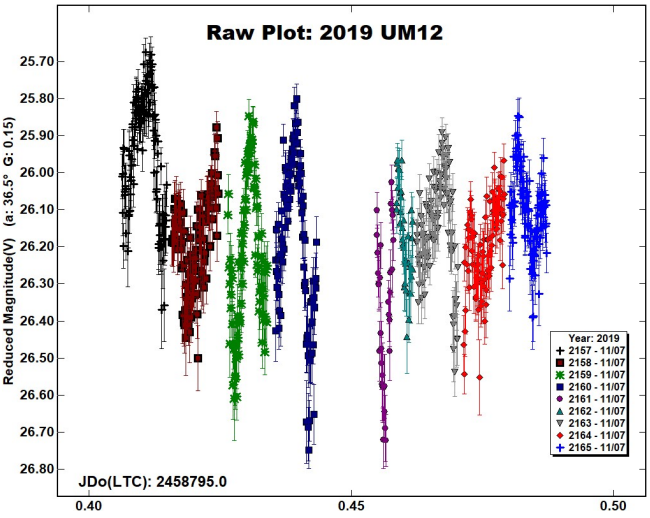

The first session (marked as 2157 in the raw plot) appears anomalously bright by ~0.17 magnitudes, this may be a consequence of tumbling, but potentially more likely is a zero-pointing issue at the start of the observing run. A best fit principal axis rotation (non-tumbling) solution is given marked as PAR rejecting the first session. It is likely that 2019 UM12 is tumbling, with principal period ~0.339 h, there are deviations from the main period and a secondary period in the range 0.2 - 0.5 h may be present but this is not established, so it is expected that it may be given a PAR rating of -2 (deviations from a single period are seen but the second period is not resolved) on the scale defined in Pravec et al. (2005).

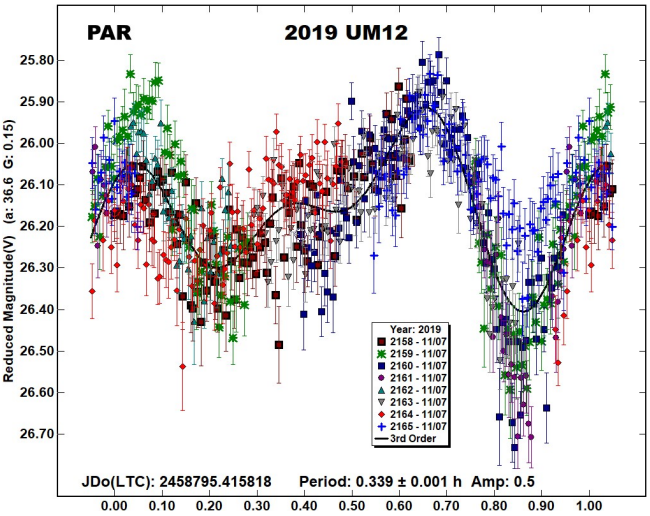

2023 TM3. This was a Catalina Sky Survey discovery from 2023 Oct 8 which made an approach to 0.4 Lunar Distances (LD) on Oct 10.54 UTC (Bacci et al., 2023). The SBDB lists it as an Aten with H = 26.9, indicating an approximate diameter of 12 m and both Sentry (JPL, 2023a) and NEODyS (NEODyS, 2023) list it as a virtual impactor with multiple low probability potential impacts starting in 2082. It was observed for 2.0 h starting at 2023 Oct 10.04 UTC and 770 photometric measurements were obtained. 2023 TM3 was within 1.3 LD and its apparent motion increased from 92 to 124

arcsec/min during observation, causing the telescope to need repositioning 12 times. Exposures lengths were reduced from 5.8 to 4.3 s to keep image trailing within the size of the annulus used in *Astrometrica*. A well defined asymmetric lightcurve was determined using *MPO Canopus* with a period of 2.3 minutes and amplitude 0.5 mag and indicating that 52 full rotations occurred during the period of observation.

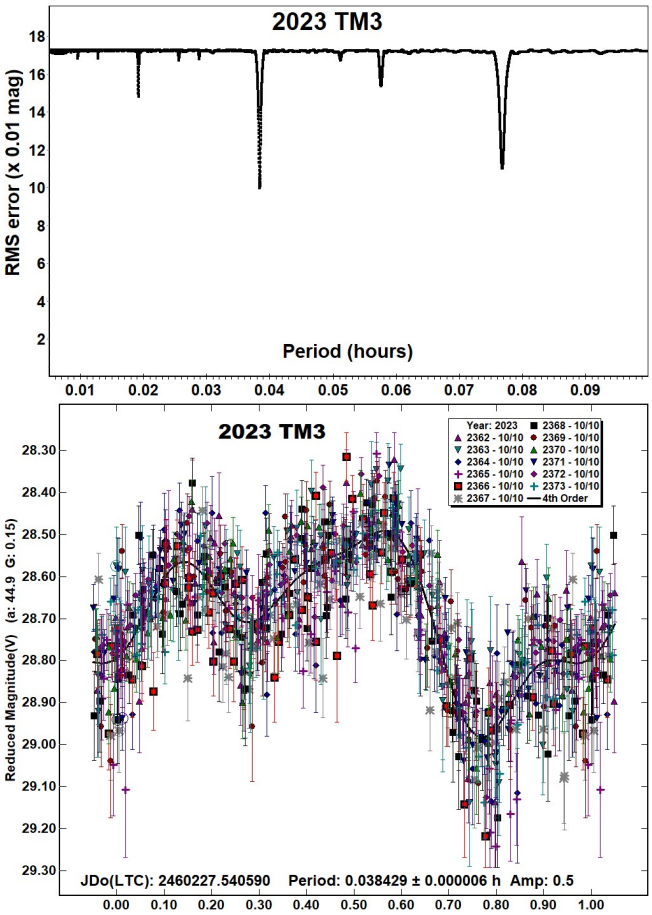

2023 TC7. Another Aten discovered by the Catalina Sky Survey, this time on 2023 Oct 11.38 UTC (Pettarin et al., 2023a). With H = 26.9 it has an estimated diameter of ~13 m and passed Earth at 1.7 LD on 2023 Oct 15.14 UTC and on its approach passed through the Earth's penumbra for an hour centred on 2023 Oct 14.31 UTC. It was observed for 9 minutes starting at 2023 Oct 13.88 UTC using 5 s exposures to obtain astrometry, when it was 16th mag and moving at 60 arcsec/min. Visual inspection of those images did not show noticeable variation, so in case rotation was very rapid a series of 2.5 and then 2 s exposures were taken 1 hour later when 2023 TC7 was at a higher altitude and those did show obvious variation between consecutive images. A quick spreadsheet determination of the possible period indicated it might be as short as 12 s and therefore an optimum exposure length to maximise signal with minimal lightcurve smoothing (Pravec et al., 2000) was estimated to be 0.185 × 12 = 2.2 s. All subsequent exposures were set at 2.4 s and further series of exposures were taken starting at 2023 Oct 14.01 UTC for 72 min and then 38 mins later another series obtained for 20 minutes. The next night 2023 TC7 was slightly brighter and reached a higher altitude and another series of images, again using 2.4 s exposure lengths was started at 2023 Oct 14.84 UTC for 57 minutes. The first night produced 1305 measurable images, the second night a further 759 and subsequent analysis with *MPO Canopus* indicated the best fit period for the asymmetric lightcurve was the same for both dates at 0.0035401 ± 0.0000001 h, or 12.7444 ± 0.0004 s. Period spectrum plots for the two nights are similar and a plot for the second date is given, covering periods from 3 - 120 s on a linear scale.

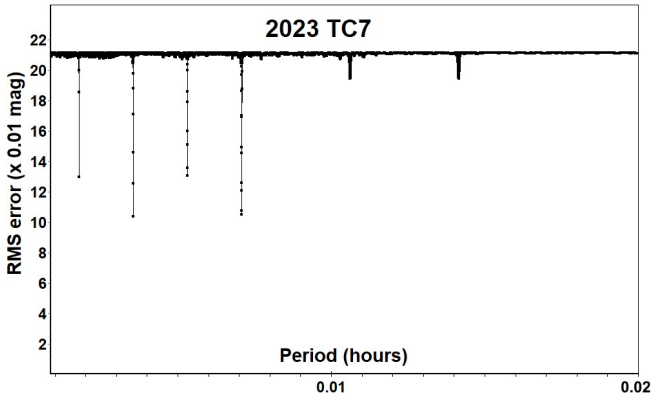

Lightcurves from the two nights are labelled Oct 13 and Oct 14 and as expected with the increasing phase angle, the amplitude also increased.

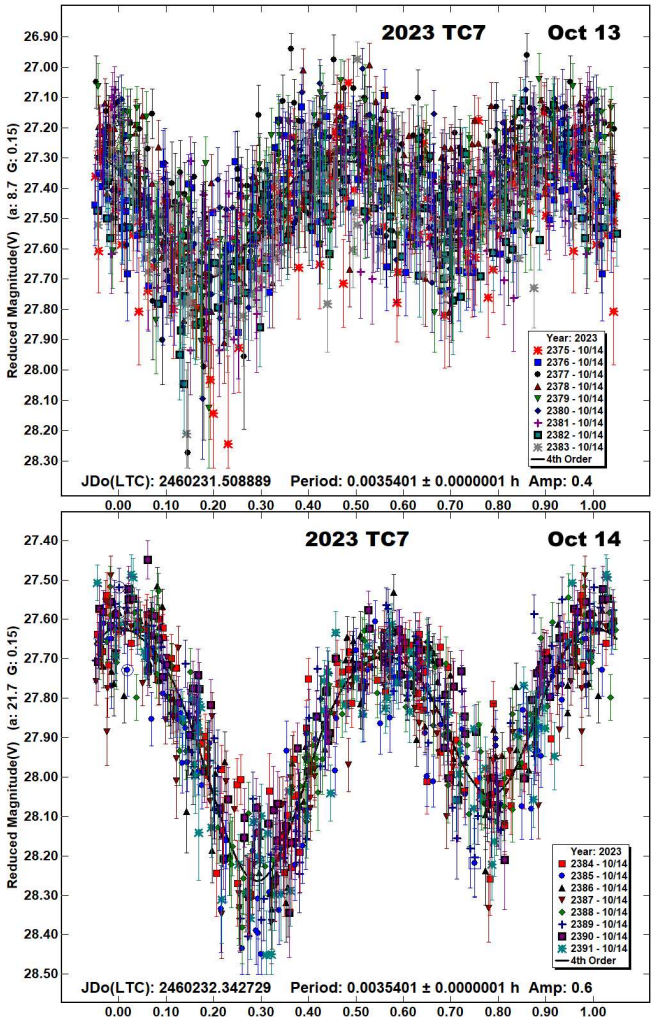

2023 TC7 was under observation for 1.5 h on the first night, during which 434 rotations occurred and for 1 h on the second night, covering a further 268 rotations. 2023 TC7 has a very short rotation period of 12.7 s, with the LCDB listing just 2017 QG18 and 2019 BE5 with periods shorter than 15 s (11.9 s and 12.0 s respectively). The detection of the very short rotation period was as a consequence of reducing the initially selected exposure length from 5 s to 2 s. The 'Smoothing of lightcurve harmonics' plot is adapted from Birtwhistle (2021) to indicate the potential effects on the first four harmonics of a lightcurve with period P = 12.7 s due to exposure lengths of Δt = 2.4 s and Δt = 5 s. The relative strength of the dominant second harmonic *f2* is reduced to 78% with exposure lengths of 2.4 s but is reduced to 25% using 5 s exposures and additionally, with the longer exposure time, any contribution from the third and fourth harmonics (*f3* and *f4*) is drastically reduced in strength but also negated, potentially causing some lightcurve distortion.

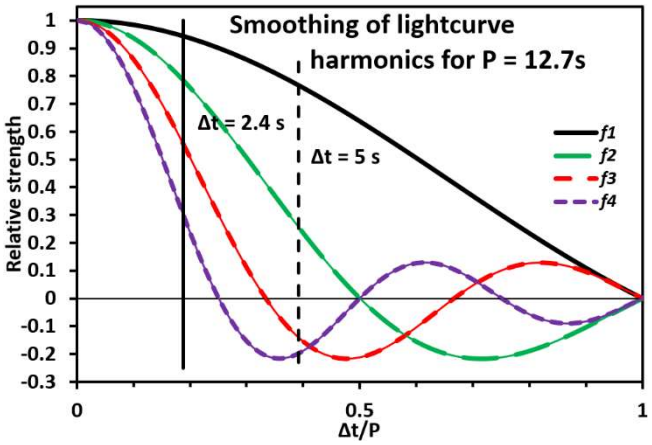

2023 VB2. This small Apollo, with H = 28.2 and an estimated dia. of ~7 m was discovered at the Nanshan Station of the Xinjiang Observatory on 2023 Nov 5.7 UTC (Pettarin et al., 2023b). It made a very close approach to 0.085 LD from Earth on 2023 Nov 7.29 UTC. Images for photometry were collected for 1.8 h starting on 2023 Nov 6.97 UTC during its approach, its apparent speed rose from 38 to 66 arcsec/min, relatively slow for an object less than 1.2 LD from Earth. Analysis with *MPO Canopus* determined an asymmetric lightcurve with period 0.06661 ± 0.00002 h and 0.5 mag amplitude. 2023 VB2 made 27 full rotations during the period of observation. The SBDB (JPL, 2023b) lists 2023 VB2 as having only one future approach to Earth in the next 100 years, with the nominal close approach distance predicted to be 1.1 LD on 2033 Nov 6 but with large uncertainties.

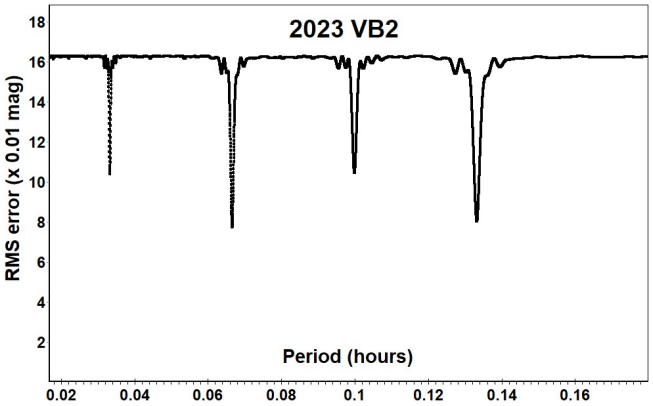

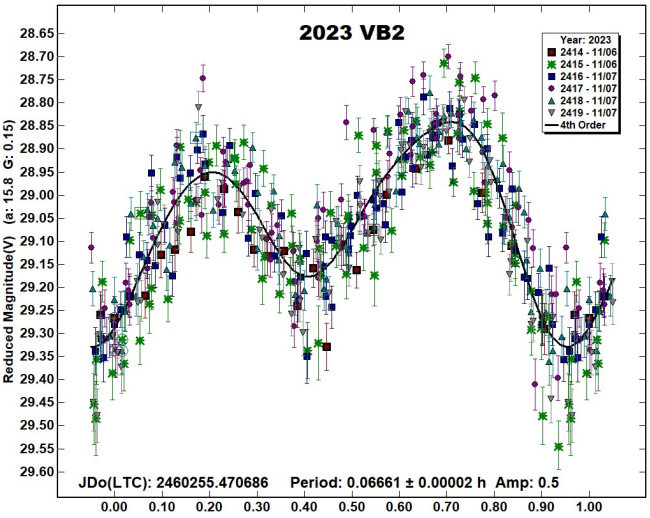

2023 WA. This small Apollo (H = 28.5, est. dia. ~7 m) was an ATLAS discovery from the Rio Hurtado station in Chile on 2023 Nov 16.2 UTC (Bulger et al., 2023), less than 24 hours before approaching Earth to 0.07 LD (27,400 km), within the distance of geostationary satellites. It brightened rapidly during the approach and was observed for 46 minutes starting on 2023 Nov 17.04 UTC as its distance decreased from 0.41 to 0.29 LD, with the apparent speed increasing from 260 to 520 arcsec/min, brightening from 14th to 13th mag. Exposures were limited to 1.9 seconds or shorter to keep trailing within the measurement annulus used in *Astrometrica* and imaging was halted when exposures would have needed to be shorter than 1 s. A linearly scaled period spectrum shows four strong, equally spaced solutions, the nominal best fit period being 0.018856 ± 0.000004 h but the resulting lightcurve labelled PAR shows definite signs of tumbling being present. Another weaker set of four equally spaced RMS minima starting at 0.0067 h can be seen in the period spectrum and the *MPO Canopus* dual period search function was used to try and resolve two periods in case non-principal axis rotation (NPAR) was present. This was successful and determined the dominant period to be 0.018857 ± 0.000003 h, shown in the lightcurve labelled P1 and a secondary period located at 0.013331 ± 0.000003 h, shown in the lightcurve labelled P2. The full amplitude suggested by the NPAR solution is 1.22 magnitudes. During the 46 minutes of observation 2023 WA completed 41 rotations of the P1 period and 58 of the P2 period. On the scale defined in Pravec et al., (2005) it is expected to be rated as PAR = -3 (NPA rotation reliably detected with the two periods resolved) (Petr Pravec, personal communication).

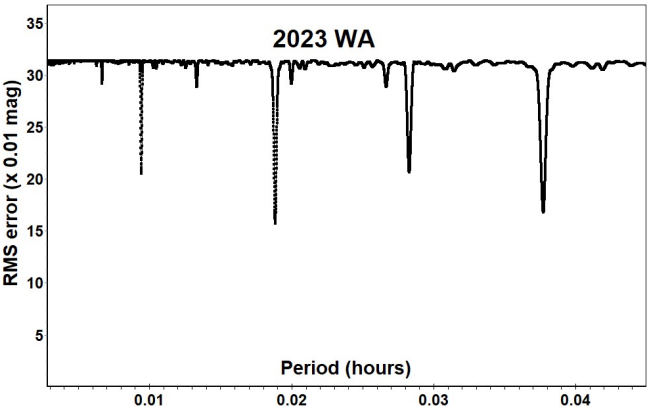

Number	Name	yyyy mm/dd	Phase	L_{PAB}	B_{PAB}	Period(h)	P.E.	Amp	A.E	PAR	H
	2009 DO111	2009 03/18-03/19	29.2-36.4	173	16	0.0488791	0.0000004	0.65	0.04		22.9
	2011 PE2	2011 08/09-08/09	52.1-51.9	341	13	0.740	0.004	1.3	0.3		23.1
	2012 TV	2012 10/06-10/07	4.0-9.8	15	-3	0.052611	0.000001	0.72	0.05		25.2
	2017 OM1	2017 07/25-07/25	84.6-87.5	342	18	0.05903	0.00003	0.3	0.1		23.4
	2019 UM12	2019 11/07-11/07	36.5-38.2	26	1	0.339	0.001	0.5	0.2	-2	24.7
	2023 TM3	2023 10/10-10/10	44.9-46.1	36	12	0.038429	0.000006	0.5	0.1		26.9
	2023 TC7	2023 10/14-10/14	*9.0-23.3	19	8	0.0035401	0.0000001	0.6	0.1		26.9
	2023 VB2	2023 11/06-11/07	16.3-17.9	39	-7	0.06661	0.00002	0.5	0.1		28.2
	2023 WA	2023 11/17-11/17	11.0-15.1	48	-1	0.018857	0.000003	0.89	0.15	-3	28.5
						0.013331	0.000003	0.33	0.15		

Table II. Observing circumstances and results. The phase angle is given for the first and last date. If preceded by an asterisk, the phase angle reached an extrema during the period. L_{PAB} and B_{PAB} are the approximate phase angle bisector longitude/latitude at mid-date range (see Harris et al., 1984). Amplitude error (A.E.) is calculated as $\sqrt{2}$ × (lightcurve RMS residual). PAR is the expected Principal Axis Rotation quality detection code (Pravec et al., 2005) and H is the absolute magnitude at 1 au from Sun and Earth taken from the Small-Body Database Lookup (JPL, 2023b).

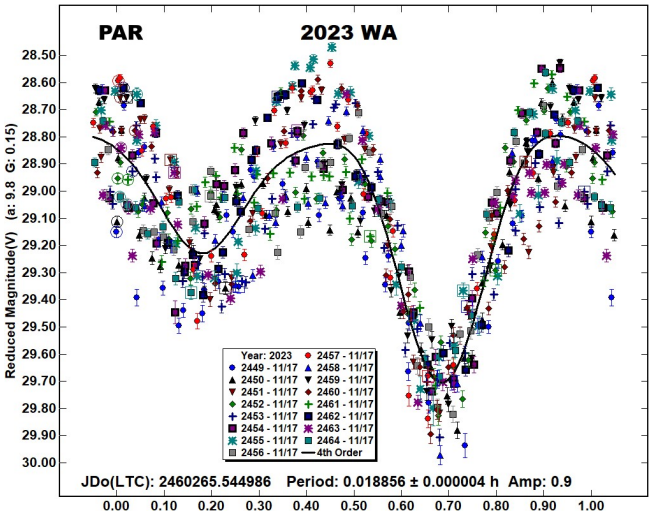

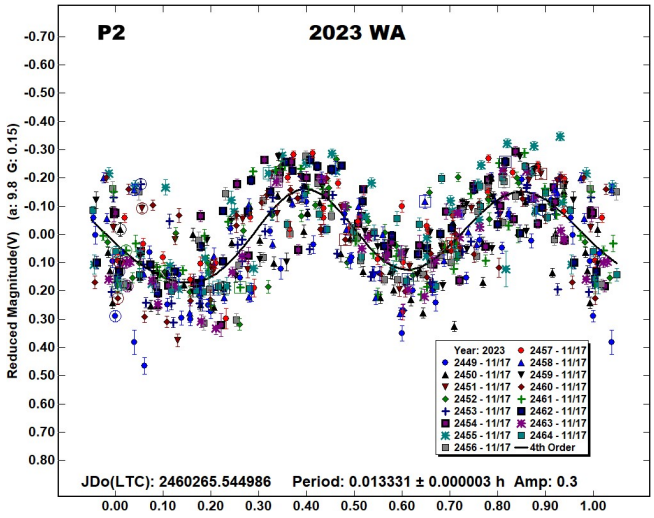

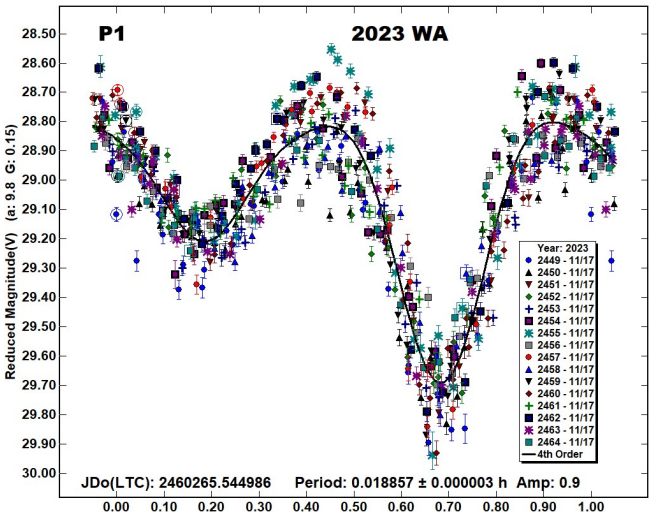

Number	Name	Integration times	Max intg/Pd	Min a/b	Pts	Flds
	2009 DO111	1.5-12	0.068	1.3[1]	1680	27
	2011 PE2	172[Σ]	0.065	1.6*	68	3
	2012 TV	2-10	0.053	1.7	790	14
	2017 OM1	2,4	0.019	1.1	607	13
	2019 UM12	5	0.004	1.2	639	8
	2023 TM3	4.3-5.8	0.042	1.2*	770	12
	2023 TC7	2.4	0.188	1.4	2064	17
	2023 VB2	8.9-13.9	0.058	1.3	408	6
	2023 WA	1.1-1.9	0.040	2.2	575	16

Table III. Ancillary information, listing the integration times used (seconds), the fraction of the period represented by the longest integration time (Pravec et al., 2000), the calculated minimum elongation of the asteroid (Zappala et al., 1990), the number of data points used in the analysis and the number of times the telescope was repositioned to different fields. Notes: 1 = Based on amplitude from 2009 Mar 16.07, * = Value uncertain, based on phase angle > 40°, Σ = Longest elapsed integration time for stacked images (start of first to end of last exposure used)

Acknowledgements

The author is indebted to Petr Pravec for reviewing the analyses of tumbling asteroids. The author also gratefully acknowledges a Gene Shoemaker NEO Grant from the Planetary Society (2005) and a Ridley Grant from the British Astronomical Association (2005), both of which facilitated upgrades to observatory equipment used in this study.

References

ADS (2023). Astrophysics Data System. *https://ui.adsabs.harvard.edu/*

Bacci, P.; Maestripieri, M.; Tesi, L.; Fagioli, G.; Pettarin, E.; Fazekas, J.B.; Beshore, E.C.; Fay, D.; Fuls, D.C.; Gibbs, A.R.; Grauer, A.D.; Groeller, H.; Hogan, J.K.; Kowalski, R.A.; Larson, S.M. and 18 colleagues (2023). "2023 TM3" MPEC 2023-T110. *https://minorplanetcenter.net/mpec/K23/K23TB0.html*

Behrend, R. (2009web). Observatoire de Geneve web site. *http://obswww.unige.ch/~behrend/page_cou.html*

Birtwhistle, P. (2021). "Ultra-Fast Rotators: Results and Recommendations for Observing Strategies" *Minor Planet Bull*. **48**, 346-352.

Boattini, A.; Christensen, E.J.; Gibbs, A.R.; Grauer, A.D.; Hill, R.E.; Kowalski, R.A.; Larson, S.M.; McNaught, R.H.; Wiggins, P.; Schwartz, M.; Holvorcem, P.R.; Dupouy, P.; de Vanssay, J.B.; Franco, L.; Pietschnig, M. and 25 colleagues (2012). "2012 TV" MPEC 2012-T16. *https://minorplanetcenter.net/mpec/K12/K12T16.html*

Bulger, J.; Chambers, K.; Dukes, T.; Lowe, T.; Magnier, E.; Schultz, A.; Willman, M.; Chastel, S.; Huber, M.; Ramanjooloo, Y.; Wainscoat, R.; Weryk, R.; de Boer, T.; Denneau, L.; Fairlamb, J. and 16 colleagues (2019). "2019 UM12" MPEC 2019-U281. *https://minorplanetcenter.net/mpec/K19/K19US1.html*

Bulger, J.; Lowe, T.; Minguez, P.; Schultz, A.; Smith, I.; Chambers, K.; de Boer, T.; Fairlamb, J.; Gao, H.; Huber, M.; Lin, C.-C.; Magnier, E.; Ramanjooloo, Y.; Wainscoat, R.; Weryk, R. and 12 colleagues (2023). "2023 WA" MPEC 2023-W10. *https://www.minorplanetcenter.net/mpec/K23/K23W10.html*

Franco, L.; Guido, E.; Sostero, G.; Howes, N.; Donato, L. (2013). "Lightcurve Photometry of NEA 2012 TV." *Minor Planet Bull.* **40**, 44-45.

Harris, A.W.; Young, J.W.; Scaltriti, F.; Zappala, V. (1984). "Lightcurves and phase relations of the asteroids 82 Alkmene and 444 Gyptis." *Icarus* **57**, 251-258.

Harris, A.W.; Young, J.W.; Bowell, E.; Martin, L.J.; Millis, R.L.; Poutanen, M.; Scaltriti, F.; Zappala, V.; Schober, H.J.; Debehogne, H.; Zeigler, K. (1989). "Photoelectric Observations of Asteroids 3, 24, 60, 261, and 863." *Icarus* **77**, 171-186.

Hoegner, C.; Stecklum, B.; Bacci, P.; Maestripieri, M.; Fragai, M.; Tesi, L.; Fagioli, G.; Ceschia, M.; Pettarin, E.; Hug, G.; Cromer, D.; Camarasa, J.; M, Bosch, J.; Hidas, A.; Cashwell, W. and 26 colleagues (2017). "2017 OM1" MPEC 2017-O47. *https://minorplanetcenter.net/mpec/K17/K17O47.html*

JPL (2023a). Sentry: Earth Impact Monitoring. *https://cneos.jpl.nasa.gov/sentry/*

JPL (2023b). Small-Body Database Lookup. *https://ssd.jpl.nasa.gov/tools/sbdb_lookup.html*

Koehn, B.W.; Bowell, E.L.G.; Skiff, B.A.; Sanborn, J.J.; McLelland, K.P.; Pravec, P.; Warner, B.D. (2014) "Lowell Observatory Near-Earth Asteroid Photometric Survey (NEAPS) - 2009 January through 2009 June." *Minor Planet Bull*. **41**, 286-300.

NEODyS (2023). Near Earth Objects Dynamic Site. *https://newton.spacedys.com/neodys*

Pettarin, E.; Leonard, G.J.; Beshore, E.C.; Fay, D.; Fazekas, J.B.; Fuls, D.C.; Gibbs, A.R.; Grauer, A.D.; Groeller, H.; Hogan, J.K.; Kowalski, R.A.; Larson, S.M.; Rankin, D.; Seaman, R.L.; Shelly, F.C. and 7 colleagues (2023a). "2023 TC7" MPEC 2023-T179. *https://minorplanetcenter.net/mpec/K23/K23TH9.html*

Pettarin, E.; Read, M.T.; Dupouy, P.; Ivanov, A.; Barcov, A.; Ivanov, V.; Lysenko, V.; Yakovenko, N.; Ivanova, N.; Gorbunov, N.; Kurbatov, G.; Shchukin, P.; Roshchupko, V.; Urbanik, M.; Fazekas, J.B. and 57 colleagues (2023b). "2023 VB2" MPEC 2023-V74. *https://www.minorplanetcenter.net/mpec/K23/K23V74.html*

Pravec, P.; Hergenrother, C.; Whiteley, R.; Sarounova, L.; Kusnirak, P.; Wolf, M. (2000). "Fast Rotating Asteroids 1999 TY2, 1999 SF10, and 1998 WB2." *Icarus* **147**, 477-486.

Pravec, P.; Harris, A.W.; Scheirich, P.; Kušnirák, P.; Šarounová, L.; Hergenrother, C.W.; Mottola, S.; Hicks, M.D.; Masi, G.; Krugly, Yu. N.; Shevchenko, V.G.; Nolan, M.C.; Howell, E.S.; Kaasalainen, M.; Galád, A. and 5 colleagues. (2005). "Tumbling Asteroids." *Icarus* **173**, 108-131.

Raab, H. (2023). Astrometrica software, version 4.14.0.452. *http://www.astrometrica.at/*

Skiff, B.A.; McLelland, K.P.; Sanborn, J.J.; Pravec, P.; Koehn, B.W.; Bowell, E. (2019). "Lowell Observatory Near-Earth Asteroid Photometric Survey (NEAPS): Paper 4." *Minor Planet Bull*. **46**, 458-503.

Tubbiolo, A.F.; Bressi, T.H.; McMillan, R.S.; Hill, R.E.; Beshore, E.C.; Boattini, A.; Garradd, G.J.; Gibbs, A.R.; Grauer, A.D.; Kowalski, R.A.; Larson, S.M.; McNaught, R.H.; Ikari, Y.; Guido, E.; Sostero, G. and 1 colleague (2009). "2009 DO111" MPEC 2009-E70. *https://minorplanetcenter.net/mpec/K09/K09E70.html*

Vaduvescu, O.; Aznar Macias, A.; Tudor, V.; Predatu, M.; Galad, A.; Gajdos, S.; Vilagi, J.; Stevance, H.F.; Errmann, R.; Unda-Sanzana, E.; Char, F.; Peixinho, N.; Popescu, M.; Sonka, A.; Cornea, R. and 12 colleagues (2017). "The EURONEAR Lightcurve Survey of Near Earth Asteroids." *Earth, Moon, and Planets* **120**, 41-100.

Warner, B.D.; Harris, A.W.; Pravec, P. (2009). "The Asteroid Lightcurve Database." *Icarus* **202**, 134-146. Updated 2023 Oct. *https://www.minorplanet.info/php/lcdb.php*

Warner, B.D. (2023). MPO Software, Canopus version 10.8.6.20. Bdw Publishing, Colorado Springs, CO.

Wiggins, P.; Hug, G.; Losse, F.; Sanchez, S.; Nomen, J.; Stoss, R.; Hurtado, M.; Jaume, J.A.; Yeung, W.K.Y.; Rios, P.; Serra, F.; Birtwhistle, P. (2011) "2011 PE2" MPEC 2011-P40. *https://minorplanetcenter.net/mpec/K11/K11P40.html*

Zacharias, N.; Finch, C.T.; Girard, T.M.; Henden, A.; Bartlett, J.L.; Monet, D.G.; Zacharias, M.I. (2013). "The Fourth US Naval Observatory CCD Astrograph Catalog (UCAC4)." *The Astronomical Journal* **145**, 44-57.

Zappala, V.; Cellini, A.; Barucci, A.M.; Fulchignoni, M.; Lupishko, D.E. (1990). "An analysis of the amplitude-phase relationship among asteroids." *Astron. Astrophys*. **231**, 548-560.

LIGHTCURVES AND COLORS OF SEVEN SMALL NEAR-EARTH ASTEROIDS: 2023 LQ1, 2023 LT1, 2023 MC, 2023 VQ5, 2023 VE6, 2023 VF6, 2023 VV7

Jean-Baptiste Kikwaya Eluo
Vatican Observatory
V-00120 Vatican City of State
jbkikwaya@arizona.edu; jbkikwaya@gmail.com

Carl W. Hergenrother
Ascending Node Technologies, LLC
Tucson, Arizona, USA

(Received: 2024 January 12 Revised: 2024 March 1)

We conducted two observation campaigns (2023 June 16-19 and 2023 November 11-13), during which we obtained photometric observations of seven small near-Earth asteroids. Lightcurves for six of the asteroids clearly showed rapid rotation, while one was inconclusive. We also computed BVRI colors for all seven asteroids to determine their taxonomy by computing color indexes and relative reflectances and comparing the results with published BVRI asteroid measurements, SMASS/SMASSII asteroid spectra.

Small near-Earth asteroid (NEA) lightcurve and color photometry were obtained with the Vatican Observatory's Vatican Advanced Technology Telescope (VATT), an aplanatic Gregorian telescope with a 1.8-m *f*/1.0 primary mirror and 0.38-m *f*/0.9 secondary mirror located at Mount Graham in southern Arizona with MPC code 290 (Kikwaya Eluo and Hergenrother, 2023). The VATT4K CCD camera equipped with a 4064×4064 detector and 15×15 µm pixels was used. The VATT4k covers the visible spectrum (300-1000 nm) with peak quantum efficiency at 450 nm. To reduce the readout time to 30 seconds, data were binned two by two, yielding a plate scale of 0.375 pixels.

For each observing campaign, ~200 bias images and about 10 to 90 images in each filter (B, V, R, and I) were obtained. Using the IRAF packages imred, ccdred, zerocombine, and flatcombine (Tody, 1986; Tody, 1993), a master bias and master flat were made and used to correct the data. Asteroid data were taken with the telescope tracking at the asteroid's rate of motion. Consequently, stars in the field were trailed and not useful for in-field relative photometry. Therefore, on each night, standard stars were observed to compute a photometric zero point and extinction coefficient for each filter (Kikwaya Eluo and Hergenrother, 2023). The IRAF ccdphot, digiphot, and apphot packages were used to produce asteroid and standard star photometry (Hergenrother et al., 2009; Kikwaya Eluo et al., 2016, 2019, 2022). Each object was measured with an aperture set to two times the FWHM (Hergenrother et al., 2009; Kikwaya Eluo et al., 2016, 2019, 2022). The sky background was set to a radius of fifteen pixels and a width of ten pixels.

As we expected the asteroid to be a fast rotator, the filter sequence used for lightcurve and colors is V-R-I-B-V (Hergenrother et al., 2009; Kikwaya Eluo et al., 2016, 2019, 2022). To ensure that the rotation period was covered, we collected several images in V at the beginning of the sequence and then observed in R, I, and B filters. The number of images in the R, I, and B filters was usually equal to one-third of the number of images taken in V. At the end, we again observed a series of images in V. To compute the lightcurve and determine the rotation period of an asteroid, we used *ALC*, Petr Pravec's Asteroid Lightcurve software.

We also used *ALC* to determine the following color indexes: V-R, B-V, and V-I. Two-color plots (B-V versus V-R, and V-I versus V-R) were utilized to estimate the taxonomy of the object (Yoshida et al., 2004; Zellner et al., 1985; Dandy et al., 2002; Dandy et al., 2003). We used spectrophotometry to compute the relative reflectance normalized to V (reflectance at the V-band equal to 1) of each asteroid from its photometric color indexes (Holmberg et al., 2006; Kikwaya Eluo et al., 2016). To refine the taxonomy classification of the asteroid, we proceeded to compare its relative reflectance using the chi-squared method (Popescu et al., 2012; Popescu et al. 2016) with the observed asteroid spectra in the SMASS/SMASSII database as presented by Bus and Binzel (2002a,b). However, our data only covered the visible part of the spectra (Kikwaya Eluo & Hergenrother, 2023). The comparison uses the M4AST (Modeling for Asteroids) engine from the Paris observatory, https://spectre.imcce.fr/m4ast/index.php/index/home.

Table I reports the absolute magnitude and orbital information of each asteroid. Table II contains the results of our observations.

Object	yyyy mm/dd	Phase	Delta (AU)	r (AU)	H	a	e	i	Bpab	Lpab	Grp
2023 LQ1	2023 06/16	42.6	0.008	1.021	27.1	1.849	0.473	3.873	259.162	20.983	Apollo
2023 LT1	2023 06/19	34.6	0.013	1.026	26.9	1.232	0.332	8.249	253.633	11.490	Apollo
2023 MC	2023 06/18	15.9	0.036	1.051	25.7	0.894	0.393	1.679	265.314	8.460	Aten
2023 VQ5	2023 11/11	23.8	0.009	0.999	27.7	0.737	0.356	5.689	60.003	1.387	Aten
2023 VE6	2023 11/11	32.1	0.011	0.999	27.2	0.857	0.225	10.403	57.636	-13.306	Apollo
2023 VF6	2023 11/11	24.9	0.019	1.007	27.2	0.920	0.118	8.993	35.270	2.281	Aten
2023 VV7	2023 11/13	13.6	0.015	1.004	26.7	1.704	0.411	8.388	53.701	5.971	Apollo

Table I: Object name, date of observation, phase angle, delta (distance to the Earth in AU), r (distance to the Sun in AU), absolute magnitude, semi-major axis, eccentricity, inclination, Bpab, Lpab, and Grp (group the object belongs to) are reported.

Object	Period (hours)	Amp(mag)	B-V	V-R	V-I	Tax. Class
2023 LQ1	0.1605+/-0.0002	0.249+/-0.075	0.805+/-0.076	0.433+/-0.091	0.715+/-0.063	X-complex (Q,Xe,Cg)
2023 LT1	0.11620+/-0.00004	0.582+/-0.079	0.754+/-0.077	0.372+/-0.081	0.716+/-0.073	C-complex (Cgh,Cg,C)
2023 MC	-----	-----	0.683+/-0.082	0.383+/-0.072	0.713+/-0.085	C-complex (C,Cgh,Xc)
2023 VQ5	0.07130+/-0.00003	0.176+/-0.072	0.699+/-0.049	0.373+/-0.052	0.788+/-0.055	X-complex (X,Xc,Xk)
2023 VE6	0.12724+/-0.00006	0 516+/-0.070	0.779+/-0.054	0.384+/-0.041	0.650+/-0.054	C-complex (Cgh,Cg,O)
2023 VF6	0.1079+/-0.0002	0.290+/-0.088	0.789+/-0.053	0.366+/-0.058	0.752+/-0.059	C-complex (Cgh,Cg,Xc)
2023 VV7	0.3036+/-0.0004	0.623+/-0.103	0.774+/-0.051	0.536+/-0.049	0.944+/-0.062	S-complex (Sv,L,S)

Table II: Rotation periods of 6 NEAs and colors and taxonomic classes of all 7 NEAs are reported.

2023 LQ1. The Catalina Sky Survey discovered this small, H = 27.1 Apollo asteroid on 2023 June 15. On 2023 June 16, shortly before the asteroid passed 0.0068 au from Earth, we collected 10 B, 64 V, 10 R, and 9 I images to determine its rotation period, colors, and taxonomic class. Its lightcurve yielded a rotation period of 0.1605 ± 0.0002 h with an amplitude of 0.249 ± 0.075 magnitude, confirming fast rotation (Fig. 1). Images taken with the B, R, and I filters were used to compute the color indexes. 2023 LQ1's colors (B-V = 0.805 ± 0.076, V-R = 0.433 ± 0.091, V-I = 0.715 ± 0.063) fall between C-type and S-type, being more consistent with the X-complex (Fig. 14, 15). The comparison of its relative reflectance with the observed asteroid spectra yielded three matches: Q, Xe, and Cg (Bus and Binzel, 2002a, 2002b), with the chi-squared value for Q being less than 0.001 (Fig. 2).

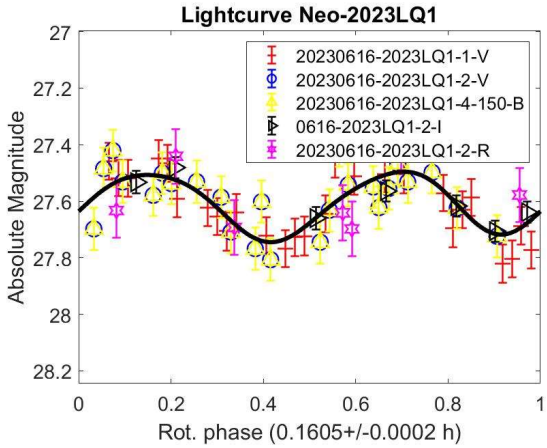

Figure 1. Lightcurve of 2023 LQ1 phased to a period of 0.1605 ± 0.0002 h.

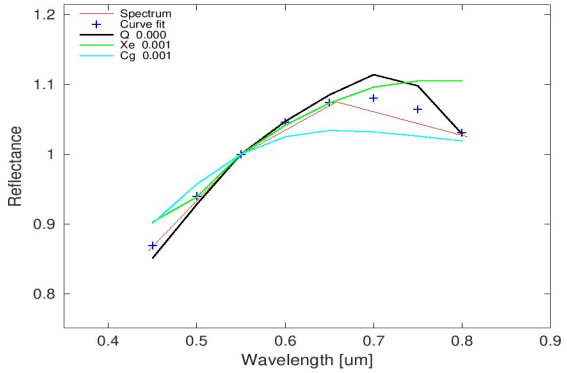

Figure 2. Relative reflectance of 2023 LQ1 compared with SMASS spectra using the chi-squared method (Bus and Binzel, 2002a, 2002b).

2023 LT1. 2023 LT1 is an Apollo asteroid with an absolute magnitude of 26.9. Eighty-four V-band images were obtained on 2023 June 19 UT. The rotation period is 0.11620 ± 0.00004 h with an amplitude of 0.582 ± 0.079 mag, confirming it is a fast rotator (Fig. 3). Images were also obtained in B, R, and I for computing colors: B-V = 0.754 ± 0.077; V-R = 0.372 ± 0.081; and V-I = 0.716 ± 0.073. 2023 LT1 is identified as a C-type from both the two-axis color plots (Fig. 14, 15), and comparison with SMASSI/II asteroid spectra showed a chi-squared value of less than 0.0001 with Cgh, Cg, and C taxonomies (Fig.4).

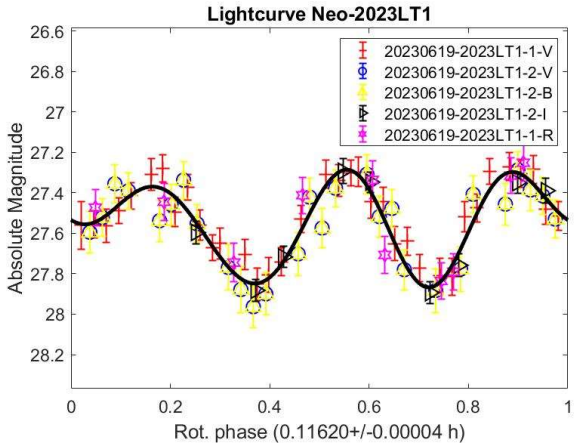

Figure 3. Lightcurve of 2023 LT1 phased to a period of 0.11620 ± 0.00004 h.

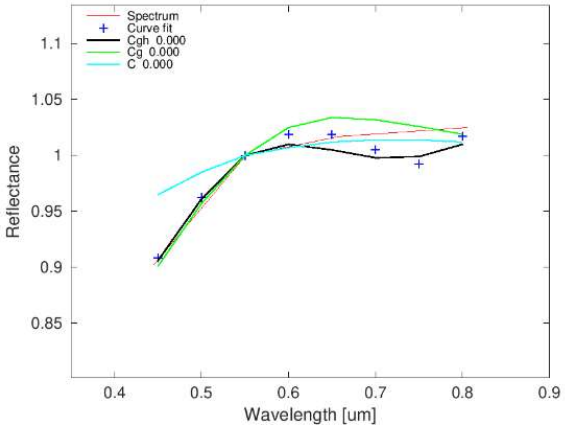

Figure 4. Relative reflectance of 2023 LT1 compared with observed asteroid spectra using the chi-squared method.

2023 MC. 2023 MC is an Aten asteroid with an absolute magnitude of 25.7. Sixty-four images were collected in the V filter to determine the lightcurve of 2023 MC. The lightcurve results were ambiguous, suggesting that 2023 MC may be a slow rotator or a very rapid rotator with a period unresolved by our 60 s exposures. The color indexes were B-V = 0.683 ± 0.082, V-R = 0.383 ± 0.072, and V-I = 0.713 ± 0.085, consistent with 2023 MC being a member of the C-complex (Fig. 14, 15). A C-type taxonomy was confirmed by comparison with SMASSI/II spectra, revealing close matches (Chi-squared value < 0.001) with C and Cgh types (Fig. 5).

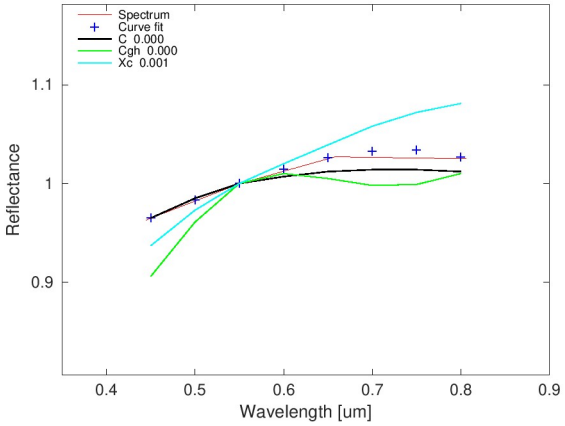

Figure 5. The relative reflectance of 2023 MC matches three taxonomies: C, Cgh, and Xc.

2023 VQ5. 2023 VQ5 is an Aten asteroid with an absolute magnitude of 27.7. We observed three long series in the V filter on November 11 UT: one at the beginning of the color sequence and two at the end for a total of ninety images. The lightcurve shows a rotation period of 0.07130 ± 0.00003 h with a small amplitude of 0.176 ± 0.072 mag (Fig. 6). The object appears to be a rapid rotator. Still, the low amplitude relative to the uncertainty of the individual observations casts doubt as to whether the 0.07130 h solution is correct.

The color indexes of B-V = 0.699 ± 0.049, V-R = 0.373 ± 0.052, and V-I = 0.788 ± 0.055 suggest an X-complex taxonomy for 2023 VQ5 (Fig. 14, 15). This is confirmed by the comparison between the relative reflectance of 2023 VQ5 and the SMASS asteroid spectra (Bus and Binzel, 2002a, 2002b) that yielded three solutions with a chi-squared value of less than 0.001 (X, Xc, and Xk) (Fig. 7).

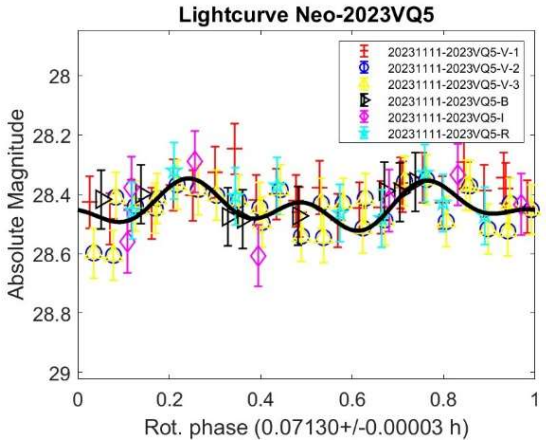

Figure. 6. Lightcurve of 2023 VQ5 phased to a period of 0.07130 ± 0.00003 h.

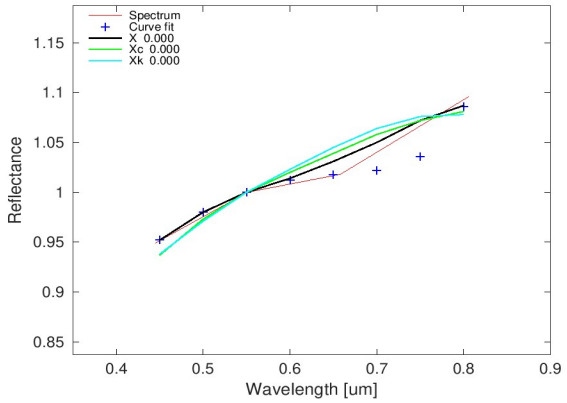

Figure 7. Relative reflectance of 2023 VQ5 compared with observed asteroid spectra using the chi-squared method.

2023 VE6. 2023 VE6 is an Aten asteroid with an absolute magnitude of 27.2. On November 11 UT, V images were obtained to construct a lightcurve of 2023 VE6. It yielded a rotation period of 0.12724 ± 0.00006 h with an amplitude of 0.516 ± 0.070 mag (Fig. 8). We found B-V = 0.779 ± 0.054, V-R = 0.384 ± 0.041, and V-I = 0.650 ± 0.054, showing that 2023 VE6 falls within the C-type taxonomy class according to the two-color plots (Fig. 14, 15). The comparison with observed asteroid spectra using the chi-squared method suggested a possible match between the relative reflectance of 2023 VE6 and asteroid spectra for Cgh, Cg, and O types. Two of these three solutions (Cgh, Cg) are clearly from the C-complex (Fig. 9).

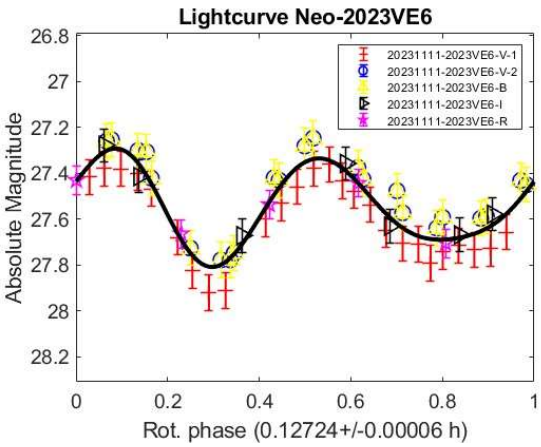

Figure 8. Lightcurve of 2023 VE6 phased to a period of 0.12724 ± 0.00006 h.

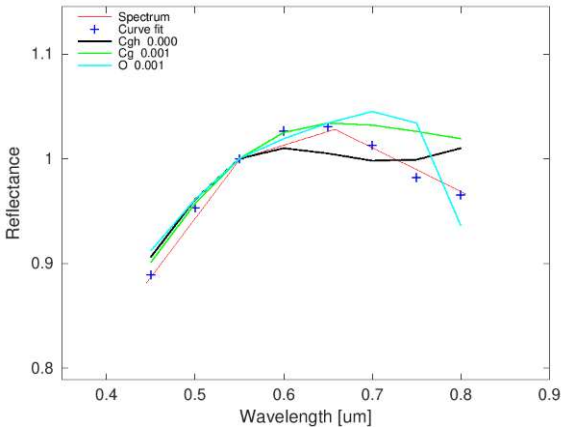

Figure 9. Among the observed spectra matching 2023 VE6 with a chi-squared value less than 0.001 are the Cgh, Cg, and O types (Bus and Binzel, 2002a, 2002b).

2023 VF6. 2023 VE6 is an Apollo asteroid with an absolute magnitude of 27.2. Three sets of V images were obtained on November 11 UT: one at the beginning of the observation sequence (V-R-I-B-V) and two at the end. We used these images to construct the lightcurve of 2023 VF6, yielding a rotation of 0.1079 ± 0.0002 h with an amplitude of 0.290 ± 0.088 mag (Fig. 10). Observations of 2023 VF6 with filters R, B, and I helped to compute its color indexes: B-V = 0.789 ± 0.053, V-R = 0.366 ± 0.058, and V-I = 0.752 ± 0.059. The two-axes-color plots showed that 2023 VF6 belongs to C-type asteroids (Fig. 14, 15), and it was confirmed by the solutions given by comparing the relative reflectance of 2023 VF6 using the chi-squared method with the observed asteroid spectra (Bus and Binzel, 2002a, 2002b). Among the three solutions Cgh, Cg, and Xc which matched the relative reflectance of 2023 VF6 with a chi-squared value less than 0.001, two belong to the C-complex (Fig. 11).

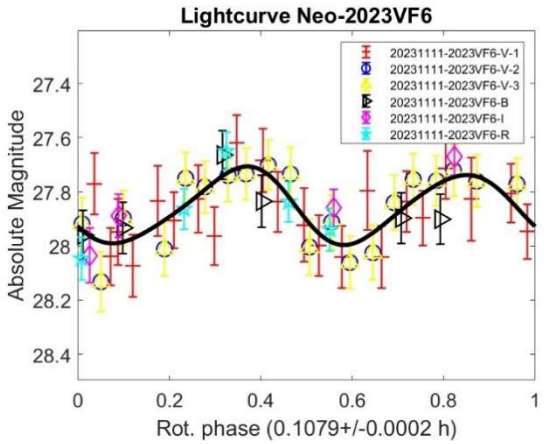

Figure 10. Lightcurve of 2023 2023 VF6 phased to a period of 0.1079 ± 0.0002h

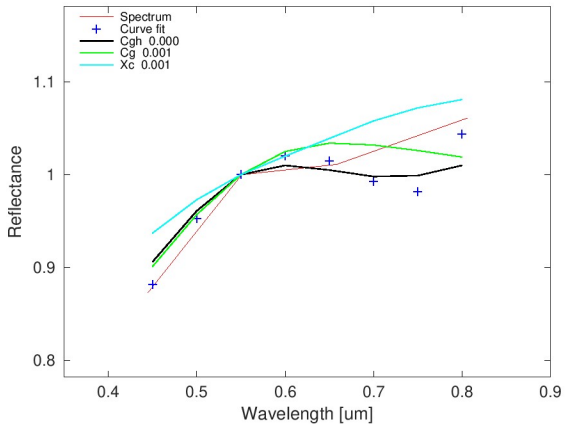

Figure 11. Relative reflectance of 2023 VF6 compared with observed asteroid spectra using the chi-squared method.

2023 VV7. 2023 VV7 is an Apollo asteroid with an absolute magnitude of 26.7. On November 13 UT, we observed 2023 VV7 with a V filter and gathered around 70 images to construct its light curve. The V photometry yielded a rotation period of 0.3036 ± 0.0004 h with an amplitude of 0.623 ± 0.103 mag, confirming that 2023 VV7 is a fast rotator (Fig. 12). Additional images in R, I, and B were obtained to help in computing the color indexes: B-V = 0.774 ± 0.051, V-R = 0.536 ± 0.049, and V-I = 0.944 ± 0.062. The two-axis color plots (B-V versus V-R, V-I versus V-R) show 2023 VV7 falling between S- and D-types, though closer to the S-type than D-type, suggesting that 2023 is more likely a member of the S-type taxonomy class (Fig. 14, 15). This is confirmed by comparing the relative reflectance of 2023 VV7 and the observed asteroid spectra as collected by SMASS and SMASSII (Bus and Binzel, 2002a, 2002b). Three solutions are given (Sv and L with a chi-squared value of 0.001, S with a chi-squared value of 0.002), suggesting that 2023 VV7 belongs to the S-type taxonomy class (Fig. 13).

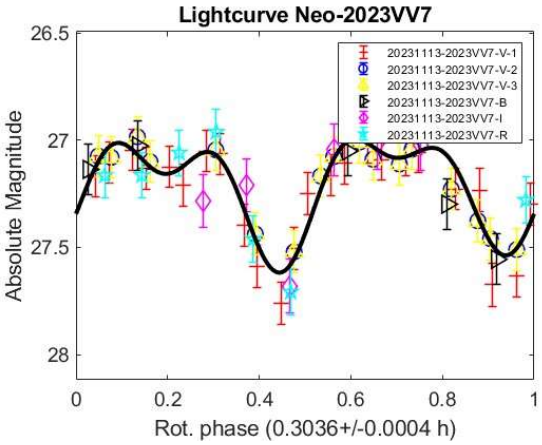

Figure 12. Lightcurve of 2023 VV7 phased to a period of 0.3036 ± 0.0004 h.

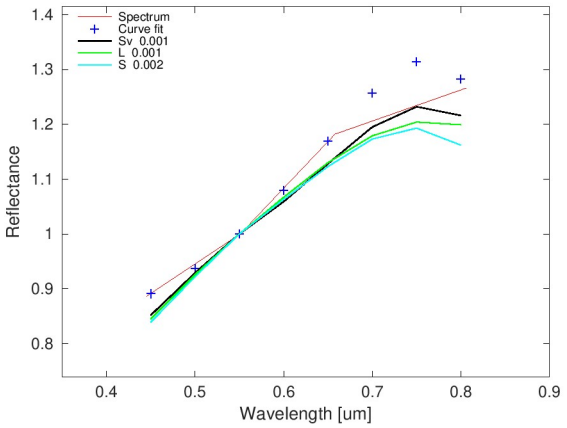

Figure 13. Relative reflectance of 2023 VV7 compared with observed asteroid spectra using the chi-squared method.

Acknowledgments

We want to thank the Vatican Observatory for allowing us to use VATT. We would also like to express our gratitude to Petr Pravec for letting us use ALC software for the lightcurve solution and also for determining the color indexes of our objects.

References

Bus, S.J.; Binzel, R.P. (2002a). "Phase II of the Small Main-Belt Asteroid Spectroscopic Survey. The Observations." *Icarus* **158**, 106-145.

Bus, S.J.; Binzel, R.P. (2002b). "Phase II of the Small Main-Belt Asteroid Spectroscopic Survey: A Feature-Based Taxonomy." *Icarus* **158**, 146-177.

Dandy, C.L.; Fitzsimmons, A.; Collander-Brown, S.J.; Asher, D.; Bailey, M.E. (2002). "Optical Colours of Near-Earth Objects." *Proceedings of Asteroids, Comets, Meteors*, ACM 2002. 915-918.

Dandy, C.L.; Fitzsimmons, A.; Collander-Brown, C.J. (2003). "Optical colors of 56 near-Earth objects: Trends with size and orbit." *Icarus* **163**, 363-373.

Hergenrother, C.W.; Whiteley, R.J.; Christensen, E.J. (2009). "Photometry observations of Five Near-Earth Asteroids: (31221) 1998 BP26, (96315) 1997 AP10, (164184) 2004 BP68, 2006 VV2, and 2006 XY." *Minor Planet Bulletin* **36**, 16-18.

Holmberg, J.; Flynn, C.; Portinari, L. (2006). "The Colours of the Sun." *MNRAS* **367**, 449-453.

Kikwaya Eluo, J.B.; Glimour; C.M.; Fedorets, G.; Boyle, R.P. (2016). "Four-color broadband photometry for physical characterization of fast rotator NEOs." *DPS-EPSC 2016*, id.325.13.

Kikwaya Eluo, J.B.; Hergenrother, C.W.; Boyle, R.P. (2019). "Physical Characterization of Fast Rotating Neos: From Spectroscopy Back to Spectrophotometry." *DPS-EPSC 2019*, 365.

Kikwaya Eluo, J.B.; Hergenrother, C.W.; Boyle, R.P. (2022). "Physical Characterization of 52 Near-Earth Objects with Absolute Magnitudes >22." *BAAS* **54**, 8, e-id 2022n8i514p04.

Kikwaya Eluo, J.B.; Hergenrother, C.W. (2023). "Lightcurves and Colors of Four Small Near-Earth Asteroids: 2020 BV14, 2023 HH3, 2023 HT3, 2023 KQ." *Minor Planet Bulletin* **50**, 300-303.

Popescu, M.; Birlan, M.; Nedelcu., D.A. (2012). "Modeling of Asteroid Spectra - M4AST." *A&A* **544**, A130.

Popescu, M.; Licandro, J.; Morate, D.; de Leon, J.; Nedelcu, D.A; Rebolo, R. (2016). "Near-Infrared Colors of Minor Planets Recovered from VISTA-VHS Survey (MOVIS)." *A&A* **591**, A115.

Tody, D. (1986). "The IRAF Data Reduction and Analysis System." In D.L. Crawford (Ed.), *Proceedings of SPIE Instrumentation in Astronomy VI* (Vol. **627**, p. 733).

Tody, D. (1993). "IRAF in the nineties." In R.J. Hanisch, R.J.V. Brissenden, & J. Barnes (Eds), *Astronomical Data Analysis Software and Systems II*, A.S.P. Conference Series (Vol. **52**, p. 173).

Yoshida, F.; Dernawan, B.; Ito, T.; Sawabe, Y.; Haji, M.; Saito, R. (2004). "Photometric Observations of a Very Young Family-Member Asteroid (832) Karin." *PASJ* **56**, 1105-1113.

Zellner, B.; Tholen, D.J.; Tedesco, E.F. (1985). "The eight-color asteroid survey: Results for 589 minor planets." *Icarus* **61**, 355-416.

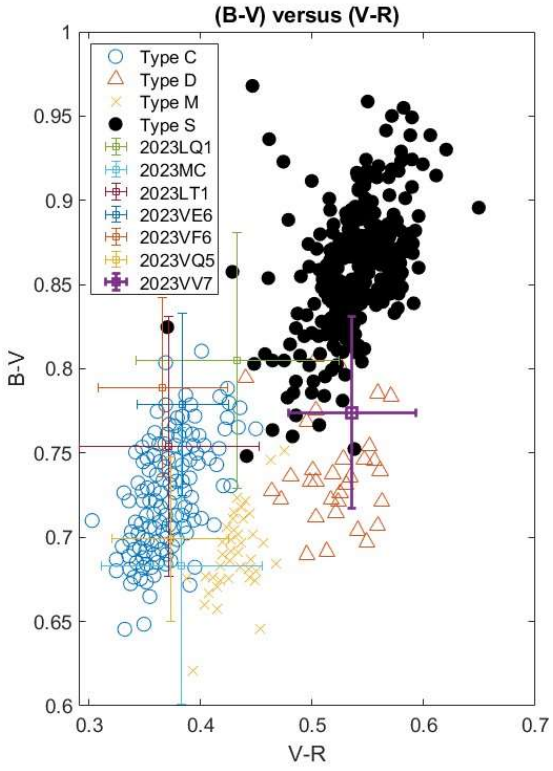

Figure 14. Two-color B-V versus V-R plot for all 7 NEAs.

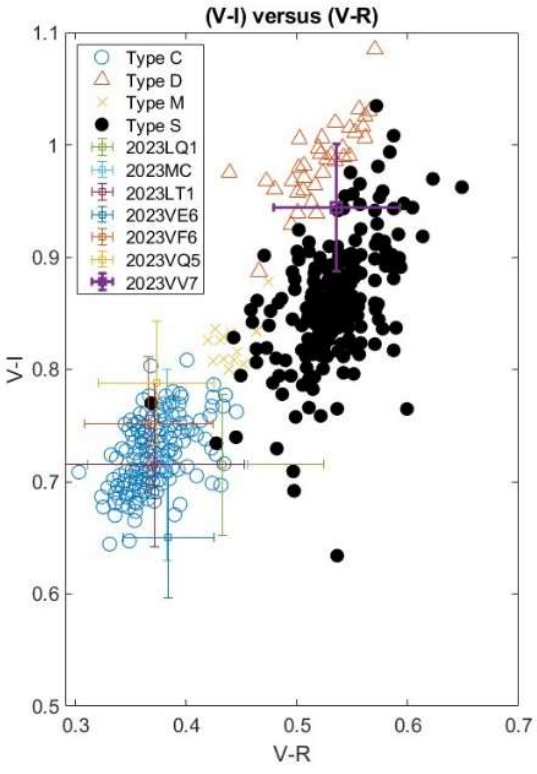

Figure 15. Two-color V-I versus V-R plot for all 7 NEAs.

SATELLITE OF 5457 QUEEN'S DISCOVERY AND CONFIRMATION BY TWO STELLAR OCCULTATIONS

Christian Weber
International Occultation Timing Association/European Section (IOTA/ES)
IOTA/ES e.V., Am Brombeerhag 13, D-30459 Hannover, Germany
camera@iota-es.de

Jan Mánek
Czech Astronomical Society (CAS), IOTA/ES
Ondrejov, Czech Republic

Serge Dramonis
Athens, Greece

Stefan Meister
IOTA/ES
Eglisau, Switzerland

Andreas Schweizer
IOTA/ES
Wettswil am Albis, Switzerland

Daniel Antuszewicz
Legionowo, Poland

Jiří Kubánek
IOTA/ES
Strašice, Czech Republic

Michal Rottenborn
Observatory Rokycany and Pilsen
Pilsen, Czech Republic

(Received: 2023 November 19)

We report the discovery and confirmation of a previously unknown satellite of the main-belt asteroid 5457 Queen's (1980 TW5) via GPS-time-stamped video recordings of two stellar occultations. The first occultation on 2023 September 4.93059 resulted in three positive chords from the Czech Republic and Switzerland for the main body, allowing an elliptical fit of 24.6 ± 0.9 km × 16.2 ± 0.7 km, and in a 2.0 ± 0.2 km chord of the presumed satellite. 15.07 days later, on September 20.00597, the satellite was confirmed by an observer in Greece, who determined a chord of 17.5 ± 0.5 km for the main body and a chord of 2.8 ± 0.5 km for the satellite. Using both satellite chords as diameters of spherical bodies, we derived the following satellite distances from the main body: 2023 September 4.93059: separation 11.4 ± 0.7 mas, p.a. 52.2 ± 3.0°; 2023 September 20.00597: separation 20.4 ± 0.5 mas, p.a. 248.8 ± 3.0°. Further observations are required to derive the orbital parameters. We indicate upcoming occultation events until October 2024.

Observations - Occultation event 2023 September 4

The observations of the two occultation events took place within the framework of the International Occultation Timing Association/European Section (IOTA/ES, 2023) and the results were recorded with its SODIS portal (SODIS, 2023). The details of the first occultation event are given in Figure 1, see also OW Cloud (OWC, 2023), *https://cloud.occultwatcher.net/event/976-5457-7484-648603-U000768*.

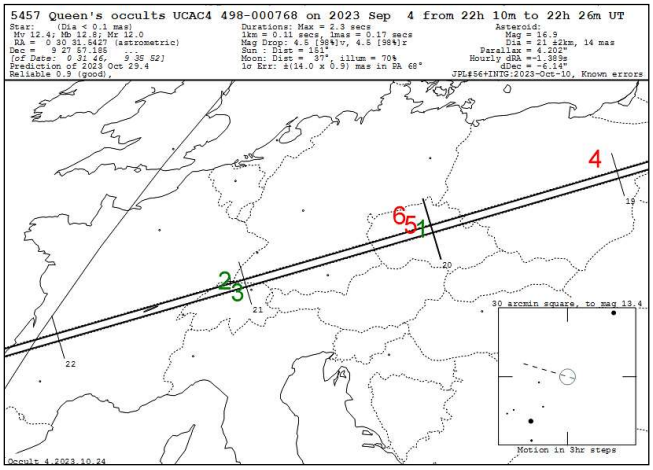

Figure 1: Occultation map (Herald, 2023) of the September 4 event, 1 - 3: stations with a positive result, among them station 1 with a double drop, 4 - 6: stations with negative results. The numbers indicate the locations of the stations only approximately, the exact geographical positions are given in Table III.

Until this event, no stellar occultation chords were known for the asteroid 5457 Queen's (Herald, 2023). Moreover, in the common databases (LCDB, 2023; Johnston, 2023) there are no indications of a possible binary nature of 5457 Queen's. Table I lists data of the asteroid, those of the occulted star are shown in Table II.

Class	Main-belt asteroid
Diameter	21 ± 2 km / 14 mas
Visual magnitude	16.9
Rotation period	4.326 h
Geometric albedo	0.048
Moons / Rings	0 / 0

Table I: Asteroid data for the occultation on 2023 September 4 (Herald, 2023; JPL, 2023).

Identifier	UCAC4 498-000768
Gaia DR3 source ID	2750746718513211520
Estimated diameter (Herald, 2023)	0.02 mas
GCRS position at 2023.6772 (Herald, 2023)	RA 0 30 31.54276 Dec + 9 27 57.18572
GDR3 BPmag	12.76
GDR3 Gmag	12.45
GDR3 RPmag	11.95
GDR3 dup flag	0
GDR3 RUWE	0.85
WDS entry	0
Subject of previous stellar or lunar occultations (Herald, 2023)	0

Table II: Data of the occulted star for the occultation on 2023 September 4.

The occultation was recorded by 6 observers getting 3 positive and 3 negative results. One of the positive recordings (station 1, J. Mánek) shows clearly two consecutive drops reaching the same depth, and indicating a possible satellite (Figure 2). The other two positive detections by the stations 2 and 3 (Figures 3 and 4) gave well positioned chords to derive an elliptical fit of the main body (Figure 9).

Table III summarizes the station details and the occultation results using PyMovie aperture photometry and PyOTE to extract the times (PyMovie/PyOTE, 2023).

Sta-tion	Observer, Lon./Lat./Height [m]	Telescope, Camera	Time	Exp. [s]	Disapp. (UT), first/sec. drop	Reapp. (UT), first/sec. drop	Occ. dur. [s]
1	J. Mánek, CZ, +14 46 47.7/+49 54 36.2/524	0.35-m Newt., DVTI+CAM 430*	GPS	0.100	22:20:00.3436 ± 0.0118 / 22:20:02.8780 ± 0.0156	22:20:02.0092 ± 0.0118 / 22:20:03.0780 ± 0.0156	1.666 / 0.200
2	S. Meister, CH, +8 31 26.4/+47 34 9.2/393	0.20-m Newt., DVTI+CAM 430*	GPS	0.065	22:20:54.737 ± 0.025	22:20:57.141 ± 0.025	2.404
3	A. Schweizer, CH, +8 34 14.3/+47 31 10.4/550	0.50-m Newt., DVTI+CAM 430*	GPS	0.020	22:20:55.268 ± 0.008	22:20:56.177 ± 0.008	0.909
4	D. Antuszewicz, PL, +20 54 9.0/+52 22 57.3/81	0.20-m Newt., ZWO ASI120MM	NTP	0.220	Non detection	Non detection	-
5	J. Kubánek, CZ, +13 44 56.3/+49 44 35.7/538	0.30-m Newt., QHY174GPS	GPS	0.040	Non detection	Non detection	-
6	M. Rottenborn, CZ, +13 44 56.3/+49 44 35.7/538	0.25-m Newt., QHY174GPS	GPS	0.025	Non detection	Non detection	-

Table III: 2023 September 4 observing stations details and derived occultation times. *(DVTI, 2023).

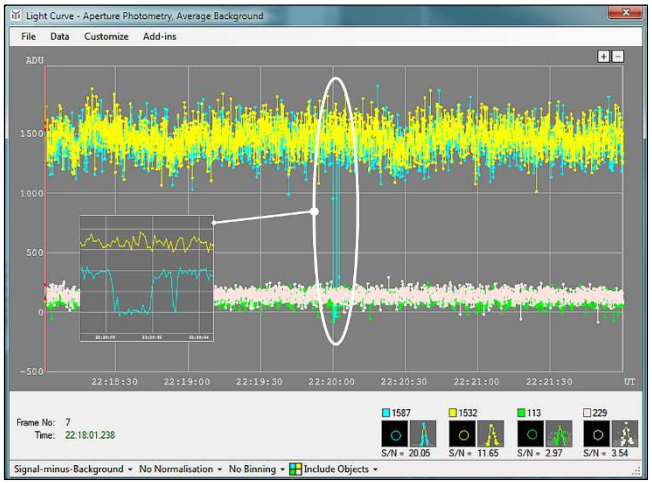

Figure 2: Station 1 Tangra lightcurves (Tangra, 2023), exposure time 100 ms, target star cyan, comparison stars yellow, green and pink.

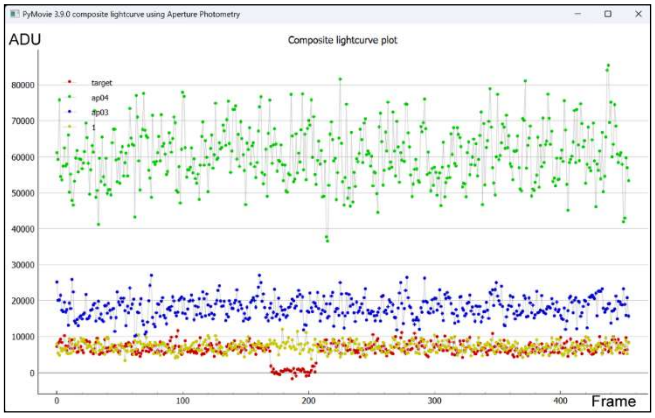

Figure 3: PyOTE lightcurves of the recording of station 2; target lightcurve in red, exposure time 65 ms.

To exclude a possible double star explanation, we determined the limiting magnitude of the recording of station 1. The faintest photometrically analyzable stars are of Gmag 13.84 (GDR3 ID 2750793997513186944) and Gmag 14.92 (GDR3 ID 2750747130830053504).

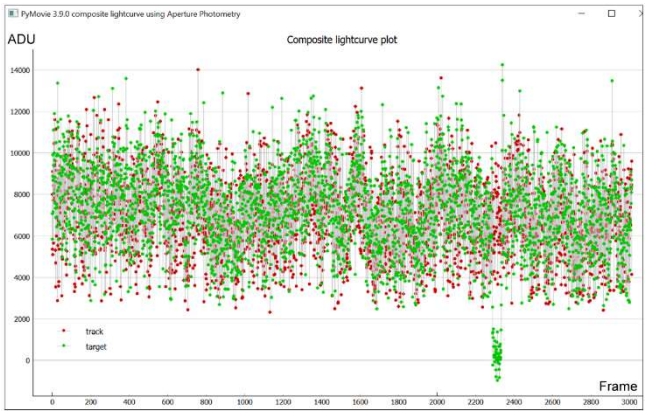

Figure 4: PyOTE lightcurves of the recording of station 3; target star lightcurve in green, exposure time 20 ms.

Figure 5 shows the lightcurves of these stars compared to both occultation drops. For the target star having a Gmag of 12.45, the measured decrease in brightness is more than 2.5 mag, relative to the magnitude of Gmag 14.92 of the faintest comparison star (c4 in Figure 5).

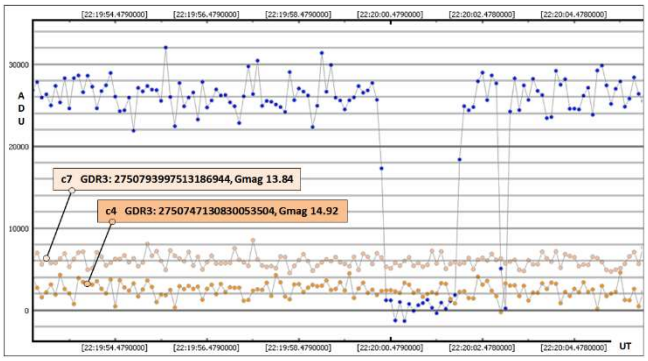

Figure 5: The lightcurves of the faintest comparison stars (c4, c7) and the occultation drops (blue) of the September 4 event.

To be a double star, the occulted star must have components showing a 0.75 mag drop each (components not fainter than 13.20 mag). It can be seen that both drops are of similar depth and fall below the magnitude of the comparison star c4 (Gmag 14.92), excluding a double star hypothesis. By a thorough analysis of all circumstances, we can also rule out the possibility that atmospheric or noise influences are the reason for the secondary drop.

Sta-tion	Observer, Lon./Lat./Height [m]	Telescope, Camera	Time	Exp. [s]	Disapp. (UT), first/sec. drop	Reapp. (UT), first/sec. drop	Occ. dur. [s]
1	S. Dramonis, GR, + 23 33 50.9/+38 37 6.4/342	0.40-m Newt., ZWO ASI183MM	GPS	0.060	00:08:36.0860 ± 0.0376 / 00:08:37.9390 ± 0.0344	00:08:36.3082 ± 0.0376 / 00:08:39.3740 ± 0.0344	0.222 1.435

Table IV: 2023 September 20 observing station details and derived occultation times.

Observations - Occultation event 2023 September 20

Figure 6 shows the shadow path and the parameters of this second occultation event of 5457 Queen's, see also OW Cloud *https://cloud.occultwatcher.net/event/992-5457-5157-648549-U000567*.

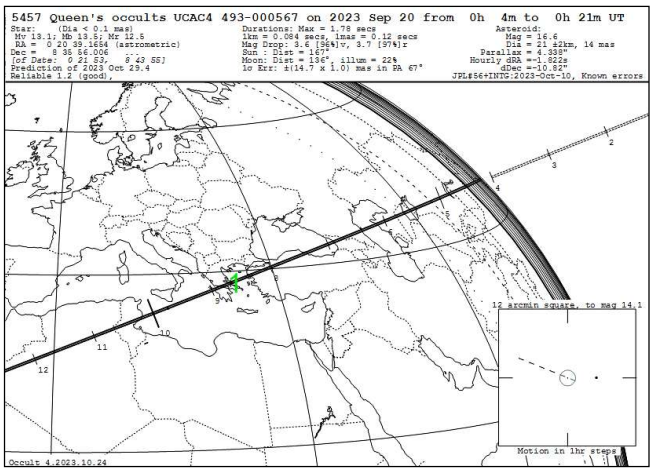

Figure 6: Occult map (Herald, 2023) of the September 20 event, 1 indicates the position of the station that has recorded a double drop.

Except for the slightly changed visual magnitude of the asteroid (16.6), its data for this occultation have not changed compared to those given in Table I for the September 4 occultation. Table V shows the parameters of the target star.

Identifier	UCAC4 493-000567
Gaia DR3 source ID	2749281138232702080
Estimated diameter (Herald, 2023)	0.02 mas
GCRS position at 2023.6772 (Herald, 2023)	RA 0 20 39.16540 Dec + 8 35 56.00643
GDR3 BPmag	13.54
GDR3 Gmag	13.08
GDR3 RPmag	12.46
GDR3 dup flag	0
GDR3 RUWE	1.2
WDS entry	0
Subject of previous stellar or lunar occultations (Herald, 2023)	0

Table V: Occulted star data for the occultation event on 2023 September 20.

As can be seen in Figure 6, only the station of S. Dramonis, Greece, observed this event. Figure 7 presents the lightcurve, showing a short drop (satellite) followed by the main body drop.

Figure 7: Station 1 Tangra lightcurves, exposure time 60 ms, target star cyan.

Table IV summarizes the station details and the occultation times, derived with PyMovie/PyOTE.

We also examined the limiting magnitude for this recording (Figure 8). Assuming the target star with a magnitude of Gmag 13.08 was a double star with the same magnitudes of both components, they would each require a magnitude of 13.83 mag. As can be seen from Figure 8, the magnitude of both drops of similar depths is at minimum light lower than that of the comparison star c5 (GDR3 source ID 2749274712961627520, Gmag 14.21). So, a double star can be ruled out. We also rule out that atmospheric effects or noise can be the cause of the secondary drop. The satellite's light fall-off comprises three images of nearly equal depth, which is not consistent with a noise event.

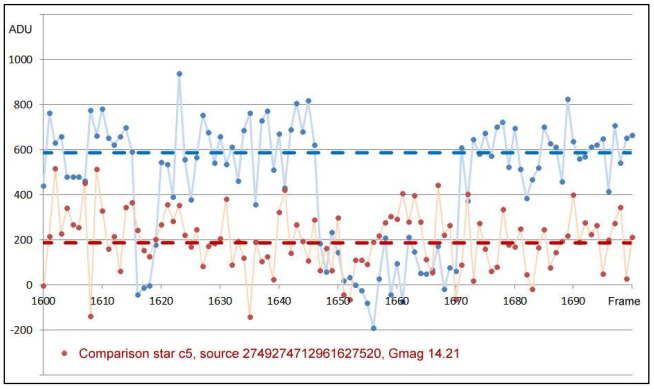

Figure 8: Part of the station 1 recording showing the target star (blue) and the faintest comparison star c5 (red brown). The dotted lines indicate the average light levels.

Reduction of the observations

We reduced both observations with the *Asteroid Observations Editor*, being part of Occult (Herald, 2023).

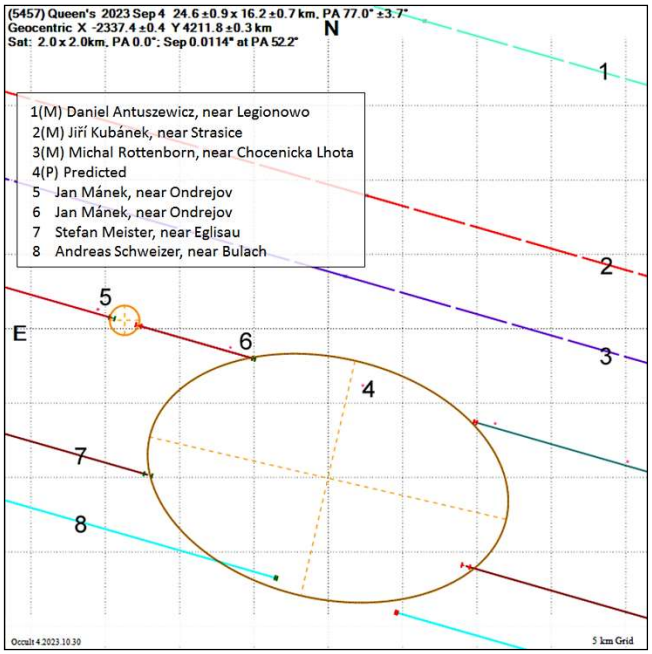

Figure 9: Occultation sky-plane plot of the September 4 event. The chord numbers do not correspond to the station numbers. In the positive chords 5 - 8, the red markings mean D (disappearance), the green ones R (reappearance). The error bars are mostly too small to be seen on the picture.

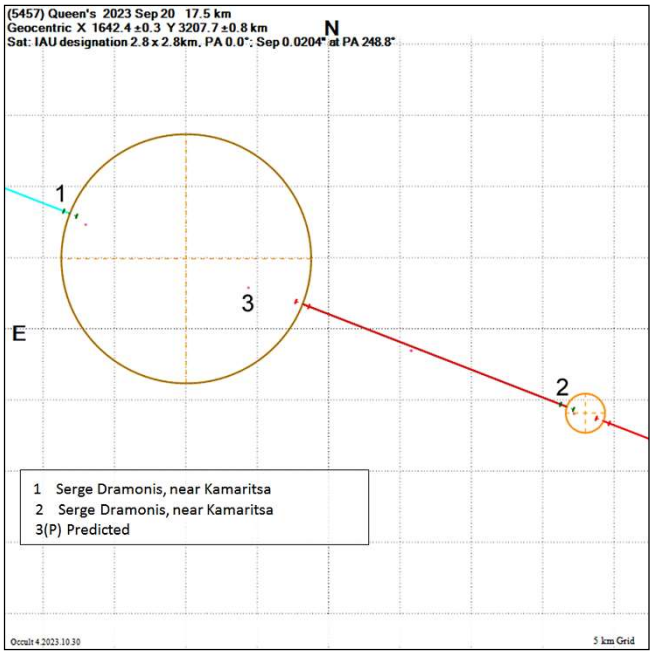

Figure 10: Occultation sky-plane plot of the September 20 event. The red marks stand for D, the green for R. The marks also show the uncertainties.

Figure 9 presents the plot of the September 4 occultation. We were able to fit the main body through an ellipse, giving the first fair shape of the asteroid (24.6 ± 0.9 km × 16.2 ± 0.7 km; p.a. 77.0 ± 3.7°). This is in rough agreement with the NEOWISE thermal diameter of 20.6 ± 2.2 km (Herald, 2023); the AKARI Acura data fit slightly better at 22.3 ± 3.4 km (Herald, 2023). Having only one chord for the satellite, we assumed a spherical shape, resulting in a diameter of 2.0 ± 0.2 km.

Figure 10 shows the reduction of the September 20 event. In this historically only second successfully observed stellar occultation by 5457 Queen's, one chord was achieved due to a single observation station. As a result, we fit the primary and secondary bodies into circles, whereby the chord of the main body with a length of 17.5 ± 0.5 km does not contradict the elliptical fit from the September 4 event. However, as there is only one chord, it is not possible to use the elliptical fit from 4 September here. The resulting diameter of the satellite is 2.8 ± 0.5 km.

Using the Asteroid Observations Editor and the diameters of the satellites derived from both occultation events, we calculate the following satellite positions relative to the main body:

2023 Sep 04.93059: separation 11.4 ± 0.7 mas, p.a. 52.2 ± 3.0°
2023 Sep 20.00597: separation 20.4 ± 0.5 mas, p.a. 248.8 ± 3.0°.

5457 Queen's system
Center of mass, orbit and upcoming occultation events

Based on the data obtained from the two occultations, the center of mass of the system will not differ significantly from the center of mass of the main body. It is therefore unlikely that wobbling effects of the photo center can be detected from current data (Gaia).

During the occultation on 20 September, 15.07 d after the first occultation, the satellite was on the opposite side of the main body. One could therefore speculate about a possible orbital period of the satellite of around 30 days. However, the period could also be a fraction of 30 days.

Our results from two occultation events do not allow to derive the orbital parameters, further observations are required.

To indicate upcoming occultation events of 5457 Queen's, Occult was used for a global search until 2024 October 31 (search parameters: JPL orbit solution #56, JPL ephemerides, Gaia EDR3 down to 16 mag). We found 116 potential occultation events. The preferred ones (most of them in America in August and September 2024) are listed in Table VI.

The observations of 2023 September 4 and September 20 are subject of CBET 5318 (CBET, 2023).

Date	UT	Region	Duration [s]	Star Vmag [mag]	Drop [mag]	UCAC4
2023 Dec 23	14:21	Indonesia	1.36	14.7	3.3	475-000153
2023 Dec 26	15:30	South Asia	1.25	14.9	3.1	476-000207
2024 Jul 24	10:42	South America	0.58	14.4	4.0	571-013135
2024 Aug 02	03:45	Great Britain	0.62	14.6	3.8	573-014688
2024 Aug 08	08:05	South America	0.65	16.0	2.5	573-016037
2024 Aug 14	22:35	Indonesia	0.70	15.7	2.7	574-016038
2024 Aug 17	21:01	USA	0.72	15.3	3.1	574-016357
2024 Aug 19	07:58	South America	0.73	15.8	2.6	574-016525
2024 Aug 23	09:55	Guatemala	0.76	15.2	3.2	574-017177
2024 Aug 31	11:27	USA	0.86	12.1	6.2	574-018794
2024 Sep 05	08:21	USA	0.92	14.8	3.5	574-019912
2024 Sep 10	11:19	USA	1.00	12.7	5.5	574-020981
2024 Sep 11	01:43	France - Latvia	1.02	15.5	2.8	574-021122
2024 Sep 13	12:07	Mexico	1.06	14.7	3.5	574-021713
2024 Sep 14	04:12	Great Britain	1.08	13.2	4.9	574-021839
2024 Sep 14	05:33	Portugal - Spain	1.08	13.7	4.5	574-021847
2024 Sep 15	09:15	Canada	1.11	12.5	5.6	* G060009.5 +244120
2024 Sep 30	07:30	Mexico, USA	1.64	15.7	2.4	573-026064
2024 Oct 04	18:40	Mexico, USA	1.93	15.7	2.4	573-026695
2024 Oct 07	06:05	Guatemala	2.10	15.9	2.2	573-026974
2024 Oct 14	17:48	Japan	3.20	14.3	3.5	573-027632

Table VI: Preferred 5457 Queen's upcoming occultation events from an Occult search until 2024 October 31 (search parameters: JPL orbit solution #56, JPL ephemerides, Gaia EDR3 to 16 mag); * Gaia RA/Dec coordinates.

Acknowledgements

We thank the maintainers of the Occult Watcher Cloud prediction feeds (J. Kubánek, CentralEurope feed; C. Perelló, IBEROC feed) who predicted the occultation events, and the SODIS team for managing the observation reports. We would like to thank D. Herald and D. Gault (both Trans-Tasman Occultation Alliance) for an independent assessment of our data. We acknowledge the developers of the software used in this work, especially D. Herald (Occult), B. Anderson (PyMovie, PyOTE) and H. Pavlov (Tangra). This work has made use of data from the European Space Agency (ESA) mission Gaia (*https://www.cosmos.esa.int/gaia*), processed by the Gaia Data Processing and Analysis Consortium (DPAC, *https://www.cosmos.esa.int/web/gaia/dpac/consortium*). Funding for the DPAC has been provided by national institutions, in particular the institutions participating in the Gaia Multilateral Agreement. This research has made use of the Washington Double Star Catalog maintained at the U.S. Naval Observatory.

References

CBET (2023). Central Bureau for Astronomical Telegrams. CBET 5318 web site. *http://www.cbat.eps.harvard.edu/iau/cbet/005300/CBET005318.txt*

DVTI (2023). DVTI+CAM web site. *https://dvticam.com/home*

Herald (2023). Herald, D. Occult4 web site. *http://www.lunar-occultations.com/iota/occult4.htm*

IOTA/ES (2023). International Occultation Timing Association / European Section web site. *https://iota-es.de/index.html*

Johnston (2023). Asteroids with satellites web site. *https://www.johnstonsarchive.net/astro/asteroidmoons.html*

JPL (2023). Small-Body Database Browser web site. *https://ssd.jpl.nasa.gov/tools/sbdb_lookup.html*

LCDB (2023). Warner, B.D.; Harris, A.W.; Pravec, P. (2009). "The Asteroid Lightcurve Database." *Icarus* **202**, 134-146. Updated 2023 August 8. *https://alcdef.org/index.php*

OWC (2023). Pavlov, H. Occult Watcher Cloud web site. *https://cloud.occultwatcher.net*

PyMovie/PyOTE (2023). Anderson, B. PyMovie/PyOTE web site. *http://occultations.org/observing/software/pymovie/*

SODIS (2023). Stellar Occultation Data Input System web site. *https://sodis.iota-es.de/*

Tangra (2023). Pavlov, H. Tangra web site. *http://www.hristopavlov.net/Tangra3/*

LIGHTCURVE PHOTOMETRY OPPORTUNITIES: 2024 APRIL-JUNE

Brian D. Warner
Center for Solar System Studies (CS3)
446 Sycamore Ave.
Eaton, CO 80615 USA
brian@MinPlanObs.org

Alan W. Harris
Center for Solar System Studies (CS3)
La Cañada, CA 91011-3364 USA

Josef Ďurech
Astronomical Institute
Charles University
18000 Prague, CZECH REPUBLIC
durech@sirrah.troja.mff.cuni.cz

Lance A.M. Benner
Jet Propulsion Laboratory
Pasadena, CA 91109-8099 USA
lance.benner@jpl.nasa.gov

We present lists of asteroid photometry opportunities for objects reaching a favorable apparition and have no or poorly-defined lightcurve parameters. Additional data on these objects will help with shape and spin axis modeling using lightcurve inversion. The "Radar-Optical Opportunities" section includes only near-Earth asteroids, some of which are planned radar targets.

We present several lists of asteroids that are prime targets for photometry and/or astrometry during the period 2024 April-June. The "Radar-Optical Opportunities" section provides an expanded list of potential NEA targets, many of which are planned or good candidates for radar observations.

In the first three sets of tables, "Dec" is the declination and "U" is the quality code of the lightcurve. See the latest asteroid lightcurve data base (LCDB from here on; Warner et al., 2009) documentation for an explanation of the U code:

http://www.minorplanet.info/lightcurvedatabase.html

The ephemeris generator on the MinorPlanet.info web site allows creating custom lists for objects reaching V ≤ 18.0 during any month in the current year and up to five years in the future, e.g., limiting the results by magnitude and declination, family, and more.

https://www.minorplanet.info/php/callopplcdbquery.php

We refer you to past articles, e.g., Warner et al. (2021a; 2021b) for more detailed discussions about the individual lists and points of advice regarding observations for objects in each list.

Once you've obtained and analyzed your data, it's important to publish your results. Papers appearing in the *Minor Planet Bulletin* are indexed in the Astrophysical Data System (ADS) and so can be referenced by others in subsequent papers. It's also important to make the data available at least on a personal website or upon request. We urge you to consider submitting your raw data to the ALCDEF database. This can be accessed for uploading and downloading data at

http://www.alcdef.org

The database contains about 10.59 million observations for 24,353 objects (as of 2024 January 6), making it one of the more useful sources for raw data of *dense* time-series asteroid photometry.

Lightcurve/Photometry Opportunities

Objects with U = 3- or 3 are excluded from this list since they will likely appear in the list for shape and spin axis modeling. Those asteroids rated U = 1 or have only a lower limit on the period, should be given higher priority over those rated U = 2 or 2+. On the other hand, do not overlook asteroids with U = 2/2+ on the assumption that the period is sufficiently established. Regardless, do not let the existing period influence your analysis since even highly-rated results have been proven wrong at times. Note that the lightcurve amplitude in the tables could be more or less than what's given. Use the listing only as a guide.

All objects are reaching one of their five brighter apparitions from 1995-2050. Bold text, if any, indicates a near-Earth asteroid (NEA). A period followed by an asterisk is sidereal.

		Brightest			LCDB Data		
Number	Name	Date	Mag	Dec	Period	Amp	U
470	Kilia	04 06.6	12.4	-2	296.2	0.15-0.40	2+
2383	Bradley	04 12.5	14.8	-10	5.823	0.67	2
5222	Ioffe	04 20.4	14.6	-23	9.72	0.18-0.28	2+
1238	Predappia	04 22.4	15.2	-6	8.94	0.03	2-
2830	Greenwich	04 23.5	14.4	+4	80.068	0.34	2
3091	van den Heuvel	04 23.5	15.4	-14	30.9	0.30	2-
3735	Trebon	04 26.8	15.5	-22	8.471	0.55	2
4733	ORO	04 27.7	15.5	-13	5.88	0.46-0.47	2
3747	Belinskij	05 07.4	15.4	-23	14.6	0.08	2
1199	Geldonia	05 14.9	14.2	-19	57.939	0.11-0.20	2
4091	Lowe	05 16.4	15.3	-21	16.59	0.10-0.11	2
1354	Botha	05 16.9	14.3	-24	8.379	0.11	2+
1145	Robelmonte	05 19.8	13.7	-31	8.002	0.13-0.18	2
13351	Zibeline	05 20.0	15.4	-12	6.8	0.06	2-
21374	**1997 WS22**	**05 20.2**	**13.4**	**-15**	**3.405**	**0.07-0.17**	**2**
6012	Williammurdoch	05 22.4	15.2	-20	2.89	0.18	2
7238	Kobori	05 25.2	15.3	-21	17.224*		2
926	Imhilde	05 26.1	13.7	-29	25.977	0.27-0.31	2+
13361	1998 UM8	05 28.8	15.4	-17	15.231	0.08	2
10422	1999 AN22	06 03.9	14.9	-26	35.157	0.43-0.50	2+
3023	Heard	06 06.8	15.5	-19	2.713	0.14	2
4428	Khotinok	06 10.3	14.6	-22	101.326*		2
18187	2000 QQ53	06 11.3	15.5	-23	67.104*		2
3413	Andriana	06 16.5	15.3	-31	11.2	0.11	2-
2554	Skiff	06 16.7	14.5	-29	273	0.9	2
3638	Davis	06 18.8	15.4	-17	8.9	0.40	2
1032	Pafuri	06 21.5	13.6	-27	113	0.14-0.51	2+
6271	Farmer	06 24.3	15.2	-37	250	0.13-0.22	2
10487	Danpeterson	06 28.2	14.1	-21	16.91	0.11	2
415029	**2011 UL21**	**06 29.2**	**11.7**	**-16**	**2.732**	**0.32**	**2+**

Low Phase Angle Opportunities

The Low Phase Angle list includes asteroids that reach very low phase angles ($\alpha < 1°$). The "α" column is the minimum solar phase angle for the asteroid. Getting accurate, calibrated measurements (usually V band) at or very near the day of opposition can provide important information for those studying the "opposition effect." Use the on-line query form for the LCDB to get more details about a specific asteroid.

https://www.minorplanet.info/php/callopplcdbquery.php

The best chance of success comes with covering at least half a cycle a night, meaning periods generally < 16 h, when working objects with low amplitude. Objects with large amplitudes and/or long periods are much more difficult for phase angle studies since, for proper analysis, the data must be reduced to the average magnitude of the asteroid for each night. Refer to Harris et al. (1989) for the details of the analysis procedure.

As an aside, it is arguably better for physical interpretation (e.g., *G* value versus albedo) to use the maximum light rather than mean level to find the phase slope parameter (*G*), which better models the behavior of a spherical object of the same albedo, but it can produce significantly different values for both *H* and *G* versus using average light, which is the method used for values listed by the Minor Planet Center. Using and reporting the results of both methods can provide additional insights into the physical properties of an asteroid.

The International Astronomical Union (IAU) has adopted a new system, H-G_{12}, introduced by Muinonen et al. (2010). It will be some years before H-G_{12} becomes widely used, and hopefully not until a discontinuity flaw in the G_{12} function has been fixed. This discontinuity results in false "clusters" or "holes" in the solution density and makes it impossible to draw accurate conclusions.

We strongly encourage obtaining data as close to 0° as possible and then every 1-2° out to 7°. It's in this range the phase curve is non-linear because of the opposition effect. From 7° out to about 30°, when the curve tends to be linear, observations at 3-6° intervals should be sufficient. Coverage beyond 50° or so is not generally helpful since the H-G system is best defined with data from 0-30°.

It's important to emphasize that all observations should (must) be made using high-quality catalogs to set the comparison star magnitudes. These include ATLAS, Pan-STARRS, SkyMapper, and Gaia2/3. Catalogs such as CMC-15, APASS, or the MPOSC from *MPO Canopus* have too high systematic errors.

Also important is that there are sufficient data from each observing run such that their location can be found on a combined, phased lightcurve derived from two or more nights obtained *near the same phase angle.* If necessary, the magnitudes for a given run should be adjusted so that they correspond to mid-light of the combined lightcurve. This goes back to the H-G system being based on average, not maximum or minimum light.

The asteroid magnitudes are brighter than in others lists because higher precision is required and the asteroid may be a full magnitude or fainter when it reaches phase angles out to 20-30°. The list includes objects that reach V ≤ 14.0 at opposition. Including fainter objects may be necessary if the list becomes too short.

Num	Name	Date	α	V	Dec	Period	Amp	U
359	Georgia	04 01.5	0.35	13.5	-6	5.537	0.14-0.54	3
615	Roswitha	04 04.5	0.19	13.2	-6	4.422	0.11	3
477	Italia	04 07.2	0.39	13.7	-8	19.413	0.15-0.32	3
796	Sarita	04 21.9	0.20	13.6	-12	8.1755	0.27-0.33	3
2063	Bacchus	04 23.2	0.44	14.0	-13	14.904	0.22-0.42	3
106	Dione	04 23.8	0.81	12.8	-10	16.210	0.08-0.18	3
50	Virginia	04 24.3	0.81	13.9	-10	14.315	0.07-0.20	3
551	Ortrud	04 24.6	0.15	14.0	-13	17.416	0.14-0.19	3
494	Virtus	04 25.1	0.21	12.8	-13	5.57	0.03-0.12	2
793	Arizona	04 27.7	0.26	14.0	-15	7.399	0.22-0.25	3
570	Kythera	05 01.2	0.09	14.0	-15	8.117	0.09-0.20	3
147	Protogeneia	05 02.7	0.40	13.1	-17	7.853	0.25-0.28	3
27	Euterpe	05 05.5	0.78	10.3	-15	10.408	0.10-0.21	3
310	Margarita	05 09.0	0.03	13.0	-17	12.070	0.14-0.37	3
712	Boliviana	05 10.2	0.14	12.7	-18	11.743	0.10-0.20	3
64	Angelina	05 15.5	0.75	11.2	-21	8.752	0.04-0.42	3
640	Brambilla	05 18.9	0.41	13.1	-19	7.768	0.25-0.31	3
49	Pales	05 21.9	0.84	13.1	-23	20.705	0.17-0.19	3
352	Gisela	05 22.8	0.25	13.0	-21	7.490	0.08-0.70	3
379	Huenna	05 23.6	0.72	13.5	-18	14.141	0.07-0.22	3
311	Claudia	05 24.6	0.52	13.8	-19	7.532	0.16-0.89	3
62	Erato	05 24.7	0.77	13.8	-18	9.221	0.12-0.28	3
940	Kordula	05 24.9	0.12	14.0	-21	15.57	0.36	3
396	Aeolia	05 29.2	0.15	12.6	-22	14.353	0.10-0.36	3
179	Klytaemnestra	06 03.0	0.05	12.1	-22	11.173	0.07-0.55	3
586	Thekla	06 06.2	0.36	13.7	-22	13.670	0.24-0.30	3
449	Hamburga	06 07.2	0.30	13.3	-22	36.516	0.06-0.17	3
1197	Rhodesia	06 09.7	0.48	13.6	-22	16.060	0.22-0.32	3-
683	Lanzia	06 15.1	0.77	12.9	-21	8.630	0.12-0.20	3
974	Lioba	06 18.0	0.03	13.7	-23	38.7	0.37	3

Shape/Spin Modeling Opportunities

Those doing work for modeling should contact Josef Ďurech at the email address above. If looking to add lightcurves for objects with existing models, visit the Database of Asteroid Models from Inversion Techniques (DAMIT) web site.

https://astro.troja.mff.cuni.cz/projects/damit/

Additional lightcurves could lead to the asteroid being added to or improving one in DAMIT, thus increasing the total number of asteroids with spin axis and shape models.

Included in the list below are objects that:

1. Are rated U = 3– or 3 in the LCDB.
2. Do not have reported pole in the LCDB Summary table.
3. Have at least three entries in the Details table of the LCDB where the lightcurve is rated U ≥ 2.

The caveat for condition #3 is that no check was made to see if the lightcurves are from the same apparition or if the phase angle bisector longitudes differ significantly from the upcoming apparition. The last check is often not possible because the LCDB does not list the approximate date of observations for all details records. Including that information is an on-going project.

With the wide use of sparse data from the surveys for modeling that produces hundreds of statistically valid poles and shapes, the need for data for main-belt objects is not what it used to be. The best use of observing time might be to concentrate on near-Earth asteroids, or on asteroids where the only period was derived from sparse data, which can help eliminate alias periods.

The latter targets are usually flagged with an 'S' on the LCDB summary line. Regardless, it's a good idea to visit the DAMIT site and see what it has, if anything, on the target(s) you've picked for observations.

All objects are at a favorable apparition. If any, those in italic text are near-Earth objects.

		Brightest			LCDB Data		
Num	Name	Date	Mag	Dec	Period	Amp	U
2074	Shoemaker	04 17.0	15.3	-11	2.533	0.06-0.13	3
2047	Smetana	04 24.0	15.4	-10	2.497	0.12-0.16	3
494	Virtus	04 25.1	12.8	-13	40.42	0.03-0.21	3
3309	Brorfelde	04 26.4	14.6	-20	2.504	0.09-0.23	3
2883	Barabashov	04 30.0	15.1	-14	2.684	0.04-0.08	3
5515	Naderi	04 30.2	15.5	+3	5.23	0.37-0.58	3
2276	Warck	05 03.0	14.9	-15	4.054	0.20-0.25	3
10997	Gahm	05 14.5	15.9	-30	3.209	0.50-0.58	3-
1593	Fagnes	05 31.7	14.6	-3	25.25	0.24-0.47	3-
3800	Karayusuf	06 07.4	15.2	-6	2.232	0.10-0.19	3
3637	O'Meara	06 08.9	14.6	-3	5.751	0.11-0.25	3-

Radar-Optical Opportunities

Table I below gives a list of near-Earth asteroids reaching maximum brightness for the current quarter-year based on calculations by Warner. We switched to this presentation in lieu of ephemerides for reasons outlined in the 2021 October-December opportunities paper (Warner et al., 2021b), which centered on the potential problems with ephemerides generated several months before publication.

The initial list of targets started using the planning tool at

https://www.minorplanet.info/php/callopplcdbquery.php

where the search was limited to near-Earth asteroids only that were V ≤ 18 for at least part of the quarter.

The final step was to cross-reference our list with that found on the Goldstone planned targets schedule at

http://echo.jpl.nasa.gov/asteroids/goldstone_asteroid_schedule.html

In Table I, objects in bold text are on the Goldstone proposed observing list as of 2024 January and often need supplemental astrometry and/photometry

It's important to note that the final list in Table I is based on *known* targets and orbital elements when it was prepared. It is common for newly discovered objects to move in or out of the list. We recommend that you keep up with the latest discoveries by using the Minor Planet Center observing tools.

In particular, monitor NEAs and be flexible with your observing program. In some cases, you may have only 1-3 days when the asteroid is within reach of your equipment. Be sure to keep in touch with the radar team (through Benner's email or their Facebook or Twitter accounts) if you get data. The team may not always be observing the target but your initial results may change their plans. In all cases, your efforts are greatly appreciated.

For observation planning, use these two sites

MPC: *http://www.minorplanetcenter.net/iau/MPEph/MPEph.html*
JPL: *http://ssd.jpl.nasa.gov/?horizons*

Cross-check the ephemerides from the two sites just in case there is discrepancy that might have you imaging an empty sky.

About YORP Acceleration

Near-Earth asteroids are particularly sensitive to YORP acceleration. YORP (Yarkovsky-O'Keefe-Radzievskii-Paddack; Rubincam, 2000) is the asymmetric thermal re-radiation of sunlight that can cause an asteroid's rotation period to increase or decrease. High precision lightcurves at multiple apparitions can be used to model the asteroid's *sidereal* rotation period and see if it's changing.

It usually takes four apparitions to have sufficient data to determine if the asteroid rotation rate is changing under the influence of YORP. This is why observing an asteroid that already has a well-known period remains a valuable use of telescope time. It is even more so when considering the BYORP (binary-YORP) effect among binary asteroids that has stabilized the spin so that acceleration of the primary body is not the same as if it would be if there were no satellite.

The Quarterly Target List Table

The Table I columns are

Num	Asteroid number, if any.
Name	Name assigned by the MPC.
H	Absolute magnitude from MPCOrb.
Dkm	Diameter (km) assuming $p_V = 0.2$.
Date	Date (mm dd.d) of brightest magnitude.
V	Approximate V magnitude at brightest.
Dec	Approximate declination at brightest.
Period	Synodic rotation period from summary line in the LCDB summary table.
Amp	Amplitude range (or single value) of reported lightcurves.
U	LCDB solution quality (U) from 1 (probably wrong) to 3 (secure).
Notes	Comments about the object.

"PHA" is a potentially hazardous asteroid. NHATS is for "Near-Earth Object Human Space Flight Accessible Targets Study." Presume that that astrometry and photometry have been requested to support Goldstone observations. The sources for the rotation period are given in the Notes column. If none are qualified with a specific period, then the periods from multiple sources were in general agreement. Higher priority should be given to those where the current apparition is the last one V ≤ 18 through 2050 or several years to come.

References

Dumitru, B.A.; Birlan, M.; Sonka, A.; Colas, F.; Nedelcu, D.A. (2018). "Photometry of asteroids (5141), (43032), (85953), (259221), and (363599) observed at Pic du Midi Observatory." *Astron. Nach.* **339**, 198-203.

Harris, A.W.; Young, J.W.; Bowell, E.; Martin, L.J.; Millis, R.L.; Poutanen, M.; Scaltriti, F.; Zappala, V.; Schober, H.J.; Debehogne, H.; Zeigler, K.W. (1989). "Photoelectric Observations of Asteroids 3, 24, 60, 261, and 863." *Icarus* **77**, 171-186.

Muinonen, K.; Belskaya, I.N.; Cellino, A.; Delbò, M.; Levasseur-Regourd, A.-C.; Penttilä, A.; Tedesco, E.F. (2010). "A three-parameter magnitude phase function for asteroids." *Icarus* **209**, 542-555.

Pal, A.; Szakáts, R.; Kiss, C.; Bódi, A.; Bognár, Z.; Kalup, C.; Kiss, L.L.; Marton, G.; Molnár, L.; Plachy, E.; Sárneczky, K.; Szabó, G.M.; Szabó, R. (2020). "Solar System Objects Observed with TESS - First Data Release: Bright Main-belt and Trojan Asteroids from the Southern Survey." *Ap. J. Suppl Ser*. **247**, id. 26.

Pravec, P.; Wolf, M.; Sarounova, L. (1998web; 2000web; 2020web; 2021web). *http://www.asu.cas.cz/~ppravec/neo.htm*

Rubincam, D.P. (2000). "Radiative Spin-up and Spin-down of Small Asteroids." *Icarus* **148**, 2-11.

Taylor, P.A.; Nolan, M.C.; Howell, E.S.; Benner, L.A.M.; et al. (2012). *CBET* **3091**.

Warner, B.D. (2014). "Near-Earth Asteroid Lightcurve Analysis at CS3-Palmer Divide Station: 2014 March-June." *Minor Planet Bull*. **41**, 213-224.

Warner, B.D. (2015). "Near-Earth Asteroid Lightcurve Analysis at CS3-Palmer Divide Station: 2015 March-June." *Minor Planet Bull*. **42**, 256-266.

Warner, B.D. (2018). "Near-Earth Asteroid Lightcurve Analysis at CS3-Palmer Divide Station: 2018 April-June." *Minor Planet Bull*. **45**, 366-379.

Warner, B.D.; Stephens, R.D. (2019). "Near-Earth Asteroid Lightcurve Analysis at the Center for Solar System Studies: 2019 January-April." *Minor Planet Bull*. **46**, 304-314.

Warner, B.D.; Harris, A.W.; Pravec, P. (2009). "The Asteroid Lightcurve Database." *Icarus* **202**, 134-146. Updated 2023 Oct. *http://www.minorplanet.info/lightcurvedatabase.html*

Num	Name	H	Diam	BDate	BMag	BDec	Period	AMn	AMx	U	Notes
	2017 MB3	**25.4**	**0.025**	**06 27.2**	**17.8**	**15**					**PHA NHATS**
439437	**2013 NK4**	**18.83**	**0.509**	**04 17.4**	**12.3**	**9**					
	2020 BP13	**21.2**	**0.171**	**04 07.6**	**16.5**	**-59**					**PHA**
415029	**2011 UL21**	**15.97**	**1.90**	**06 29.2**	**11.6**	**-16**	**2.732**		**0.32**	**2+**	**PHA** Warner (2018)
517681	**2015 DE198**	**18.91**	**0.491**	**04 09.6**	**15.8**	**75**	**33.558**		**0.27**	**2**	**PHA** Pal et al. (2020)
363599	**2004 FG11**	**21.04**	**0.184**	**04 08.8**	**17.3**	**31**	**7.021**		**0.30**	**2**	**PHA Binary** Taylor et al. (2012) Dumitru et al. (2018)
469445	2002 LT24	22.19	0.108	06 26.3	16.9	-10					
504034	**2005 UJ159**	**17.64**	**0.881**	**06 20.0**	**15.3**	**-38**					**PHA**
388945	**2008 TZ3**	**20.46**	**0.24**	**05 10.3**	**18.0**	**11**	**39.15**	**0.47**	**0.59**	**2+**	**PHA** Pravec et al. (2020web)
14827	Hypnos	18.87	0.500	05 29.0	15.3	-27					
385843	2006 JY25	20.51	0.235	06 20.8	17.8	-48	7.8		1.0	2	
21374	1997 WS22	17.47	0.953	05 20.2	13.4	-15	3.405	0.07	0.17	2	Warner (2014)
612970	2005 HN3	21.23	0.169	05 11.9	17.4	-7					
2063	Bacchus	17.23	1.06	04 22.9	13.9	-13	14.904	0.22	0.42	3	Pravec et al. (1998web)
381677	2009 BJ81	18.32	0.644	05 27.5	15.8	22	325		0.40	2	Warner & Stephens (2019) P2 ~ 27 h reported.
162472	2000 LL	19.17	0.435	05 27.6	16.4	-12					
482049	2009 XG8	18.82	0.512	05 11.3	15.6	-17					
302523	2002 KH3	17.62	0.889	06 14.0	16.0	-6					
25330	1994 KV4	16.76	1.32	04 20.3	15.0	15	4.919	0.14	0.15	3	Pravec et al. (2000web)
86667	2000 FO10	17.54	0.923	05 06.5	15.7	9	53.756	1.01	1.30	3-	Pravec et al. (2021web)
1566	Icarus	16.59	1.43	06 19.2	14.8	-29	2.2726	0.05	0.22	3	Warner (2015)

Table I. A list of near-Earth asteroids reaching brightest in 2024 April-June. PHA: potentially hazardous asteroid. NHATS: Near-Earth Object Human Space Flight Accessible Targets Study. Diameters are based on p_V = 0.20. The Date, V, and Dec columns are the mm/dd.d, approximate magnitude, and declination when at brightest. Amp is the single or range of amplitudes. The references in the Notes column are those for the adopted period.

Warner, B.D.; Harris, A.W.; Durech, J.; Benner, L.A.M. (2021a). "Lightcurve Photometry Opportunities" 2021 January-March." *Minor Planet Bull.* **48**, 89-97.

Warner, B.D.; Harris, A.W.; Durech, J.; Benner, L.A.M. (2021b). "Lightcurve Photometry Opportunities" 2021 October-December." *Minor Planet Bull.* **48**, 406-410.

IN THIS ISSUE

This list gives those asteroids in this issue for which physical observations (excluding astrometric only) were made. This includes lightcurves, color index, and H-G determinations, etc. In some cases, no specific results are reported due to a lack of or poor-quality data. The page number is for the first page of the paper mentioning the asteroid. EP is the "go to page" value in the electronic version.

THE MINOR PLANET BULLETIN (ISSN 1052-8091) is the quarterly journal of the Minor Planets Section of the Association of Lunar and Planetary Observers (ALPO, http://www.alpo-astronomy.org). Current and most recent issues of the *MPB* are available on line, free of charge from:

https://mpbulletin.org/

The Minor Planets Section is directed by its Coordinator, Prof. Frederick Pilcher, 4438 Organ Mesa Loop, Las Cruces, NM 88011 USA (fpilcher35@gmail.com). Robert Stephens (rstephens@foxandstephens.com) serves as Associate Coordinator. Dr. Alan W. Harris (MoreData! Inc.; harrisaw@colorado.edu), and Dr. Petr Pravec (Ondrejov Observatory; ppravec@asu.cas.cz) serve as Scientific Advisors. The Asteroid Photometry Coordinator is Brian D. Warner (Center for Solar System Studies), Palmer Divide Observatory, 446 Sycamore Ave., Eaton, CO 80615 USA (brian@MinorPlanetObserver.com).

The Minor Planet Bulletin is edited by Professor Richard P. Binzel, MIT 54-410, 77 Massachusetts Ave, Cambridge, MA 02139 USA (rpb@mit.edu). Brian D. Warner (address above) is Associate Editor. Assistant Editors are Dr. David Polishook, Department of Earth and Planetary Sciences, Weizmann Institute of Science (david.polishook@weizmann.ac.il) and Dr. Melissa Hayes-Gehrke, Department of Astronomy, University of Maryland (mhayesge@umd.edu). The *MPB* is produced by Dr. Pedro A. Valdés Sada (psada2@ix.netcom.com).

Effective with Volume 50, the *Minor Planet Bulletin* is an electronic-only journal; print subscriptions are no longer available. In addition to the free electronic download of the *MPB* as noted above, electronic retrieval of all *Minor Planet Bulletin* articles (back to Volume 1, Issue Number 1) is available through the Astrophysical Data System:

http://www.adsabs.harvard.edu/

Authors should submit their manuscripts by electronic mail (rpb@mit.edu). Author instructions and a Microsoft Word template document are available at the web page given above. All materials must arrive by the deadline for each issue. Visual photometry observations, positional observations, any type of observation not covered above, and general information requests should be sent to the Coordinator.

* * * * *

The deadline for the next issue (51-3) is April 15, 2024. The deadline for issue 51-4 is July 15, 2024.

THIS PAGE INTENTIONALLY LEFT BLANK